

**Oxidation Reactions of *Lucina pectinata* hemoglobins:
Model system to design heme protein based blood substitutes**

By

Walleska De Jesús Bonilla

A thesis submitted in partial fulfillment of the requirements for the degree of

DOCTOR OF PHILOSOPHY

In

Applied Chemistry
(Biophysics)

UNIVERSITY OF PUERTO RICO

MAYAGÜEZ CAMPUS

2008

Approved by:

Madeline Torres Lugo, Ph.D.
Member, Graduate Committee

Date

José E. Cortés Figueroa, Ph.D.
Member, Graduate Committee

Date

Elsa M. Cora, Ph.D.
Member, Graduate Committee

Date

Juan López Garriga, Ph.D.
President, Graduate Committee

Date

Nelson Cardona Martínez, Ph.D.
Representative, Graduate Studies

Date

Francis Patrón, Ph.D.
Chairperson, Chemistry Department

Date

ABSTRACT

Today, efforts are focused in the production of a second-generation blood substitutes that minimizes the oxidative stress and the tissue vasoactivity. The infused cell-free hemoglobin's can act as nitric oxide (NO) scavenger inducing vasoconstriction and affecting blood pressure. Also, it can autoxidize producing reactive oxygen species such as the superoxide ion and H_2O_2 . These reactions produce the heme-Fe(IV) ferryl species, which promote hemolysis.

Regarding this, *Lucina pectinata* hemoglobins HbI and HbII were used to explore correlations between structure and the oxidative stability in the reactions with H_2O_2 and NO. The HbI and HbII distal pocket active site has the conserved amino acids GlnE7 (also present in elephant and shark myoglobin), PheCD1, and PheE11. The other amino acid is PheB10 in HbI, while HbII has TyrB10. The HbI PheB10Tyr replacement was used to compare the active centers.

The results indicate that the human cross-linked α -DBBF-Hb has an autoxidation rate constant (k_{autox}) of 0.090 h^{-1} . The autoxidation rate constant for HbI was 0.055 h^{-1} . However, HbII and HbI PheB10Tyr have significant lower autoxidation rates of 0.003 h^{-1} , and 0.008 h^{-1} , respectively. The kinetic rate constant for the reaction of α -DBBF-Hb with H_2O_2 producing high amounts of fluorescent heme degradation products is $8.0 \text{ M}^{-1}\text{s}^{-1}$. The heme degradation for HbII ($0.61 \text{ M}^{-1}\text{s}^{-1}$) and HbI PheB10Tyr ($0.58 \text{ M}^{-1}\text{s}^{-1}$) is the smaller of the hemoglobins, while HbI has the higher rate constant ($16.73 \text{ M}^{-1}\text{s}^{-1}$). This data suggests that TyrB10 significantly contributes to reduce the oxidation caused by H_2O_2 . The kinetic rate constant for the oxy Hb oxidation with NO for α -DBBF-Hb and HbII is $18.95 \mu\text{M}^{-1}\text{s}^{-1}$, and

$2.8 \mu\text{M}^{-1}\text{s}^{-1}$, and for HbI and HbI PheB10Tyr is $91.6 \text{ M}^{-1}\text{s}^{-1}$, and $49.97 \text{ M}^{-1}\text{s}^{-1}$, respectively. These reactions suggest that in addition to TyrB10, there are other factors in HbII affecting the NO entrance to the distal site leading to the slow HbII oxidation by this ligand.

Furthermore, experiments with endothelial cells show that under induced oxidative stress *L. pectinata* hemoglobins stimulate mild apoptosis to cells when forming the ferryl species in the reactions with hydrogen peroxide. Moreover, the exposition of the hemoglobins during hypoxia increases the HIF-1 α levels, thus suggesting that the cell redox signaling and death pathways are altered. This suggests novel capabilities, especially for HbII, to carry oxygen under hypoxic conditions or oxygen stress. Taken together, our results suggest that *L. pectinata* HbII may represent a good model for the design of future oxidative stable oxygen carrier with little or no vasoactivity.

RESUMEN

Hoy día continúan los esfuerzos para producir un sustituto de hemoglobina que genere poco estrés oxidativo y poca vasoactividad. La administración de hemoglobina modificada y fuera del glóbulo rojo, reacciona con el óxido nítrico (NO) disponible en los tejidos causando vasoconstricción y afectando la presión sanguínea. La hemoglobina se auto oxida y produce especies reactivas a oxígeno, como por ejemplo el ión superóxido y peróxido de hidrógeno. Por lo que la hemoglobina también reacciona con estas especies produciendo las especies ferryl, hemo-Fe(IV), las cuales promueven el rompimiento del grupo hemo.

Es por esto que en este estudio se han utilizado las hemoglobinas HbI y HbII de la almeja *Lucina pectinata* para correlacionar estructura y estabilidad oxidativa en las reacciones con H_2O_2 y NO. El centro activo de HbI y HbII contienen amino ácidos conservados como GlnE7 (también presente en la mioglobina de elefante y de tiburón), PheCD1 y PheE11. En el centro activo difieren en el amino ácido en la posición B10, el cual es Phe en HbI y Tyr en HbII. El mutante de HbI PheB10Tyr fue utilizado para comparar los centros activos entre las hemoglobinas.

Los resultados muestran que la hemoglobina humana modificada α -DBBF tiene una constante de auto oxidación (k_{autox}) de 0.090 h^{-1} , mientras que para HbI el valor de k_{autox} es 0.055 h^{-1} . Sin embargo, HbII y HbI PheB10Tyr tienen una constante de auto oxidación bien pequeña con valores de 0.010 h^{-1} y 0.008 h^{-1} , respectivamente. La constante cinética para la formación de productos de degradación fluorescentes es grande para α -DBBF Hb, con un valor de $8.0 \text{ M}^{-1}\text{s}^{-1}$. Sin embargo, las constantes de degradación para HbII ($1.1 \text{ M}^{-1}\text{s}^{-1}$) y HbI PheB10Tyr ($1.2 \text{ M}^{-1}\text{s}^{-1}$) mostraron ser las más bajas, mientras que HbI ($37 \text{ M}^{-1}\text{s}^{-1}$) obtuvo el

valor más alto para la formación de productos de degradación del hemo. Estos datos sugieren que TyrB10 contribuye significativamente a reducir la oxidación causada por H_2O_2 . Las constantes cinéticas para la oxidación de las hemoglobinas en su estado oxigenado en la reacción con NO son $18.95 \mu\text{M}^{-1}\text{s}^{-1}$, $2.8 \mu\text{M}^{-1}\text{s}^{-1}$, $91.6 \text{ M}^{-1}\text{s}^{-1}$ y $49.97 \text{ M}^{-1}\text{s}^{-1}$ para α -DBBF Hb, HbII, HbI y HbI PheB10Tyr, respectivamente. Estas reacciones sugieren que hay otros factores, además de TyrB10, afectando la entrada de NO al centro activo permitiendo que la oxidación de HbII por este ligando sea lenta.

Además, los experimentos realizados con células endoteliales mostraron que bajo estrés oxidativo inducido, la reacción de hemoglobinas de *L. pectinata* con peróxido de hidrógeno forman las especies ferryl, estimulando la apoptosis celular. También, los niveles de la proteína HIF-1 α aumentan cuando las células son tratadas con las hemoglobinas durante un periodo de hipoxia, sugiriendo que tanto las rutas de señal para estrés oxidativo como las que llevan a muerte celular son afectadas. Esto sugiere que durante estrés inducido por hypoxia HbII tiene la capacidad de transportar oxígeno al medio celular y de alterar las reacciones que fisiológicamente se llevan a cabo. Resumiendo todos los aspectos de este estudio, los resultados sugieren que *L. pectinata* HbII representa un buen modelo para el diseño de un transportador de oxígeno que sea estable en términos de oxidación y que tenga poca actividad de vasoconstricción.

© 2008 Walleska De Jesús-Bonilla

To God, my guide and my strength.

*To my kids Adrián, Natalia, Paola, and Isabel, for being my inspiration.
To my husband Artemio, for his patience and all these years of trust, support and love.
To my lovely mother Nancy, for her love, prayers and help.*

ACKNOWLEDGEMENTS

During these years of doctoral studies, several persons collaborated directly and indirectly with my research. First of all I would like to thank God, for giving me patience, strength and health to complete this research. Special thanks to my advisor Dr. Juan López Garriga who believed in me and gave me the scientific vision and tools to fulfill this research. Thanks for your friendship, guidance and support. I also would like to thank my committee: Dr. José E. Cortés, Dr. Madeline Torres, and Dr. Elsa Cora, for your time and availability, and to help me during this process of my life.

Part of this research was performed in the Laboratory of Biochemistry and Vascular Biology, Division of Hematology, Center for Biologics Evaluation and Research (CBER), Food and Drug Administration (FDA). I would like to thank Dr. Abdu Alayash, Yiping Jia, Francine Wood and Paul Yeh for my training and experimental assistance.

I would like to acknowledge my laboratory and Science on Wheels partners, for their help when I most needed them. And special thanks to Dr. Madeline Torres' laboratory group, for their guidance and make me feel part of your group.

Thanks Professor Víctor Ramírez, Dr. Juan González Lagoa and Dr. Mayra Cadiz for my English writing corrections.

Alfred P. Sloan Foundation, NIH-NIGMS/ MBRIS-Score-2 (Grant S06GM08103-34), and Graduate and Undergraduate Students enhancing Science and Technology in K-12 Schools (GUEST K-12) are acknowledged for the financial support.

Table of Contents

Abstract	ii
Resumen	iv
Acknowledgements	viii
List of Symbols and Abbreviations	xiii
List of Figures	xv
List of Tables	xxvi
Table of Contents	
1	INTRODUCTION
1.1	Motivation1
1.2	Human hemoglobin physiology3
1.2.1	pH and CO ₂ activity in human hemoglobin7
1.2.2	Nitric oxide and peroxynitrite formation in human Hemoglobin10
1.2.3	Human hemoglobin oxidation and denaturation12
1.3	Blood substitutes15
1.3.1	Effects of the hemoglobin outside the red blood cells; cell free-hemoglobins18
1.3.2	Effects of hemoglobins on endothelial cells22
1.4	<i>Lucina pectinata</i> hemoglobins27
1.5	Objectives33
2	MATERIALS AND METHODS
2.1	Heme proteins preparation36
2.1.1.	Hemoglobin isolation and purification36

2.1.2.	Hemoglobin spectral analysis	43
2.2	Redox chemistry of <i>L. pectinata</i> hemoglobins	
2.2.1	Hemoglobins autoxidation	47
2.2.2	Reaction of the hemoglobins with hydrogen peroxide	48
2.2.3	Detection of heme degradation products	53
2.2.4	Hemoglobin reactions with nitric oxide	54
2.2.5	Catalase assay	55
2.3	Redox chemistry of <i>L. pectinata</i> hemoglobins <i>in vitro</i>	
2.3.1	Endothelial cell culture	56
2.3.2	Cell viability assay	56
2.3.3	Exposition of endothelial cells to a hypoxic environment	57
2.3.4	Detection of the HIF inducible factor HIF-1 α	57
2.3.5	Intracellular superoxide determination	58
2.3.6	Oxygen tension measurements	59
2.3.7	Endothelial cells exposition to glucose oxide	59
2.3.8	Cell morphology after exposed to hemoglobins and glucose oxidase	60
2.3.9	Statistical analysis	61
3	HEMOGLOBIN REACTION WITH NITRIC OXIDE	
3.1	Introduction	62
3.2	Nitric oxide reaction results	63
3.2.1.	NO-induced oxidation	63
3.2.2.	Reaction of ferric hemoglobins with nitric oxide	71

	3.2.3. Hemoglobins NO dissociation	71
	3.3 Discussion	75
4	HEMOGLOBINS REDOX CHEMISTRY IN THE REACTION WITH HYDROGEN PEROXIDE	
	4.1 Introduction	87
	4.2 Autoxidation results	89
	4.3 Oxidation reactions with hydrogen peroxide	97
	4.4 Discussion	113
5	REACTION WITH GLUCOSE OXIDASE IN BOVINE AORTIC ENDOTHELIAL CELLS	
	5.1 Introduction	123
	5.2 <i>L. pectinata</i> hemoglobins oxidation with glucose oxidase	125
	5.3 Apoptosis and cell morphology in the reaction of the hemoglobins with glucose oxidase	135
	5.4 Discussion	159
6	REDOX CHEMISTRY OF THE HEMOGLOBINS EXPOSED TO BOVINE AORTIC ENDOTHELIAL CELLS DURING HYPOXIA	
	6.1 Introduction	166
	6.2 Intracellular superoxide ion formation and oxygen tension results	167
	6.3 <i>Lucina pectinata</i> redox chemistry during hypoxia	171
	6.4 HIF-1 α protein expression during hypoxic conditions	178
	6.5 Discussion	181
7	CONCLUSIONS	189
	REFERENCES	192

APPENDIX A	Student's t-Test statistical analysis for the bovine aortic endothelial cells apoptotic levels cells incubated for 2 hours, 6 and 24 hours	203
APPENDIX B	Student's t-Test statistical analysis for the HIF-1α expression in bovine aortic endothelial cells incubated with HbII for 2 hours, 4, 6, 8, and 24 hours	219

List of Symbols and Abbreviations

BAEC	Bovine aortic endothelial cells
CO ₂	Carbon dioxide
α-DBBF Hb	Diaspirin cross-linked hemoglobin
DETA/NOOate	Diethyltriamine nitric oxide adduct (NOC-18)
2,3-DPG	2,3-diphosphoglycerate
EC	Endothelial cells
FDA	Food and Drug Administration
GOX	Glucose oxidase
H ₂ O ₂	Hydrogen peroxide
Hb	Hemoglobin
HbI	<i>Lucina pectinata</i> HbI
HbII	<i>Lucina pectinata</i> HbII
HbIII	<i>Lucina pectinata</i> HbIII
HbA ₀	Adult human hemoglobin
HbCO	Carboxy hemoglobin
HbO ₂	Oxy hemoglobin
HbOC	Hemoglobin-based oxygen carrier
HIF	Hypoxia inducible factor
HIV	Human Immunodeficiency virus
k _{off}	Kinetic rate constant for dissociation
k _{on}	Kinetic rate constant for association

<i>L. pectinata</i>	<i>Lucina pectinata</i>
Mb	Myoglobin
mmHg	Millimeters of mercury
NO	Nitric oxide
NOS	Nitric oxide synthase
O ₂	Oxygen
O ₂ ^{•-}	Superoxide anion
•OH	Hydroxyl radical
ONOO ⁻	Peroxynitrite
RBC	Red blood cells
RNS	Reactive nitrogen species
ROS	Reactive oxygen species
SOD	Superoxide dismutase

List of Figures

Figures		Page
1.1	Human hemoglobin crystallographic structure. PDB: 1GZX. The hemoglobin consists of two alfa and two beta chains (ribbons red, gray, gold and blue), each one containing a heme prosthetic group (cyan).....	6
1.2	The heme group (Fe-protoporphyrin IX). The iron has six coordination sites: four are bonded to the pyrrole rings, another to an imidazole nitrogen of a histidine proximal residue and the sixth coordination position is available for binding with oxygen and other small molecules.....	7
1.3	Hemoglobin in both: the oxy and deoxy state. In the deoxy state (A), the protoporphyrin is out of the plane in a T-state. When the molecule is oxygenated (B), it is in the R-state.....	10
1.4	Mechanisms of nitric oxide binding to hemoglobin. The reaction of deoxy Hb with NO forms the complex Hb-NO, while the reaction with oxy Hb and NO oxidizes the hemoglobin and forms the peroxynitrite compound (A). The reaction of nitric oxide binding to ferric hemoglobin forms the ferric Hb-NO complex (B) (Privalle et al., 2000)..	13
1.5	Schematic representation of hemoglobin autoxidation and formation of reactive oxygen species. Oxy Hb autoxidizes producing the superoxide ion, which dismutates to hydrogen peroxide. The oxy Hb or ferric Hb consumes the hydrogen peroxide in a pseudoperoxidative cycle, forming the ferryl compounds. The presence of superoxide dismutase and catalase in the red blood cell controls these oxidation reactions converting the superoxide ion to oxygen and water (Modified from Alayash, 1999).....	16
1.6	Schematic representation of NO production in presence of hemoglobin inside the red blood cells (A). (B) Hemoglobin outside the red blood cells scavenges NO leading to the production of ROS. Model adapted from Dou et al., 2002 & Alayash, 2004.....	23
1.7	Mechanism for HIF-1 α degradation under normoxic conditions via the activation of HIF-1 α proline hydroxylase (Sharp et al., 2004).....	27
1.8	Mechanism for the inhibition of the HIF-1 α target genes under normoxic conditions via the activation of HIF-1 α asparagine hydroxylase (Sharp et al., 2004).....	28

1.9	<i>Lucina pectinata</i> HbI crystallographic structure, PDB code 1FLP (Rizzi et al., 1994). HbI is a monomeric hemoglobin of 142 amino acids, and is a sulfide reactive hemoglobin.....	31
1.10	<i>Lucina pectinata</i> HbII crystallographic structure, PDB code 2OLP (Gavira et al., 2008). HbII consists of two dimmers of 163 amino acids, and is an oxygen binding hemoglobin.....	32
1.11	Heme pocket amino acids from <i>Lucina. pectinata</i> HbI (A) PDB: 1FLP, and HbII (B) PDB: 2OLP. In the distal site of the heme pocket of the Hbs is GlnE7 instead of the classical histidine. The other surrounding amino acid residues are PheCD1, PheE11, PheB10 for HbI, while HbII and HbIII have PheCD1, PheE11 and TyrB10.....	34
2.1	Elution chromatogram for the size exclusion chromatography purification of the <i>L. pectinata</i> ctenidia extract. (1) HbII/HbIII mixture, (2) HbI/Cysteine rich protein mixture.....	37
2.2	Elution chromatogram for the purification of <i>L. pectinata</i> HbI by ion exchange chromatography monitored at 280 nm. (1) ferric HbI, (2) oxy HbI, (3) cystein rich protein.....	38
2.3	Elution chromatogram for the HbII/HbIII mixture purification by ion exchange chromatography. A FPLC with an ion exchange chromatography column was used and monitored at 280 nm. Peak 1 corresponds to other protein impurities, peak 2 and 3 were assigned to HbII and HbIII, respectively.....	40
2.4	HbI PheB10Tyr elution chromatogram after purification by size exclusion chromatography using the FPLC instrument and monitored at 280 nm.....	42
2.5	Polyacrylamide gel electrophoresis for the <i>L. pectinata</i> hemoglobins. (1) broad range prestained protein ladder, (2) and (5) HbI, (3) and (6) HbII, (4) and (7) HbIII, (8) HbI/Cysteine rich protein mixture, (9) HbII/HbIII mixture, (10) protein extract.....	43
2.6	<i>L. pectinata</i> HbII oxidation states spectra. The Soret band at 414 nm with Q bands at 542 nm and 576 nm represents the oxy HbII species. The ferric species show a Soret band at 404 nm and Q bands at 502 nm and 633 nm. The heme-Fe(II) deoxy species has a Soret band at 432 nm with a Q band at 556 nm.....	46
2.7	UV-Vis overlaid spectra of the α -DBBF Hb bands in the Q region for	

	the oxy (heme-Fe(II)), ferric (heme-Fe(III)) and ferryl (heme-Fe(IV)) forms, used to identified the oxidation state of the hemoglobins.....	49
2.8	Schematic representation of the UV-Vis spectrophotometer instrument used to study the kinetic data in the reaction of the hemoglobins from <i>L. pectinata</i> with hydrogen peroxide.....	50
2.9	UV-Vis overlaid spectra for the reaction of <i>L. pectinata</i> HbI with hydrogen peroxide. The Soret band at 416 nm shifts to 419 nm, characteristic of the ferryl species.....	51
2.10	Kinetic trace for the reaction of HbI with hydrogen peroxide, 1:2000 ratio, at 400 nm for 10 seconds, using the a UV-Vis spectrophotometer with an stopped-flow apparatus.....	52
2.11	Bovine aortic endothelial cells after exposed to α -DBBF Hb. Endothelial cells morphology was monitored for 24 hrs during incubation with 50 μ M α -DBBF Hb.....	61
3.1	Oxidation reaction of 0.5 μ M oxy α -DBBF Hb by 10 μ L NO. Oxy α -DBBF Hb (416 nm) shifts to ferric α -DBBF Hb (407 nm). The oxy α -DBBF Hb Q bands broaden and decrease, while increase the bands characteristic of the ferric species.....	64
3.2	Oxidation reaction of 0.5 μ M oxy HbII by 10 μ L NO. Oxy HbII (414 nm) shifts to ferric HbII (404 nm). The absence of ferric Q bands evidences the hemoglobin resistance to oxidation by nitric oxide.....	66
3.3	Oxidation reaction of 0.5 μ M oxy HbI by 10 μ L NO. Oxy HbI (416 nm) shifts to ferric HbII (407 nm). Up arrows represent increasing of the ferric bands, while down arrows represent the decrease in oxy bands.....	67
3.4	Stopped-flow kinetics of NO-induced oxidation of <i>L. pectinata</i> HbI and HbII. Normalized time courses for the reactions of 0.5 μ M NO and 0.5 μ M HbI or HbII. The solid lines are the nonlinear least-square fits to the exponential decay equations. The kinetic rate constants were obtained from the fit of the average of at least three independent experiments.....	68
3.5	Plot of the apparent rate constants for the NO-induced oxidation of <i>L. pectinata</i> hemoglobins and α -DBBF Hb. (a) HbI, (b) HbI PheB10Tyr, (c) α -DBBF Hb, (d) HbII.....	69
3.6	Stopped-flow time courses of rapid reactions of 0.5 μ M ferric HbI and HbII with 15 μ M NO solution measured at 420 nm in 50 mM sodium	

	phosphate buffer at pH 7.4 and 20°C. The solid lines were obtained from the nonlinear least-square fits to the exponential increase equations of the average of 3 - 5 independent experiments	72
3.7	Plot of the apparent rate constants of NO association to ferric HbI, ferric HbI PheB10Tyr, and ferric HbII. Each protein (15 μ M) was mixed 20-50 μ M NO in a stopped-flow apparatus and monitored at 420 nm.....	73
3.8	Kinetic traces for the NO dissociation from the NO-Hb complex. ■ HbII, ○ HbI, ● α -DBBF Hb. Deoxygenated Hbs (5 μ M) were mixed with equal molar ratio of NO, and then incubated with 1 mM CO and 10 mM sodium dithionite in 100 mM sodium phosphate buffer, pH 7.4, in sealed cuvettes. NO dissociation was measured at 420 nm in a spectrophotometer. The solid lines are the non-linear least-square fits to the single exponential fit of the average for three independent kinetic traces.....	74
3.9	Proposed mechanism for the nitric oxide-induced oxidation of the <i>L. pectinata</i> HbII hemoglobin. Oxy HbII reacts with NO forming the peroxynitrite complex. The peroxynitrite isomerizes to nitrate. Nitrate releases from HbII forming ferric HbII. In the left corner: HbII crystallographic structure, PDB 2OLP, Gavira et al., 2008. Model adapted from Gardner et al., 2006.....	80
3.10	Stereo diagrams of the orientations of the distal residues of <i>L. pectinata</i> HbII and HbI. The distances (\AA) from the residues to the heme iron atom were calculated from the C- ζ in the PheE11 and PheCD1, the N of the amide in the GlnE7, and from the oxygen in the TyrB10.....	83
3.11	<i>Lucina pectinata</i> ferric HbI (A) and oxy HbII (B) heme pocket amino acids. These amino acids are directly linked to the conformational change that allows heme stability with bound molecules.....	85
3.12	Superposition of oxy HbII and ferric HbI <i>Lucina pectinata</i> hemoglobins. The oxy HbII structure (red, PDB 2OLP), highlighting the heme and residues GlnE7, PheCD1, TyrB10, TyrG5, and proximal HisF8, is overlaid with the ferric HbI structure (cyan, PDB 1FLP), highlighting the heme, GlnE7, PheCD1, PheB10, PheG5, and proximal HisF8	86
4.1	Autoxidation reaction of <i>L. pectinata</i> HbII. 20 μ M HbII was incubated in a Chelex-treated 50 mM phosphate buffer, pH 7.4 at 37°C, and monitored over a time period of 6 hours. The oxy species (414 nm) shifts to 404 nm characteristic of ferric HbII. Insert: Displacement of the oxy Q bands from 540 nm and 576 nm to 633nm	90

4.2	Autoxidation of α -DBBF Hb in the absence (●) and presence (○) of SOD/catalase. The autoxidation of 20 μ M of α -DBBF was monitored over a period of 6 hours. The α -DBBF Hb solution was incubated in a chelex-treated 50 mM phosphate buffer, pH 7.4, at 37 °C. The percentage changes of oxy α -DBBF Hb were calculated using the UV-Vis spectra following the Winterbourn equations (Materials and Methods, Section 2.1.2).....	91
4.3	Autoxidation of HbI in the absence (●) and presence (○) of SOD/catalase. The autoxidation of 20 μ M of HbI was monitored over a period of six hours. The HbI solution was incubated in a Chelex-treated 50 mM phosphate buffer, pH 7.4, at 37 °C. The percentage changes of oxy HbI were plotted over time.....	94
4.4	Autoxidation of HbII in the absence (●) and presence (○) of SOD/catalase. The autoxidation of 20 μ M of HbII was monitored over a period of six hours. The HbII solution was incubated in a Chelex-treated 50 mM phosphate buffer, pH 7.4, at 37 °C. The percentage changes of oxy HbII were plotted over time.....	95
4.5	Autoxidation of HbI PheB10Tyr in the absence (●) and presence (○) of SOD/catalase. The autoxidation of 20 μ M of HbI PheB10Tyr was monitored over a period of 6 hours. The HbI PheB10Tyr solution was incubated in a Chelex-treated 50 mM phosphate buffer, pH 7.4, at 37 °C. The percentage changes of oxy HbI PheB10Tyr were plotted over time.....	96
4.6	Catalase assay for the hemoglobins α -DBBF Hb (a), HbI (b), and HbII (d). Catalase concentrations of 0.3 nM (c) and 3.0 nM (e) were used as control. The kinetic was monitored by mixing 8.4 μ L of H ₂ O ₂ 30% with 1 μ M hemoglobin in 50mM potassium phosphate buffer, pH 7, for 122 seconds, at 240 nm	98
4.7	Reaction of 8 μ M ferric HbII (A) and HbI PheB10Tyr (B) with hydrogen peroxide, pH 5.0, at 1:400 ratio, respectively. The formation of the ferryl species was monitored at 400 nm at 22°C over a period of 10 seconds. After 5 seconds, the ferric hemoglobin shifts from 407 nm to 416 nm with an isobestic point at 419 nm.....	99
4.8	Reaction of ferric HbII with hydrogen peroxide, pH 7.4, at 1:400 ratio. The Soret band shifts from 407 nm to 419 nm with isosbestic point at 416 nm, confirming the formation of the ferryl compound II.....	101
4.9	Reaction of ferric HbI PheB10Tyr with hydrogen peroxide, pH 7.4, at	

	1:400 and 1:1000 ratios, respectively. The Soret band shifts from 407 nm to 419 nm with isosbestic point at 416 nm, confirming the formation of the ferryl compound II	102
4.10	Overlaid spectra for the reaction of ferric <i>L. pectinata</i> HbI PheB10Tyr with hydrogen peroxide. 18 M HbI PheB10Tyr was reacted with a large H ₂ O ₂ excess. (a) Unreacted HbI PheB10Tyr; (b) reaction after 2 minutes; (c) reaction after 8 minutes.....	103
4.11	Compound I formation in the reaction of ferric recombinant HbI with H ₂ O ₂ . A: kinetic traces of 1 equivalent of recombinant HbI with different equivalents of H ₂ O ₂ ; (a) 1:100, (b) 1:250, (c) 1:500, (d) 1:1000, (e) 1:2000, and (f) 1:3000. B: Spectra for the progress of the reaction at 648 nm, and 1:2000 (Hb:H ₂ O ₂) ratio. The ferryl species Compound I was formed upon 1 second (a) of the reaction.....	105
4.12	Stopped-flow kinetic trace for the reaction of <i>L. pectinata</i> HbII and HbI PheB10Tyr with hydrogen peroxide for 10 seconds at 400 nm. (a) HbII and (b) HbI PheB10Tyr in the reaction at pH 7.5. (c) HbI PheB10Tyr and (d) HbII in the reaction at pH 5.0.....	107
4.13	Plot of the apparent rate constants for the reaction of <i>L. pectinata</i> hemoglobins with H ₂ O ₂ as function of H ₂ O ₂ . (a) HbII at pH 5, (b) HbI PheB10Tyr mutant at pH 5, (c) HbII at pH 7.5, (d) HbI PheB10Tyr at pH 7.5, (e) HbII at pH 11.2, (f) HbI PheB10Tyr at pH 11.2. The hemoglobins were reacted with H ₂ O ₂ in ratios from 1:100 to 1:5000. The formation of the ferryl compound I was monitored at 400 nm, at 5 ms intervals and over periods ranging from 1 to 10 seconds. The kinetic rate constants are the mean of four independent experiments.....	108
4.14	Stopped-flow fluorescence time courses of the reaction between 10 μ M <i>L. pectinata</i> HbI, HbII, and HbI PheB10Tyr and 4 mM H ₂ O ₂ (after mixing). The fluorescence was measured using a stopped-flow spectrophotometer in 50 mM sodium phosphate buffer, pH 7.4, with an excitation wavelength of 321 nm and emission at 360 nm.....	110
4.15	Plot of the apparent rate constants for the formation of heme degradation products. Reaction of 10 μ M oxy HbI (a), HbII (b), and HbI PheB10Tyr (c) as function of H ₂ O ₂ monitored in a stopped-flow spectrophotometer. The kinetic rate constants are the mean of at least three independent experiments.....	111
4.16	<i>L. pectinata</i> oxy HbII hydrogen bonding network. The TyrB10 and GlnE7 point towards the bound oxygen stabilizing it by means of hydrogen bonding. Fe - O1, 2.94 Å; Fe - O2, 2.14 Å; O1 - GlnE7 (NE1),	

	3.00 Å; TyrB10 (OH) – O1, 1.94 Å; TyrB10 (OH) - GlnE7 (NE2), 3.00 Å; GlnE7 (OE1) - LysF3 (NZ), 2.64 Å; heme (O1D) - LysF3 (NZ), 2.71 Å; heme (O2A) - ArgF11 (NH1), 2.95 Å; heme (O1A) - ArgF11 (NH2), 2.64 Å; HisF8 (NE2) - Fe, 2.11 Å (Gavira et al., 2008).....	116
4.17	Proposed mechanism for the reaction of HbII and PheB10Tyr HbI with H ₂ O ₂ . The oxy hemoglobin [2] autoxidizes to form the ferric heme [1], which reacts with H ₂ O ₂ to form, compound I [3] or compound II [4]. The formation of the ferryl compound I proceeds by the decay to compound II or depending on the H ₂ O ₂ concentration can go back to the ferrous heme. The reaction at high concentrations tends to the production of degradation species and to heme degradation.....	118
5.1	Hemoglobins redox cycle. The hemoglobins autoxidation forms the superoxide ion which dismutates to hydrogen peroxide. The hemoglobin reacts with hydrogen peroxide in a ferric-ferryl cycle that produces high concentrations of ROS. This balance disruption alters cell death pathways.....	124
5.2	Overlaid spectra for the reaction of 50 µM oxy HbI with 250 µM H ₂ O ₂ . Oxy HbI 541nm and 576 nm bands decrease while increase the ferryl band at 648 nm and the formation of hemichrome species.....	126
5.3	Overlaid spectra for the reaction of 50 µM HbI with 10 mU/mL GOX. Oxy HbI 541nm and 576 nm bands decrease while increase ferric bands at 502 nm and 633 nm. The change in baseline between spectra and the decrease in the bands intensity suggest heme degradation.....	128
5.4	UV-vis spectra for the reaction of 50 µM HbI with 10 mU/mL GOX after 6 hrs (A), and after the addition of sodium dithionite (B). After 6 hours the spectrum only shows the hemichrome band at 561 nm. The addition of sodium dithionite did not form the deoxy hemoglobin, instead forms a band at 648 nm.....	129
5.5	Overlaid spectra for the reaction of 50 µM HbII with 250 µM H ₂ O ₂ . Oxy HbII 541nm and 576 nm bands have a small decrease while increase the heme-tyrosianate moiety band at 603 nm	130
5.6	Overlaid spectra for the reaction of 50 µM HbII with 10 mU/mL GOX. Oxy HbII 541nm and 576 nm bands have a very small reduction, but without signals of ferric or ferryl species	132
5.7	UV-Vis spectra for the reaction of 50 µM HbII with 10 mU/mL GOX after 6 hrs, and addition of sodium dithionite. In spectrum A, the reaction at 6 hours resemble the reaction with 250 µM H ₂ O ₂ , with an	

	increase in the 605 nm band. Deoxy HbII was formed after the addition of sodium dithionite (B).....	133
5.8	Schematic representation for the reaction of <i>Lucina pectinata</i> HbII and HbI with glucose oxidase. A. HbII reacts with the H ₂ O ₂ produced by GOX forming the ferryl species. Continuous flux of H ₂ O ₂ makes HbII to act as a pseudoperoxidase, thus consuming H ₂ O ₂ in a ferric-ferryl cycle. B. HbI reacts with the produced H ₂ O ₂ forming ferric and the ferryl species. Continuous H ₂ O ₂ production leads to HbI heme degradation.....	134
5.9	Bovine aortic endothelial cells viability assay after exposed to α -DBBF Hb, HbII, HbI, and HbI PheB10Tyr mutant. ■ 2 hr, ■ 6hr, ■ 24 hr. Values at each time represent the mean \pm SE of 15 - 30 assays for three different experiments	136
5.10	Bovine Aortic Endothelial Cells Viability Assay after exposed to α -DBBF Hb, HbII, HbI, and HbI PheB10Tyr mutant and GOX. ■ 2 hr, ■ 6hr, ■ 24 hr. Values at each time represent the mean \pm SE of 15 - 30 assays for three different experiments.....	138
5.11	UV-Vis spectra of the hemoglobins after incubated with BAEC for 2 hours. (A) The incubation of 50 μ M hemoglobin in the cells media at 37°C only shows bands for oxy hemoglobin. (B) Hemoglobins after reaction with 10 mU/mL GOX in the cells media for 2 hours. α -DBBF Hb and HbII exhibit oxidation and ferryl formation, while the HbI PheB10Tyr mutant forms the ferryl species. The band at 561 nm suggests the HbI hemichrome species.....	140
5.12	UV-Vis spectra of the hemoglobins after incubated with BAEC for 6 hours. (A) The incubation of 50 μ M hemoglobin in the cells media at 37°C remains in the oxy species. (B) Hemoglobins after reaction with 10 mU/mL GOX in the cells media for 6 hours. α -DBBF Hb shows ferric-ferryl bands, HbII oxidizes and forms hemichrome species, HbI PheB10Tyr mutant shows ferryl bands, and HbI is almost degrade.....	142
5.13	UV-Vis spectra of the hemoglobins after incubated with BAEC for 24 hours. (A) α -DBBF Hb shows oxy bands, while HbII and HbI PheB10Tyr oxidize and form hemichrome species. (B) Hemoglobins after reaction with 10 mU/mL GOX in the cells media for 24 hours. α -DBBF Hb shows ferric-ferryl bands and small degradation. <i>L. pectinata</i> hemoglobins forms hemichrome species and degrade.....	143
5.14	Morphologic changes in endothelial cells induced by the redox cycling	

	of the hemoglobins for 2 hours. Arrows in micrograph D and G show cell elongation. Arrows in H show cell detachment and rounding	146
5.15	Morphologic changes in endothelial cells induced by the redox cycling of the hemoglobins during 6 hours. Arrows in micrograph D show initial steps of hemoglobin aggregation. Arrows in micrographs E and G show cells elongation. Micrograph H shows that all the cell have elongated morphology	148
5.16	Morphologic changes in endothelial cells induced by the redox cycling of the hemoglobins during 24 hours. Micrograph B shows cells rounding and fragments. The cells exposed to <i>L. pectinata</i> hemoglobins show cell detachment from the layer. Micrographs D and H show the hemoglobin aggregation on the cell monolayer	149
5.17	Endothelial cells treated with hemoglobins and 10 mU/mL GOX for 24 hours. Micrographs A and B show cells treated only with GOX, C – F show cells treated with GOX and α -DBBF Hb, HbII, HbI, or HbI PheB10Tyr, respectively. Examples of nucleus condensation are point up with white arrows	150
5.18	Endothelial cells DNA extraction. Agarose gels A and B show the extracted DNA of cells treated for 2 hours and 6 hours, respectively. Lanes were filled with: 1- 123 bp DNA ladder marker; 3- untreated cells DNA; 4 to 7- DNA of cells treated with HbII, HbI PheB10Tyr, HbI, and α -DBBF Hb, respectively; 9- 1 kb DNA ladder. Agarose gel C and D show the extracted DNA of cells treated with 10 mU/mL GOX for 2 hours and 6 hours, respectively. Lanes 1 and 10 were filled with the 123 bp and 1 kb DNA ladder marker; 3- untreated cells DNA; 4 to 8- DNA of cells treated with HbII, HbI PheB10Tyr, HbI, α -DBBF Hb, and cells only with GOX, respectively	154
5.19	Bovine aortic endothelial cells apoptosis assay after exposed to HbII, HbI PheB10Tyr, HbI, or α -DBBF Hb for ■ 2 hours, ■ 6hours, and ■ 24 hours. Values at each time represent the mean \pm SE of 5-7 samples.....	156
5.20	Bovine aortic endothelial cells apoptosis assay after exposed 10 mU/mL GOX and HbII, HbI PheB10Tyr, HbI, or α -DBBF Hb for ■ 2 hours, ■ 6hours, and ■ 24 hours. Values at each time represent the mean \pm SE of 5-7 samples	158
5.21	Schematic representations of HbII and HbI hemoglobins when treated with endothelial cells and GOX incubated at 37°C without (A) or with (B) a CO ₂ atmosphere.....	162

5.22	Proposed mechanism for the reaction of <i>L. pectinata</i> HbI and HbII when exposed to the endothelial cells media. The hemoglobins autoxidize producing the superoxide ion. In addition, the hemoglobins react with NO forming ferric hemoglobin and the peroxynitrite ion. The accumulation of H ₂ O ₂ , formed by GOX, produces the ferryl species and subsequent heme degradation. The formation of high concentrations of ROS create a balance disruption that can cause physiological diseases, for example vasoconstriction.....	164
6.1	Time course for the intracellular O ₂ ⁻ formation during hypoxia in the presence or without SOD. Cells were incubated under hypoxic conditions (95%N ₂ , 5% CO ₂) with 50 μM Hb and with or without 100 U SOD for 12 hrs. The O ₂ ⁻ was measured in a TopCount Luminescence counter. ● α-DBBF Hb/hypoxia; ○ α-DBBF Hb/hypoxia/SOD; ◆ HbII/hypoxia; ◇ HbII/hypoxia/SOD; ▲ HbI/hypoxia; △ HbI/hypoxia/SOD.....	168
6.2	Oxygen tension of endothelial cells medium during hypoxia. Confluent endothelial cells were placed inside a chamber containing 3mL of basal medium and with or without 50 μM Hb (◆: α-DBBF Hb; ▲: HbII; ■: HbI). Normoxia experiments (□: control) were carried out when 5% CO ₂ and 95% air were flushed into the chamber. Hypoxia experiments (○: cells during hypoxia) were conducted when mixed gas (5% CO ₂ and 95% N ₂) was flushed into the chamber. Values at each time represent the mean ± SE of 3 independent experiments.....	170
6.3	UV-Vis overlaid spectra of <i>Lucina pectinata</i> HbII after exposed to bovine aortic endothelial cells subjected to hypoxia. The formation of reactive oxygen species lead to the production of the ferryl HbII.....	172
6.4	Time course spectra analysis for the oxidation of HbII in cells culture media under normoxic and hypoxic conditions. HbII (25μM) was incubated with BAEC's at 2, 4, 6, 8, 12 and 24 hrs. At each time interval the spectrum was recorded and the percentage of oxy, ferric and hemichrome was calculated following the Winterbourn equations (Material and methods, Section 2.1.2)	174
6.5	UV-Vis overlaid spectra of <i>Lucina pectinata</i> HbI after exposed to bovine aortic endothelial cells subjected to hypoxia. The initial spectrum at 2 hours already shows a mixture between the ferric and the ferryl species with a Soret band at 412 nm and Q bands at 543 nm and 577 nm	176
6.6	Time course spectra analysis for the oxidation of HbI in cells culture	

	media under normoxic and hypoxic conditions. HbI (25 μ M) was incubated with BAEC's at 2, 4, 6, 8, and 12 hrs. At each time interval the spectrum was recorded and the percentage of oxy, ferric and hemichrome was calculated following the Winterbourn equations.....	177
6.7	HIF-1 α expression in bovine aortic endothelial cells under hypoxia with or without 25 μ M oxy HbII (A) or HbI (B). Hypoxic gas (95% N ₂ , 5% CO ₂) was flushed in a sealed chamber containing the cell cultured media with or without 50 μ M HbII or HbI. After each experiment, cell lysates were analyzed by western blot for HIF-1 α protein	179
6.8	Relative HIF-1 α protein expression levels in BAEC's during incubation with (A) HbII or (B) HbI under hypoxia. Densitometry for the immunoblot detection of HIF-1 α was performed and plotted as function of time. ▲-cells under normoxia, ■-cells under hypoxia treated with HbII (A) or HbI (B), ◆-untreated cells under hypoxia. The probability (<i>p</i>) is less than 0.05; therefore the increase between cells in hypoxia and with Hb is significant.....	180
6.9	Schematic representation for the reaction of the <i>Lucina pectinata</i> hemoglobins HbI and HbII. During the hypoxic period, oxy hemoglobin down loads the oxygen which is converted to superoxide ion by Nox1. The reaction of the hemoglobin with the hydrogen peroxide, formed by the superoxide dismutation, produces the Hb-ferryl species. Model adapted from Dworakowski et al., 2008 & Alayash, 2004	183
6.10	Correlation between the percent of oxy (A) or ferric (B) HbII and HIF-1 α relative levels. Graph A shows a negative correlation between the decrease in the percent of oxy HbII and the expression of HIF-1 α . Graph B shows a positive correlation between the increase in the percent of ferric HbII and the expression of HIF-1 α	186
6.11	Correlation between the percent of oxy (A) or ferric (B) HbI and HIF-1 α relative levels. Graph A shows a negative correlation between the decrease in the percent of oxy HbI and the expression of HIF-1 α . Graph B shows a positive correlation between the increase in the percent of ferric HbI and the expression of HIF-1 α	187

List of Tables

Tables	Page
1.1 Adverse effects associated to the administration of hemoglobin based oxygen carriers	5
1.2 Advantages and necessities of the production of a blood substitute	19
1.3 Hemoglobin structural modifications to maintain the tetramer structure..	21
1.4 Kinetic oxygenation and autoxidation characteristics of HbA ₀ and α -DBBF human hemoglobins.....	22
1.5 Kinetic rate constants for the reaction of HbA ₀ and α -DBBF Hb with hydrogen peroxide and nitric oxide.....	24
2.1 Spectral properties of HbI and HbII from <i>L. pectinata</i>	45
3.1 Kinetic and equilibrium rate constants for the reaction of NO with the oxy, deoxy and ferric forms of <i>L. pectinata</i> and α -DBBF Hb hemoglobins	70
3.2 Kinetic rate constants for myoglobin NO-induced oxidation and myoglobin mutants	77
3.3 Kinetic rate constants for oxygen reactions of <i>L. pectinata</i> hemoglobins and α -DBBF Hb	79
4.1 Oxidative reaction rate constants of <i>L. pectinata</i> hemoglobins compared to α -DBBF Hb. k_{autox} is the rate constant for the spontaneous autoxidation of the hemoglobins at 37°C in the presence or absence of the enzymes SOD and catalase	93
4.2 Kinetic rate constants for the hydrogen peroxide oxidation of <i>L. pectinata</i> complexes monitored at 400 nm	109
4.3 Peroxide-mediated oxidation reactions rate constants of ferric Hb by H ₂ O ₂ measured at 400 nm, and the formation of heme fluorescent products induced by H ₂ O ₂	112
4.4 Proposed heme pocket interactions when HbII is exposed to different pHs	120

5.1	Spectral characteristic of the hemoglobins exposed to endothelial cells with and without glucose oxidase	145
5.2	Endothelial cell morphological changes and media features after treatment with hemoglobins	152
5.3	Endothelial cell morphological changes and media features after treatment with hemoglobins and glucose oxidase.....	153

1 INTRODUCTION

1.1 Motivation

Hospitals need nearly 20 million units of blood daily to be used in surgical procedures and when treating diseases related to chronic anemia. To overcome this necessity, about 11 million units of blood are transfused each year, yet this is still not enough. Furthermore, recent efforts to produce a blood substitute show an increasing trend (Chang, 1997; Chang, 2003; Tinmouth et al., 2008; Rousselot et al., 2006; Alayash, 2004), first because the shelf life of donated blood is only six weeks (Chang, 1997), and second because people do not want blood transfusions to avoid the risk of HIV infection (Tinmouth et al., 2008), hepatitis B and C, urticaria, and hemolytic transfusion infection (Chang 1997). For these reasons, the testing and screening procedures of the donated blood increased to ensure good quality, but also increased the cost of a blood unit from \$130 to \$170 (Becker, 2001). A blood substitute or an hemoglobin-based oxygen carrier (HBOC) needs to fulfill many requirements, not only to be an oxygen carrier, but to have an oxygen affinity to adequately oxygenate the tissues (Dimino et al., 2007; Jia et al., 2004) without the production of oxygen radicals, and must have antioxidant properties and low reaction with nitric oxide (NO) (Kim, 2004; Alayash, 1999).

Under physiological conditions, hemoglobin (Hb) in human beings is inside the red blood cells (RBC) and carries oxygen in the heme-Fe(II) state with oxygen as a ligand (oxy Hb). Oxy hemoglobin spontaneously oxidizes to ferric hemoglobin, a non functional heme-Fe(III) form, which cannot bind oxygen. In this reaction the superoxide anion ($O_2^{\cdot-}$) is formed and can dismutate to hydrogen peroxide (H_2O_2). This reactive oxygen species (ROS)

can react with hemoglobin producing the highly reactive ferryl species, heme-Fe(IV), that leads to heme degradation with cell damage. It has been suggested (Therade-Matharan et al., 2004) that the mitochondrial electron transport system is the major source of ROS. The HbOC's are cell free-hemoglobins that are not toxic to cells or tissues, but can induce toxicity when autoxidizing, thus generating ROS and reactive nitrogen species (RNS). Therefore, the hemoglobin redox chemistry limits the efficacy of the proposed oxygen carriers.

In spite of years of research, the mechanism by which hemoglobin reacts or generates ROS is not completely understood. New studies are focused in finding the mechanism to decrease or eliminate the reactivity of the hemoglobin with oxidants like hydrogen peroxide, and nitric oxide. Table 1.1 shows the adverse effects associated to HBOC's that are under clinical trials, where the vasoconstriction complications and the increase in arterial pressure are the most common effects (Tinmouth et al., 2008). In this respect, the special properties and the arrangement of the amino acids in *Lucina pectinata* heme pocket hemoglobins allow us to study more deeply the redox chemistry, specially the reactions with NO and its behavior in cell culture. The kinetic and structural data presented here suggest that the proximity of the tyrosine B10 and the glutamine E7 to the heme iron in HbII minimizes the exposure of its heme to solvent, thus maintaining oxidative stability and reducing the reactivity toward nitric oxide. Therefore, these studies help to envision new reaction mechanisms that can improve the production of blood substitutes.

Table 1.1 Adverse effects associated to the administration of hemoglobin based oxygen carriers.

Hemoglobin	Adverse effects
Hemopure, Biopure, MA	<ul style="list-style-type: none"> • Vasoconstrictive effect.
HemAssist, Baxter Health Group	<ul style="list-style-type: none"> • Higher mortality in treatment group than in the control group • Hypertension • Severe vasoconstriction complications
Hemolink, Hemosol Inc.	<ul style="list-style-type: none"> • Severe abdominal pain • Increase in mean arterial pressure
Other HBOC's prototypes	<ul style="list-style-type: none"> • Relative short half-life after administration • Renal toxicity • Adverse effects in vascular tone and blood pressure.

Modified after Tinmouth et al., 2008.

1.2 Human hemoglobin physiology

Human hemoglobin is the oxygen carrier protein of the RBC with an approximate concentration of 2 mM (Alayash, 1999). Mammalian hemoglobins have molecular weights of about 64,500 Daltons. Figure 1.1 shows the human hemoglobin crystal structure, consisting of a tetramer of two alpha (α) subunits and two beta (β) subunits called globins each of which is bound to a heme. The heme group is the name for the prosthetic group with an iron in the central pocket (Figure 1.2). This iron atom can be either in the ferric (heme-Fe(III)) or ferrous (heme-Fe(II)) form. The heme moiety has a molecular weight of 616.48 Daltons and gives blood its characteristic red color. The iron has octahedral

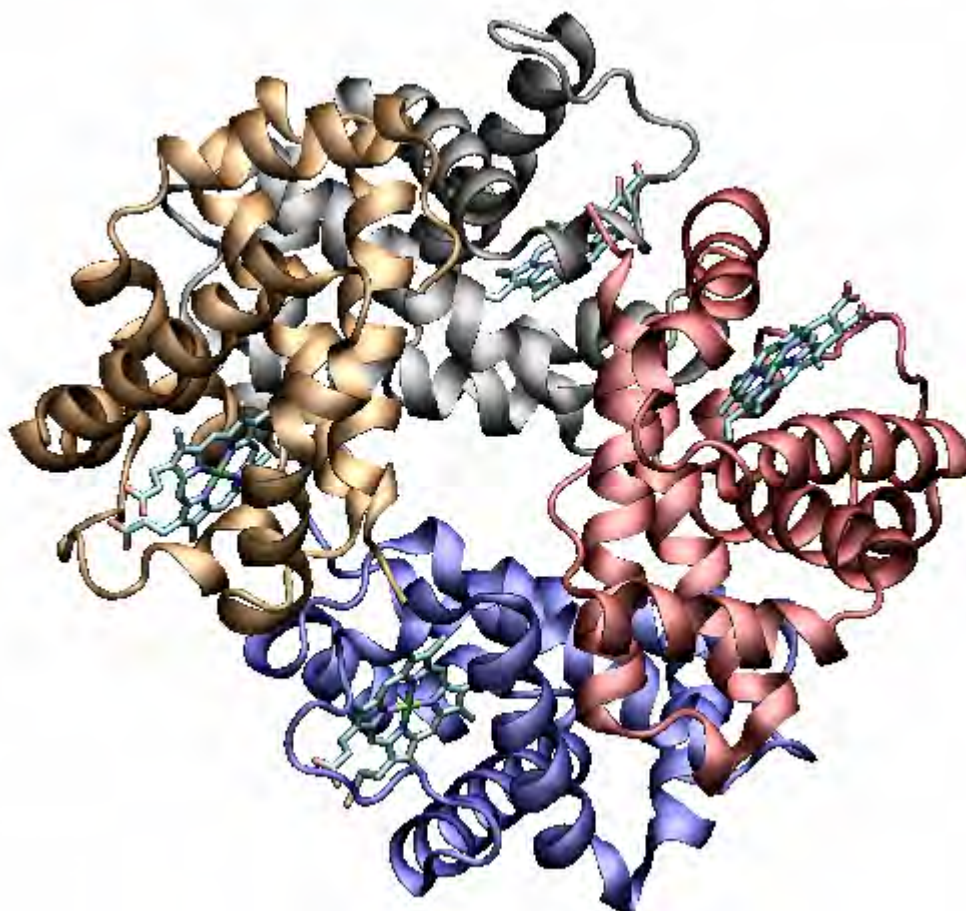


Figure 1.1 Human hemoglobin crystallographic structure. PDB: 1GZX. The hemoglobin consists of two alfa and two beta chains (ribbons red, blue, gray and gold), each one containing a heme prosthetic group (cyan).

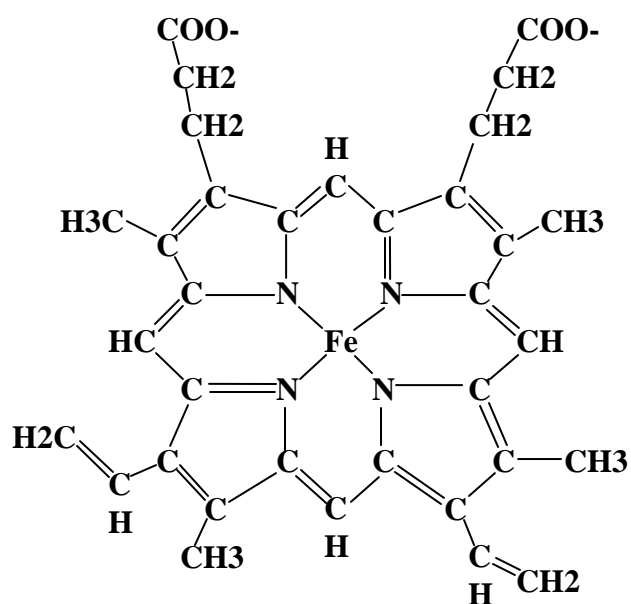


Figure 1.2 The heme group (Fe-protoporphyrin IX). The iron has six coordination sites: four are bonded to the pyrrole rings, another to an imidazole nitrogen of a histidine proximal residue and the sixth coordination position is available for binding with oxygen and other small molecules.

coordination geometry with six binding sites. It is coordinated to four pyrrole nitrogens, as electron-pair donors of protoporphyrin IX, and to an imidazole nitrogen of a histidine proximal residue from the globin side of the porphyrin that is invariant in all known hemoglobins. The sixth coordination position is used for binding oxygen and other small molecules. Vertebrate hemoglobins and myoglobins, with the exception of elephant Mb, have His and Leu at the distal positions E7 and B10 respectively, with the distal His able in some cases to hydrogen bond with the bound O₂, thus stabilizing the oxygenated structure. In many non-vertebrate globins, the HisE7 and LeuB10 residues are replaced by Gln and Tyr, respectively, resulting in a tight cage for O₂ and much higher O₂ binding affinities relative to vertebrate myoglobin (Weber & Vinogradov, 2001).

Tetrameric hemoglobins, stabilized by the RBC's, bind four oxygen molecules, one per heme, in the lungs, generally with a cooperative mechanism, releasing the diatomic ligand into the peripheral organs and tissues to support respiration. Such a mechanism, which may be modulated by allosteric effectors, is based on concerted tertiary and quaternary conformational changes, coupled to oxygen binding (Bolognesi et al., 1999). In this respect, the hemoglobin structure is known for both its deoxygenated state when it has no oxygen, and its oxygenated form when carries a full load of four oxygen atoms. The heme group is nonplanar when it is not bound to oxygen; the iron atom is pulled out of the plane of the porphyrin, toward the proximal histidine residue to which it is attached and the molecule is then in the tense or T-state (Figure 1.3, left). This nonplanar configuration is characteristic of the deoxygenated heme group and it is commonly referred to as a dome shape. The valence electrons in the atoms surrounding the iron in the heme group and the valence electrons in the histidine residue form clouds of electron density. However, when the iron in the heme group

binds to an oxygen molecule, the porphyrin ring adopts a planar configuration and hence the iron lies in the plane of the porphyrin ring (Figure 1.3, right), and the hemoglobin is in the relaxed or R-state. When the iron atom moves into the porphyrin plane upon oxygenation, the proximal histidine is drawn closer to the heme group. This movement of the histidine residue then shifts the position of other amino acids that are near the histidine. When the amino acids in a protein are shifted in this manner (by the oxygenation of one of the heme groups in the protein), the structure of the interfaces between the four subunits is altered. Hence, when a single heme group in the hemoglobin protein becomes oxygenated, the whole protein changes its shape. In the new shape, it is easier for the other three-heme groups to become oxygenated. Thus, the binding of one molecule of O_2 to hemoglobin enhances the ability of hemoglobin to bind more O_2 molecules with a Hill coefficient (n) of 2.8. This property of hemoglobin is known as cooperative binding and allows the hemoglobin to deliver 1.83 times more oxygen (Chang, 1997). When the oxygen is displaced by carbon monoxide the hemoglobin is called carboxy hemoglobin (HbCO). When the iron in hemoglobin is oxidized from the oxy to the ferric state, the compound is called ferric hemoglobin or met hemoglobin and it is accompanied by a loss of oxygen-binding capacity. The cover of hydrophobic groups of the globin prevents the autoxidation.

1.2.1 pH and CO_2 activity in human hemoglobin

The conformational change between the deoxy and the oxy states is a function of the presence of 2,3-diphosphoglycerate (2,3-DPG) produced by the RBC. The 2,3-DPG facilitates the release of oxygen when the tissue oxygen tension is approximately 26 mmHg.

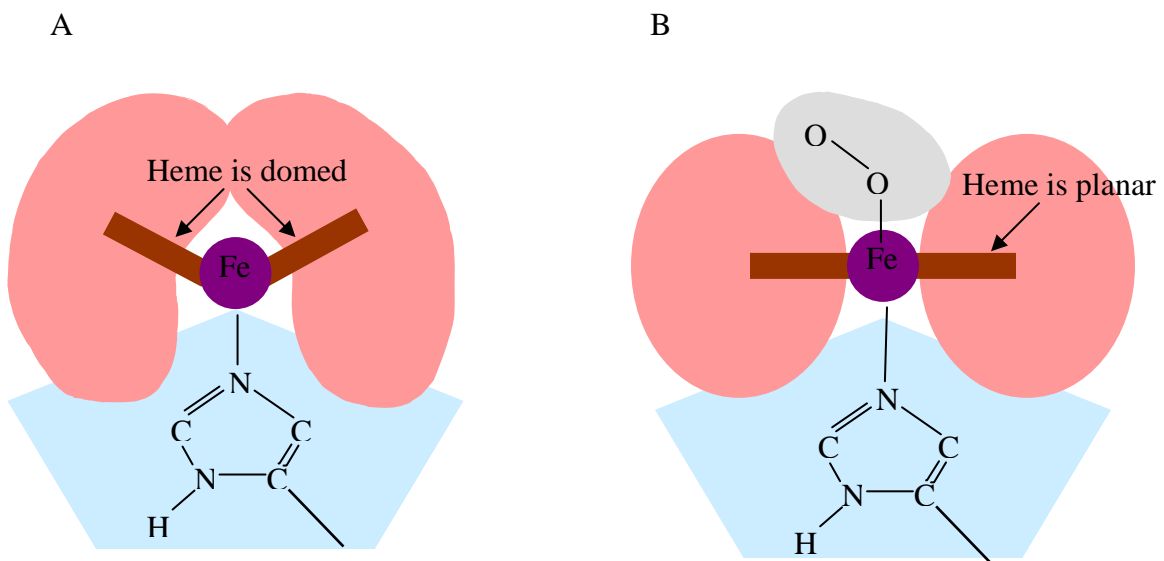
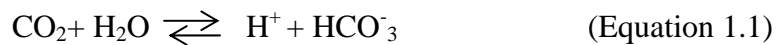


Figure 1.3 Hemoglobin in both: the oxy and deoxy state. In the deoxy state (A), the protoporphyrin is out of the plane in a T-state. When the molecule is oxygenated (B), it is in the R-state.

When the hemoglobin is outside the red blood cells, the 2,3-DPG is not available, thus increasing the affinity for the oxygen. Another factor that affects the oxygen binding is the pH. If the blood pH is lower than the normal physiological pH of 7.4, the ability of hemoglobin to bind oxygen decreases. The oxygen dissociation curve of hemoglobin shows that the oxygen partial pressure at 50% saturation (P_{50}) is 26 mmHg. As blood circulates from arterial to venous, the dissociation curve shifts to the right because the carbon dioxide (CO_2) concentration increases. This facilitates the dumping of O_2 at the tissue level, thus decreasing the affinity for O_2 . If the tissue uses more oxygen, the amount of oxygen ($p\text{O}_2$) is lower. In this case, more oxygen is delivered to the tissue. Another indicator that a tissue has a high metabolic rate and a need for increased oxygen delivery, is the production of CO_2 . Studies indicate that CO_2 binds the two chains of the hemoglobin at the N-terminal valine (Manning, 1995). When a tissue is more active, the amount of carbon dioxide produced is increased and the $p\text{CO}_2$ is higher. Equation 1.1 shows the reaction of CO_2 with water, which under normal equilibrium produces carbonic acid. This reaction indicates that as the amount of CO_2 increases, more hydrogen ions are formed and as a result the pH will decrease.



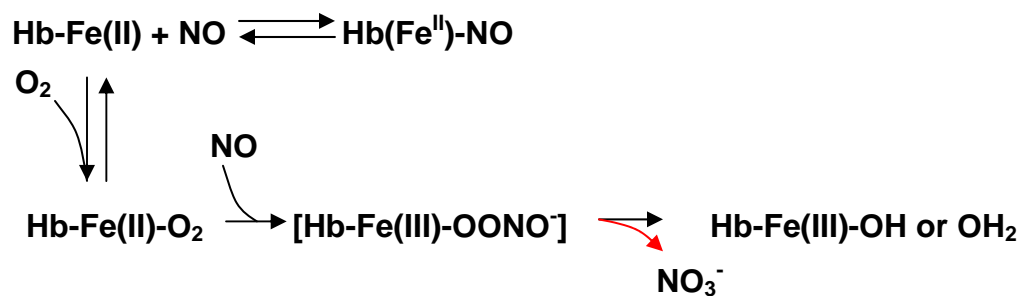
Thus, lower pH in the blood suggests an increase of carbon dioxide concentration, which in turn implies a more active tissue that requires more oxygen. The Bohr effect aids in this function by releasing oxygen to the tissues when the concentration of hydrogen ions becomes large. At low pH the Bohr effect allows the blood to unload oxygen usage by the muscles.

1.2.2 Nitric oxide and peroxynitrite formation in human hemoglobin

Nitric oxide (NO), a diatomic free radical, is the endothelium-derived relaxing factor that acts as a signaling molecule in the tissues regulating many physiological processes. In the endothelium, NO is produced by the endothelial nitric oxide synthase (NOS) with a half-life of 5 seconds or less, and concentrations from 0.01 to 1 μM (Ignarro et al., 1993). Previous studies suggest that nitric oxide regulates the calcium channels and the calcium entry in vascular smooth muscle. In this respect, the decrease in the NO biological activity is attributed to vascular diseases, as for example hypertension (Cohen, 1999). Moreover, it was suggested a protective role for NO during inflammation, through the inactivation of NADPH oxidase and the consequent inhibition of the superoxide ion ($\text{O}_2^{\cdot-}$) (Ródenas et al., 1998). Thus, the superoxide dismutase (SOD), catalases and the antioxidant function of NO suppresses the formation of ROS and RNS that leads to cell-mediated injury. Other studies suggested that in the vasculature, between the smooth muscle and the endothelial cells, the NO has a higher concentration than $\text{O}_2^{\cdot-}$ (Alayash, 1999). In cases of non-physiological conditions, in trauma or in cell stress, the NO is consumed in the tissues in a rapid reaction which produces $\text{O}_2^{\cdot-}$. Therefore, increases the superoxide ion concentration and as a consequence, increases the formation of H_2O_2 and peroxynitrite ($\text{ONOO}^{\cdot-}$), which are also highly toxic. Moreover, several peroxidases function as catalytic sink consuming NO in the presence of hydrogen peroxide affecting NO biological activity (Abu-Soud & Hazen, 2000).

The hemoglobin in the red blood cell also scavenges NO, and two mechanisms are suggested for the reaction (Privalle et al., 2000, Chen et al., 2008). Figure 1.4 A shows the

A.



B.

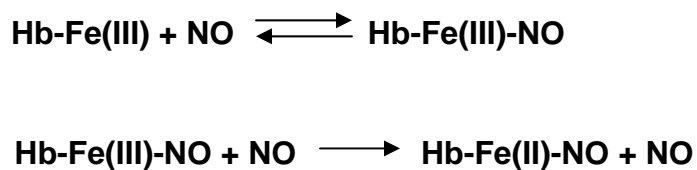


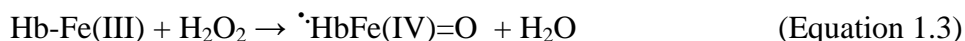
Figure 1.4 Mechanisms of nitric oxide binding to hemoglobin. The reaction of deoxy Hb with NO forms the complex Hb-NO, while the reaction with oxy Hb and NO oxidizes the hemoglobin and forms the peroxynitrite compound (A). The reaction of nitric oxide binding to ferric hemoglobin forms the ferric Hb-NO complex (B) (Privalle et al., 2000).

reaction of NO with deoxy hemoglobin producing the Hb-NO complex. In the equilibrium reaction between oxy and deoxy hemoglobin, the NO dioxygenase activity of oxy Hb has been suggested to scavenge the excess of NO (Privalle et al., 2000). The oxy Hb can be autoxidized when the NO enters the heme pocket and reacts with the bound oxygen forming Hb-Fe(III)-ONOO⁻, the peroxynitrite complex, which then isomerizes to NO₃⁻ and ferric Hb. Previous observations indicate that the first decomposition product of NO in aqueous solution is nitrite, and that further oxidation to nitrate requires the presence of the oxidizing species oxy hemoglobin (Ignarro et al., 1993). Figure 1.4B shows the reaction of ferric Hb with NO producing the Hb-Fe(III)-NO complex. When the physiology concentration of NO is disturbed, leading to an excess, the NO molecule can react with the Hb-Fe(III)-NO complex to produce an Hb-Fe(II)-NO complex. Subsequent reactions also lead to the formation of ONOO⁻. This reaction is thought to be the major route of NO destruction *in vivo* (Alayash et al., 1998). It induces the formation of tyrosyl radicals in the oxy hemoglobin of RBC and nitrate tyrosine residues damaging and destabilizing the protein (Alayash et al., 1998; D'Agnillo et al., 2000).

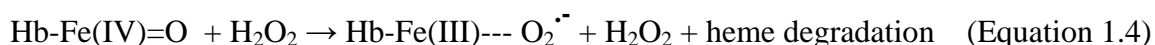
1.2.3 Human hemoglobin oxidation and denaturation

Inside the red blood cells, hemoglobin autoxidizes from oxy Hb to ferric Hb, and produces a non-functional protein. The mechanism of autoxidation involves the production of O₂^{•-} and H₂O₂. Figure 1.5 shows that O₂^{•-} can be formed by the transfer of one electron from the oxy heme to bound O₂. Moreover, in the cell-leakage of electrons from the electron transport chain, the oxygen molecule produces the superoxide anion, which in turn can dismutate to H₂O₂ (Ho, 1995). This ROS oxidizes Hb, both in the heme-Fe(II) or in the

heme-Fe(III) forms, producing the ferryl heme-Fe(IV) species (King & Winfield, 1963; Nagababu & Rifkind, 2004). Equation 1.2 shows the formation of the ferryl compound II in the two equivalent oxidative reactions of oxy heme with H₂O₂. In Equation 1.3, the second electron is taken from the heme, producing a protein radical, compound I (Alayash, 2004). Under normal conditions, in which there are no H₂O₂ excess, the heme center is reduced back to ferric Hb.



The ferryl species are very cytotoxic and lead to heme degradation and cell damage (Trent & Hargrove, 2002; Nagababu et al., 2002). In this cyclic reaction (Figure 1.5), the hemoglobin can act as a pseudoperoxidase, thus protecting the cells from the H₂O₂ toxicity (D'Agnillo & Alayash, 2002; Chang, 2004). At very high concentrations of H₂O₂, the hemoglobin can further react with the remaining H₂O₂ reducing the ferryl species (Equation 1.4). This reaction leads to the formation of different degradation products and promotes hemolysis, lipid peroxidation and interprotein cross-linking (Nagababu & Rifkind 2004; Fridovich, 1995).



Sometimes the binding of the distal His to the iron changes the structure conformation inducing the formation of ferric Hb from the ferryl or from the hemichrome species. If this reaction and conformational change does not take place, the hemichrome formation is irreversible and the protoporphyrin loses the iron. As a natural mechanism, other plasma

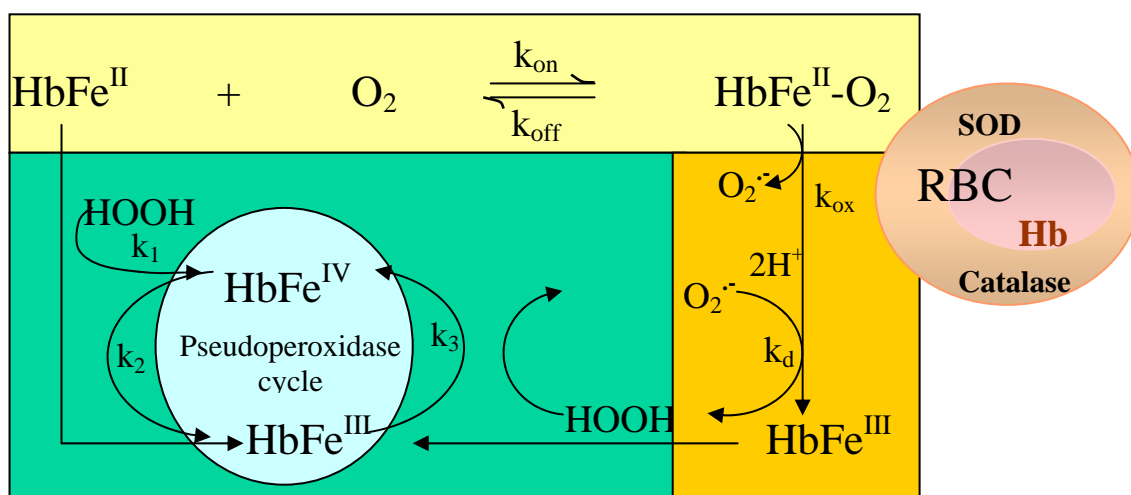


Figure 1.5 Schematic representation of hemoglobin autoxidation and formation of reactive oxygen species. Oxy Hb autoxidizes producing the superoxide ion, which dismutates to hydrogen peroxide. The oxy Hb or ferric Hb consumes the hydrogen peroxide in a pseudoperoxidative cycle, forming the ferryl compounds. The presence of superoxide dismutase and catalase in the red blood cell controls these oxidation reactions converting the superoxide ion to oxygen and water (Modified from Alayash, 1999).

proteins remove the breakdown products during this reaction. For example, ferric Hb reductase reduces the hemoglobin back to oxy Hb, and the enzyme SOD converts $O_2^{\cdot-}$ to H_2O_2 , which is eliminated by glutathione peroxidase (Privalle et al., 2000). The hemichrome species is a low spin hexacoordinated heme with an endogeneous ligand coordinated to the sixth position of the heme. Hemichrome species are function of the temperature, pH, and the structure of the globin chains, and can be detected by spectral bands at 530 nm and 565 nm with an increase in the baseline (Vitaglianai et al., 2004; Sugawara et al., 2003). Moreover, during physiological imbalance, the NO reacts with $O_2^{\cdot-}$ producing $ONOO^{\cdot-}$. The $ONOO^{\cdot-}$ causes the oxidation of the Hb to ferric and ferryl species, and can also induce the nitration of tyrosine residues (Alayash, 1999). This change also weakens the interaction between the heme and the hemoglobin, and as a result, the heme can dissociate to produce an apohemoglobin that is insoluble at physiological pH.

1.3 Blood substitutes

In the last two decades the efforts to produce a blood substitute have increased, because safe alternatives for blood transfusions are needed to avoid the risk of infection with HIV and other blood borne pathogens (Herold & Rock, 2003; Burmester et al., 2000). The possible lack of supplies after a serious accident or in cases of anemia has also motivated the search for blood substitutes (Tinmouth et al., 2008; Therade-Matharan et al., 2004). These are liquid substances prepared from hemoglobin or perfluorocarbon solutions that when injected into the human blood stream, contribute significantly to the transport of oxygen in the body. Other names used to refer to a blood substitute are cell-free oxygen carrier, red cell substitutes, oxygen therapeutics, and hemoglobin-based oxygen carriers HBOCs. Table 1.2

shows the advantages of producing a blood substitute (Tinmouth et al., 2008; Euro Blood Substitutes, 2008).

Current designs of HBOC products are made of modified stroma-free Hb from human, animal, or recombinant origin (Becker, 2001). Examples that reach the level of Phase III in clinical trials are HemolinkTM (O-raffinose-polymerized human Hb), HemopureTM (Polymerised bovine Hb), α -DBBF-Hb (diaspirin cross-linked human Hb), PolyHbBv (glutaraldehyde-polymerized bovine Hb), HemospanTM (Conjugated human Hb), and OptroTM (Cross-linked Hb from genetically modified *E. coli* bacteria). Some of them present side effects such as adverse cardiac events, tissue damage, coagulation changes, and others (Trent and Hargrove, 2002; Euro Blood Substitutes, 2008). Currently, the Food and Drug Administration (FDA) is performing clinical studies with diaspirin cross-linked human hemoglobin (α -DBBF Hb). The α -DBBF hemoglobin is an intramolecularly cross linked tetramer produced via chemical reaction with bis(3,5- dibromosalicyl) fumarate. Also, invertebrate hemoglobins show to be a potential alternative as hemoglobin-based oxygen carriers. For example, European researchers are producing a blood substitute using the *Lumbricus terrestris*, commonly known as earth worm, and the *Arenicola marina*, a marine worm (Rousselot et al., 2006; Euro Blood Substitutes, 2008; Hemarina, 2008).

The overall panorama shows that the production of a good hemoglobin-based oxygen carrier has to meet many requirements, not only to be a good oxygen carrier. One problem that is still unsolved in this field is the oxidative stress. Studies demonstrate that cell free-Hb could turn out to be a toxic substance by autoxidizing and generating ROS, or can be oxidized by its interaction with the ROS (Estep et al., 2008). The oxidative stress can cause

Table 1.2 Advantages and necessities of the production of a blood substitute.

Compatibility	<ul style="list-style-type: none">• Universal compatibility.• Can be transfused to a human of any blood type without any tests.
Safety	<ul style="list-style-type: none">• No necessity to make any tests for risk of infection.• Easy to sterilize.
Purity and Non-toxicity	<ul style="list-style-type: none">• Composed of pure compounds.• Free of infectious agents and allergens.• Non-toxic and disease-free product.• Free of any side effects.
Physiological function	<ul style="list-style-type: none">• Adequate oxygen uptake in the lungs.• Adequate oxygen delivery to the tissues.• Long circulation time.
Storability/Shelf Life	<ul style="list-style-type: none">• Long storage life.• Ideally will not need refrigeration.
Availability	<ul style="list-style-type: none">• Composed of readily and reliably available materials.
Predictability	<ul style="list-style-type: none">• Made up of reactants that are completely understood.
Reduce Cost	<ul style="list-style-type: none">• Cheap to manufacture.

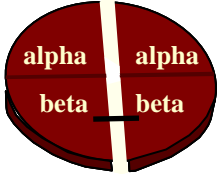
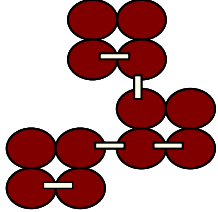
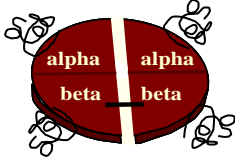
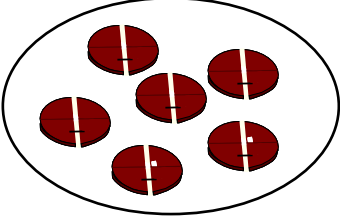
Tinmouth et al., 2008; Euro Blood Substitutes, 2008.

growth stimulation, arrest or adaptation, apoptosis or necrosis, depending on the duration and on its strength. Also, modified hemoglobin solutions can be toxic to the human system causing vasoconstriction (Chang, 2004). Therefore, the ideal oxygen carrier needs to induce few oxygen radicals and have antioxidant properties. For instance, it should have low autoxidation rates and low reaction with NO (Joyner et al., 2003).

1.3.1 Effects of the hemoglobin outside the red blood cells; cell free-hemoglobins

The first problem of the hemoglobin outside the RBC is that the infused hemoglobin loses up to 40% its capacity to carry oxygen (Chang, 1997). Another problem is the tetramer dissociation into dimers or monomers, in which the dissociated chains are filtered through the kidneys injuring the kidney tubules. Also, once the hemoglobin is dissociated, the iron can be lost faster from the dimer than from a tetramer. This problem is assisted using structural modifications of the molecule (Table 1.3), for example with genetic recombinant expression techniques, crosslinking, and by the encapsulation of the hemoglobin in liposomes or nanoparticles (Chang, 1997; Becker, 2001; Privalle et al., 2000; Mackenzie, 2005; Zhang et al., 2008; Sakai et al., 2008). Moreover, out of the cell the hemoglobin loses its interaction with 2, 3-DPG and therefore, increases the oxygen affinity inhibiting the cooperativity and the oxygen off loading to the tissues (Chang, 1997). Table 1.4 shows the kinetic rate constants for stroma free human hemoglobin, HbA₀ and α -DBBF Hb oxygenation and autoxidation. Another important feature is that without the reductases and peroxidases and other antioxidants produced in the RBC (Alayash, 1999), the hemoglobin autoxidation occurs at a bigger rate producing ferric Hb, H₂O₂, and O₂^{•-}. There are two

Table 1.3 Hemoglobin structural modifications to maintain the tetramer structure

Intramolecularly cross-linked hemoglobin	<ul style="list-style-type: none"> Intramolecular cross-link between the two alphas or the two beta sub units. 	 <p>A diagram of a single hemoglobin molecule, represented as a red circle divided vertically. The left half is labeled 'alpha' and the right half is labeled 'alpha'. A horizontal line connects the two 'alpha' halves, indicating a cross-link between them. The bottom half is labeled 'beta'.</p>
Polymerized hemoglobin	<ul style="list-style-type: none"> The formation of fumarate bridges between alpha molecules can result in oligomers or polymers of hemoglobin. 	 <p>A diagram showing a chain of four hemoglobin molecules. Each molecule is a red circle with 'alpha' and 'beta' labels. They are connected by horizontal lines, representing fumarate bridges between alpha subunits of adjacent molecules.</p>
Conjugated hemoglobin	<ul style="list-style-type: none"> The linkage of free hemoglobin molecules to a soluble non-hemoglobin polymer 	 <p>A diagram of a hemoglobin molecule (red circle with 'alpha' and 'beta' labels) connected by a wavy line to a larger, more complex wavy line representing a polymer chain.</p>
Microsphere hemoglobin	<ul style="list-style-type: none"> Hemoglobin molecules are exposed to a high intensity ultrasound, which creates 'shells' of approximately one million hemoglobin molecules cross-linked by the superoxides formed during the sonication process. 	<p>Liposome</p>  <p>A diagram of a liposome, which is a large oval structure. Inside the oval, there are several smaller red circles, each representing a hemoglobin molecule with 'alpha' and 'beta' labels.</p>
Liposome-encapsulation of hemoglobin	<ul style="list-style-type: none"> Phospholipid bilayer, with molecules of cholesterol added for increased rigidity and mechanical stability. This liposome then encloses a stroma free hemoglobin solution and 2,3 DPG or inositol hexaphosphate as a gelatinous fluid. 	

Modified from Alayash, 1999 & Chang, 2003.

Table 1.4 Kinetic oxygenation and autoxidation characteristics of HbA₀ and α -DBBF human hemoglobins.

Hemoglobin	P ₅₀ (mmHg)	k _{off, O₂} (s ⁻¹)	k _{autox} (h ⁻¹)	k _{autox} SOD/catalase (h ⁻¹)
HbA ₀	14 ^a	33.3 ^a	0.018 ^a	0.009 ^a
α -DBBF Hb	32 ^b	56.0 ^c	0.09 ^d	0.05 ^d

^a Jia et al., 2004.

^b Nagababu et al., 2002.

^c Cashon et al., 1995.

theories that account for the side effects that the infused cell free-hemoglobins show in clinical trials (Tinmouth et al., 2008). The first one is shown in Figure 1.6B, where the Hb (red circles) flowing through or near the endothelial cells can react with NO, disturbing the NO balance. This causes the smooth muscle cells to contract, leading to vasoconstriction. Figure 1.6A shows the production of NO under physiological conditions and in presence of the red blood cells. The NO scavenging capacity for cell-free Hb is 500 fold higher than the capacity of the Hb in the RBC (Kim, 2004). From this NO balance disruption, an excess of ONOO⁻, H₂O₂, and O₂⁻ is produced, thus causing oxidative stress (Yeh & Alayash, 2003). Table 1.5 shows the kinetic rate constants for the reaction of HbA₀ and α -DBBF Hb with hydrogen peroxide and nitric oxide. At high concentrations of cell-free Hb, the NO is scavenged, releasing endothelin and producing a vasopressor effect (Chang, 1997). A second

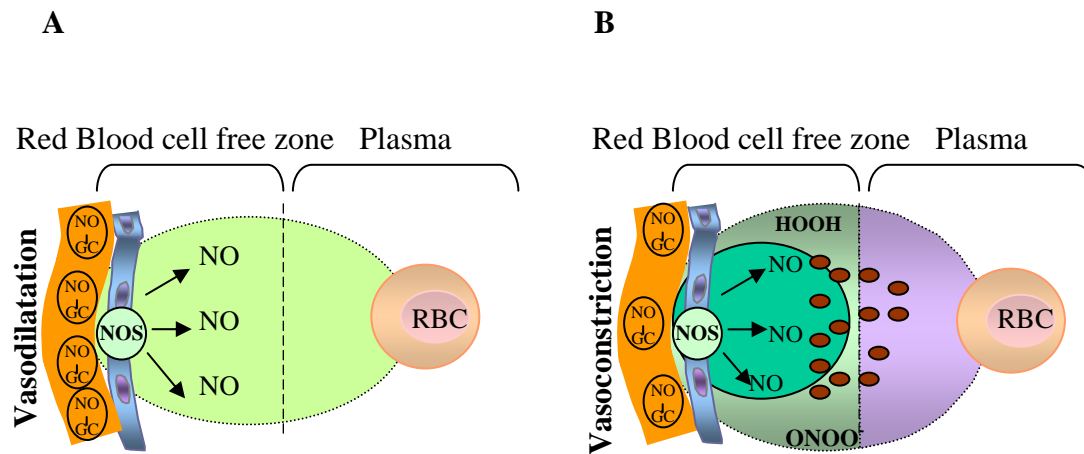


Figure 1.6 Schematic representation of NO production in presence of hemoglobin inside the red blood cells (A). (B) Hemoglobin outside the red blood cells scavenges NO leading to the production of ROS. Model adapted from Dou et al., 2002 & Alayash, 2004.

Table 1.5 Kinetic rate constants for the reaction of HbA₀ and α -DBBF Hb with hydrogen peroxide and nitric oxide

Hemoglobin	$k_{\text{ox, NO}}$ ($\mu\text{M}^{-1}\text{s}^{-1}$)	$k_{\text{H}_2\text{O}_2}$ ($\text{M}^{-1}\text{s}^{-1}$)	$k_{\text{Heme degradation}}$ ($\text{M}^{-1}\text{s}^{-1}$)
HbA ₀	$18.8 \pm 1.2^{\text{a}}$	$8.8 \pm 2.3^{\text{a}}$	$5.2 \pm 0.4^{\text{a}}$
α -DBBF Hb	$19.0 \pm 1.4^{\text{b}}$	$120.5 \pm 5.6^{\text{b}}$	$8.0 \pm 1.6^{\text{a}}$

^a Jia et al., 2004.

^b De Jesús-Bonilla et al., 2007

group of scientists did not observe any correlation between vasoconstriction and NO scavenging. Their studies suggested that the clue piece in the clinical side effects is the oxygen affinity. The cells free hemoglobin needs to have an oxygen affinity higher than usual, so in this manner decrease vasoconstriction (Alayash, 2004, Rohlf et al., 1998; Martin et al., 1986).

1.3.2 Effects of hemoglobins on endothelial cells

The endothelial cells (EC) are capable of producing internally or externally ROS. As a result, they can cause different forms of oxidative stress leading to tissue injury to the endothelium, cell death, and functional abnormality. The cytotoxic effects of intracellular H₂O₂ can affect signaling pathways (physiological events) in EC, for example, apoptosis.

The extracellular oxidative stress in the endothelium can be studied by the direct exposure of cell cultured endothelial cells to H_2O_2 , glucose oxidase (GOX), xanthine oxidase, activated leukocytes, or by using physiological inducers like hypoxia. The reaction of xanthine oxidase produces O_2^- and H_2O_2 , while the reaction with GOX generates glucose, H_2O_2 , and uric acid, which is a weak antioxidant. The use of xanthine oxidase or radio-labeled GOX helps in the quantization of the ROS delivered to the cultured cells (Gow et al., 1999). The endothelial cells are exposed to cell-free Hb, and therefore they are susceptible to the cytotoxic side effects produced by the oxidation of oxy Hb (Privalle et al., 2000). For endothelial cell cultured studies, GOX produces an appropriate flux of H_2O_2 (3-4 μM), which mimics the H_2O_2 production *in vivo*. Previous studies show that when Mb or α -DBBF Hb is added to the cell system, the apoptosis is reduced or inhibited due to a rapid elimination of the H_2O_2 (D'Agnillo & Alayash, 2002) by the hemoglobin. This redox cycle of hemoglobin consuming the H_2O_2 produced by GOX damage the cells causing apoptosis (D'Agnillo & Alayash, 2002; D'Agnillo & Alayash, 2001). Therefore, it was suggested that the hydroxyl radical formed when the heme is lost, or the formation of the ferryl species in the oxidation of hemoglobin can play an important role in DNA damage and apoptosis of the cells (D'Agnillo & Alayash, 2001).

During the apoptotic process the cell morphology changes, for example, chromatin condensation, the nucleolus disintegrates, and the nucleus shrinks. Moreover, the total volume of the cell is reduced, the cell shrinks and is denser, the cytoplasmic organelles condensed and the endoplasmic reticulum dilated. Thereafter, the nucleus and the cytoplasm fragments in small corpuscles with membrane named apoptotic bodies. As part of the process, endonucleases are activated and cut the genomic DNA in fragments of 180-200 pb.

There is also a loss in the mitochondrial potential and in the plasmatic membrane where the phosphatidylserine residues, which normally are faced to the inner of the cellular membrane, are also faced to the exterior. The activation of the caspases is fundamental in the apoptosis cellular death process. The caspases that are activated in response to stress or cellular damage are caspases-8, -9, -10 and 12. The caspase-3 is an effector's caspase, and is responsible for the chromatin condensation, DNA fragmentation and formation of apoptotic bodies.

The cells under hypoxic conditions also generate ROS, which lead to cell apoptosis and tissue damage. The hypoxia inducible factor-1 α (HIF-1 α) is expressed in the endothelial cells, and is a transcription factor that regulates adaptative responses to the lack of oxygen in mammalian cells. It consists of two proteins, HIF-1 α and HIF-1 β . Figure 1.7 shows the process for HIF-1 α degradation under normoxic conditions (Sharp et al., 2004; Kvietikova et al., 1995). An adequate oxygen supply and in the presence of oxyglutarate, the HIF-1 α hydroxylase is activated and hydroxylates two HIF-1 α proline residues. The conformational change in HIF-1 α allows the binding of the von Hippel-Lindau protein (pVHL), and subsequently, the binding of a complex formed by elongin C (eC), elongin B (eB), Rbx and Cul2, which acts as an E3 ubiquitin ligase, degrading the HIF-1 α . HIF-1 α accumulates under hypoxic conditions and is an important mediator of the hypoxic response of tumor cells and controls the up-regulation of a number of factors important for solid tumor expansion including the vascular endothelial growth factor (VEGF). Figure 1.8 depicts the mechanism under normoxia that inhibits the production of HIF target genes. In the process, the HIF-asparagine hydroxylase hydroxylates the HIF-1 α asparagine 803 residue preventing the binding of p300 in the HIF-1 α /HIF-1 β complex, consequently, preventing the activation of

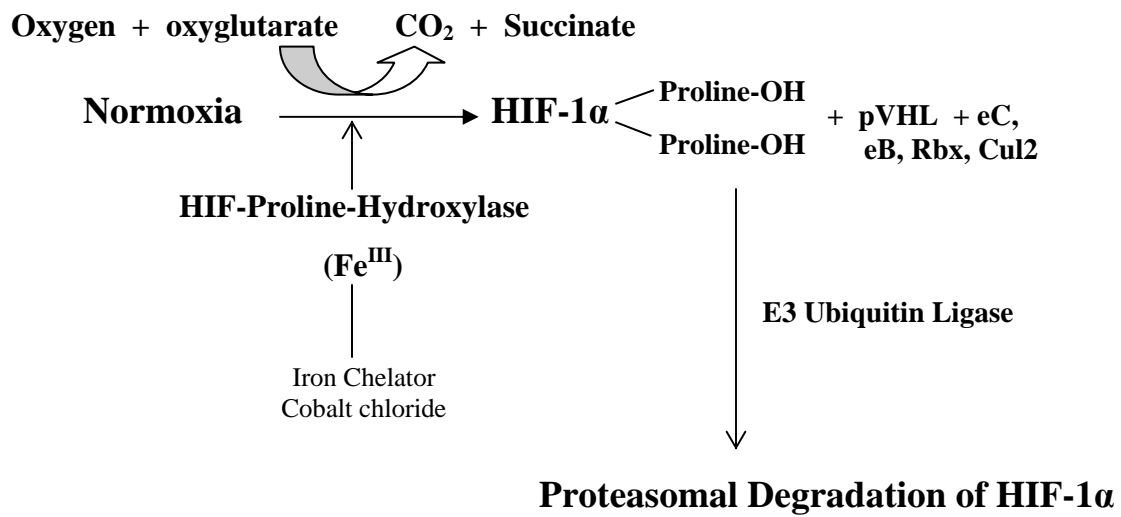


Figure 1.7 Mechanism for HIF-1 α degradation under normoxic conditions via the activation of HIF-1 α proline hydroxylase (Sharp et al., 2004).

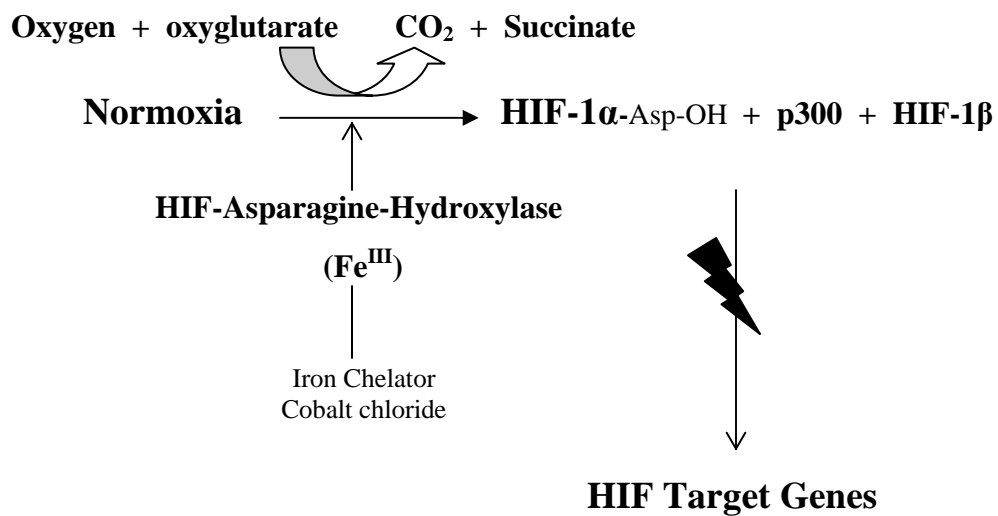


Figure 1.8 Mechanism for the inhibition of the HIF-1 α target genes under normoxic conditions via the activation of HIF-1 α asparagine hydroxylase (Sharp et al., 2004).

the HIF-1 α target genes. Independently of the mechanism, during hypoxic conditions the HIF-1 α hydroxylases are inhibited allowing the expression of the HIF-1 α protein. Therefore, during hypoxic conditions, HIF-1 α expression can be used to monitor the oxidative reactions and O₂ transport properties (Scharte et al., 2003).

In addition, the expression of HIF-1 α is activated when the levels of O₂^{•-} are decreased. The O₂^{•-} can be produced by the cells, and can act on them or in nearby cells to activate or inhibit a signal. That is why it is considered a cell-signaling molecule (Yeh & Alayash, 2004). The decrease in HIF-1 α expression can be explained as a result of different mechanisms, for example of a low O₂ delivery by the hemoglobin, the hemoglobin turnover consuming the radical, or that the O₂^{•-} is being dismutated to H₂O₂ in the mitochondria (Buehler & Alayash, 2004). Other experiments done showed that the addition of superoxide dismutase (SOD) to the samples decreases the O₂^{•-} levels during hypoxia. These experiments indicate that the ROS and NO balance are altered when α -DBBF Hb is added to the cell environment. The modulation of the HIF-1 α expression by NO suggests that the reaction of NO with O₂^{•-} is a mechanism of cell signaling (Yeh & Alayash, 2004).

1.4 *Lucina pectinata* hemoglobins

Symbiotic systems between mollusks and intracellular chemoautotrophic bacteria are characterized by the presence of hemoglobins located in the cytoplasm of the bacteriocyte gill cells, which are specialized to house symbiotic bacteria. The main biological function of these hemoglobins is related to the transport of oxygen and other compounds from the external environment to the symbiotic bacteria. The bivalve mollusk *Lucina pectinata* is a

clam that inhabits the sulfide-rich coastal sediments of tropical shallow embayments, houses a dense population of chemoautotrophic symbiotic bacteria, which employ the energy coming from the oxidation of the environmental hydrogen sulfide to fix carbon dioxide into hexoses, which are the only source of carbon for the mollusk (Read, 1965; Wittenberg & Wittenberg, 1990; Wittenberg & Kraus, 1991; Kraus & Wittenberg, 1990). *L. pectinata* uses three hemoglobins to supply the O₂ and H₂S to the bacteria. The first hemoglobin isolated using size exclusion chromatography is HbI (14,443 Daltons). Figure 1.9 shows the HbI X-Ray crystallography structure (Rizzi et al., 1994). HbI is a monomer at all concentrations and binds hydrogen sulfide in the presence of oxygen, to yield the ferric heme-sulfide adduct (Kraus & Wittenberg, 1990; Kraus et al., 1990). The other two hemoglobins are hemoglobin II (HbII) and hemoglobin III (HbIII) (16,128 and 17,762 Daltons, respectively). HbII and HbIII are oxygen reactive hemoglobins, and exist as monomers at low concentrations. Recently, the HbII crystal structure (Figure 1.10) was resolved showing to be a homodimer at concentration ~ 1-2 mM (Gavira et al., 2006; Gavira et al., 2008) with a heme pocket more collapsed than HbI. At high concentrations (~4mM) HbII tends to form oligomers of more than 4 subunits, and HbIII tends to form a dimer (~1mM). A mixture of HbII/HbIII of ~6mM exhibits self-association and can form a non-interactive heterotetramer (Kraus & Wittenberg, 1990). It has been suggested that HbI is used to transport the sulfide to the bacteria while HbII and HbIII provide oxygen to the gills and to the bacterial symbionts (Rizzi et al., 1996).

The amino acid sequence and crystallography data show that the proximal ligand is histidine (Rizzi et al., 1994; Gavira et al., 2008; Antommatei et al., 1999; Torres et al., 2003), as in other hemoglobins. But in the heme cavity, this clam has an unusual collection of

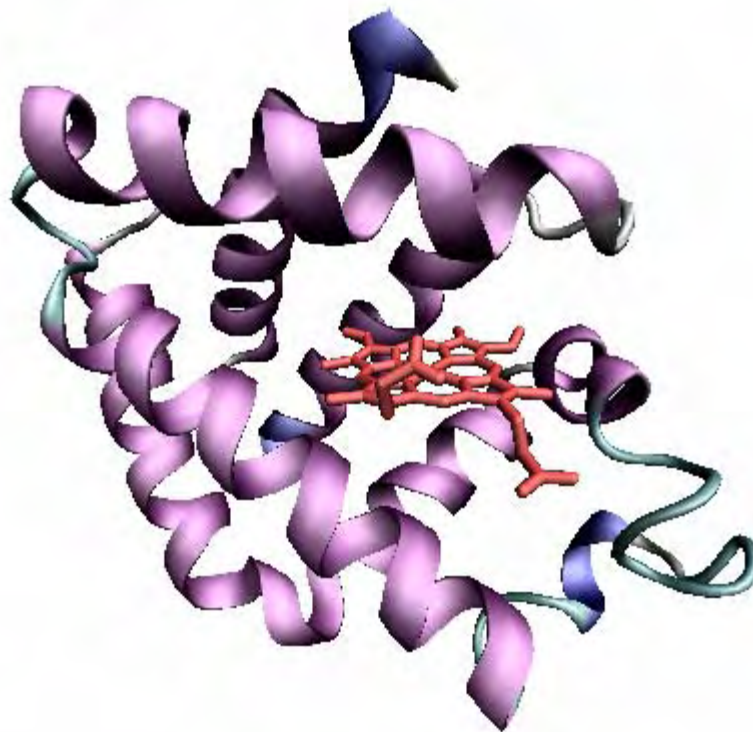


Figure 1.9 *Lucina pectinata* HbI crystallographic structure, PDB code 1FLP (Rizzi et al., 1994). HbI is a monomeric hemoglobin of 142 amino acids, and is a sulfide reactive hemoglobin.

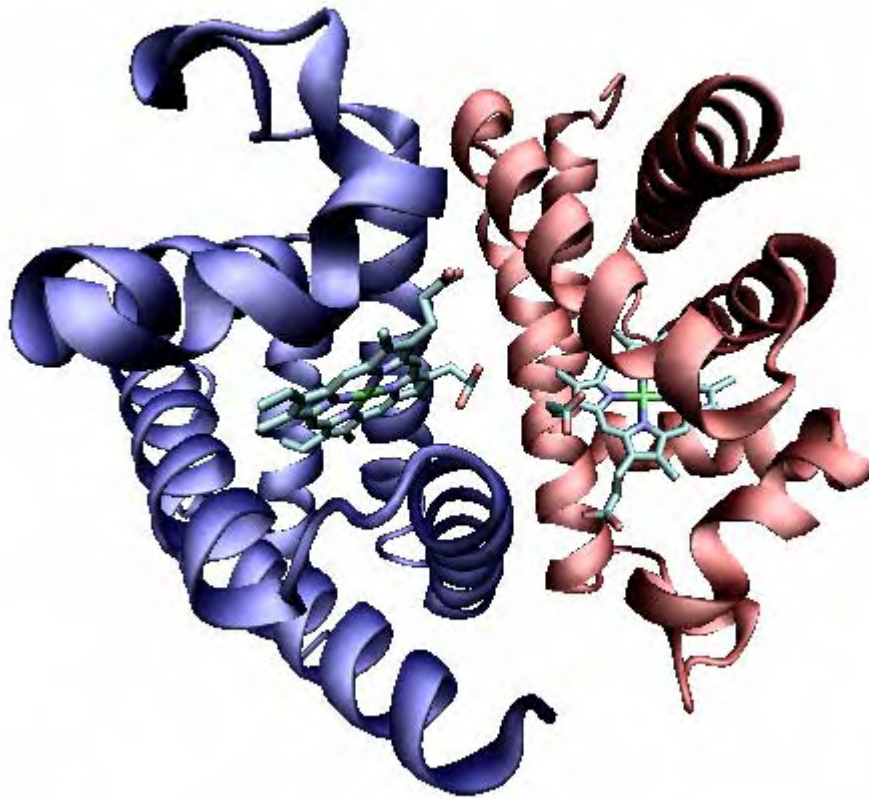


Figure 1.10 *Lucina pectinata* HbII crystallographic structure, PDB code 2OLP (Gavira et al., 2008). HbII consists of two dimers of 163 amino acids, and is an oxygen binding hemoglobin.

amino acids. There is a glutamine (Gln64 or E7) in the distal site of the heme pocket in the three hemoglobins instead of the classical histidine. This glutamine is also present in elephant myoglobin and shark myoglobin. The other surrounding amino acid residues are three phenylalanines (Phe43, Phe68, Phe29) for HbI (Figure 1.11A), while HbII (Figure 1.11B) and HbIII have two phenylalanines (Phe43, Phe68) and a tyrosine residue (Tyr30 or B10). At alkaline pH, the tyrosyl competes with hydroxyl radical as a ligand to the heme iron. At acid pH, the tyrosyl is assumed to be protonated and water ligates to the ferric heme (Kraus & Wittenberg 1990; Pietri et al., 2005). The low oxygen dissociation rate of HbII and HbIII suggested that these Hbs may accept electrons from the symbiont, assuming the character of a terminal oxidase (Wittenberg & Wittenberg, 1990). The kinetic rate constants for oxygen association and dissociation, k_{on} and k_{off} , are fast for HbI and very slow for HbII. This gave equilibrium oxygen affinities of approximately the same with a $P_{50} = 0.1-0.2$ mmHg. This affinity is very high compared to human hemoglobin (HbA₀) or other oxygen prototypes.

Recombinant HbI and several site-directed mutants were cloned and expressed in the bacteria *E. coli*. Infrared studies of HbI, and different HbI variants including the HbI PheB10Tyr mutant suggest a conformational equilibrium between an open and closed configuration due to the interactions of the TyrB10, ligand, and heme iron (Antommatei et al., 1999). Previous studies of *Lucina pectinata* HbI show resistance to ferryl formation (De Jesús-Bonilla et al., 2001). Stopped flow kinetics and resonance Raman data showed that the formation of the ferryl species compound I and compound II varies with pH, and it is suggested that in HbII this dependence is associated with the disruption of the heme

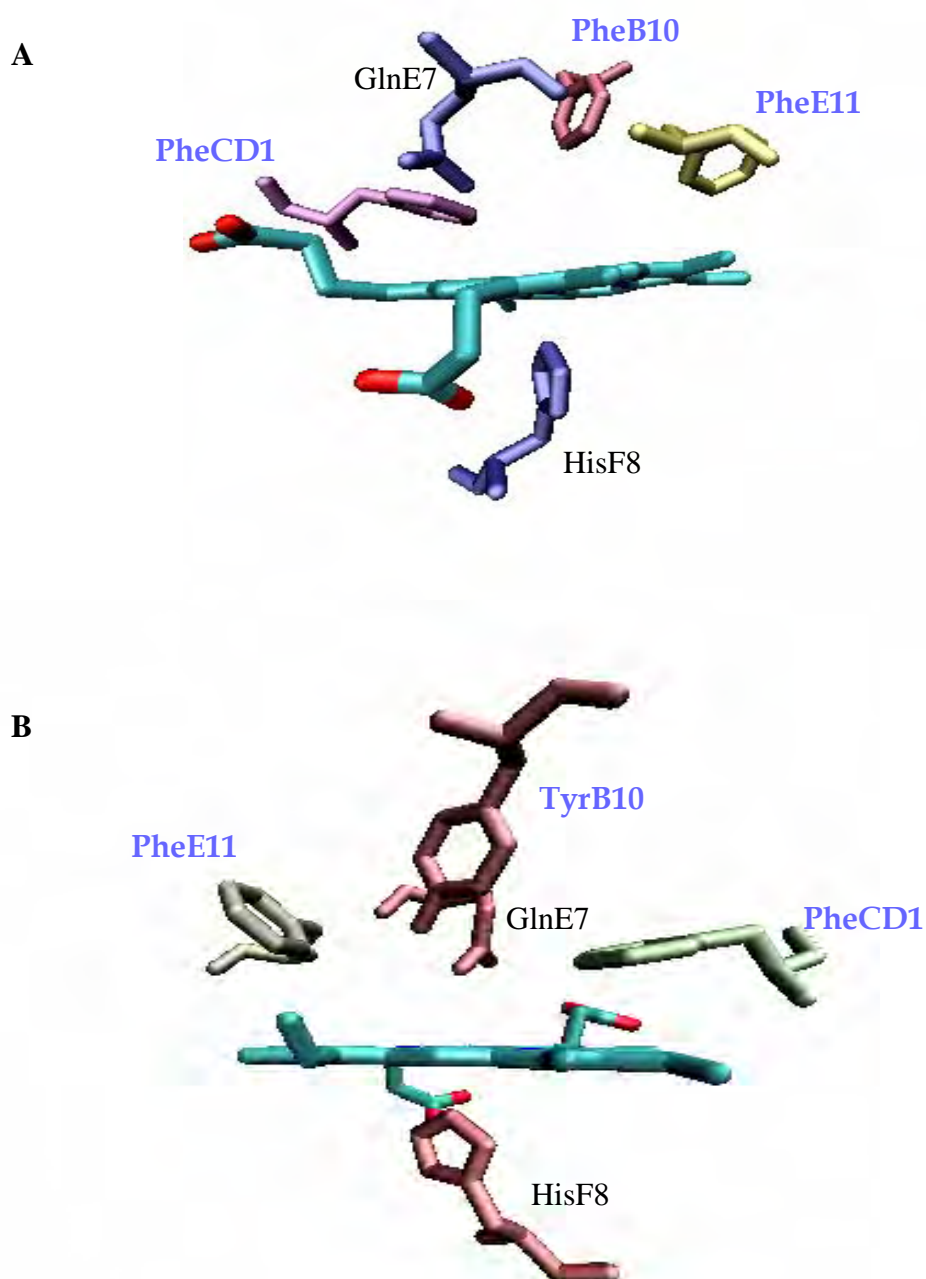


Figure 1.11 Heme pocket amino acids from *Lucina pectinata* HbI (A) PDB: 1FLP, and HbII (B) PDB: 2OLP. In the distal site of the heme pocket of the Hbs is GlnE7 instead of the classical histidine. The other surrounding amino acid residues are PheCD1, PheE11, PheB10 for HbI, while HbII and HbIII have PheCD1, PheE11 and TyrB10.

tyrosinate protein moiety which controls the access of H_2O_2 to the hemeprotein active center (De Jesús-Bonilla et al., 2002).

Recent studies with *L. pectinata* showed that the HbII is resistant to hydrogen peroxide oxidation due to the Tyr in the B10 position. The tyrosine creates a hydrogen networking that stabilizes the radical form of the compound II ferryl species. This special feature of HbII and other studies made with Mb mutants that resemble HbI allow us to study these hemoglobins with different oxidant species. The studies discussed here give us another insight in the role of the amino acids in the heme pocket, and an understanding for the design of safer hemoglobin blood substitutes.

1.5 Objectives

The challenge for researchers in the production of a heme protein based blood substitute is to decrease the interaction of the protein model with nitric oxide (NO) and side oxidative reactions to avoid the several side effects in humans. Thus, the purpose of this research was to pursue the factors that modulate the reaction of the *L. pectinata* hemoglobins with nitric oxide and hydrogen peroxide, which may lead to the development of new heme protein models useful for blood substitutes. This was achieved under the following objectives:

- 1) To define the kinetic reactions of the hemoglobins HbI, HbII and HbI PheB10Tyr with NO in terms of the structure and its relation to the physiological function based on:
 - Oxidation reaction of the oxy hemoglobins by nitric oxide

- Association reaction of ferric hemoglobin with nitric oxide
- Dissociation reaction of nitric oxide from the nitrosyl-hemoglobin (Hb(II)-NO) complex

2) One hypothesis is that the heme proteins containing a Gln in the E7 position have a rapid oxidation and high production of heme degradation products, thus another objective is to understand the oxidative reactions of HbI, HbII and the HbI PheB10Tyr mutant to predict a possible structure that limits the oxidation of the heme group in terms of:

- Autoxidation of the hemoglobins.
- Oxidation reaction of the hemoglobins by hydrogen peroxide.
- Formation of heme degradation products in the reactions with hydrogen peroxide.

3) To establish a comparison between the behavior of the HbI, HbII, and HbI PheB10Tyr mutant hemoglobins exposed to physiological conditions in a cell media culture under conditions of oxidative stress versus the kinetic experiments. To achieve this objective the studies were based on:

- The exposure of the hemoglobins to an endothelial cell media with glucose oxidase to evidence the formation of ferryl species and to monitor changes in cell morphology and apoptosis in endothelial cells.

- The exposure of the hemoglobins to an endothelial cell media under hypoxia to evidence the intracellular production of superoxide ion and to monitor the hemoglobins capability to transport oxygen during hypoxia.
- Formation of the ferryl species in the reaction with glucose oxidase.
- Expression of the HIF-1 α factor to evidence that hemoglobins can affect cell signaling pathways.

Overall, the study provided valuable information for a better comprehension of the role of the heme pocket amino acids in the peroxidative and oxidative reactions. The results also examine the possibility of *L. pectinata* HbII as a model system to design heme protein based blood substitutes with better resistant to oxidative damage and with little vasoactivity.

2 MATERIALS AND METHODS

2.1 Heme proteins preparation

2.1.1 Hemoglobin isolation and purification

The hemoglobins from the clam *Lucina pectinata* were extracted following previous methodology with slight modifications (Navarro et al., 1996). Briefly, 100 mL of extraction solution (10mM HEPES, 5mM EDTA, 1mM DTTR) adjusted to pH 7.5 was used per 25 g of ctenidia tissue. The extract was homogenized, bubbled for 15 minutes with CO and centrifuged at 19,000 rpm for 1 hour. The supernatant was collected, filtered and stored at -80°C for further purification of the hemoglobins. A HiLoad 26/60 Superdex 200 preparation grade (ÄKTA FPLC, Amersham Bioscience) column was used to initially isolate the protein samples. The column was equilibrated to pH 7.5 with 0.5mM EDTA and 50mM sodium phosphate buffer at a flow rate of 4.4ml/min and 0.5 MPa and the proteins concentration in each fraction was identified by absorbance at 280 nm. Figure 2.1 shows the elution chromatogram for the hemoglobin's isolation from the ctenidia extract, where peaks 1 and 2 corresponds to the HbII/HbIII mixture and HbI/cysteine rich protein mixture, respectively. The HbI was purified from the cysteine rich protein by ion exchange chromatography using a DEAE Fast Flow 16/62 column (ÄKTA FPLC, Amersham Bioscience) in 25mM NH_4HCO_3 , pH 8.3 buffer. The elution chromatogram for the purification of HbI shows 3 peaks corresponding to HbI in the ferric state (peak 1), HbI in the oxy state (peak 2), and the cysteine rich protein (peak 3). The HbII and HbIII proteins were isolated and purified from the HbII/HbIII fraction by ion exchange chromatography with a

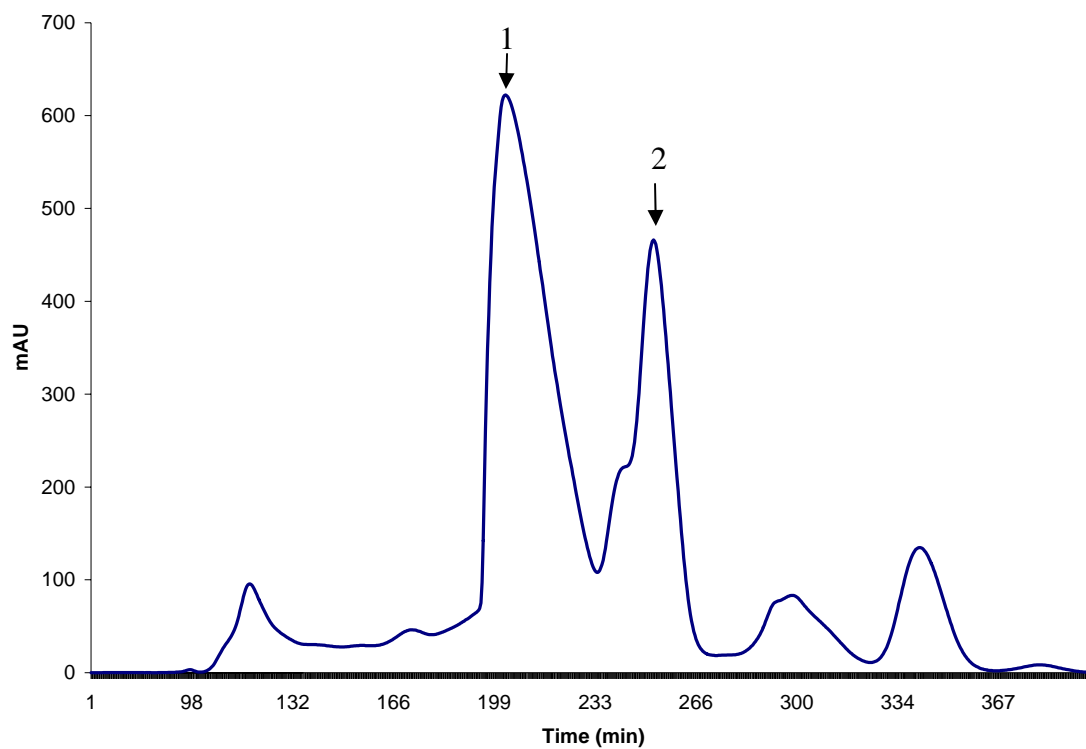


Figure 2.1 Elution chromatogram for the size exclusion chromatography purification of the *L. pectinata* ctenidia extract. (1) HbII/HbIII mixture, (2) HbI/Cysteine rich protein mixture.

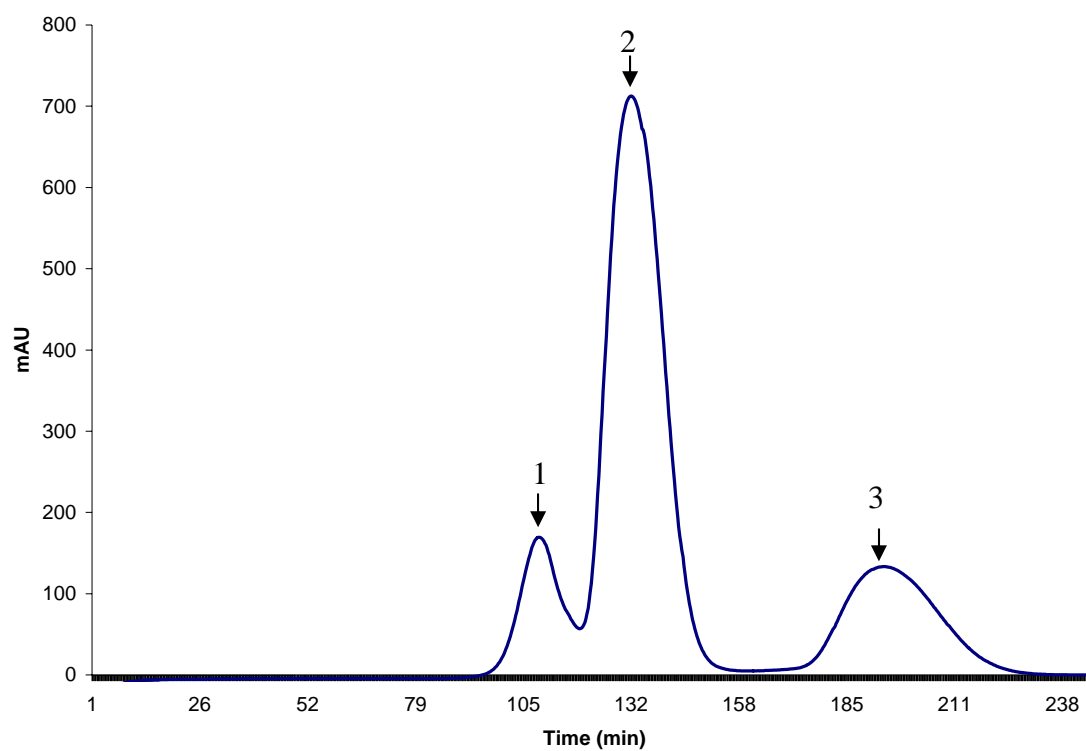


Figure 2.2 Elution chromatogram for the purification of *L. pectinata* HbI by ion exchange chromatography monitored at 280 nm. (1) ferric HbI, (2) oxy HbI, (3) cystein rich protein.

HiPrep 16/10 Q FF (ÄKTA FPLC, Amersham Bioscience) column equilibrated with 10 mM triethanolamine/acetate buffer at pH 8.3, and eluted with a gradient of sodium chloride concentration from 0 to 180mM. Figure 2.3 shows the elution chromatogram for the separation of the HbII/HbIII mixture, where peak 1 corresponds to other protein impurities, while peak 2 and 3 were assigned to HbII and HbIII, respectively.

The recombinant protein HbI PheB10Tyr was prepared as described by León and collaborators (León et al., 2004). The *E. coli* Bli5 competent cells with the plasmid were developed at the Biomolecular Laboratory of Dr. Carmen Cadilla (University of Puerto Rico, Medical Sciences Campus), and provided in scraped Petri dishes. The large-scale expression process was performed in a 5-L BioFlo 3000 Bioreactor (New Brunswick) following Collazo procedures with minor modifications (Collazo et al., 2004). Briefly, colonies from the scrapped dishes were grown in a 250 mL sterilized Erlenmeyer containing 50 mL of the Terrific Brooth (TB) medium. The culture was incubated for 12 hours at 120-150 rpm, and 37°C. After 12 hours, the culture was transferred to a 2500 mL culture flask with 450 mL of the TB medium, and incubated overnight with the same conditions. The 4 L TB media for the large-expression was prepared directly inside the bioreactor vessel, and sterilized for 60 min at 121°C. When the media reached a temperature of 37°C, 30 µg/mL of chloramphenicol, 70 µg/mL of kanamycin, 500 µL of antifoam solution (Sigma), 0.17 M KH₂PO₄, 0.72 M K₂HPO₄, and 75 mL of the glucose (50% w/v) were added. The dissolved oxygen (dO₂) and the pH were controlled during the experiment. The media was inoculated with the overnight culture prepared before the fermentation. The cell growth was monitored measuring the optical density at 600 nm (OD₆₀₀). When the OD₆₀₀ value was between 1 or 2, the protein expression was induced by adding 5 mL of 1 M IPTG solution and 33 mg/mL

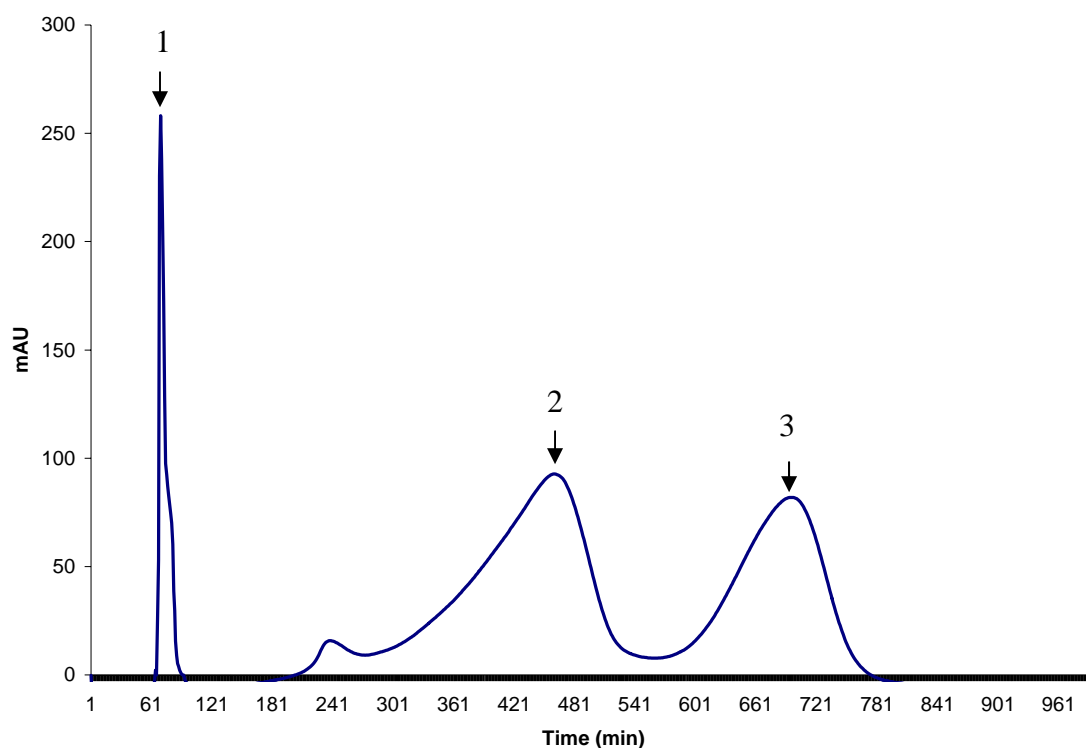


Figure 2.3 Elution chromatogram for the HbII/HbIII mixture purification by ion exchange chromatography. A FPLC with an ion exchange chromatography column was used and monitored at 280 nm. Peak 1 corresponds to other protein impurities, peak 2 and 3 were assigned to HbII and HbIII, respectively.

hemin chloride in NH_4OH . The OD_{600} was taken every 30 minutes after the induction until the lag phase was reached. The expression process was finished when two or three constant values of OD_{600} reading were obtained in the lag phase. The cell culture was centrifuged for 20 minutes at 4,000 rpm, 4 °C in a Beckman J2-HS Centrifuge. The cell pellet was stored at -56°C for further lysis and purification procedures.

The reddish-brown pellets were lysed by 5 cycles of sonication using 10 mL of tris-EDTA buffer (10 mM Tris-HCl, 0.1 mM EDTA, pH of 8.0) for every 50 mL of culture centrifuge. The protein was purified by adding the lysate to a cobalt metal affinity resin (Talon, Invitrogen). The resin was washed with wash buffer (50 mM Na_2PO_4 , 0.3M NaCl and 15 mM imidazole, pH 7.6). After the last wash, 15-20 mL (for each 5mL of resin) of elution buffer (Na_2PO_4 50 mM, NaCl 0.3M, 150 mM imidazole, pH 7.6) were used to elute the protein. The imidazole and salts were removed with ultra filtration, and the final purification step was achieved using the HiLoad 26/60 Superdex 200 preparation grade (ÄKTA FPLC, Amersham Bioscience) column. Figure 2.4 shows the HbI PheB10Tyr elution chromatogram after purification by size exclusion chromatography.

The endothelial cell culture studies required hemoglobins with high purity and sterility. Therefore, the hemoglobins for these studies were eluted through an endotoxin removing gel (Thermo Scientific, IL, USA) followed by a 0.22 μm filtration under sterile conditions. The hemoglobin's oxidation state was verified with a spectrophotometer, while the sample purity was determined using sodium dodecylsulphate polyacrylamide gel electrophoresis (SDS-PAGE). Figure 2.5 shows the polyacrilamide gel after the electrophoresis for two different purifications of the hemoglobins. HbI shows a band near 14,000 Da in lanes 2 and 5, while HbII shows to be purified from HbIII in lanes 3, 6 and 4, 7,

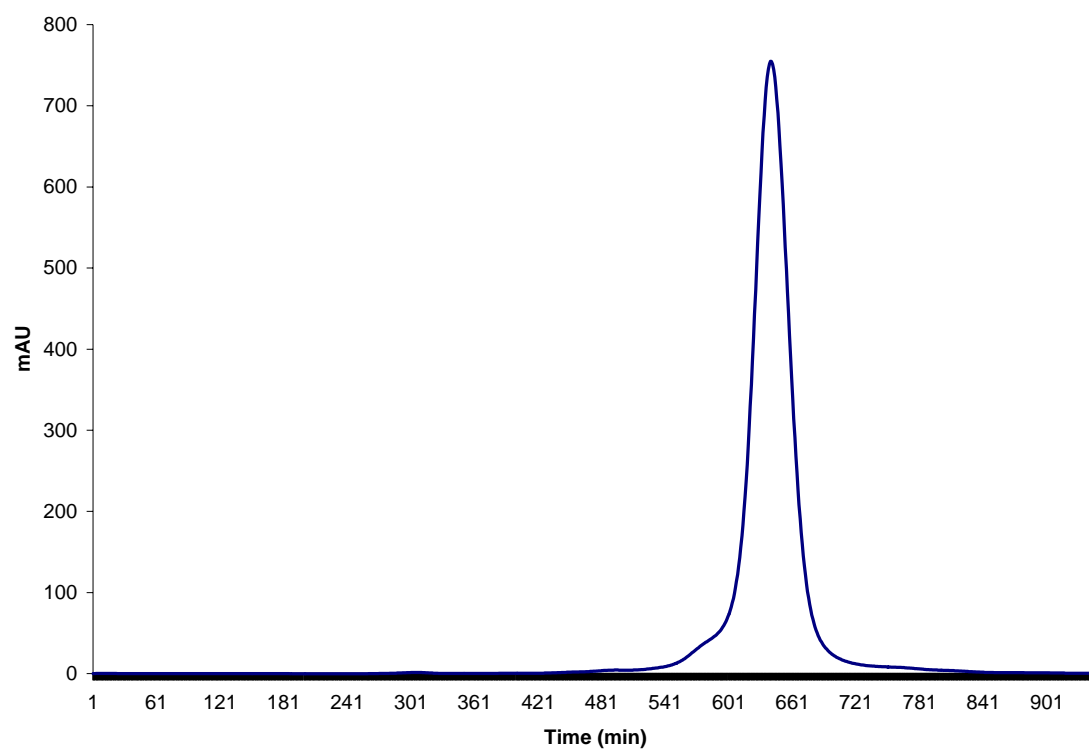


Figure 2.4 HbI PheB10Tyr elution chromatogram after purification by size exclusion chromatography using the FPLC instrument and monitored at 280 nm.

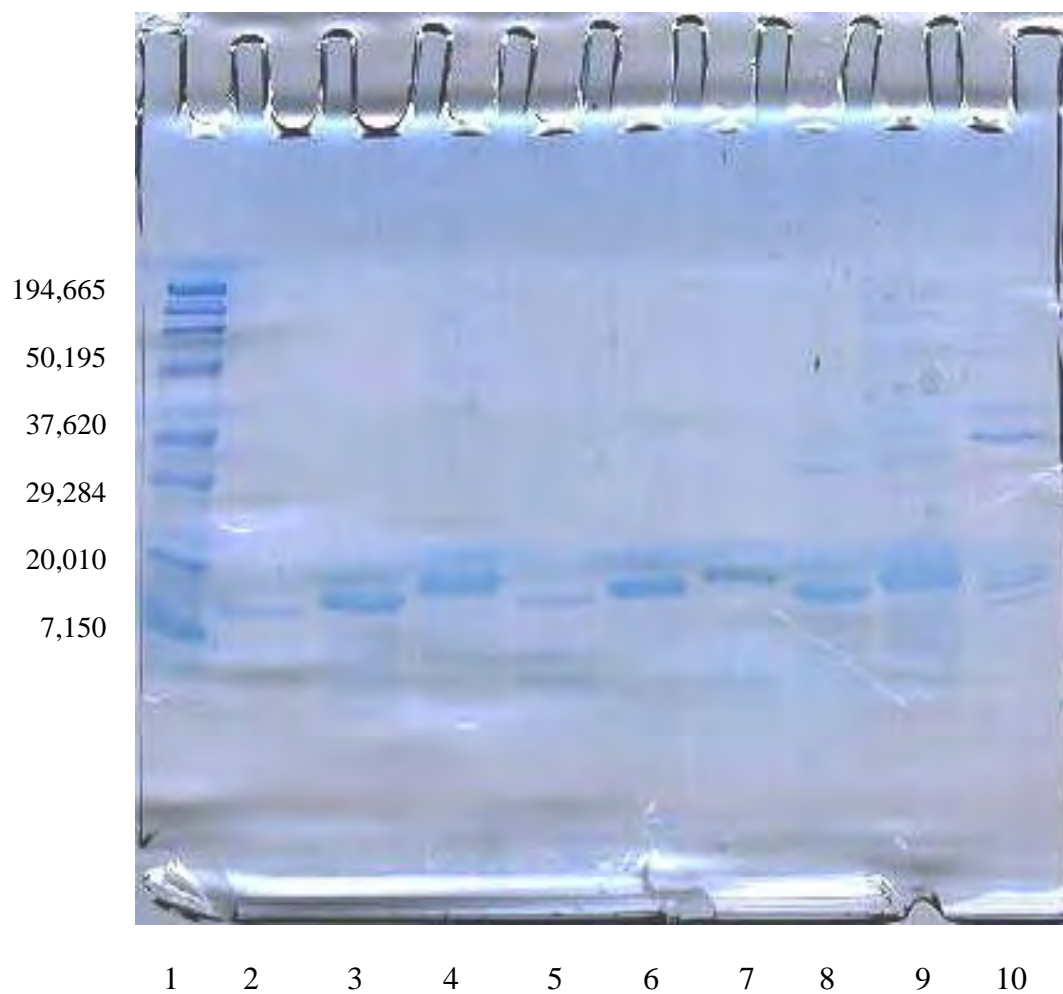


Figure 2.5 Polyacrylamide gel electrophoresis for the *L. pectinata* hemoglobins. (1) broad range prestained protein ladder, (2) and (5) HbI, (3) and (6) HbII, (4) and (7) HbIII, (8) HbI/Cysteine rich protein mixture, (9) HbII/HbIII mixture, (10) protein extract.

respectively. Lane 8 contains the HbI/cystein rich protein mixture before purification, where can be seen the cystein rich protein band near 32,000 Da. Lanes 9 and 10 correspond to a mixture of HbII/HbIII before purification and to a dilute ctenidia extract, respectively.

2.1.5 Hemoglobin spectral analysis

The oxy Hb species were prepared reducing the sample by adding sodium dithionite ($\text{Na}_2\text{S}_2\text{O}_4$) to the hemoglobin and eluting through a Sephadex G-25 gel column in 50mM potassium phosphate buffer. The ferric species were prepared by oxidizing the oxy Hb with potassium ferricyanide followed by an Amicon ultrafiltration with YM 10 membranes to remove unreacted ferricyanide. During the preparation of the samples, the concentrations and formation of the complexes were verified using their absorption spectrum. Table 2.1 shows the λ_{max} of each complex and the corresponding absorptivity coefficient (ϵ) for HbI and HbII in the ferric, oxy and deoxy species. Figure 2.6 shows an example of the different oxidation states for the *L. pectinata* HbII. The heme protein concentration for each species was determined using the Winterbourn (Winterbourn, 1985) equations 2.1 through 2.3, in which:

$$[\text{Oxy hemoglobin}] = 119(A_{576} - A_{700}) - 39(A_{630} - A_{700}) - 89(A_{560} - A_{700}) \quad (\text{Equation 2.1})$$

$$[\text{Ferric hemoglobin}] = 28(A_{576} - A_{700}) + 307(A_{630} - A_{700}) - 55(A_{560} - A_{700}) \quad (\text{Equation 2.2})$$

$$[\text{Hemichrome species}] = -133(A_{576} - A_{700}) - 114(A_{630} - A_{700}) + 233(A_{560} - A_{700}) \quad (\text{Equation 2.3})$$

The hemoglobin concentration was calculated with the overall sum of the equations 2.1 to 2.3. In this mathematic operation, the concentration for each oxidation state is calculated

Table 2.1 **Spectral properties of HbI and HbII from *L. pectinata***

Hemoglobin complex	λ_{\max} (Soret) (nm)	ϵ (mM⁻¹cm⁻¹)	λ_{\max} (Q) (nm)	ϵ (mM⁻¹cm⁻¹)
<i>Deoxy HbI</i>	433	119	557	12.2
<i>Oxy HbI</i>	416	135	576	13.0
<i>Ferric HbI</i>	407	178	633	4.2
<i>Deoxy HbII</i>	432	120	556	12.5
<i>Oxy HbII</i>	414	129	576	12.6
<i>Ferric HbII</i>	404	130	632	3.6

based on the extinction coefficient of the oxy, ferric and hemichrome species multiplied by the absorbance of the bands in the visible spectrum at 576, 630 and 560 nm. The background was subtracted with the absorbance at 700 nm.

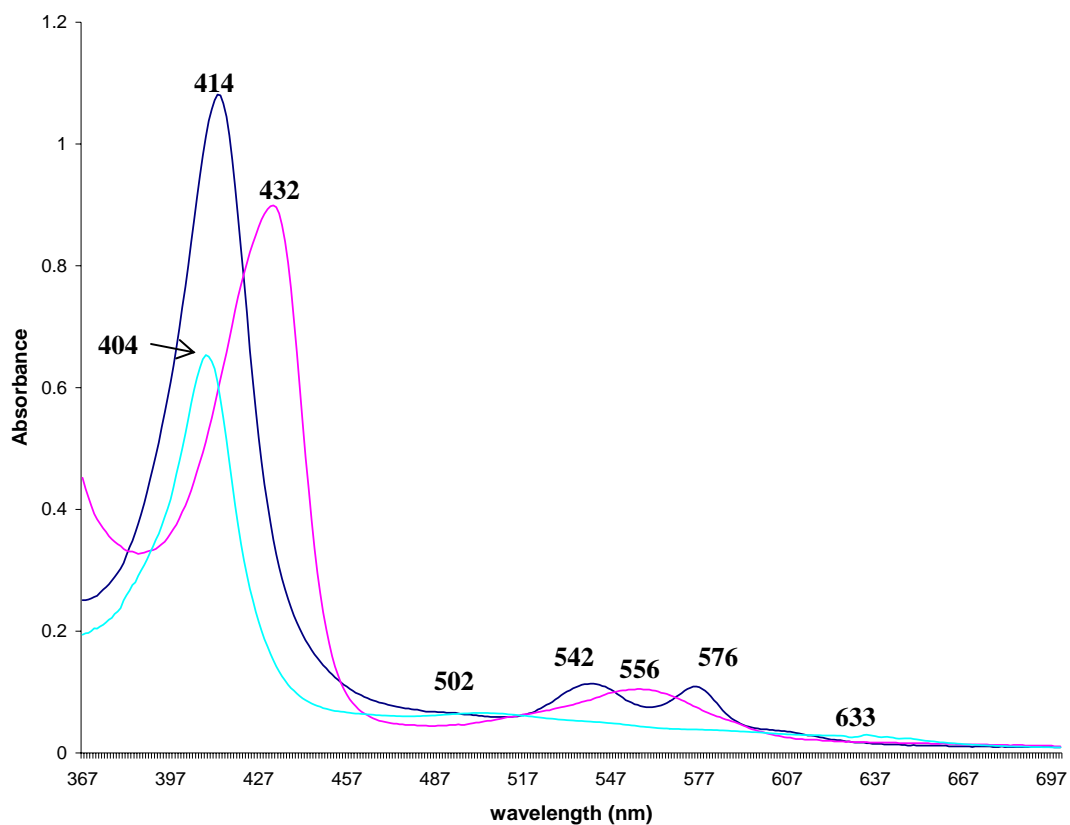


Figure 2.6 *L. pectinata* HbII oxidation states spectra. The Soret band at 414 nm with Q bands at 542 nm and 576 nm represents the oxy HbII species. The ferric species show a Soret band at 404 nm and Q bands at 502 nm and 633 nm. The heme-Fe(II) deoxy species has a Soret band at 432 nm with a Q band at 556 nm.

2.2 Redox chemistry of *L. pectinata* hemoglobins

2.2.5 Hemoglobins autoxidation

The hemoglobin autoxidation reaction was performed at 37°C for 6 hours following Jia (Jia et al., 2004) procedures with slight modifications. Briefly, the hemoglobins were reduced to maximum levels of the oxy form prior to autoxidation experiments and verified spectrophotometrically. Approximately 20 μ M Hb solutions were incubated in air equilibrated 50 mM Chelex-treated phosphate buffer with or without the antioxidant enzymes, catalase (414 U/ml) and superoxide dismutase (4.6 U/ml). The autoxidation rate constants were obtained by nonlinear least-squares curve fitting using the single exponential Equation 2.4 (SigmaPlot software).

$$y = B_0 + A \exp(-k_1 t) \quad (\text{Equation 2.4})$$

The absorbance spectra between 400 and 700 nm were recorded as a function of time in a temperature-controlled photodiode array spectrophotometer (HP-8453). The proportions of oxy, ferric, and hemichrome Hb species were calculated from each spectrum by multicomponent analysis based on their extinction coefficients using the Winterbourn algorithm (Section 2.1.2) (Winterbourn, 1985). The oxy Hb percentage changes due to the autoxidation of the hemoglobins were plotted as a function of time.

2.2.2 Reaction of the hemoglobins with hydrogen peroxide

The ferryl (heme-Fe(IV)=O) species was detected using an Applied Photophysics SF-17 microvolume stopped-flow apparatus with a diode array detector. The dead time of the instrument is 1.3 ms. Spectral data was acquired between 1 second to 8.2 seconds at 25°C.

Figure 2.7 shows a UV-Vis overlaid spectra of the α -DBBF Hb bands in the Q region for the oxy (heme-Fe(II)), ferric (heme-Fe(III)) and ferryl (heme-Fe(IV)) forms, used to identify the oxidation state of the hemoglobins. The ferric hemoglobin solutions (8 μ M) were diluted in 0.5 mM Tris buffer, pH 7.4 with a final concentration of 4 μ M. The ferryl species was formed for the reaction of hemoglobin with an initial H₂O₂ concentration of 10mM to 200 mM H₂O₂ (Nagababu et al., 2002).

Kinetic experiments were performed using a RSM Rapid-scanning monochromator (Olis, Inc.) with a stopped-flow apparatus. Figure 2.8 shows the schematic representation of the instrument. The scans were recorded for up to ten seconds. HbI recombinant, HbII and the HbI Phe(B10)Tyr mutant were mixed with H₂O₂ (Hb:H₂O₂ ratios from 1:100 to 1:6500). The formation of the ferryl compound I was monitored at 648 nm while the formation of the compound II was monitored at 400 nm and 540 nm. To validate the experimental method, ferric HbI was reacted with H₂O₂, 1:2000 ratio, at 400 nm for 10 seconds (De Jesús-Bonilla et al., 2001). Figure 2.9 shows the overlaid spectra for the reaction, in where the oxy HbI bands shifts to 419 nm, characteristic of the ferryl compound. Figure 2.10 shows the kinetic trace for the oxidation of the ferric heme with H₂O₂, with a kinetic rate constant value for the formation of the ferryl species of $1.93 \times 10^2 \text{ M}^{-1}\text{s}^{-1}$, and $R^2 = 0.992$, which is comparable to previous work, with a rate constant value of $2.0 \times 10^2 \text{ M}^{-1}\text{s}^{-1}$ (De Jesús-Bonilla et al., 2001). The rate constants values (k_{obs}) at each concentration were calculated using standard value decomposition (SVD) and global analysis, and subjected to curve fitting routines included in the Olis software, using similar approximations reported previously (Egawa et al., 2000). The double exponential equation (Equation 2.5) used was

$$y = A_1 \exp(-k_1 t) + A_2 \exp(-k_2 t) + c \quad (\text{Equation 2.5})$$

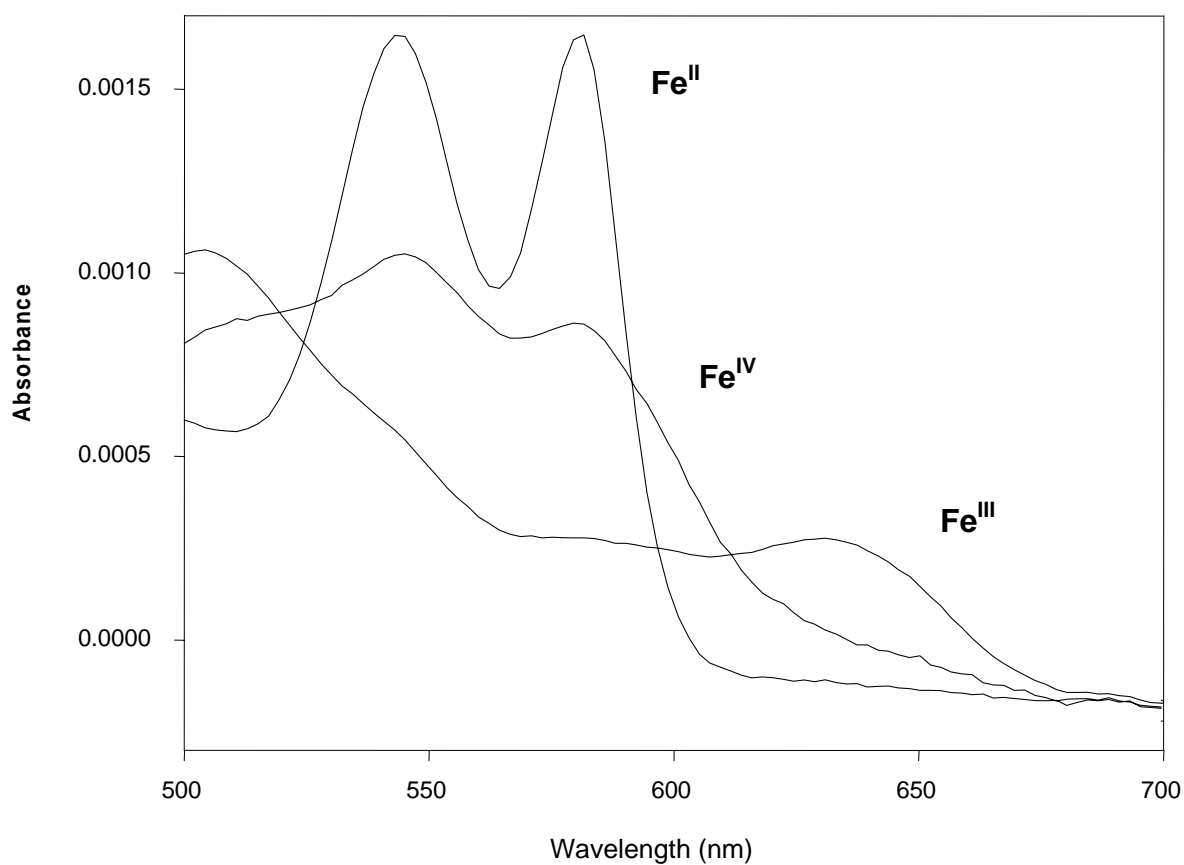


Figure 2.7 UV-Vis overlaid spectra of the α -DBBF Hb bands in the Q region for the oxy (heme-Fe(II)), ferric (heme-Fe(III)) and ferryl (heme-Fe(IV)) forms, used to identify the oxidation state of the hemoglobins.

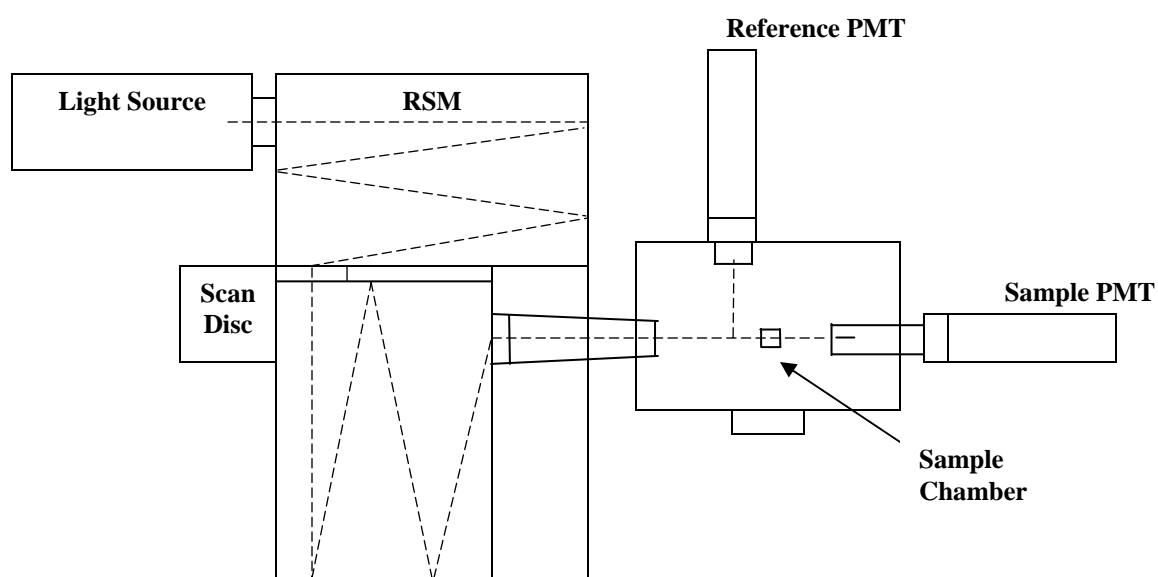


Figure 2.8 Schematic representation of the UV-Vis spectrophotometer instrument used to study the kinetic data in the reaction of the hemoglobins from *L. pectinata* with hydrogen peroxide.

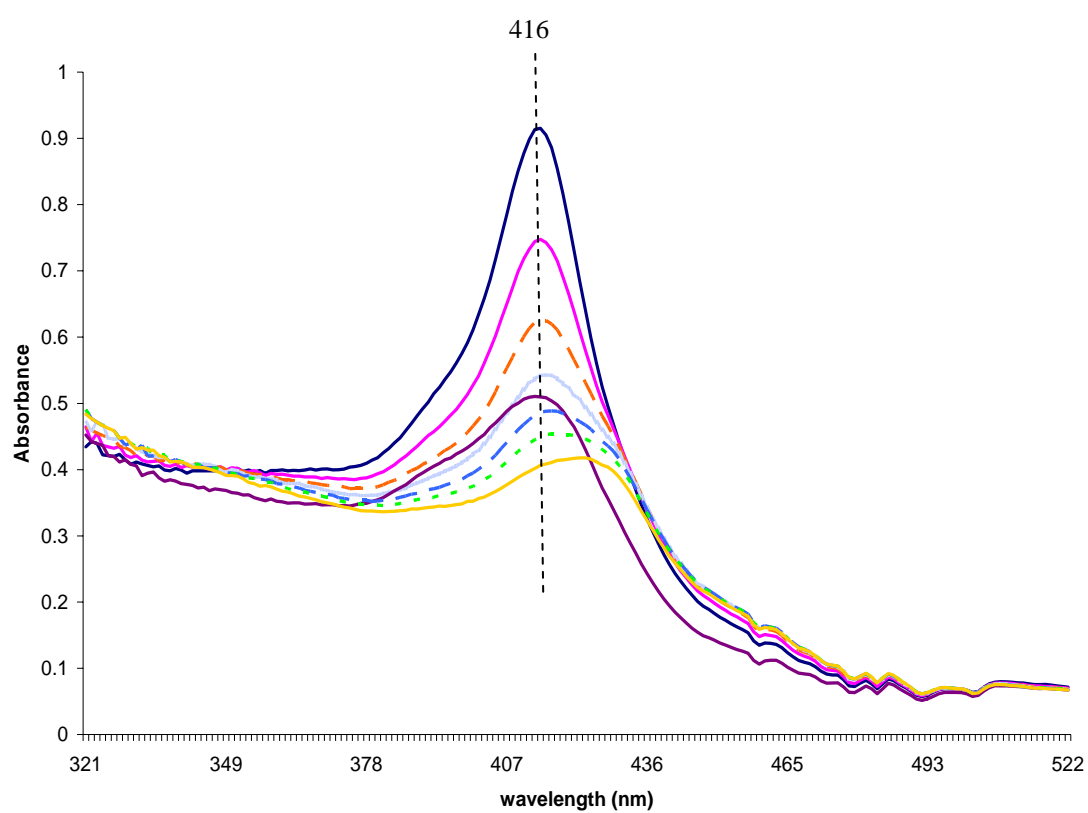


Figure 2.9 UV-Vis overlaid spectra for the reaction of *L. pectinata* HbI with hydrogen peroxide. The Soret band at 416 nm shifts to 419 nm, characteristic of the ferryl species.

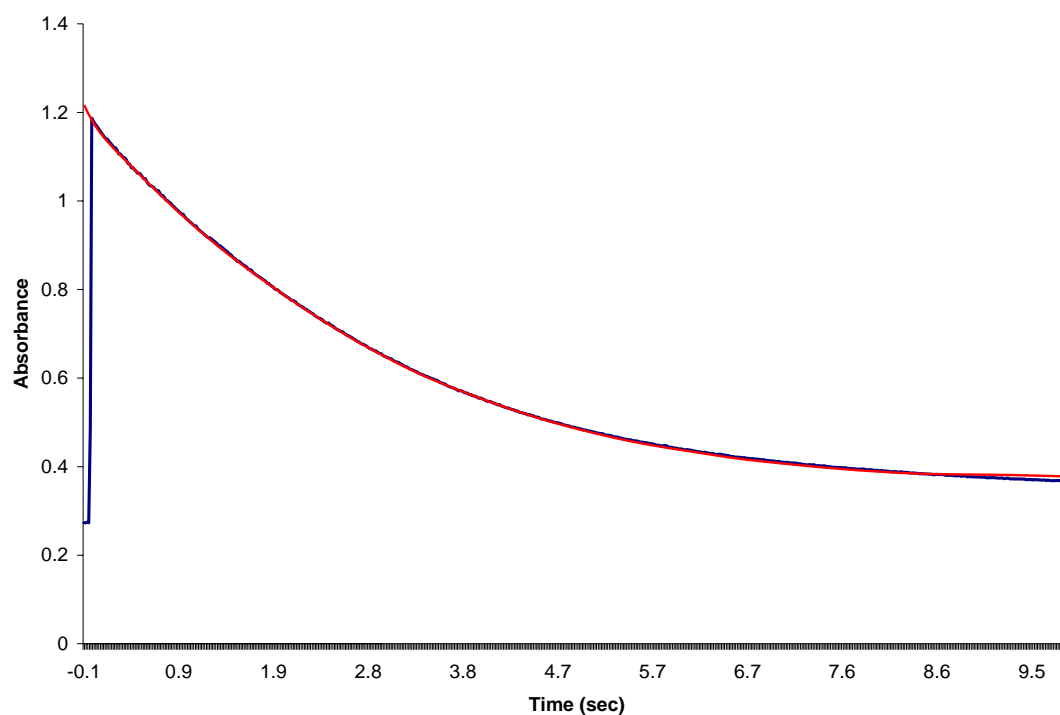


Figure 2.10 Kinetic trace for the reaction of HbI with hydrogen peroxide, 1:2000 ratio, at 400 nm for 10 seconds, using a UV-Vis spectrophotometer with an stopped-flow apparatus.

in which A_1 and A_2 are the amplitudes, k_1 and k_2 are the exponential rate constants, and c is the fluorescence intensity at $t = \infty$. Then, the constants were plotted against H_2O_2 concentration to obtain the pseudo first-order rate constant for the ferryl formation. The effect of the pH in the ferryl formation was studied by changing the buffer pH to 4.86, 7.50, and 11.2.

2.2.5 Detection of heme degradation products

The reactions of hydrogen peroxide provoked the formation of heme degradation fluorescent products. The oxy hemoglobin solutions were diluted in 50mM sodium phosphate buffer, pH 7.4, with a final concentration of 20 μ M. The degradation products were induced in the reaction of the hemoglobin with 4, 6 and 8 mM H_2O_2 , and detected using an Applied Photophysics SF-17 microvolume stopped-flow apparatus as described previously (Jia & Alayash, 2002). The dead time of the instrument is 1.3 ms. Time courses were acquired between 500 and 1000 seconds at 25°C, 378.0 volts, with an excitation of 321 nm. A 360 nm band pass interference filter was placed over the exit to the photomultiplier tube to observe the fluorescence emission. The pseudo first order rate constants were fitted with double exponential function (Equation 2.5) using a Marquard-Levenberg fitting routine included in the instrument software program. The rate constants values were determined from at least four individual traces. The rate constant for the formation of degradation products was obtained from the slope of the plot of the observed pseudo first-order rate constant versus H_2O_2 concentration.

2.2.5 Hemoglobin reactions with nitric oxide

The nitric oxide stock solution was prepared by flushing the gaseous NO through a degassed NaOH solution, washed with a 50mM bis/Tris buffer to remove higher nitrogen oxides, and finally through a previously degassed 0.1M sodium phosphate buffer with a pH 7.4. Aliquots of this stock solution were injected into syringes containing anaerobic buffer to achieve the desired dilution.

Time courses for NO oxidation of oxy Hb were measured using the Applied Photophysics SF-17 microvolume stopped-flow apparatus at 20°C, and 420 nm (Alayash et al., 2001). The mixing time of the instruments was 1-2 ms. The nitric oxide concentrations were between 1-25 μ M and the hemoglobin concentration was kept in 0.5 μ M, after mixing. The pseudo first order rate constants were calculated using double exponential fitting with the Equation 2.5 (Origin software). The NO-induced oxidation rate constant was obtained from the slope of the plot of the observed pseudo first-order rate constant versus NO concentration. Reactions of 15 μ M ferric Hbs, after mixing, with various concentrations of NO were monitored at 420 nm in an oxygen-free environment using the stopped-flow apparatus (Alayash et al., 1993).

The nitric oxide dissociation rate constants were measured following Farrés (Farrés et al., 2005) procedures. Briefly, the dissociation of the Hb-NO complex was achieved by molecular replacement in the reaction with 1 mM CO/ 10 mM sodium dithionite solution, which represents flooding conditions. The changes in absorption were monitored at 420 nm using a HP UV Spectrophotometer and recording the spectra every 10 minutes during the first three hours, and every 30 minutes for a second three hours period. The kinetic rate

constant value for the NO dissociation was obtained from the exponential decay fit with equation

$$y = A_1 \exp (-x/t_1) + y_0 \quad (\text{Equation 2.6})$$

where y is the dependent variable, y_0 is the y offset, A_1 is the amplitude, x is the independent variable, and t_1 is the decay constant. The kinetic rate constant value is the average for three independent kinetic traces.

2.2.5 Catalase assay

A catalase assay was performed to detect a possible enzymatic behavior in the hemoglobins. The experiment was performed by adding 8.4 μL of 30% H_2O_2 to a 3.0 mL cuvette containing 1 μM hemoglobin in 50mM potassium phosphate buffer, pH 7.4. The kinetic trace was obtained for 122 seconds at 1second interval, at 240 nm. Catalase at 3 nM and 0.3 nM was used as control of the enzymatic activity.

2.3 Redox chemistry of *L. pectinata* hemoglobins *in vitro*

2.3.1 Endothelial cell culture

Bovine aortic endothelial cells (BAECs) were obtained from Clonetics (BW-6002, San Diego, CA, USA). Cells were grown in endothelial basal medium (EGM) supplemented with 5% fetal bovine serum (FBS), 10 ng/mL human recombinant epidermal growth factor, 1 $\mu\text{g/mL}$ hydrocortisone, 10 $\mu\text{g/mL}$ bovine brain extract, 50 $\mu\text{g/mL}$ gentamicin, and 50 ng/mL amphotericin-B. Cells were cultured in 25 cm^3 diameter cell culture dishes at 37°C in a humidified incubator (5% CO_2 , 95% air). For harvesting, cells were washed in HEPES-

buffered saline and incubated with 0.025% trypsin- 0.01% EDTA for three minutes at 37°C. After cell detachment, trypsin neutralization solution was added, and cells were centrifuged at 157 rpm for 6 minutes at 4°C. The experimental data were obtained from BAECs in the second to eight passages.

2.3.2 Cell viability assay

The number of viable cells under each experimental condition was estimated using the Cell Titer-Blue Cell Viability Assay (Promega Co, USA). Briefly, the cells were sub-cultured in a 96-well plate, and when confluence was reached, were exposed to media with 50 μ M Hb, 10 mU/mL glucose oxidase, or both, from 2 to 24 hrs. At each end period, the cells were washed twice with phosphate buffered saline (PBS). Cell Titer-Blue reagent (20 μ L) was added to the cells, and mixed with appropriate free-phenol red fresh cell medium, for a final volume of 120 μ L in each well. The cells were incubated at 37°C and the fluorescence at 560 nm_{Ex}/590 nm_{Em} was recorded after 1 hour with the spectrofluorometer Spectra MAX GEMINI EM (Molecular Devices). Viable cells reduced the resazurin present in the CellTiter-Blue reagent to resorufin, which is pink and fluorescent. Therefore, fluorescent signal is proportional to the number of viable cells at the end of each experiment. Cells without treatment were used as positive control.

2.3.3 Exposition of the endothelial cells to a hypoxic environment

The hypoxic measurements were done following Yeh and Alayash procedures with slight modifications (Yeh & Alayash, 2004). Briefly, the cells were grown until confluence in 60 mm flasks. The medium was replaced with free-phenol red endothelial growth medium

without supplements. The flasks were placed in a polycarbonate chamber with medium containing or not 25 μ M oxy Hb. Then, the chamber was flushed with hypoxic gas (5% CO₂, 95% N₂) for 20 min and clamp-locked. The incubation time was 2, 4, 8, 12, 24 and 48 hours.

After incubation under either normoxic or hypoxic conditions, the media of BAECs treated with or without Hb were collected and spectral analysis of Hb oxidation products in the media was performed following the methodology described in 2.1.2 section (Winterbourn, 1985). The cells were washed in ice cold phosphate buffered saline and harvested in cell lysis buffer (145 mM NaCl, 0.1mM MgCl₂, 15mM HEPES, 10mM EDTA, 1mM Na₃VO₄, 2% leupeptin, 0.5% 4-(2-aminoethyl) benzenesulfonyl fluoride, 1% Triton X-100, pH 7.2). The cells were scrapped and stored in dry ice until analysis.

2.3.4 Detection of the HIF inducible factor HIF-1 α

The protein extract from the cells lysis in the hypoxic experiments was separated on a 4–20% polyacrylamide gel (Novex, Carlsbad, CA, U.S.A.), and electro blotted by western blot on a polyvinylidene difluoride (PVDF) membrane. The membrane was blocked with Casein in PBS blocking solution (Pierce, Rockford, IL, USA) and then probed with HIF-1 α mouse monoclonal antibody (1:1,000 dilution) (StressGen, Victoria, Canada) for 1 hour at room temperature. The membrane was washed three times in PBS-T (PBS (1X), Tween-20) wash buffer and then incubated with biotin-conjugated goat antimouse or antirabbit (1:1,000) antibody (Zymed, San Francisco, CA, U.S.A.) for 1 hour. The membranes were washed again for three times and then incubated with Streptavidin-Alkaline Phosphatase (1:5000) (Zymed, San Francisco, CA, USA) for 30 minutes. After washing for three times, the membranes were incubated with NBT/CIP ready to use substrate for alkaline phosphates

(Pierce) until bands were seeing. Total protein was determined using the bicinchoninic acid protein (BCA) assay kit (Pierce, Rockford, IL, U.S.A.). The bands on the membrane were scanned and the density was measured in a FluorChem 5500 analyzer (Alpha Innotech).

2.3.5 Intracellular superoxide determination

Hypoxic experiments were carried with 50 μ M Hbs at 30 min, 1 hour, 2, 4, 6, 8, and 12 hour with or without 100 U of superoxide dismutase (SOD), an $O_2^{\bullet -}$ scavenger. At the end of the hypoxic experiment, the cells were harvested in ice-cold phosphate buffered saline, centrifuged at 1000 rpm for 3.5 minutes, and suspended in a salt solution buffer (130 mM NaCl, 5 mM KCl, 1 mM $MgCl_2$, 1 mM $CaCl_2$, 35 mM phosphoric acid, 20 mM HEPES, pH 7.4). The cell suspensions were added to 96-well plates containing dark-adapted lucigenin (250 μ M) in PBS (1X) balance salt solution, at room temperature. Lucigenin is a compound that emits light upon interaction with $O_2^{\bullet -}$. The increases in photon emission were measured every 20 seconds thereafter for 10 minutes in a Microplate Luminescence Counter (TopCount NXT, Packard, Meriden, CT, U.S.A.). A standard curve generated using xanthine/xanthine oxidase and normalized by protein content as determined by BCA protein assay was used to calculate the net increases in $O_2^{\bullet -}$ generation.

2.3.6 Oxygen tension measurements

A polarographic oxygen electrode placed in the hypoxic chamber allowed the measurement of oxygen partial pressure (pO_2) in the cell culture medium with or without the hemoglobins. The electrode was calibrated with KCl electrolyte solution. Briefly, a 60-mm

confluent cell dish was placed in the hypoxic chamber with 3 mL EGM, without FBS, containing or not the hemoglobin. Hypoxic gas (95% N₂, 5% CO₂) was flushed through the chamber for 20 minutes to ensure an oxygen free atmosphere. The oxygen partial pressure was measured at different intervals for 1 hour.

2.3.7 Endothelial cells exposition to glucose oxide

The experiments for the reaction of glucose oxidase in the cells were done following D'Agnillo and Alayash procedures (D'Agnillo and Alayash, 2002). Briefly, the cells were seeded in six-well plates and grown in complete medium for six days. The redox transitions of the hemoglobins were measured in cultures containing 50 µM Hb with and without 10 mU/mL GOX for periods between 2 hour and 24 hour. At each time interval the hemoglobin solution was removed from cells and the composition of oxy, ferric and hemichrome species were calculated as described in section 5.1.2. The cells were washed twice and trypsinized, and the DNA was extracted using a DNA ladder extraction kit (BioVisions). The electrophoresis technique using 1.2% agarose gel was used to monitor the apoptosis in cells. Also, cells were seeded in 96-well plates and incubate under the same conditions with the hemoglobins with or without GOX. Cell apoptotic levels were measured using the Apo-One Caspase 3/7 kit from Promega, Inc. The caspase activity was detected with the spectrofluorometer Spectra MAX GEMINI EM (Molecular Devices) at 485 nm_{Ex}/521 nm_{Em}. The Apo-One Caspase-3/7 contains a rhodamine 110, bis-(N-CBZ-L-aspartyl-L-glutamyl-L-valyl-L-aspartic acid amide) (Z-DEVD-R110) substrate that when cleaved by the caspases activated by apoptosis forms the fluorescent rhodamine 110. Therefore, the fluorescent

product is proportional to apoptotic levels in cells. The non-treated cells and cells with 1.5% Clorox were used as negative and positive controls, respectively. The results are expressed in relative fluorescence units (RFU).

2.3.8 Cell morphology after exposure to hemoglobins and glucose oxidase

The endothelial cells were subcultured and treated as described in section 2.3.7. At the end of each incubation time with hemoglobin, GOX or both, the media was aspirated and the cell morphology was analyzed using a phase contrast microscope. Figure 2.11 shows the morphology of the bovine aortic endothelial cells after exposure to α -DBBF Hb for 24 hours. In one set of experiments, the cells were incubated in 1mL staining buffer (10mM HEPES/NaOH, 140 mM NaCl, 2.5 mM CaCl₂, pH 7.4) containing 2.5 μ g/mL propidium iodide, 7.5 μ g/mL Hoechst 33342, and 15 μ L Alexa Fluor 488-annexin V conjugate (Molecular Probes, Eugene, OR, USA) for 20 minutes at 25°C. Fluorescence microscopy was used to monitor the apoptosis or necrosis in cells.

2.3.9 Statistical analysis

Experiments were performed at least three times. Levels of statistical significance were determined by using the unpaired two-tailed Student's *t*-test. Results are presented as means \pm SD. Probability (*p*)-values of less than 0.05 were considered significant.

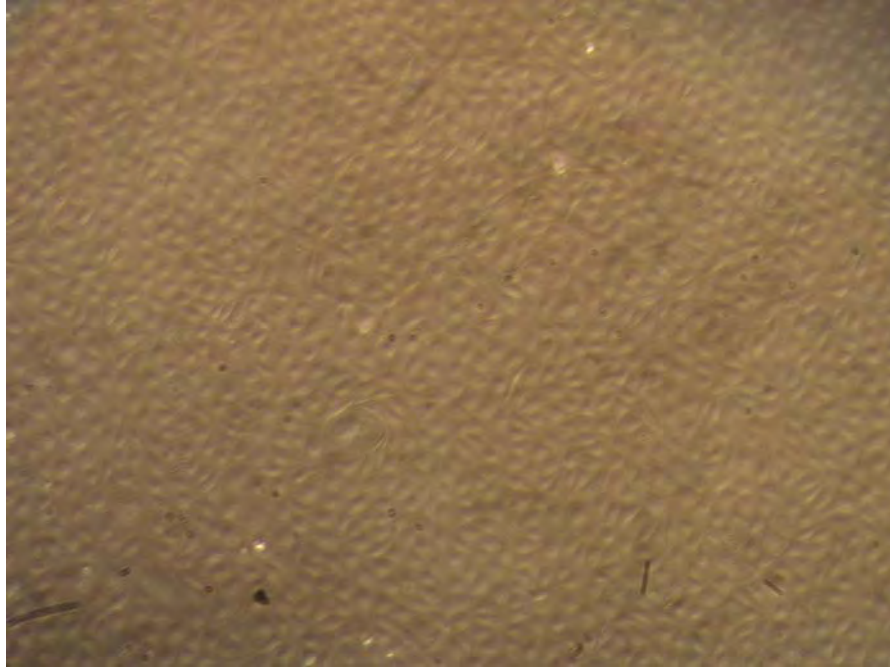


Figure 2.11 Bovine aortic endothelial cells after exposure to α -DBBF Hb. Endothelial cells morphology was monitored for 24 hrs during incubation with 50 μ M α -DBBF Hb.

3 HEMOGLOBINS REACTION WITH NITRIC OXIDE

3.1 Introduction

For many years the cell free hemoglobins, commonly known as hemoglobin-based oxygen carriers (HBOCs), have been studied to find the ideal oxygen carrier prototype. But, clinical trials have revealed adverse effects resulting from infusion of the HBOC's (Vandergriff, 2000; Mackenzie & Bucci, 2004; Stowell et al., 2001; Sakai et al., 2008) in which most of the hemoglobin based oxygen carriers have demonstrated vasoconstrictive properties as result of nitric oxide scavenging. These reactions result in imbalance for blood pressure control mechanisms in humans and animals (Alayash, 2004). Experimental heme protein prototypes from sperm whale myoglobins have been used to investigate the effect of the amino acid residues in and around the heme pocket with the purpose of produce mutants with favorable ligand binding characteristics. These characteristics include moderate oxygen affinity and the resistance to spontaneous and chemically NO-driven oxidation. Generally, the focus of current site directed mutagenesis strategies on hemoglobins and myoglobin is to alter electrostatic and steric interactions between the bound ligand and residues at the LeuB10, HisE7, and ValE11 positions. It has been shown, for example, that large apolar residues (Leu, Phe, Trp) at the B10 and E11 positions inhibit the NO-induced and spontaneous oxidation in both Mb and Hb by excluding oxidants and proton donors from the immediate vicinity of the bound ligand (Eich et al., 1996).

The study of the reaction of the hemoglobins with NO is important to understand biological processes such as the vasoconstriction effects produced by the cell free

hemoglobins. Therefore, this part of the investigation is focussed on the ligand interactions of the *L. pectinata* HbI, HbII and a recombinant HbI, in which PheB10 was replaced by TyrB10 with nitric oxide. This study reports the kinetic rate constants for the reaction of the NO-induced oxidation, the ferric association to the hemoglobins, and the NO dissociation. All the reactions were compared with those of the human chemically modified α -DBBF hemoglobin. Among the three hemoglobins studied from *L. pectinata* both oxy and ferric forms of HbII reacted extremely slowly with NO and its metabolites. The kinetic and structural data suggest that the proximity of TyrB10 and GlnE7 to the heme iron in HbII minimize the exposure of heme to solvent thus maintaining an oxidative stability and reducing its reactivity towards NO.

3.2 Nitric oxide reaction results

3.2.1 NO-induced oxidation

The reaction of the different hemoglobins with nitric oxide shows the overlaid spectra for the transition from the oxy Hb to ferric Hb. As a result of the reaction, the oxy hemoglobin is oxidized in the presence of NO in the reaction:



Thus, Figure 3.1 shows the overlaid spectra for the reaction of 0.5 μM oxy α -DBBF Hb with 10 μL of a saturated NO solution. The initial spectrum is that of the oxy species with a band at 416 nm, which at 20 seconds shifts to 412 nm, and at 40 seconds was displaced to 407 nm. The Q bands also show the transition to the ferric species with broad bands at 540 nm and 576 nm, and an initial increase in the 633 nm band. Once the Soret band reached a maximum at 407 nm, the intensity of the band starts to decrease suggesting a rapid oxidation and

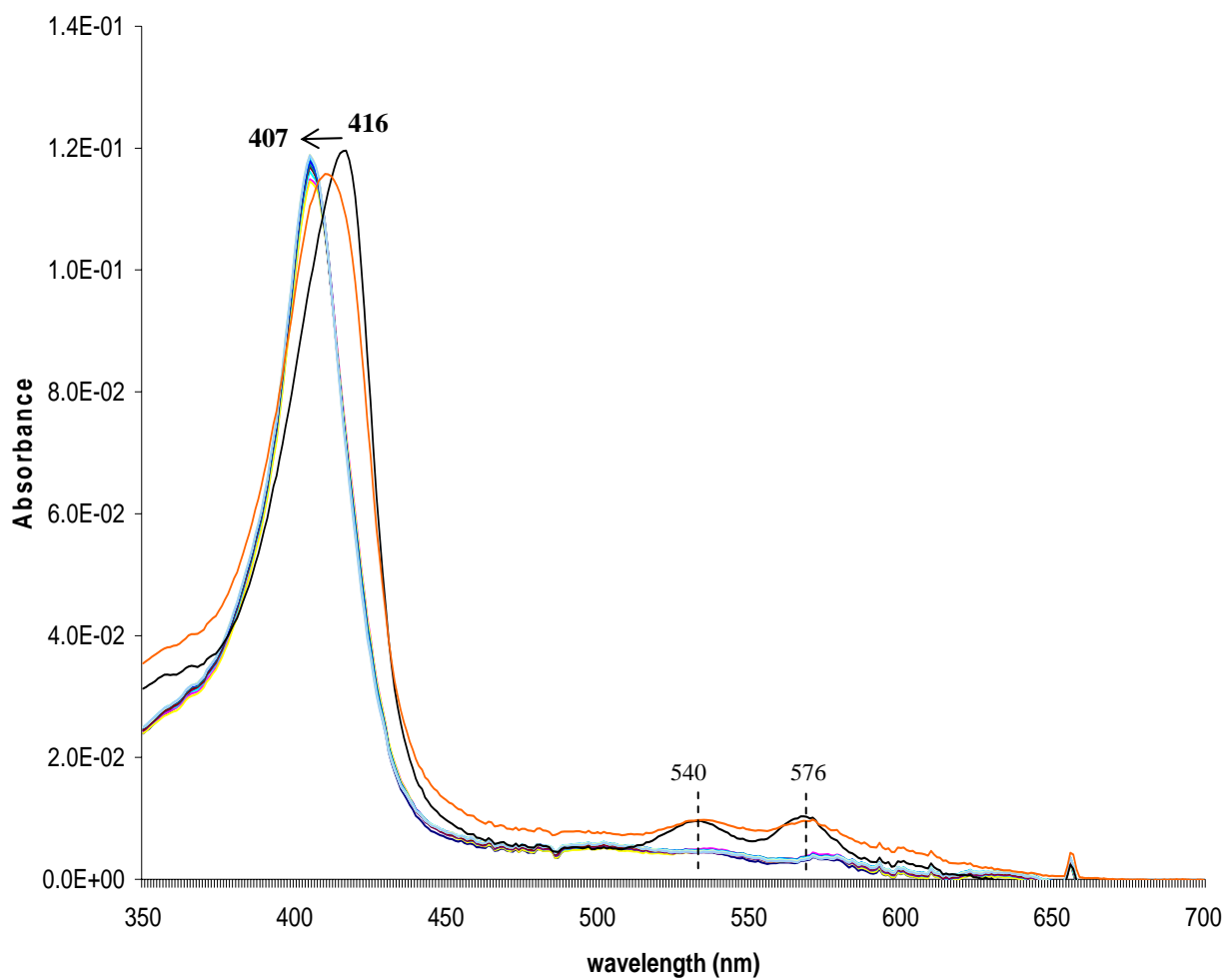


Figure 3.1 Oxidation reaction of 0.5 μ M oxy α -DBBF Hb by 10 μ L NO. Oxy α -DBBF Hb (416 nm) shifts to ferric α -DBBF Hb (407 nm). The oxy α -DBBF Hb Q bands broaden and decrease, while increase the bands characteristic of the ferric species.

possible heme degradation by the production of other ROS. Figure 3.2 shows the NO-induced oxidation for oxy HbII under the same experimental conditions. A very similar sequence of spectra was obtained for the HbI PheB10Tyr mutant. The initial spectrum shows a Soret band maximum at 414 nm representative of the oxy HbII species, which decreases and shifts to the left, reaching the ferric species band at 404 nm, near 200 seconds. But, it is important to mention that although the Soret band represents a ferric species, the Q bands suggest that HbII was not completely oxidized, showing a band at 605 nm and a mixture between the oxy and the ferric oxidation states. Similarly, the NO-induced oxidation for 0.5 μM HbI is shown in Figure 3.3. The shift in the Soret band from 416 nm to 407 nm is accompanied with a gradual increase in the absorption of the bands. The Q bands show the formation of the ferric species with a decrease in the 541 nm and 576 nm, and increases in the 502 nm and 633 nm bands.

Figure 3.4 shows the time courses for the NO-induced oxidation of oxy HbI in comparison to that obtained for oxy HbII under the same stopped-flow conditions. These time courses were fitted well to a single exponential expression with an offset (Materials and Methods, Section 2.2.4). Plots of the pseudo first-order rate constants, k_{obs} versus NO concentrations are linear, as shown in Figure 3.5, for HbI, HbII and the HbI PheB10Tyr mutant. Also, Figure 3.5 shows the plot derived for the reaction of human cross-linked α -DBBF Hb, a well documented vasoactive oxygen carrier in animals and humans because of its avid NO binding (Abassi et al., 1997). The second order kinetic rate constants for the NO-induced oxidation are shown in Table 3.1 with values of $18.95 \mu\text{M}^{-1}\text{s}^{-1}$, $2.76 \mu\text{M}^{-1}\text{s}^{-1}$, and $91.65 \mu\text{M}^{-1}\text{s}^{-1}$ for HbI PheB10Tyr, HbII and HbI, respectively. The rate constant for α -DBBF

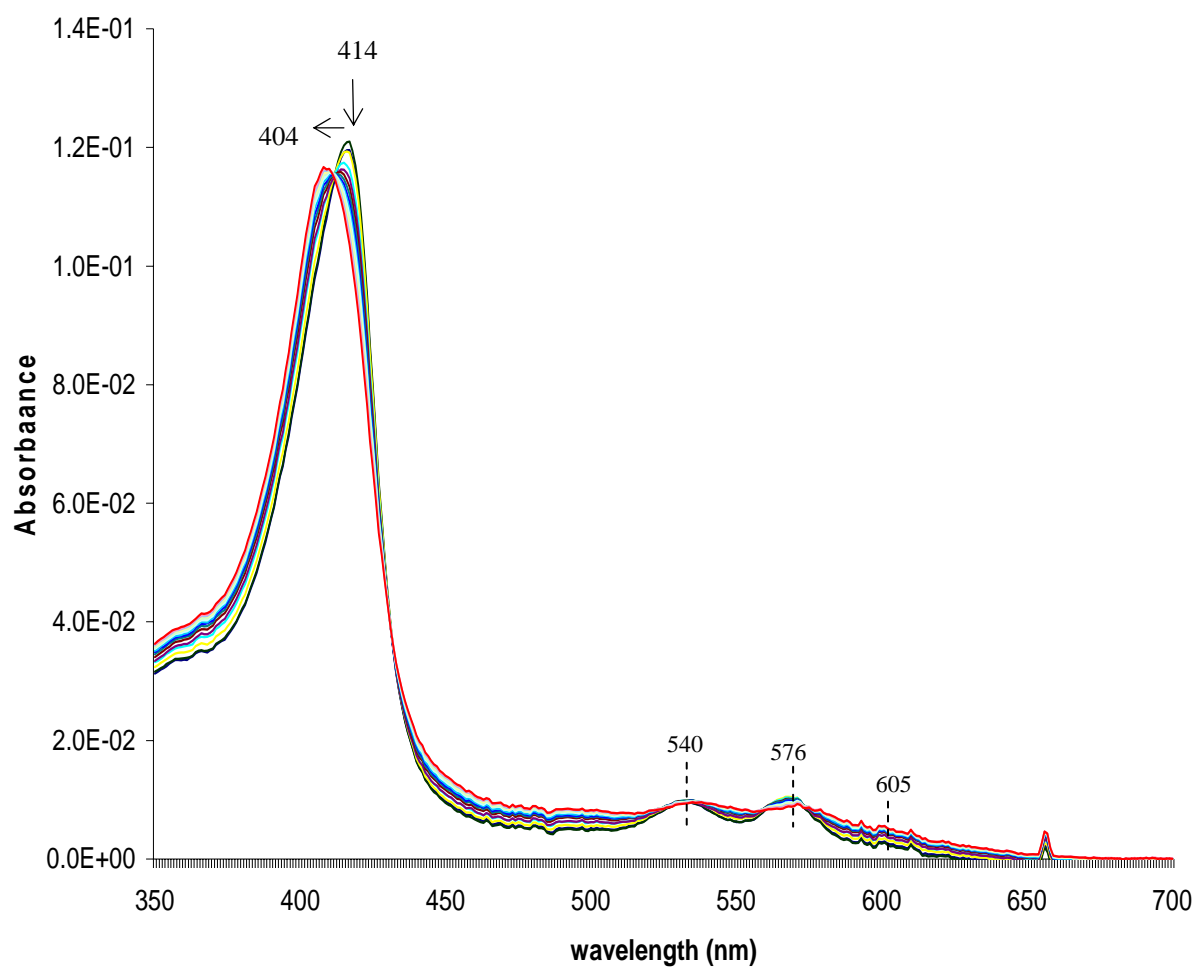


Figure 3.2 Oxidation reaction of 0.5 μM oxy HbII by 10 μL NO. Oxy HbII (414 nm) shifts to ferric HbII (404 nm). The absence of ferric Q bands evidences the hemoglobin resistance to oxidation by nitric oxide.

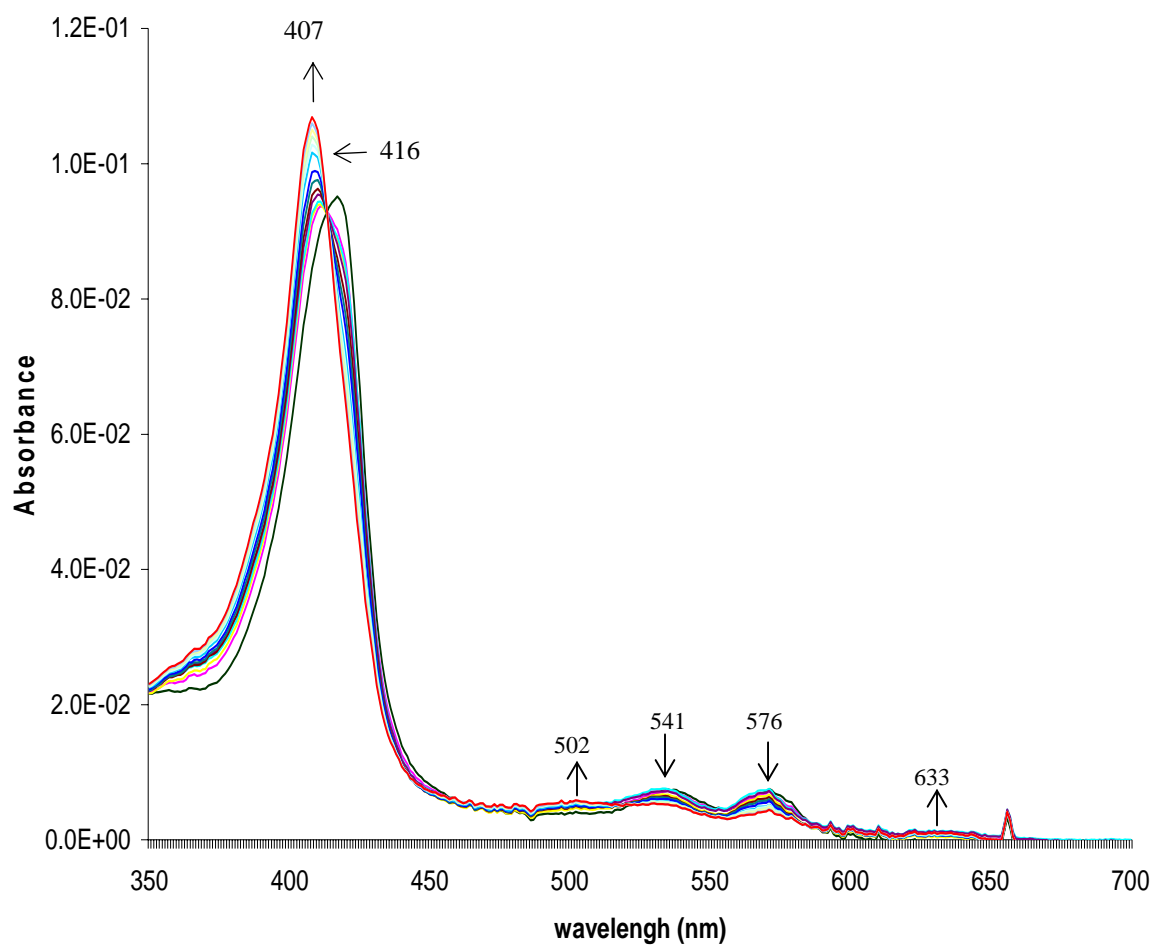


Figure 3.3 Oxidation reaction of 0.5 μM oxy HbI by 10 μL NO. Oxy HbI (416 nm) shifts to ferric HbII (407 nm). Up arrows represent increasing of the ferric bands, while down arrows represent the decrease in oxy bands.

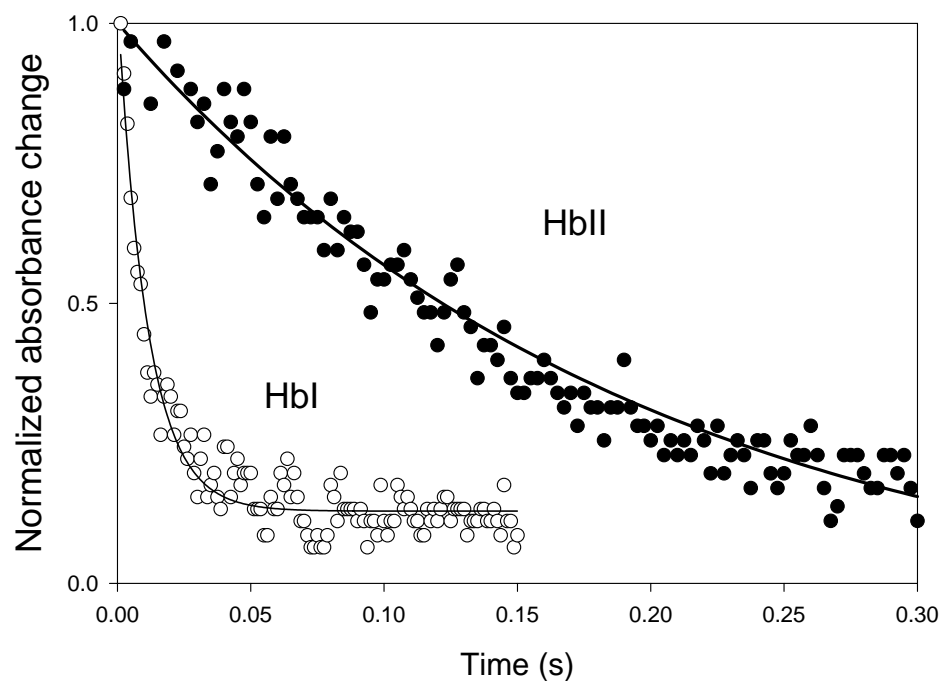


Figure 3.4 Stopped-flow kinetics of NO-induced oxidation of *L. pectinata* HbI and HbII. Normalized time courses for the reactions of 0.5 μM NO and 0.5 μM HbI or HbII. The solid lines are the nonlinear least-square fits to the exponential decay equations. The kinetic rate constants were obtained from the fit of the average of at least three independent experiments.

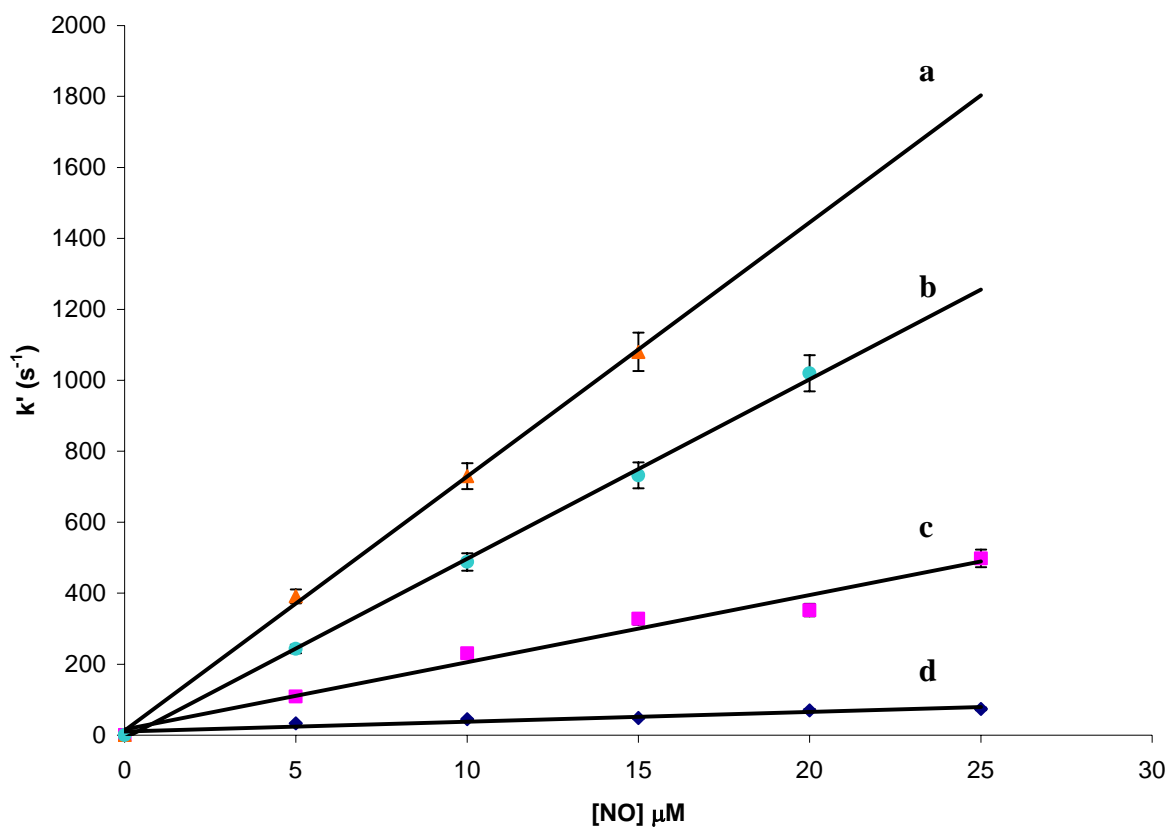


Figure 3.5 Plot of the apparent rate constants for the NO-induced oxidation of *L. pectinata* hemoglobins and α -DBBF Hb. (a) HbI, (b) HbI PheB10Tyr, (c) α -DBBF Hb, (d) HbII.

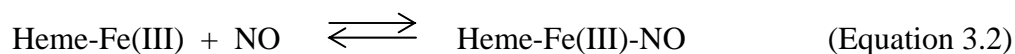
Table 3.1 Kinetic and equilibrium rate constants for the reaction of NO with the oxy, deoxy and ferric forms of *L. pectinata* and α -DBBF Hb hemoglobins.

Hemoglobin	$k'_{\text{ox, NO}},$ $\mu\text{M}^{-1}\text{s}^{-1}$	$k'_{\text{NO}}(\text{Fe}^{2+}),$ $\mu\text{M}^{-1}\text{s}^{-1}$	$k_{\text{off, NO}},$ 10^{-4}s^{-1}	$k'_{\text{NO}}(\text{Fe}^{3+}),$ $\mu\text{M}^{-1}\text{s}^{-1}$
α -DBBF Hb	19.0 ± 1.4	8.0 ± 1.6	1.2 ± 0.14	0.019 ± 0.0021
HbI	~ 91.6	37.0 ± 6.3	4.0 ± 0.37	3.85 ± 0.70
HbII	2.8 ± 0.4	1.1 ± 0.6	7.1 ± 0.53	0.66 ± 0.04
HbI PheB10Tyr	49.9 ± 0.6	1.2 ± 0.04	5.6 ± 0.26	3.09 ± 0.38

Hb is $49.9 \mu\text{M}^{-1}\text{s}^{-1}$, similar to the value previously reported (Eich et al., 1996). As can be seen in Table 3.1, the rate derived for the clam HbI is approximately 4-5 folds faster than that of α -DBBF Hb and 30 times higher in magnitude to that calculated for HbII. However, the HbI PheB10Tyr kinetic rate constant for the reaction with the nitric oxide is not similar to HbI neither to HbII, obtaining an intermediate value. This behavior is different to the one observed in the reactions with hydrogen peroxide, where the rate constant values for HbI PheB10Tyr and HbII are very similar.

3.2.2 Reaction of ferric hemoglobins with nitric oxide

Reaction of NO with the ferric forms of unmodified and chemically cross-linked Hbs have been reported to be a sensitive probe for heme pocket alterations irrespective of their oxygen affinities (Alayash et al., 1993). Figure 3.6 shows the average of the time courses for the initial events in the reaction of ferric hemoglobin with NO where



The graph illustrates that the reaction for HbI (a) is faster than for HbII (b). Figure 3.7 shows the plots for the pseudo first-order rate constants, k_{obs} versus NO concentrations for the reaction. The trend line for HbI and the mutant were forced to pass through the intercept, suggesting that for these two samples the reaction can be oxygen dependent, and not a simple bimolecular process. Table 3.1 reports the second order kinetic rate constant values for the combination of NO with the ferric hemoglobins. The values are $3.85 \mu\text{M}^{-1}\text{s}^{-1}$, 0.66 , and $3.09 \mu\text{M}^{-1}\text{s}^{-1}$ for HbI, HbII and HbI PheB10Tyr, respectively. Compared to α -DBBF Hb, which has a value of $0.019 \mu\text{M}^{-1}\text{s}^{-1}$, the reaction of HbII is approximately 35 fold faster. *L. pectinata* HbII again shows a much slower binding rate to the ferric iron compared to the rates calculated for HbI and HbI PheB1010Tyr mutant included in this study under the same experimental conditions. These results suggest that when the ferric hemoglobin is formed by the normal process of autoxidation, HbII is also less reactive towards nitric oxide compared with the other *L. pectinata* hemoglobins.

3.2.3 Hemoglobins NO dissociation

The molecular replacement of the hemoglobins bound to NO by CO in the reaction



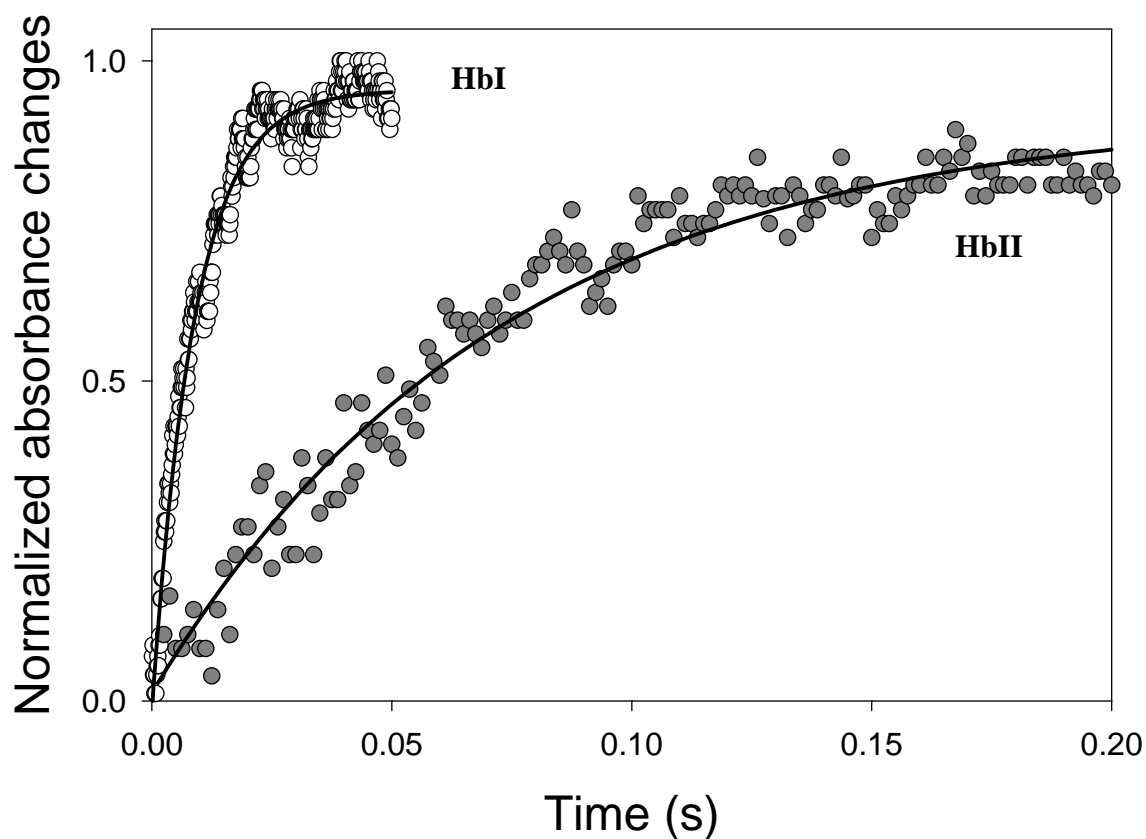


Figure 3.6 Stopped-flow time courses of rapid reactions of 0.5 μM ferric HbI and HbII with 15 μM NO solution measured at 420 nm in 50 mM sodium phosphate buffer at pH 7.4 and 20°C. The solid lines were obtained from the nonlinear least-square fits to the exponential increase equations of the average of 3 - 5 independent experiments.

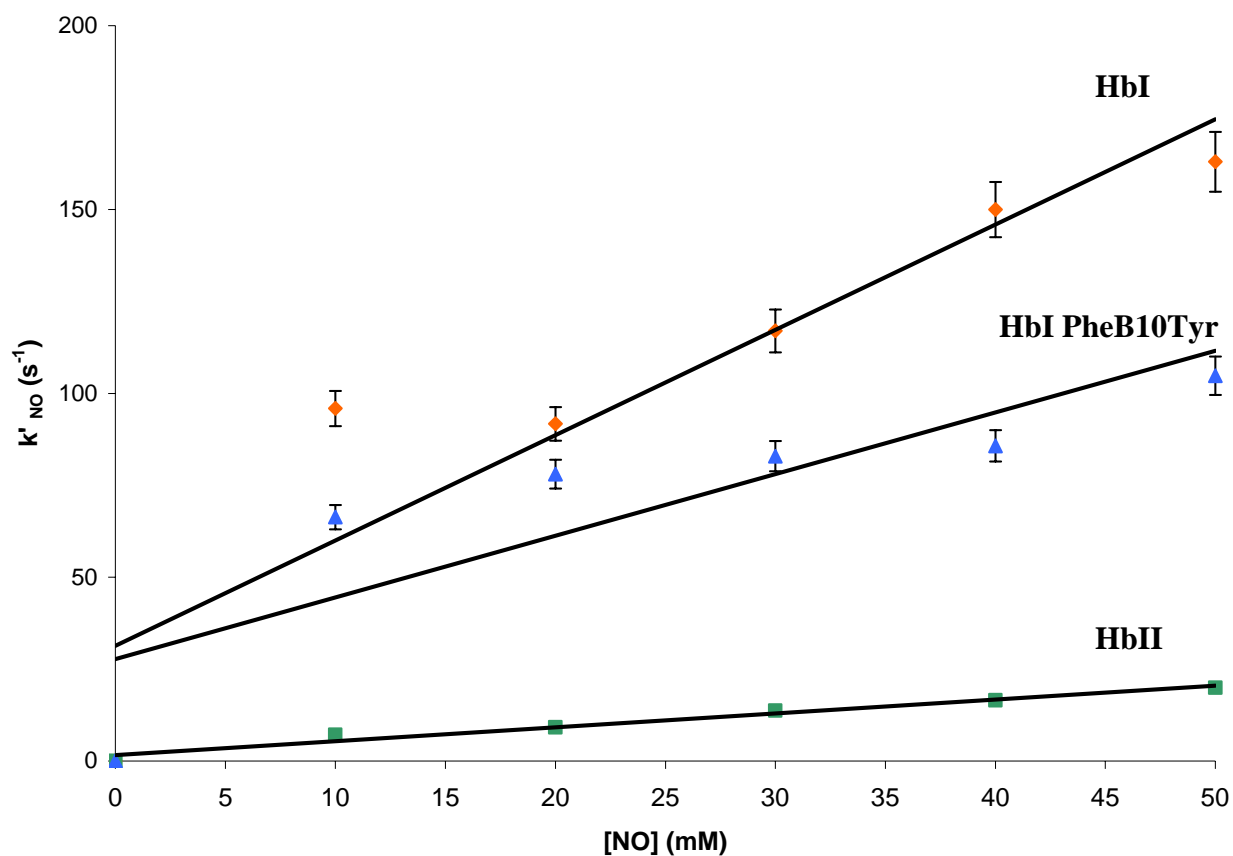


Figure 3.7 Plot of the apparent rate constants of NO association to ferric HbI, ferric HbI PheB10Tyr, and ferric HbII. Each protein (15 μ M) was mixed with 20-50 μ M NO in a stopped-flow apparatus and monitored at 420 nm.

allowed for the measurement of the NO dissociation rate constants. Figure 3.8 shows the kinetic traces for the Heme-Fe(II)-NO dissociation monitored at 420 nm. This reaction indicates that once the NO complex is formed, HbII releases completely the NO at approximately 115 minutes. This is very fast compared to our control α -DBBF Hb, where the reaction still continues to 250 minutes. The kinetic rate constant values for the hemoglobin's NO dissociation ($k_{\text{off, NO}}$) are $4.0 \times 10^{-4} \text{s}^{-1}$, $7.1 \times 10^{-4} \text{s}^{-1}$, $5.6 \times 10^{-4} \text{s}^{-1}$, and $1.2 \times 10^{-4} \text{s}^{-1}$ for HbI, HbII, HbI PheB10Tyr, and α -DBBF Hb, respectively (Table 3.1). The rate constant value for α -DBBF Hb is similar to those reported for native Hb and is significantly lower than the calculated for the *L. pectinata* hemoglobins. The kinetic rate constant for the NO dissociation from HbII is 1.5 fold higher than that of HbI and HbI PheB10Tyr, confirming that there is a different mechanism between the *L. pectinata* hemoglobins for their interaction with NO.

3.3 Discussion

One of the most widely accepted interpretations of blood pressure imbalances in patients receiving hemoglobin-based transfusion therapy is the inactivation of NO by extracellular hemoglobin. Therefore, considerable efforts have been focused in recent years to engineering second generation oxygen carriers with reduced reactivity toward NO, but at the same time their design must retain acceptable oxygen carrying capabilities. In this respect, the substitution of HisE7 with Gln, the only other residue able to establish a H-bond with oxygen has been the target of oxygen affinity lowering effects. It has also been shown that the flexibility of the flavohemoglobin heme pocket allows the movement of both

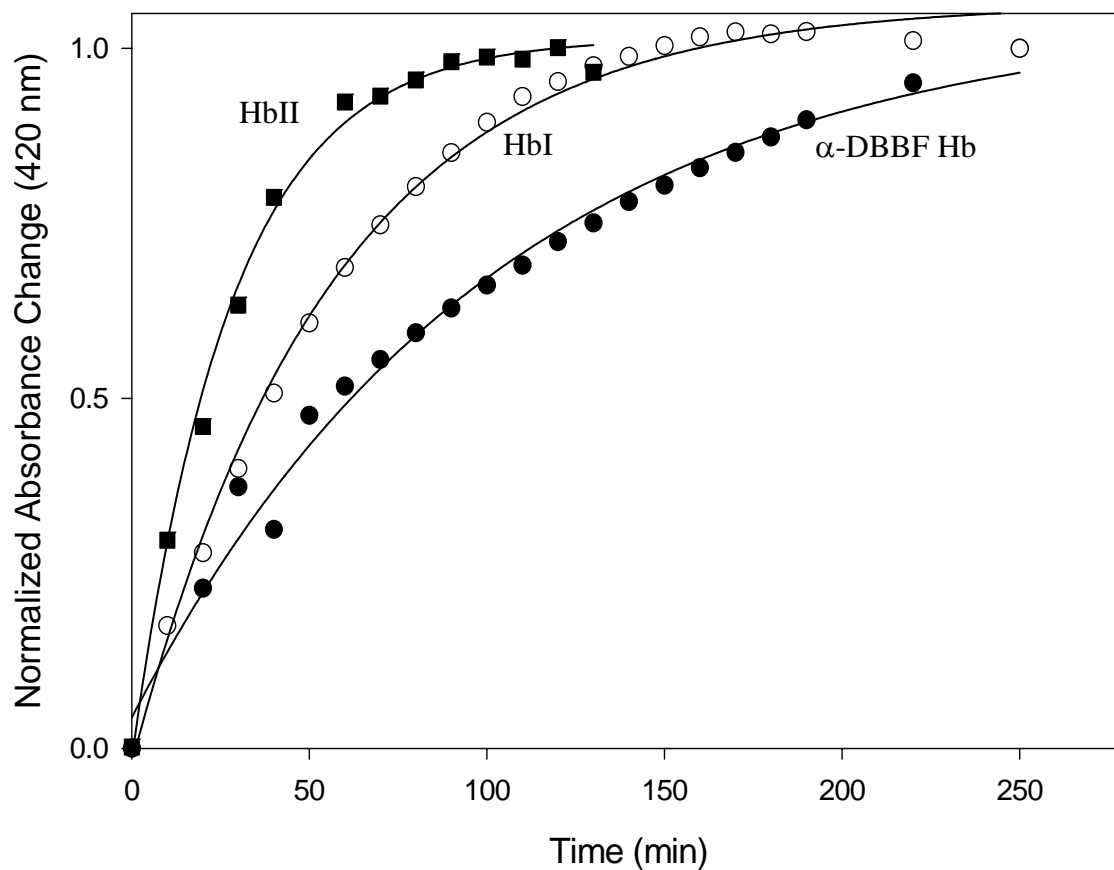


Figure 3.8 Kinetic traces for the NO dissociation from the NO-Hb complex. ■ HbII, ○ HbI, ● α-DBBF Hb. Deoxygenated Hbs (5 μM) were mixed with equal molar ratio of NO, and then incubated with 1 mM CO and 10 mM sodium dithionite in 100 mM sodium phosphate buffer, pH 7.4, in sealed cuvettes. NO dissociation was measured at 420 nm in a spectrophotometer. The solid lines are the non-linear least-square fits to the single exponential fit of the average for three independent kinetic traces.

GlnE7 and TyrB10 closer to the heme to accommodate both O₂ and NO molecules simultaneously to function as NO dioxygenase to provide protection against NO and related reactive species, and adopt a peroxidases-like structure in order to perform its function (Mukai et al., 2001, Gardner, 2008). Moreover, Eich and coworkers (Eich et al., 1996) showed that increasing the steric hindrance of the distal heme pocket leads to significant reduction in the NO association rate constants. In this respect, site directed mutations of Mb prototypes have generally replaced HisE7, LeuB10 and ValE11 by large apolar residues. Comparison studies of the NO-induced oxidation showed decreases with the substitution of LeuB10 and ValE11 by phenylalanine or tryptophan. Therefore, it was suggested that the substitution at PheB10 and PheE11 are good candidates to increase resistance to NO-induced oxidation. Other studies with a series of genetically modified hemoglobins containing Phe, Gln and Trp mutations in the α and β subunits produced a mutant with a very low reactivity towards NO (Olson et al., 2004). Effects of some of these recombinant hemoglobins were tested in several animal models of exchange transfusion and showed improved blood pressure control as well as improvement in blood flow and tissue oxygenation. However, clinical development of new recombinant hemoglobins with heme pocket alterations was recently abandoned due to several side reactions (Winslow, 2006).

Table 3.2 shows the kinetic rate constants for the NO-induced oxidation of several myoglobin mutants. The wild type myoglobin oxidation by NO has a kinetic rate constant value of 35 $\mu\text{M}^{-1}\text{s}^{-1}$. The variation of ValE11 to Phe or Trp reduces the rate constant value to 10 $\mu\text{M}^{-1}\text{s}^{-1}$ and 4.1 $\mu\text{M}^{-1}\text{s}^{-1}$, respectively. The change in the amino acid LeuB10 by Phe and

Table 3.2 Kinetic rate constants for myoglobin NO-induced oxidation and myoglobin mutants.

Heme Protein	$k'_{\text{ox, NO}}$ ($\mu\text{M}^{-1}\text{s}^{-1}$)
Wild type Mb	35
ValE11Phe	10
ValE11Trp	4.1
LeuB10Phe	8.1
LeuB10Trp	3.2
HisE7Gln	160
LeuB10Phe/HisE7Gln	17
LeuB10Trp/HisE7Gln	2.0
Mb	13
Leu(B10)Phe/His(E7)Gln/Val(E11)Phe	

Dou et al., 2002

Trp also causes a decrease in the rate constant with values of $8.1 \mu\text{M}^{-1}\text{s}^{-1}$ and $3.2 \mu\text{M}^{-1}\text{s}^{-1}$, respectively. However, the mutation in the HisE7 position increases the kinetic rate constant to $160 \mu\text{M}^{-1}\text{s}^{-1}$. This study demonstrates that the steric effects caused by the substitution of large and aromatic amino acids in position E11 and B10 decreases the interactions with NO, as for example the Trp. The heme pocket of *L. pectinata* HbI mimics the triple mutant of sperm whale Mb, Leu(B10)Phe/His(E7)Gln/Val(E11)Phe, that has similar oxygen affinity but higher association and dissociation rate constants (Table 3.3). Engineering of these three residues in sperm whale Mb produced 7-fold lower sulfide affinity to Mb compared to that of *Lucina pectinata* HbI. Comparison of solution and crystal structure between the triple mutant and HbI from the clam showed that HbI has a significantly larger ligand-binding site than that found in Mb mutants, which should facilitate the binding of large H_2S ligand. In addition, changes in the orientation of PheB10 and PheE11, and the decrease in the size of the distal pocket in the mutant may have accounted for these differences. The NO-induced oxidation rate constant for the triple mutant is $13 \mu\text{M}^{-1} \text{s}^{-1}$ (Dou et al., 2002), and is smaller than the value of $91 \mu\text{M}^{-1} \text{s}^{-1}$ calculated for HbI (Table 3.1). This unusually high rate for the NO-oxidation for HbI is matched by higher association and dissociation rate constants (Table 3.3) than the other heme proteins listed in the same table.

Lucina pectinata HbII has a heme pocket similar to many invertebrate hemoglobins which contain GlnE7 and TyrB10. The nitric oxide-induced oxidation for HbII follows the same antioxidant pattern as in the reactions with hydrogen peroxide, discussed in Chapter 4. Figure 3.9 shows the proposed mechanism of the NO-induced oxidation for HbII showing the distal GlnE7 and TyrB10 interactions. The oxy HbII (1) reacts with nitric oxide forming the peroxynitrite complex (2). It was suggested that previous to the NO binding, the hemoglobin

Table 3.3 Kinetic rate constants for oxygen reactions of *L. pectinata* hemoglobins and α -DBBF Hb.

Heme protein	$k'_{\text{on, O}_2}$ ($\mu\text{M}^{-1}\text{s}^{-1}$)	$k_{\text{off, O}_2}$ (s^{-1})	P_{50} , mm Hg
HbI	$\sim 200^a$	92.2^b	0.18^a
HbII	0.39^a	0.146^b	0.13^a
HbI PheB10Tyr	6.8^b	0.6^b	0.05^b
α -DBBF Hb	17^c	56^c	27.0^c
Mb Leu(B10)Phe/His(E7)Gln/Val(E11)Phe	16^d	3^d	0.11^d

^a Kraus and Wittenberg, 1990

^b De Jesús-Bonilla et al., 2007

^c D'Agnillo & Alayash, 2000

^d Dou et al., 2002.

has to be a ferric-iron-superoxo species to react with NO (Gardner et al., 2006). The next step in the mechanism is the isomerization of the heme-peroxynitrite complex to nitrate (3), thus allowing the release of a nitrate molecule producing ferric HbII (4). The reactions of heme reductase and oxygen with the ferric heme convert it again to oxy hemoglobin. The kinetic data show that the oxidation by NO is 6.5 times smaller in HbII ($2.8 \pm 0.4 \mu\text{M}^{-1}\text{s}^{-1}$)

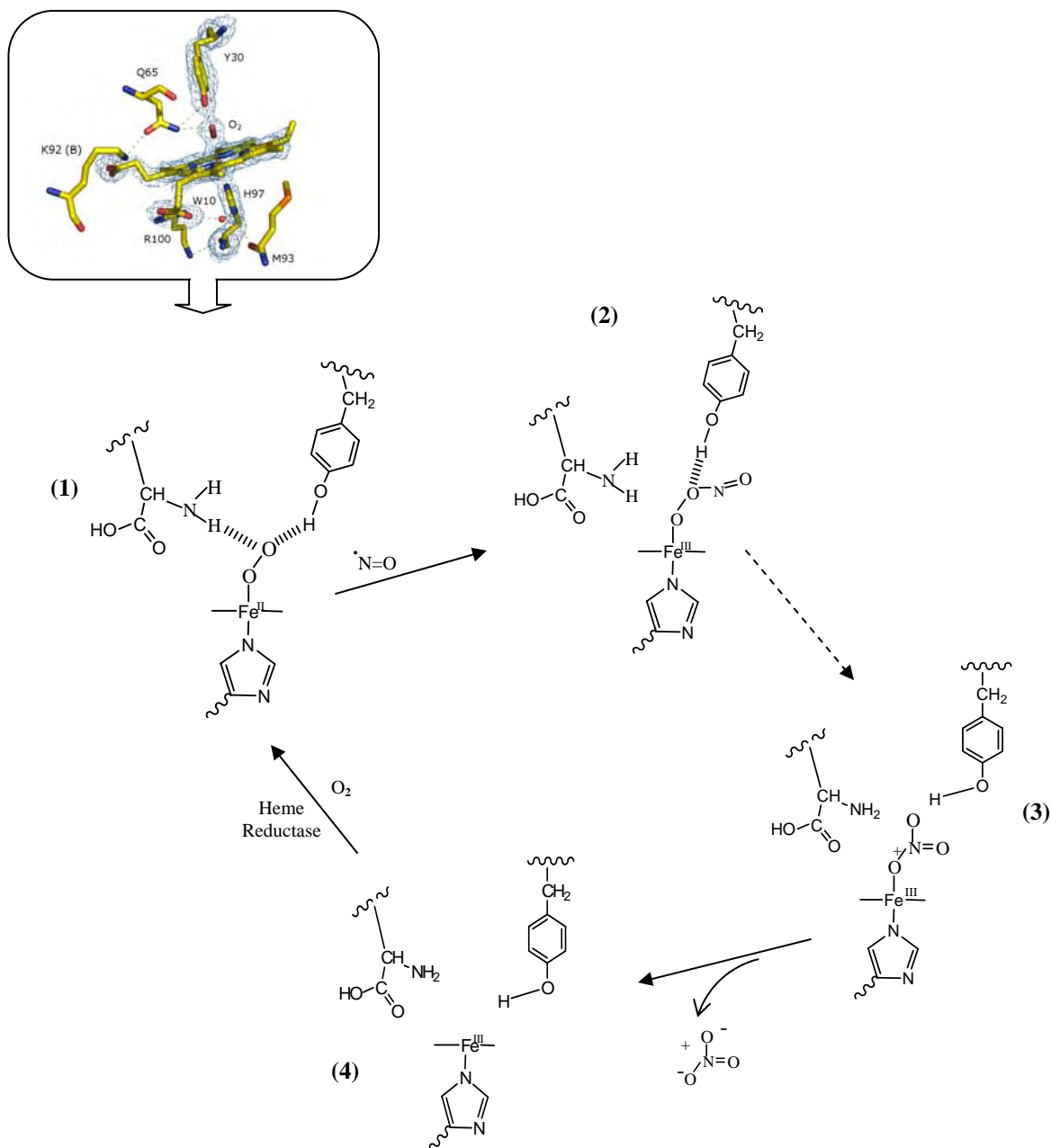


Figure 3.9 Proposed mechanism for the nitric oxide-induced oxidation of the *L. pectinata* HbII hemoglobin. Oxy HbII reacts with NO forming the peroxynitrite complex. The peroxynitrite isomerizes to nitrate. Nitrate releases from HbII forming ferric HbII. In the left corner: HbII crystallographic structure, PDB 2OLP, Gavira et al., 2008. Model adapted from Gardner et al., 2006.

than in the α -DBBF Hb ($19.0 \pm 1.4 \mu\text{M}^{-1}\text{s}^{-1}$; Table 3.1). Once formed the Hb-NO complex, HbII releases quickly the NO showing a very high dissociation rate constant of $7.1 \pm 0.53 \mu\text{M}^{-1}\text{s}^{-1}$, compared to α -DBBF Hb with a rate constant value of $1.2 \pm 0.14 \mu\text{M}^{-1}\text{s}^{-1}$. It has been suggested that the NO-induced oxidation is favored in those heme proteins that have larger oxygen association rate constants and smaller oxygen dissociation as the heme-Fe(II)-O₂ intermediate is required for this reaction (Olson et al., 2004). Therefore, it is not surprising that the NO oxidation rate for HbII is extremely low compared to that for all heme proteins including α -DBBF Hb. Previous studies for HbII showed a pH dependence in which at neutral pH coexists a mixture of a ferric hydroxide and a ferric tyrosinate-ligated structure (Pietri et al., 2005). The flexibility of this pocket allows the protein to adopt conformational changes that give the TyrB10 some freedom to control ligand reactivity (Pietri et al., 2005). However, the introduction of TyrB10 in the heme pocket of HbI in combination with Gln and the two Phe's did not completely reverse the NO-induced oxidation of this HbI mutant, which was only reduced by approximately 50% (HbI $k'_{\text{ox, NO}} = 91.6 \mu\text{M}^{-1}\text{s}^{-1}$; HbI PheB10Tyr $k'_{\text{ox, NO}} = 49.9 \mu\text{M}^{-1}\text{s}^{-1}$; Table 3.1).

In wild type ferric Mb, the rate constants for the NO binding were approximately 100 times smaller than the rate constants for the NO binding and oxidation of the corresponding oxy hemoglobin. However, aromatic substitutions at the B10 and E11 positions caused a much smaller decrease in the association of the ferric hemoglobin, $k_{\text{NO heme-Fe(III)}}$, than those observed for the NO-induced oxidation, $k_{\text{ox, NO}}$, and the NO association to deoxy hemoglobin, $k_{\text{NO heme-Fe(II)}}$. The rate for NO binding to the ferric form of HbI and its mutant were approximately 23 and 16 times smaller than their respective oxidation of their oxy species by NO. The NO binding to the ferric HbII is again the lowest among the clam

hemoglobins. Similar to the triple mutant Mb, the kinetic rate constant is only 4-5 times smaller in magnitude than the rates of the respective reactivity of their oxy hemoglobin with NO. The kinetics of reaction of this ligand with the ferric iron is controlled by a completely different stereochemistry than in the NO binding to the oxy heme. In the case of ferric Mb, a water molecule coordinates with the iron atom and as a result, the ligand binding is limited in part by the strength of the heme-Fe(III)-OH₂ bond (Sharma & Ranney, 1978, Sharma et al., 1983).

Dynamical features were examined for HbI, Mb, and the Leu(B10)Phe/His(E7)Gln/Val(E11)Phe triple mutant of sperm whale Mb, in both unligated and bound to hydrogen sulfide (Fernández-Alberti et al., 2006). The parameters included rigid body motion, relative orientation of the heme prosthetic group within the HbI, hydrogen bond formation between the heme propionate groups and nearby amino acid residues, and changes in the distal cavity volume. These studies revealed the existence of a greater heme freedom in HbI than in sperm whale Mb. The active-site residues GlnE7, PheCD1, and HisF8 are also shown to be more flexible in unligated HbI than in the Mb mutant and sperm whale Mb. This dynamic behavior is absent in HbII where the heme group is firmly anchored in place. HbII, a dimer (Figure 1.10) with the characteristic globin fold with six α -helices surrounding the heme pocket, shows a hydrophobic distal cavity containing (Figure 3.9), GlnE7, TyrB10, PheCD1 and PheE11 at a distance from the heme Fe atom of 4.45 Å, 4.83 Å, 4.73 Å, and 5.78 Å, respectively. This heme pocket is much smaller than that of HbI distal center (Figure 3.10), in where GlnE7, PheB10, PheCD1 and PheE11, show a distance from the heme Fe atom of 4.32 Å, 6.26 Å, 4.92 Å, and 6.34 Å, respectively. In addition, HbII heme cavity is more collapsed than the *Mycobacterium* hemoglobin, where an average

size of 873 Å³ have been reported for the heme cavity of the former, while the latter is represented by an average volume of 1000 Å³. Furthermore, the heme pocket in the chain B of the HbII dimer is slightly more collapsed than in the chain A, as shown by the shorter distance between the O of the distal tyrosine and the iron atom (4.81 Å in chain A and 4.56 Å in chain B), and the volume size of the heme cavity (911.6 Å³ in chain A and 834.9 Å³ in chain B) (Gavira et al., 2008). These distances suggest that the architecture of HbII heme pocket is slightly narrower than that of HbI.

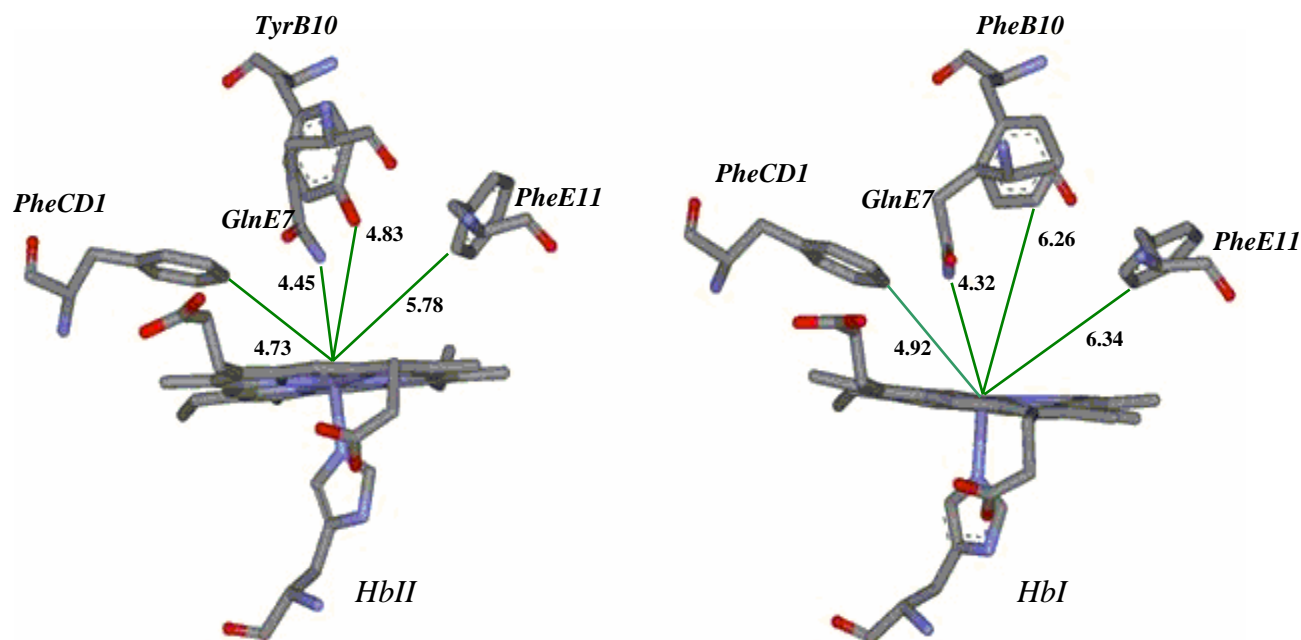
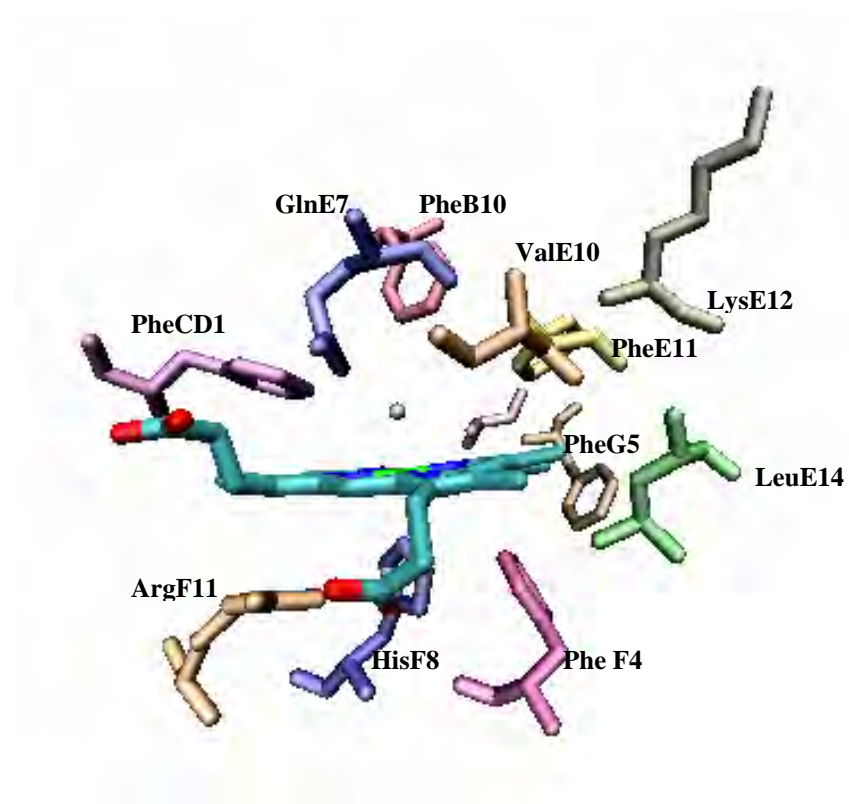


Figure 3.10 Stereo diagrams of the orientations of the distal residues of *L. pectinata* HbII and HbI. The distances (Å) from the residues to the heme iron atom were calculated from the C-ζ in the PheE11 and PheCD1, the N of the amide in the GlnE7, and from the oxygen in the TyrB10.

In addition to the smaller heme pocket due mainly to the short distance between the heme iron and the TyrB10 OH, there are other amino acids that hamper the NO entrance to the heme cavity. For example, Draghi (Draghi et al., 2001) showed that the TrpG5 in *Ascaris suum* fills all the side space, and in the case of myoglobin fills the cavity which corresponds to the xenon cavity Xe1. Figure 3.11 shows the amino acids that surrounds the heme pocket cavity of *L. pectinata* HbI (A) and the chain A of HbII (B). Heme pocket nearby residues for HbI are ValE10, LysE12, PheG5, LeuE14 and PheF4 that are substitute in HbII by SerE10, CysE12, TyrG5, GlyE14 and MetF14. Previous experiments (Draghi et al., 2001) showed that the replacement of LeuG5 by TrpG5 causes a 5 fold increase in the protein oxygen affinity. When the LeuG5 was replaced by PheG5 only has a small effect in the oxygen affinity. Thus, the position of this amino acid is relevant in the oxygen affinity and the NO entrance to the heme pocket. Figure 3.12 shows the superposition of HbI and HbII, based on the heme iron illustrating the higher electron density of the HbII TyrG5. Also, MetF4 and GlyE14 in HbII are less restrictive than PheF4 and LeuE14 in HbI, allowing a change in TyrG5 conformation that slows down the NO entrance to the heme pocket.

Clams and other water-breathing organisms are regularly and naturally exposed to NO, H₂S, and CO, for these gases occur normally in seawater. In general, the concentration of NO particularly in seawater is in the order of approximately 2×10^{-12} M. Recently it has been reported that both H₂S and NO are involved in seasonally modulating branchial muscle concentration in another Clam, *Mercenaria mercenaria* through the NO/cyclic GMP/protein kinase pathway (Gainey & Greenberg, 2005). The scavenging of NO by extracellular hemoglobin appears to have been at least partially reduced by evolutionary process leading to structural changes in the distal heme pocket in one of the three hemoglobins in the clam

A



B

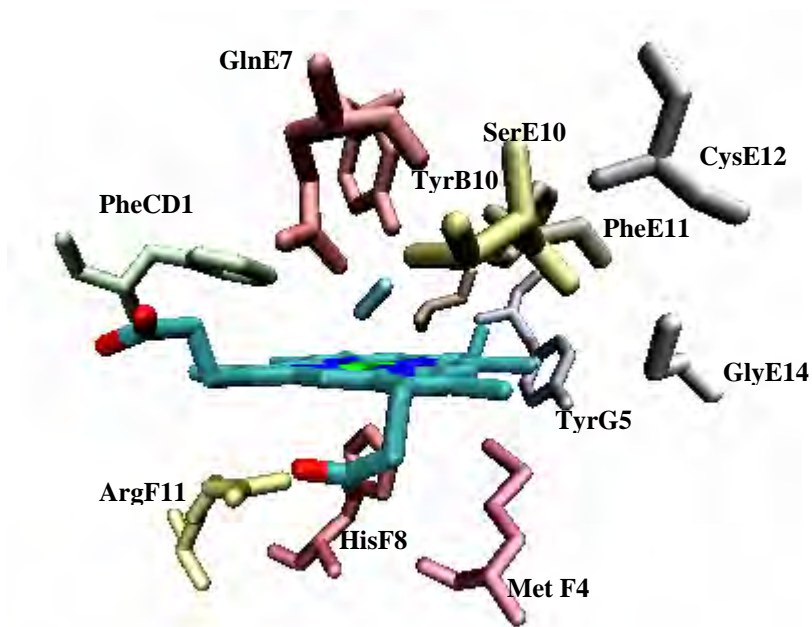


Figure 3.11 *Lucina pectinata* ferric HbI (A) and oxy HbII (B) heme pocket amino acids. These amino acids are directly linked to the conformational change that allows heme stability with bound molecules.

Lucina pectinata, particularly HbII. The co-existence of cysteine rich proteins, sulfur and NO carrying proteins in the clam blood, together with the strategic positioning of few amino acids in the heme pocket in HbII, may be involved in a regulatory mechanism against nitrosative stress (Gow et al., 2005). In the overall reactions, the HbII shows to produce low concentrations of ROS and RNS with no significant signs of formation of intermediate complexes, for example peroxynitrite. Therefore, regardless of the precise role of HbII in the NO physiology of the clam *Lucina pectinata*, the unusually well controlled NO entry in heme pocket, based on the kinetic and structural data presented may represent a model for the design of future oxidatively stable oxygen therapeutics with little or no vasoactivity.

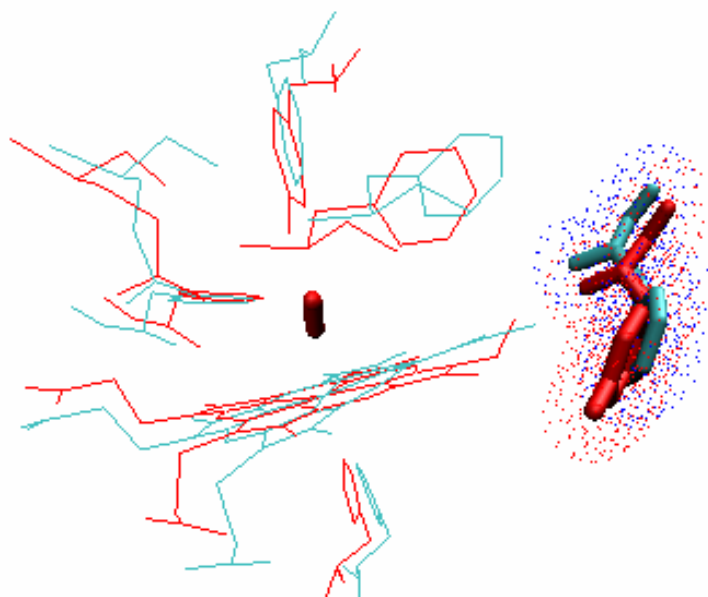


Figure 3.12 Superposition of oxy HbII and ferric HbI *Lucina pectinata* hemoglobins. The oxy HbII structure (red, PDB 2OLP), highlighting the heme and residues GlnE7, PheCD1, TyrB10, TyrG5, and proximal HisF8, is overlaid with the ferric HbI structure (cyan, PDB 1FLP), highlighting the heme, GlnE7, PheCD1, PheB10, PheG5, and proximal HisF8.

4 HEMOGLOBIN REDOX CHEMISTRY IN THE REACTION WITH HYDROGEN PEROXIDE

4.1 Introduction

In addition to the vasoconstrictive problems, infusion of the hemoglobin based oxygen carriers (HBOCs), also showed elevated rates of spontaneous oxidation (autoxidation) of their heme iron *in vivo*, and induced oxidative toxicity which are factors that significantly affects the outcome role of HBOCs (Vandergriff, 2000; Mackenzie, 2005; Stowell et al., 2001). Previous work suggested that peroxidative activity of the hemoglobins modify the heme oxidation state affecting the oxygen binding and the redox side reactions (Yeh & Alayash, 2003). One of the most studied reactions is that of the hemoglobin with the oxidant hydrogen peroxide. This reaction produces the high valent iron species, porphyrin π -cation radical ferryl compound I (heme-Fe(IV)=O Por⁺) that can be relatively stable or can spontaneously decay to its one-electron reduction product, which is the ferryl compound II, heme-Fe(IV)=O. In the blood, the oxy hemoglobin autoxidizes to form a non-functional ferric hemoglobin. At high concentrations of hydrogen peroxide, like in the case of ischemia or reperfusion, the ferric moiety forms the ferryl species by oxidation of another electron (Galaris et al., 1989, Jia et al., 2007). Various mechanisms for the oxidative process associated with hemoglobins have been reported (Nagababu & Rifkind, 2004, Nagababu et al., 2008). Both, reactions or mechanisms, agree that when an excess of H₂O₂ is present, the reaction leads to a chemical modification of the heme, in which the heme loses its tetragonal symmetry and adapts a new rhombic shape. The final product with this change in symmetry is the degradation of the heme protein or the loss of the porphyrin iron. Previous studies

show that the peroxidative reactions constrain the delivery and turnover of oxygen to cells, and the autoxidation and formation of radicals lead to heme damage and degradation (D'Agnillo & Alayash, 2002). Moreover, the reactions of H_2O_2 with proteins and its superoxide anions are detrimental in red cell pathological conditions. Studies with human hemoglobin HbA_0 conjugated to carboxylate dextran (Dex-BTC-Hb) were performed to investigate its autoxidation and redox reactions with H_2O_2 (Jia & Alayash, 2004). But this hemoglobin shows insensitivity to pH changes, a parameter that may be significant in physiological conditions.

The distal and proximal sites of the hemoglobin are the targets to study how the polarity, charge, pH, and the overall environment can affect the role of the molecule. Studies suggested that the distal histidine in myoglobin destabilizes the compound I and that the reaction of the compound I with peroxide occurs via a radical mechanism (Galaris et al., 1989; Ouellet et al., 2007). Site-directed mutation studies in Mb and Hb also suggested the myoglobin double mutation in HisE7Glu/LeuB10Phe as a blood substitution prototype (Rydberg et al., 2004). This double mutant enhances the pseudoperoxidase activity of the myoglobin. In this respect, previous studies for the reaction of HbI from the clam *Lucina pectinata* with hydrogen peroxide show a stable and characteristic band for the ferryl Compound I at 648nm, and was suggested that the stabilization of the compound I is attributed to the unusual collection of amino acid residues (GlnE7, PheB10, PheCD1, PheE11) in the heme pocket active site (De Jesús-Bonilla et al., 2001). Resonance Raman studies for this hemoglobin showed the formation of the ferryl compound II and indicated the absence of hydrogen bonding between the carbonyl group of E7 and the HbI ferryl moiety, heme-Fe(IV)=O (De Jesús-Bonilla et al., 2006).

The study of oxygen reactive hemoglobins is important to understand biological processes. Therefore, this part of the study investigates the oxidation reactions and ligand interactions of hydrogen peroxide with HbII, HbI, and a recombinant HbI, in which PheB10 was replaced by TyrB10, and compared these reactions with those of α -DBBF Hb, a chemically stabilized human Hb. This study reports the kinetic rate constants for the autoxidation of HbI, HbII and HbI PheB10Tyr mutant. Also are reported the kinetic rate constants for the reaction with H_2O_2 at various pHs, and for the formation of fluorescent heme degradation products. One of the findings in this work is that HbII oxidizes in air slowly and exhibits unusual stability towards H_2O_2 and ferryl iron formation. The kinetic and structural data suggest that the proximity of TyrB10 and GlnE7 to the heme iron in HbII minimizes the exposure of the heme to the solvent, thus maintaining an oxidative stability.

4.2 Autoxidation results

The rate of spontaneous oxidation of the hemoglobins was measured in the presence and absence of the antioxidant enzymes superoxide dismutase (SOD) and catalase at 37°C. The heme undergoes autoxidation from the oxy heme-Fe(II) to the ferric heme-Fe(III) form of the hemoglobin releasing oxygen as a superoxide ion.

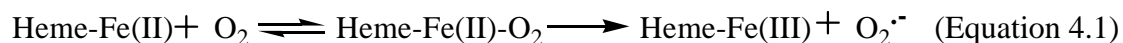


Figure 4.1 shows the overlaid spectra for the autoxidation reaction of HbII, in where the Soret band characteristic of the oxy species at 414 nm is displaced to the left up to the 404 nm band of the ferric Hb. The insert in Figure 4.1 shows the vanishing of the oxy bands at 540 and 576 nm forming the ferric species 633 nm band. Figure 4.2 shows the kinetic

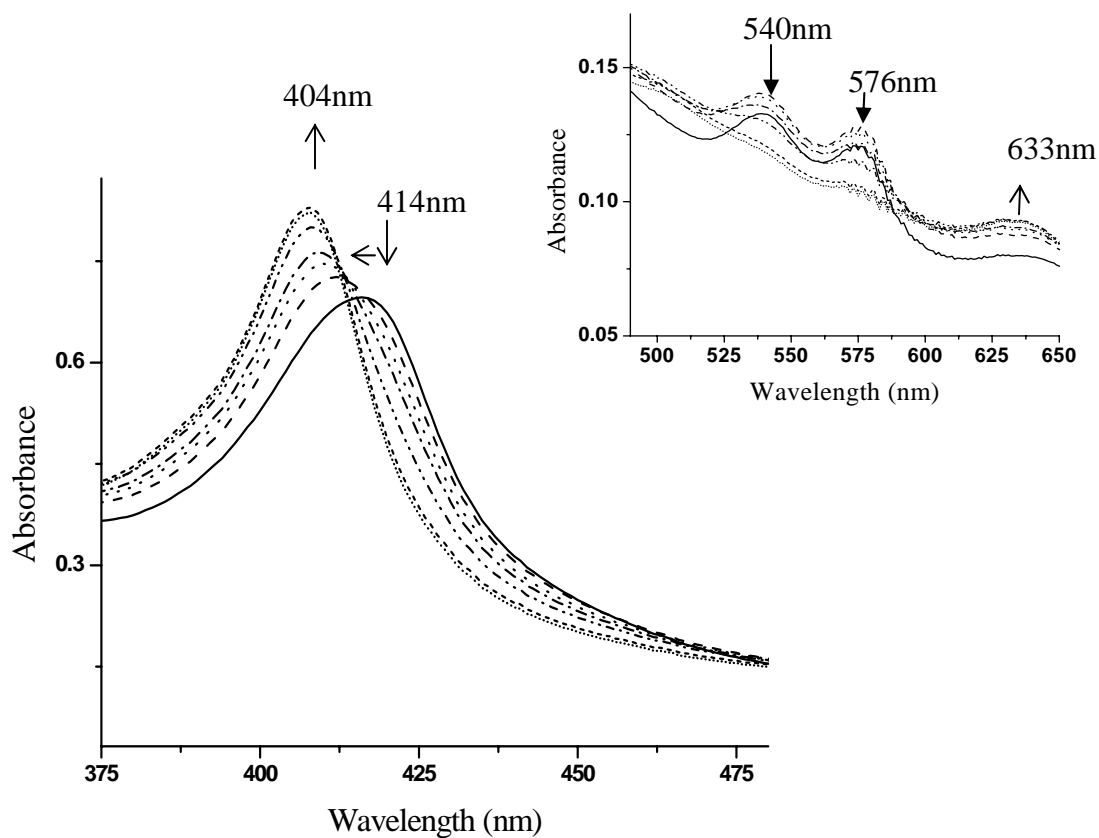


Figure 4.1 Autoxidation reaction of *L. pectinata* HbII. 20 μ M HbII was incubated in a Chelex-treated 50 mM phosphate buffer, pH 7.4 at 37°C, and monitored over a time period of 6 hours. The oxy species (414 nm) shifts to 404 nm characteristic of ferric HbII. Insert: Displacement of the oxy Q bands from 540 nm and 576 nm to 633nm.

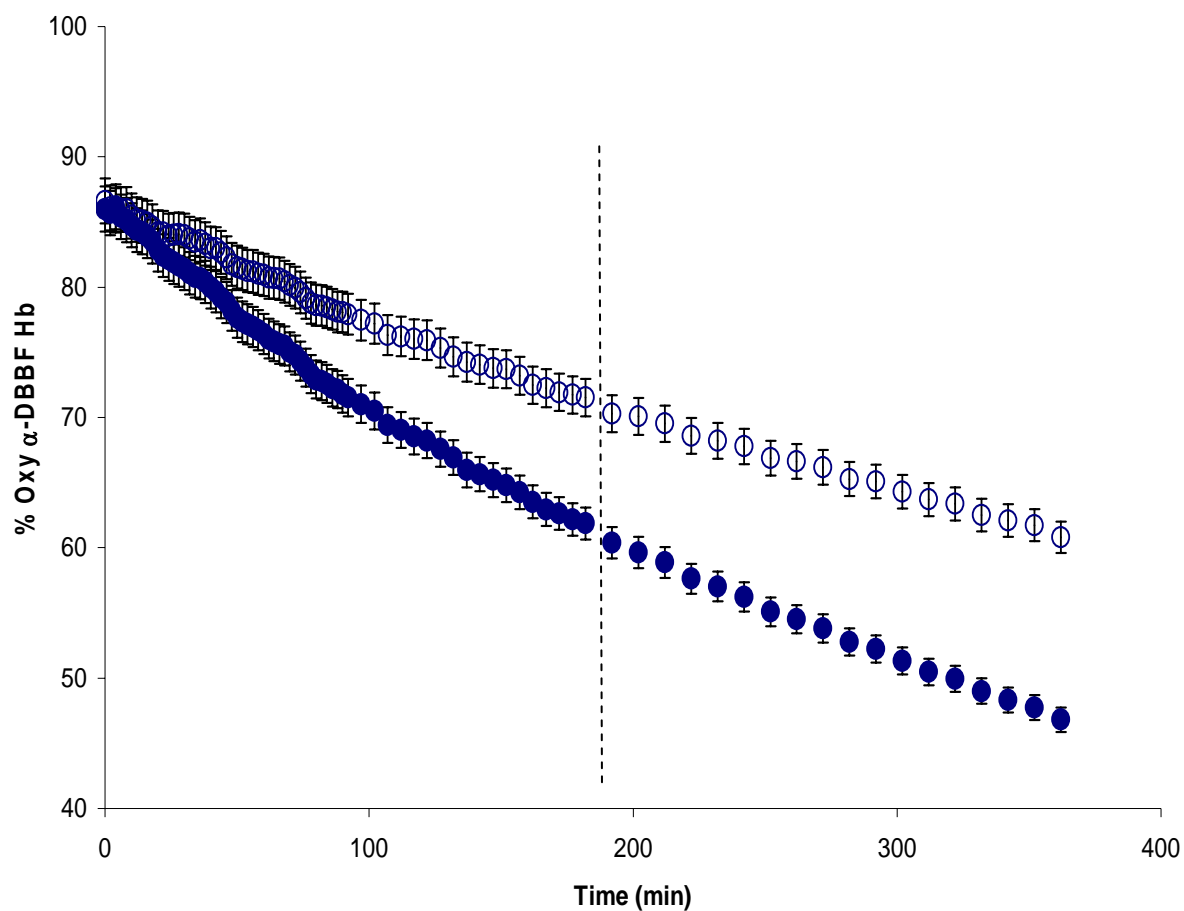


Figure 4.2 Autoxidation of α -DBBF Hb in the absence (●) and presence (○) of SOD/catalase. The autoxidation of 20 μ M of α -DBBF was monitored over a period of 6 hours. The α -DBBF Hb solution was incubated in a chelex-treated 50 mM phosphate buffer, pH 7.4, at 37 °C. The percentage changes of oxy α -DBBF Hb were calculated using the UV-Vis spectra following the Winterbourn equations (Materials and Methods, Section 2.1.2).

trace for the autoxidation reaction (black dots) of α -DBBF-Hb in which the percent of oxy hemoglobin is plotted as a function of time. The percent of oxy hemoglobin was calculated from the spectrum following Winterbourn equations (Winterbourn, 1985; Materials and Methods, Section 2.1.2), and is an average from three independent experiments. The white dots represent the autoxidation reaction in the presence of the antioxidant enzymes SOD and catalase. The kinetic traces for the α -DBBF-Hb autoxidation are represented by a single exponential, with a kinetic rate constant of 0.090 h^{-1} . When the antioxidant enzymes SOD and catalase were added to the protein solution prior to start the autoxidation experiment the rate of autoxidation of human cross-linked α -DBBF Hb was reduced by approximately 40% (0.050 h^{-1}). This result confirms the build up of oxygen free radicals during the autoxidation process, which are consumed when antioxidant enzymes are added to the system, thus decreasing the oxidation rate (Watkins et al., 1985, Yang & Olsen, 1994). Table 4.1 shows the kinetic rate constants for α -DBBF-Hb, and *L. pectinata* hemoglobins autoxidation measured at 37°C . Under the same experimental conditions, Figures 4.3 to 4.5 show the kinetic traces for the autoxidation reaction (black dots) of HbI, HbII, and HbI PheB10Tyr, respectively, in which the percent of oxy hemoglobin is plotted as a function of time. The kinetic traces for *L. pectinata* hemoglobins show that the autoxidation reaction is slower, with kinetic rate constants several fold lower than the α -DBBF Hb. Initially, HbI only reached an 80 percent of oxy hemoglobin, maybe due to its physiological role as H_2S transport in the ferric form. The kinetic rate constant for the HbI autoxidation was 0.055 h^{-1} , the higher among the *L. pectinata* hemoglobins that decreased 93% in the presence of antioxidant enzymes with a rate constant value of 0.0058 h^{-1} . HbII, that its physiological role is carried on in the oxy form, shows an autoxidation rate

Table 4.1 Oxidative reaction rate constants of *L. pectinata* hemoglobins compared to α -DBBF Hb. k_{autox} is the rate constant for the spontaneous autoxidation of the hemoglobins at 37°C in the presence or absence of the enzymes SOD and catalase.

Hemoglobin	$k_{\text{autox}} (\text{h}^{-1})$	$k_{\text{autox}} (\text{h}^{-1})$ with SOD and catalase
HbI	0.055 ± 0.008	0.0058 ± 0.0001
HbII	0.010 ± 0.002	0.010 ± 0.002
HbI PheB10Tyr	0.008 ± 0.001	0.005 ± 0.0001
α -DBBF Hb	0.090 ± 0.001	0.050 ± 0.001

constant value of 0.010 h^{-1} , which is 9 times lower than α -DBBF-Hb (0.090 h^{-1}). The HbII autoxidation reaction did not show a significant difference when SOD and catalase were added to the system. The HbI PheB10Tyr mutant oxidation rate constant is 0.008 h^{-1} which decreased a 40% in the presence of the antioxidant enzymes. This suggests that *L. pectinata* HbII may produce low concentrations of ROS, while HbI produces large concentrations of radicals in the autoxidation process. Long term stability studies in the absence of antioxidant enzymes showed that at the end of 24 hour of incubation, there were 22% and 41% ferric Hb present in HbI PheB10Tyr and HbII solutions and almost equal amount of hemichrome species, respectively. However, very little ferric HbI was formed, instead 40% of the total

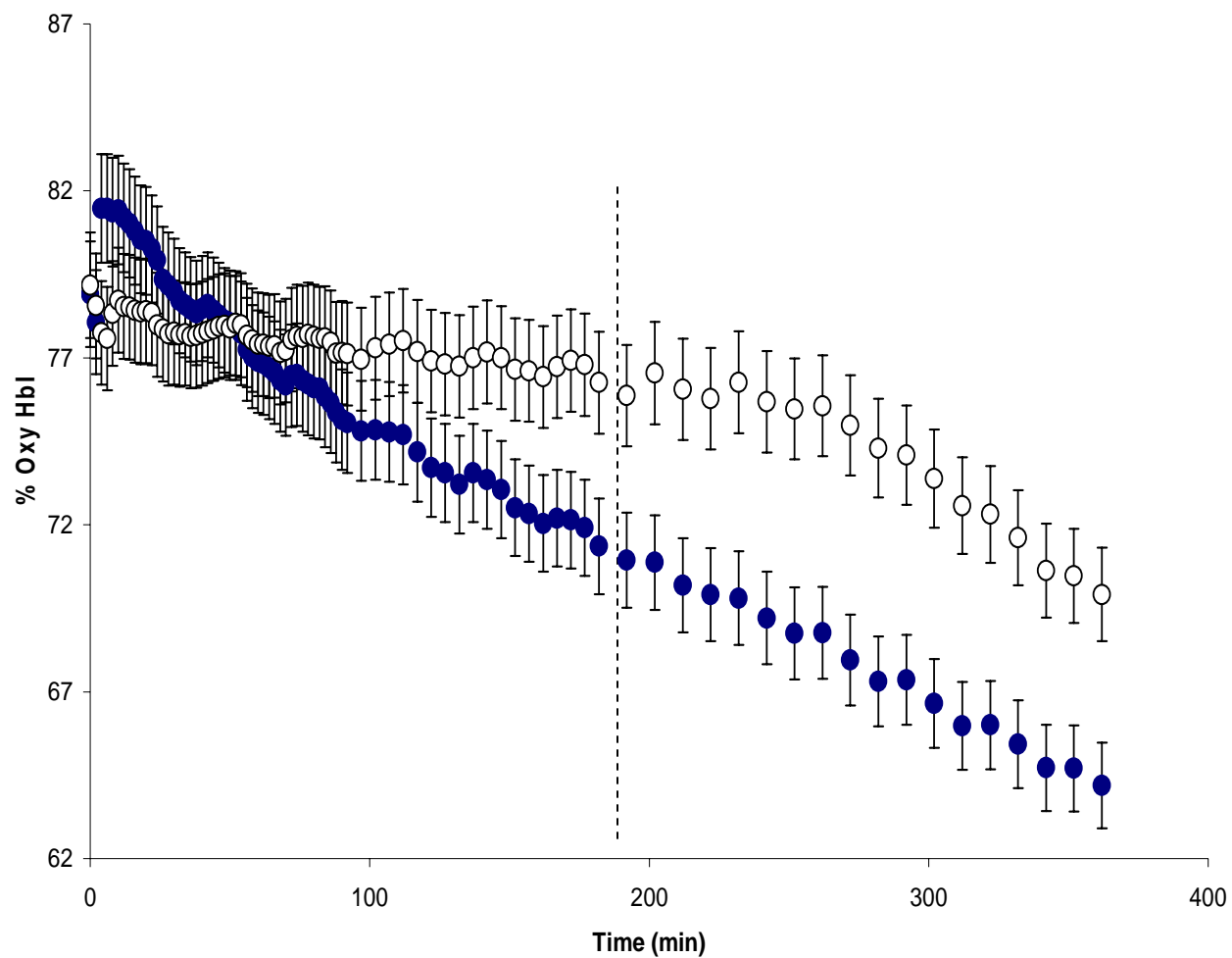


Figure 4.3 Autoxidation of HbI in the absence (●) and presence (○) of SOD/catalase. The autoxidation of 20 μ M of HbI was monitored over a period of six hours. The HbI solution was incubated in a Chelex-treated 50 mM phosphate buffer, pH 7.4, at 37 °C. The percentage changes of oxy HbI were plotted over time.

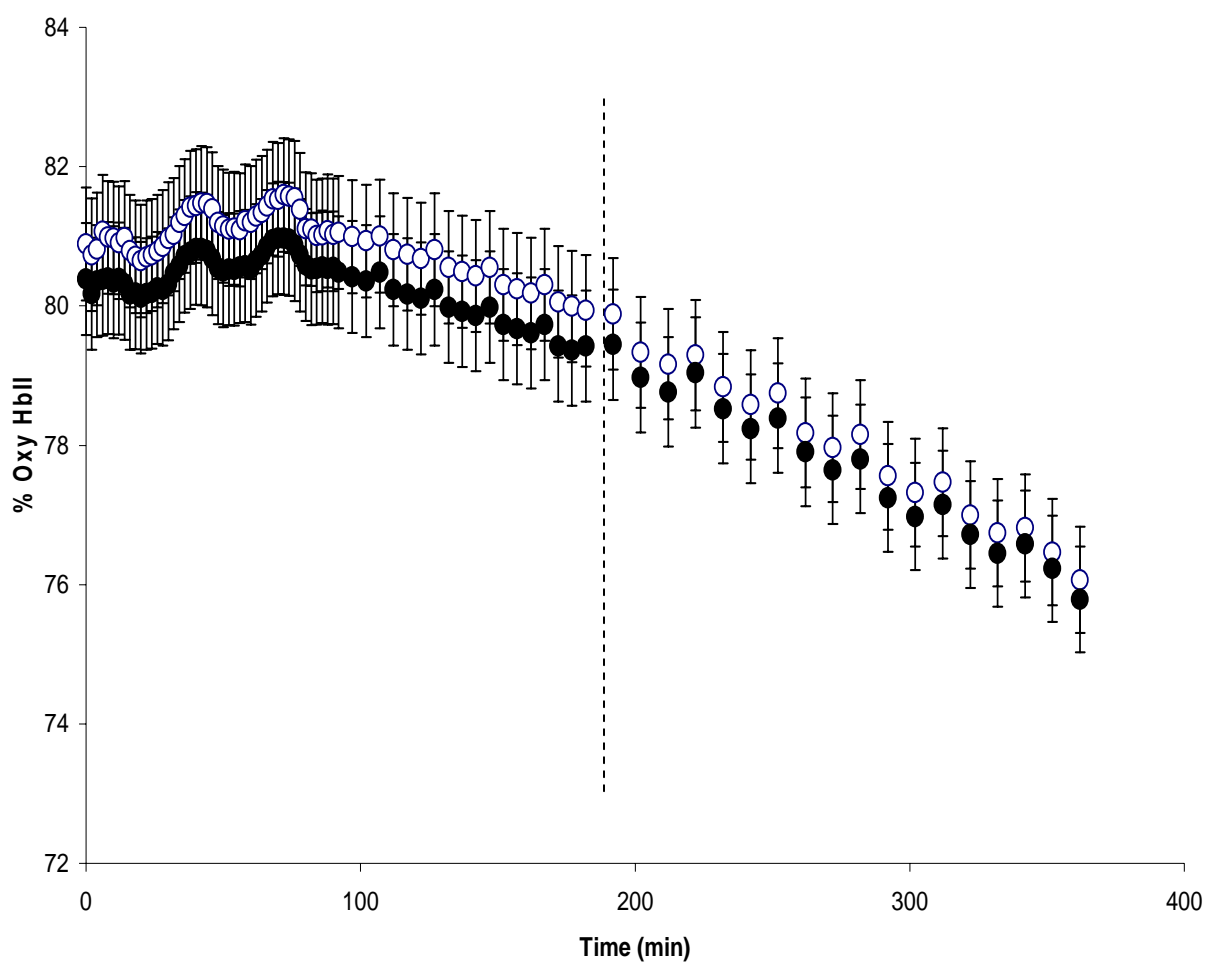


Figure 4.4 Autoxidation of HbII in the absence (●) and presence (○) of SOD/catalase. The autoxidation of 20 μ M of HbII was monitored over a period of six hours. The HbII solution was incubated in a Chelex-treated 50 mM phosphate buffer, pH 7.4, at 37 °C. The percentage changes of oxy HbII were plotted over time.

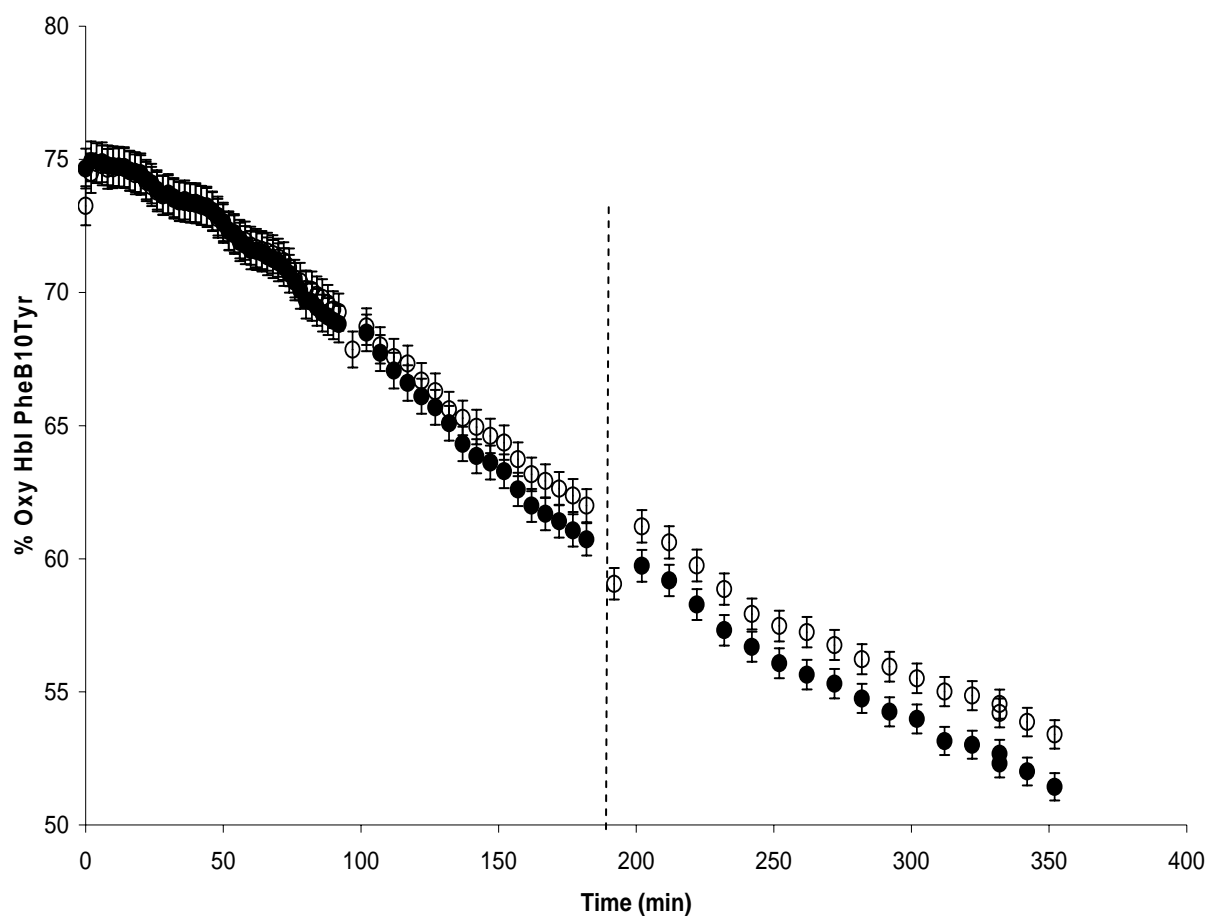


Figure 4.5 Autoxidation of HbI PheB10Tyr in the absence (●) and presence (○) of SOD/catalase. The autoxidation of 20 μ M of HbI PheB10Tyr was monitored over a period of 6 hours. The HbI PheB10Tyr solution was incubated in a Chelex-treated 50 mM phosphate buffer, pH 7.4, at 37 °C. The percentage changes of oxy HbI PheB10Tyr were plotted over time.

heme was transformed to other oxidized denatured products such as hemichromes within the first 6 hour incubation. This susceptibility of HbI to oxidative modification was confirmed by spectral changes, and by its high reaction rate with H_2O_2 and formation of fluorescent heme degradation products when compared to the other hemoglobins.

Since there is a significant difference in the autoxidation between HbI and HbII, a catalase assay was performed to monitor the enzymatic activity of the hemoglobins in terms of catalase enzymatic activity. The slopes of the trend lines for 0.3 nM and 3.0 nM catalase were -0.0392 and -0.2162, respectively. Figure 4.6 shows that neither HbI nor α -DBBF Hb have enzymatic activity similar to catalase, with slopes of -0.0035 and 1.2×10^{-7} , respectively. The effect was different for HbII, where the trace for the reaction had a slope of -0.0512. This result shows that HbII has enzymatic activity as compared to the catalase control with a concentration of 0.3 nM. This enzymatic activity suggests a different role for HbII in its physiological environment.

4.3. Oxidation reactions with hydrogen peroxide

The reaction of ferric hemoglobins with hydrogen peroxide produces a short lived ferryl hemoglobin radical, which is not stable and is converted back to ferric hemoglobin.



Figure 4.7 A monitors the reaction of ferric hemoglobin HbII with H_2O_2 at 1:400 ratio in acidic media (pH 5.0), from 350 to 500 nm. The first spectrum (a) is for 8 μM ferric HbII, at zero time of reaction, which shows a Soret band at 407 nm. After five seconds in the

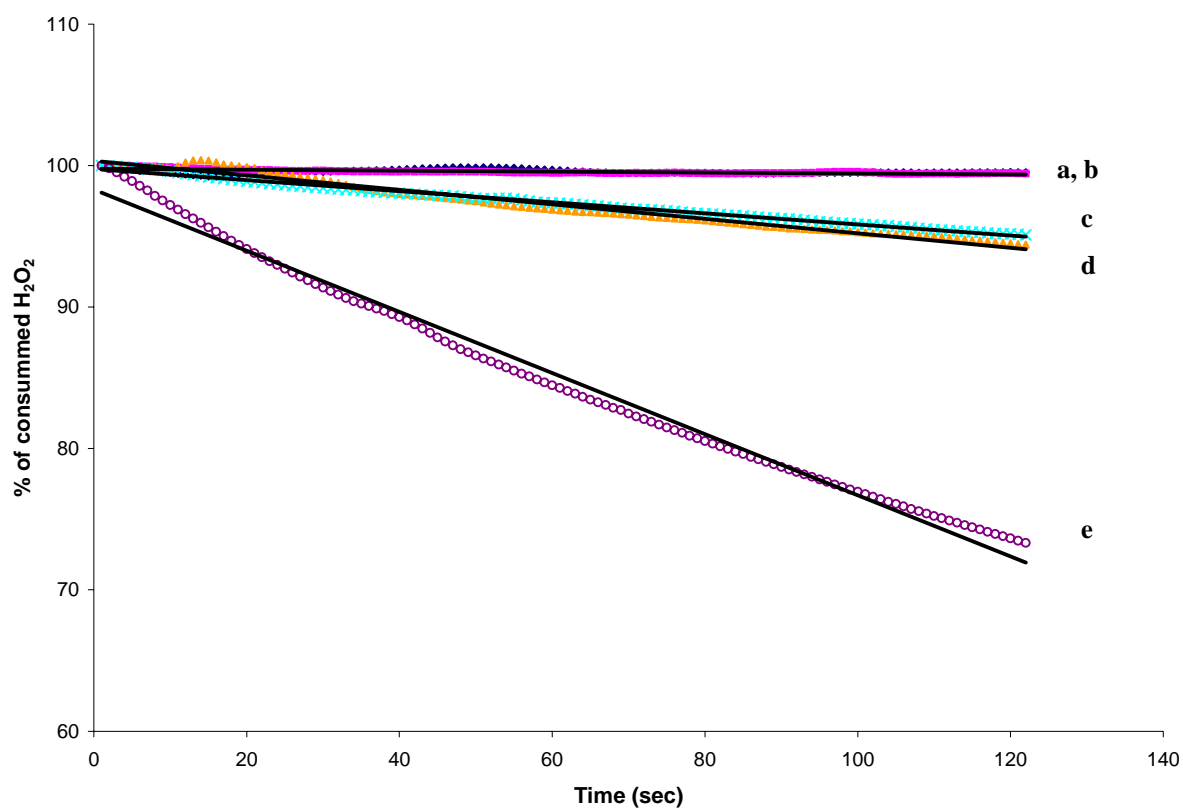


Figure 4.6 Catalase assay for the hemoglobins α -DBBF Hb (a), HbI (b), and HbII (d). Catalase concentrations of 0.3 nM (c) and 3.0 nM (e) were used as control. The kinetic was monitored by mixing 8.4 μ L of H_2O_2 30% with 1 μ M hemoglobin in 50mM potassium phosphate buffer, pH 7, for 122 seconds, at 240 nm.

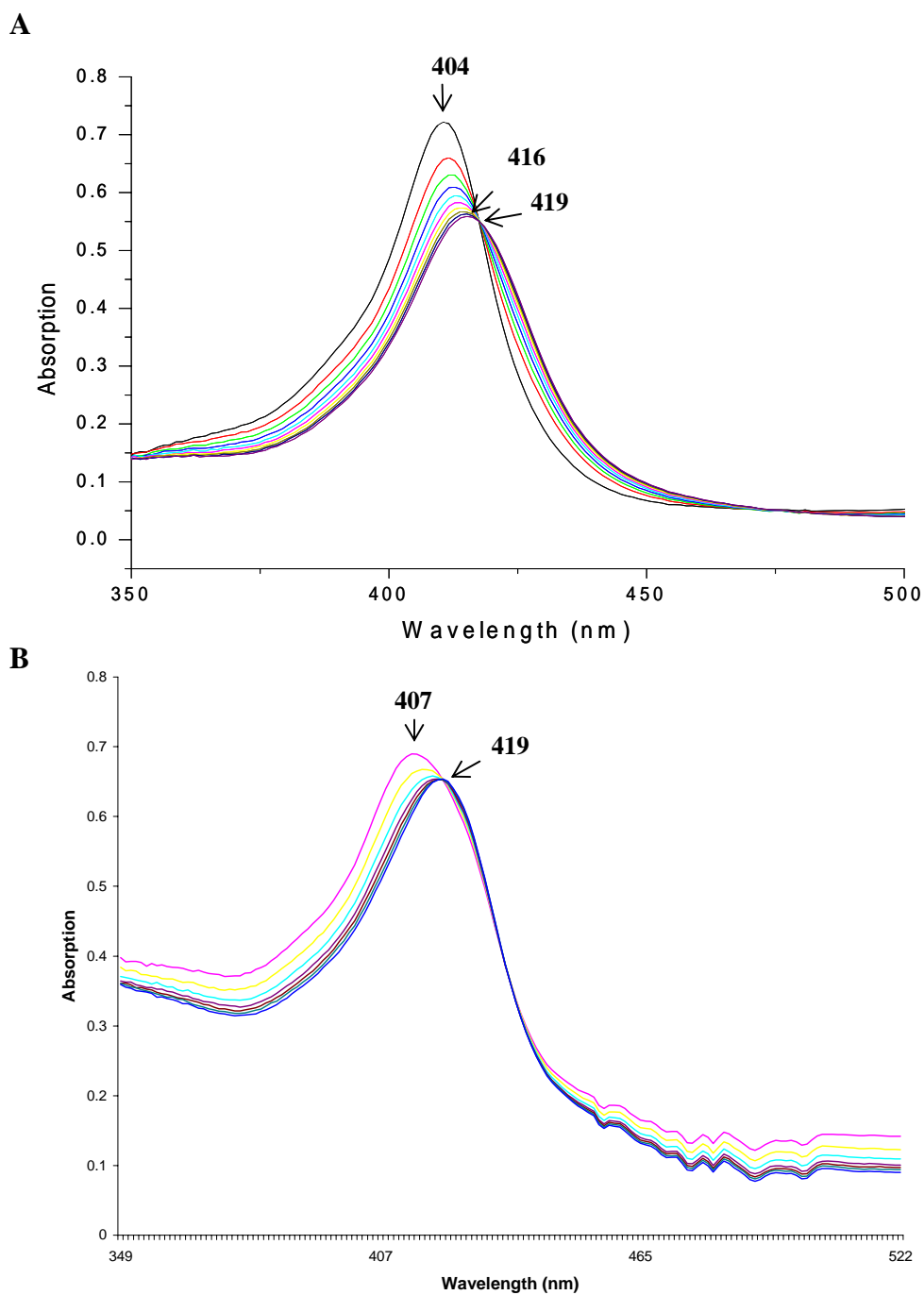


Figure 4.7 Reaction of 8 μM ferric HbII (A) and HbI PheB10Tyr (B) with hydrogen peroxide, pH 5.0, at 1:400 ratio, respectively. The formation of the ferryl species was monitored at 400 nm at 22°C over a period of 10 seconds. After 5 seconds, the ferric hemoglobin shifts from 407 nm to 416 nm with an isobestic point at 419 nm.

reaction with H_2O_2 , at 1:400 ratio, the Soret band shifts to the right and reaches a maximum at 416 nm. This band never shifts to 419 nm but the reaction shows an isobestic point at 419 nm. This isobestic point suggests a mixture between the ferryl compound II and the oxy species. It is also evident that the intensity of the bands start to decrease indicating the loss of the heme iron. The same behavior was seeing for the HbI PheB10Tyr mutant, as is shown in Figure 4.7 B. Figure 4.8 shows the reaction for HbII with hydrogen peroxide at 1:400 ratio at pH 7.0, from 350 to 500 nm. The Soret band presents a shift from 407 nm to 419 nm. The Soret band for the last three spectra showed a clear formation of the 419 nm band characteristic of the ferryl species and a little increase in absorption. This increase is indicative that up to 10 seconds there is no heme degradation, and that the hemoglobin has a change in its extinction coefficient. The reaction presents the isobestic point at 416 nm suggesting the presence of other species in the reaction. When the reaction was performed with HbI PheB10Tyr at 1:400 ratio and pH 7.4 (Figure 4.9 A), showed a similar sequence of spectrum as in pH 5.0. However, the reaction of HbI PheB10Tyr with hydrogen peroxide at 1:1000 ratio and pH 7.4, Figure 4.9 B, shows similar spectra as the reaction of HbII at 1:400, pH 7.4. The spectra for the reaction of the wild type and mutant hemoglobins with H_2O_2 at pH 11.2 did not show any shift in the bands. This results show that the progress of the reaction for HbII is faster than for HbI PheB10Tyr evidencing that the mutant is more resistant to react with hydrogen peroxide.

Figure 4.10 shows the overlaid spectra for the reaction of HbI PheB10Tyr with an excess of H_2O_2 . This reaction did not form the band at 648 nm, characteristic of the ferryl compound I. The reaction also indicates that large excess of H_2O_2 produces heme loss and degradation, as in wild type HbI (De Jesús et al., 2001). The same pattern was observed in

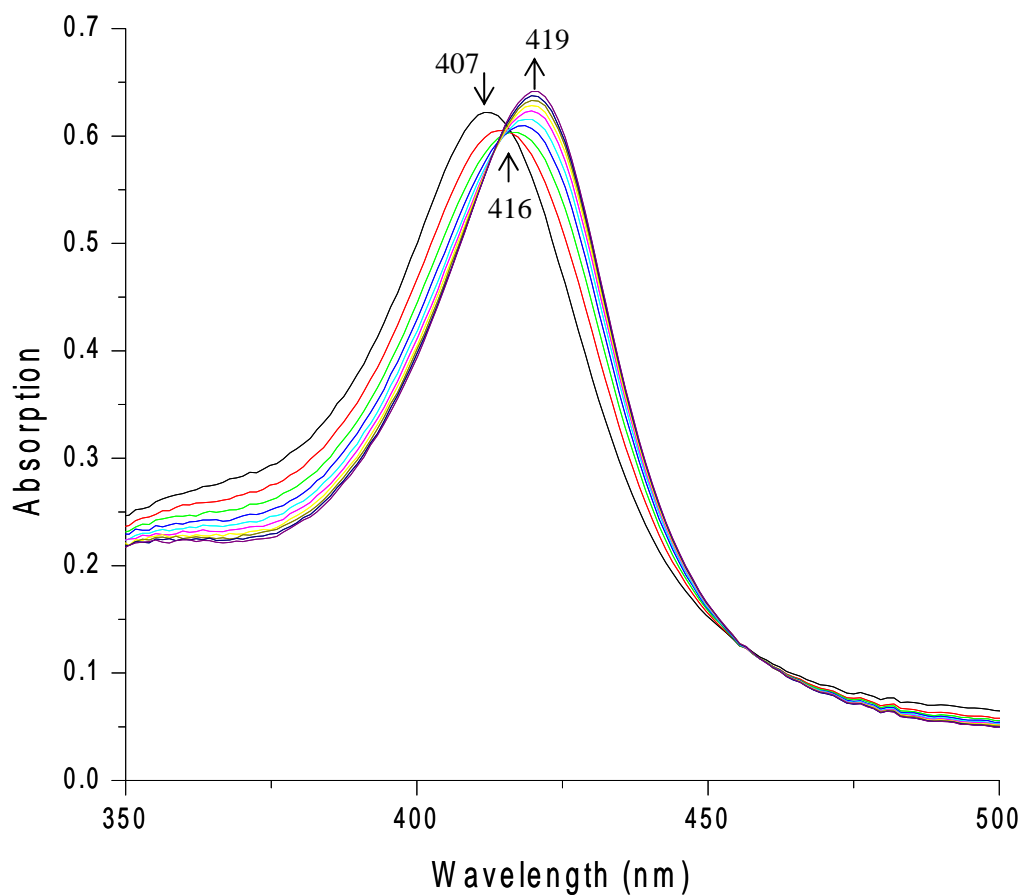


Figure 4.8 Reaction of ferric HbII with hydrogen peroxide, pH 7.4, at 1:400 ratio. The Soret band shifts from 407 nm to 419 nm with isosbestic point at 416 nm, confirming the formation of the ferryl compound II.

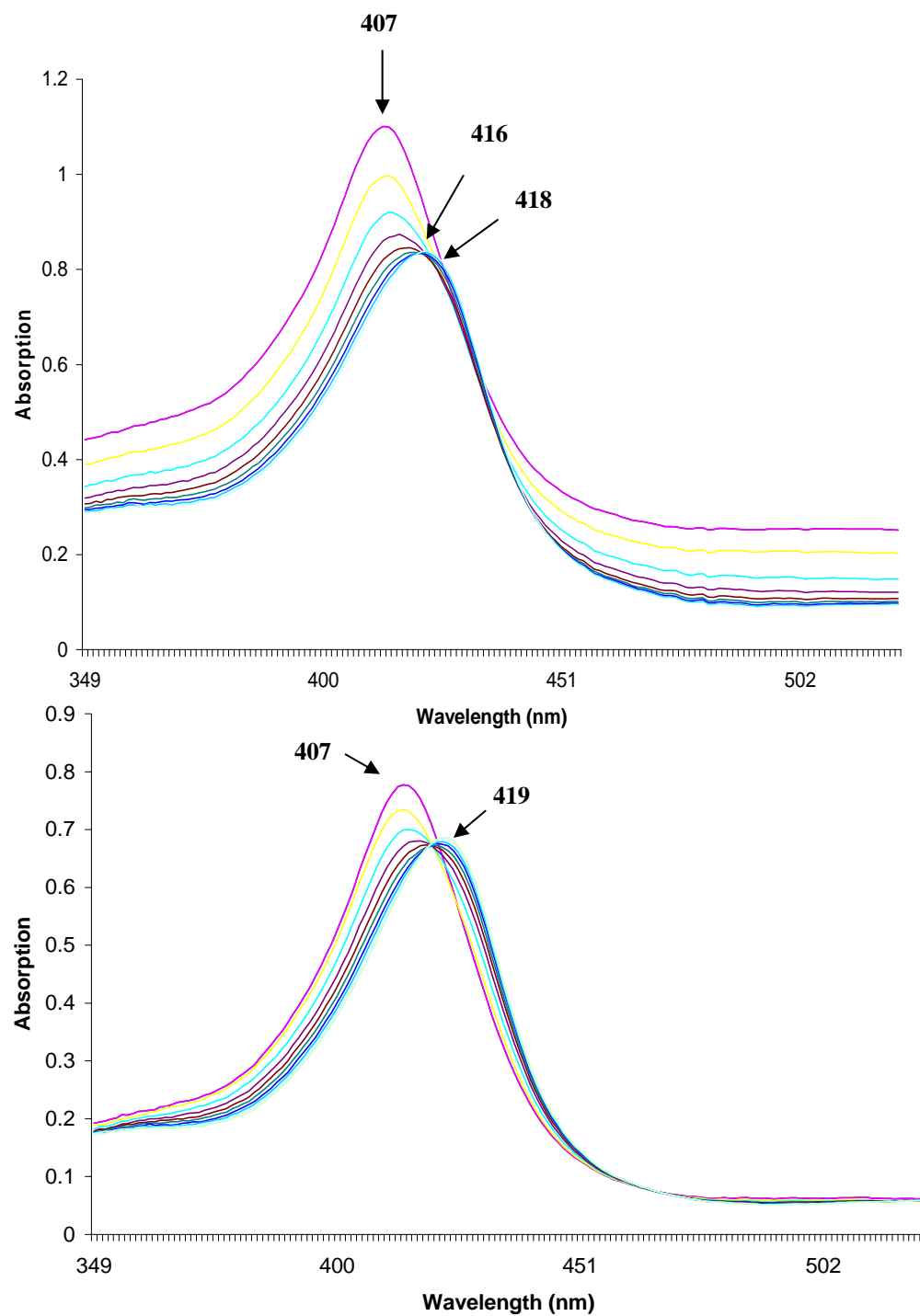


Figure 4.9 Reaction of ferric HbI PheB10Tyr with hydrogen peroxide, pH 7.4, at 1:400 and 1:1000 ratios, respectively. The Soret band shifts from 407 nm to 419 nm with isosbestic point at 416 nm, confirming the formation of the ferryl compound II.

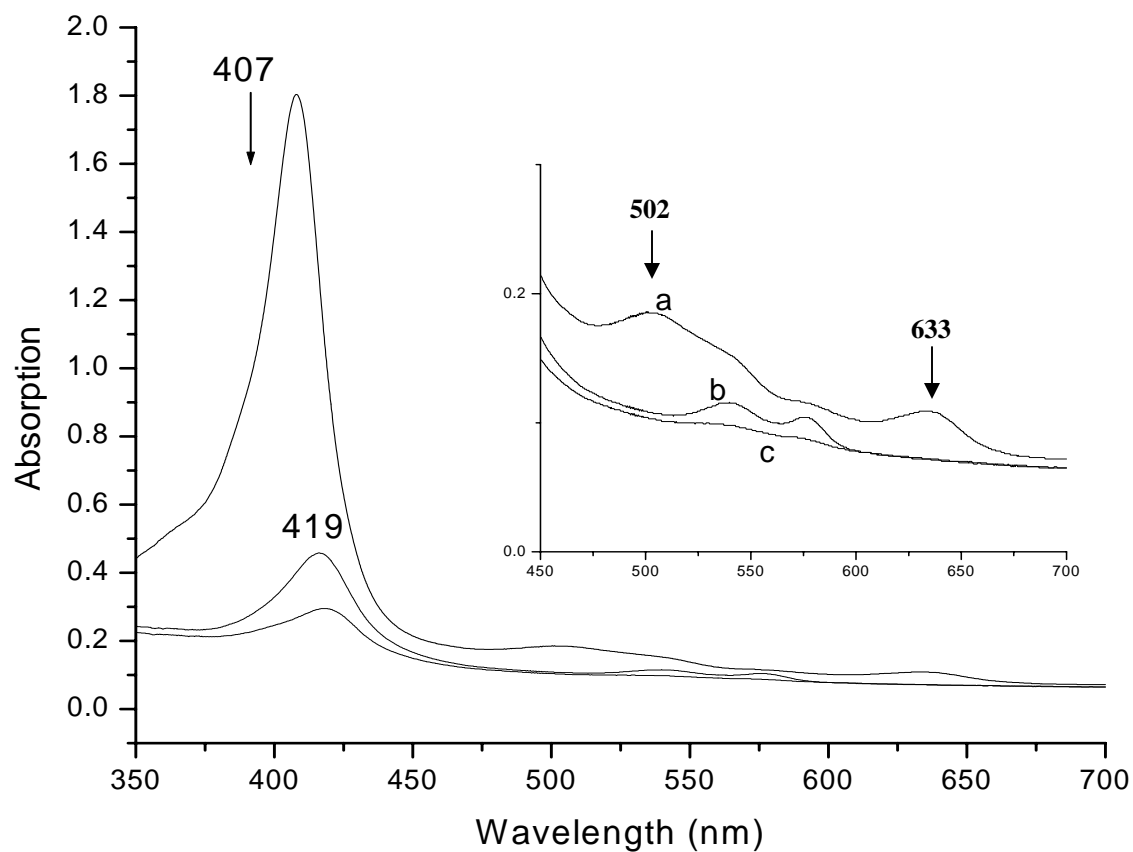


Figure 4.10 Overlaid spectra for the reaction of ferric *L. pectinata* HbI PheB10Tyr with hydrogen peroxide. 18 M HbI PheB10Tyr was reacted with a large H_2O_2 excess. (a) Unreacted HbI PheB10Tyr; (b) reaction after 2 minutes; (c) reaction after 8 minutes.

the reaction of HbII with large excess of H_2O_2 . However, in spite that both spectra are similar, the formation of the compound II ferryl species in the HbI PheB10Tyr mutant reaction shows a longer lifetime. At eight minutes the Soret and the Q bands are well defined for the HbI mutant, while at three minutes, the bands for the HbII wild type have less intensity than that for the mutant at eight minutes. The Figure 4.10 insert shows bands characteristic of the ferryl species at 2 minutes of the reaction. The decrease in the Soret band during the formation of the ferryl species suggests the formation of heme degradation products 8 minutes after H_2O_2 addition, which are thereafter evident by the vanishing of the bands. This data suggests that the orientation of the tyrosine in the B10 position and the volume of the heme pocket play a distinctive role in the ferryl formation of the hemeproteins.

Figure 4.11 A shows the kinetic traces for the reaction of the recombinant HbI with hydrogen peroxide at different ratios, at 648 nm. The reaction of 1:100 and 1:250 presents an increase in the kinetic trace, which reaches a plateau between the 1:500 and 1:1000 ratios. From 1:2000 to 1:4000 the kinetic traces show a biphasic behavior. The spectra of the progress for the reaction at 648 nm at 1:2000 ratio is shown in Figure 4.11 B. The first spectrum is from the ferric species with the characteristic Q band at 633 nm. This band shifts to the right with a broad band at 648 nm. At four seconds the 648 nm band shifts to 655 nm and this band continues increasing for 10 seconds. The kinetic measurements and the spectra for the reaction of HbII or HbI PheB10Tyr with H_2O_2 did not show the formation of the 648 nm band characteristic of the ferryl compound I. These results support the idea that the TyrB10 ligation to the metallo active center in hemeproteins and the hydrogen bonding between the ferryl in compound I and the TyrB10 hydroxyl group increased the rate of reaction, thus stabilizing the radical in compound I and forming rapidly the ferryl compound

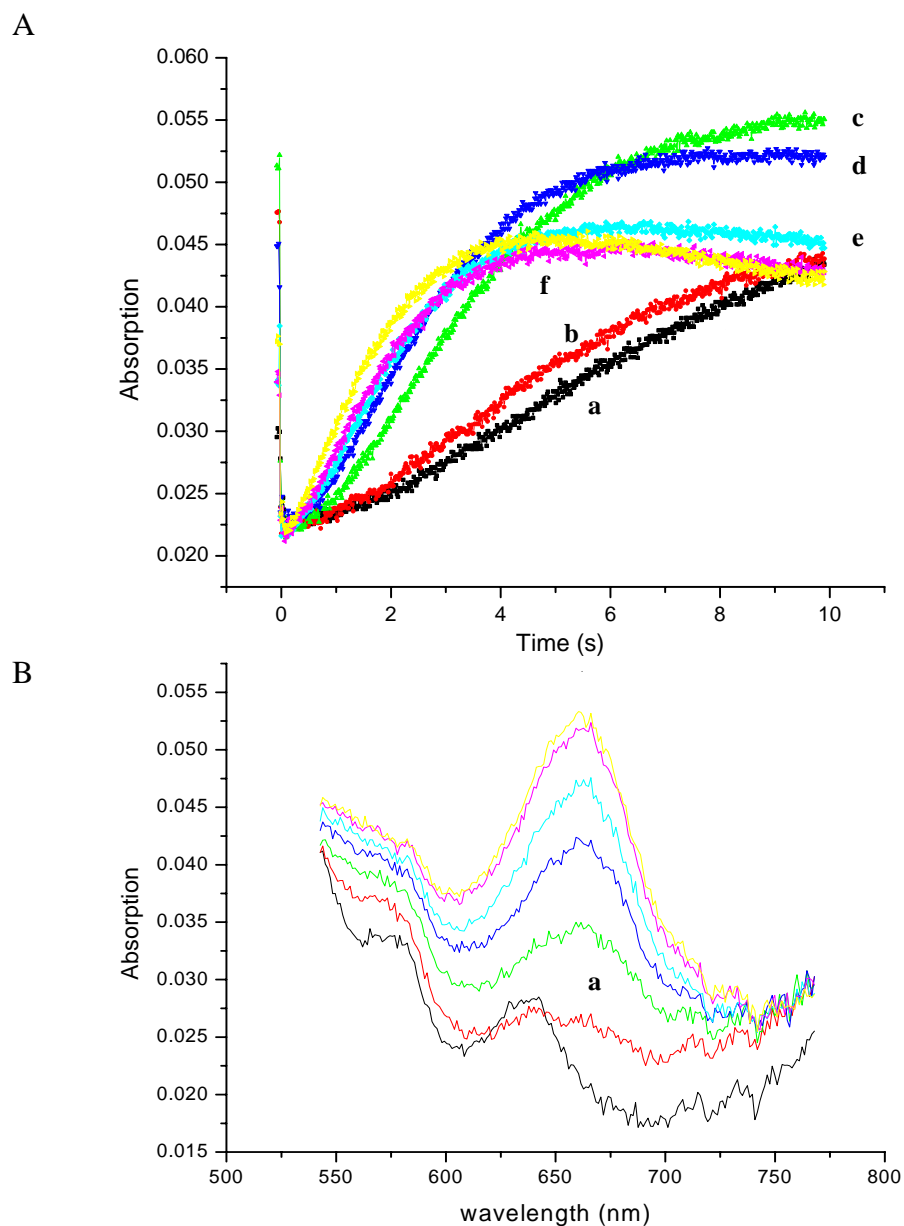


Figure 4.11 Compound I formation in the reaction of ferric recombinant HbI with H_2O_2 . **A:** kinetic traces of 1 equivalent of recombinant HbI with different equivalents of H_2O_2 ; (a) 1:100, (b) 1:250, (c) 1:500, (d) 1:1000, (e) 1:2000, and (f) 1:3000. **B:** Spectra for the progress of the reaction at 648 nm, and 1:2000 (Hb: H_2O_2) ratio. The ferryl species Compound I was formed upon 1 second (a) of the reaction.

II. Therefore, this hydrogen bonding plays a significant role in defining the presence of the 648 nm band and in the reactivity of ferryl species.

Figure 4.12 shows the kinetic trace for the reaction of HbII and HbI PheB10Tyr mutant with H_2O_2 at 400 nm for 10 seconds. HbII shows a biphasic behavior, which is marked for pH 5.0, and slight for pH 7.5. The kinetic trace for HbI PheB10Tyr mutant shows a continuum decrease in intensity, which appears to be faster at pH 7.5. Figure 4.13 plots the apparent kinetic rate constants for this reaction as function of the hydrogen peroxide concentration, and at different pH. This graph indicates that the formation of the ferryl species is faster for HbII. This can be explained in terms of the heme pocket cavity. HbI has a greater heme freedom, observed when compared to sperm whale Mb (Fernández-Alberti, 2006), that also suggests a heme freedom in the HbI PheB10Tyr mutation. Therefore, for the mutant the heme pocket amino acids allow a change in the structure conformation that slows the entrance of H_2O_2 ; thus it is also slower the formation of the compound II ferryl species. Table 4.2 shows the second order kinetic rate constants for the formation of HbII and the HbI PheB10Tyr mutant ferryl species at 400 nm. At a pH 5.0 the rate constants are around $103 \text{ M}^{-1}\text{s}^{-1}$ and $141 \text{ M}^{-1}\text{s}^{-1}$ for HbI PheB10Tyr and HbII, respectively. In the manner that the pH gets basic, the rate constants for the reaction decreases. For the neutral pH, the rate constants are between $69 \text{ M}^{-1}\text{s}^{-1}$ and $78 \text{ M}^{-1}\text{s}^{-1}$, and at a pH 11.0 are $1.5 \text{ M}^{-1}\text{s}^{-1}$ and $3.0 \text{ M}^{-1}\text{s}^{-1}$ for HbI PheB10Tyr and HbII, respectively. In all cases the rate constant for HbI PheB10Tyr is smaller than HbII. The difference in the kinetic rate constant values can be explained by changes in the heme coordination and ligation state. However, this pH behavior is not observed for the reaction of HbI with H_2O_2 , and for HbI PheB10Tyr, which both have a phenylalanine in the B10 position instead of the tyrosine (De Jesús-Bonilla et al., 2006).

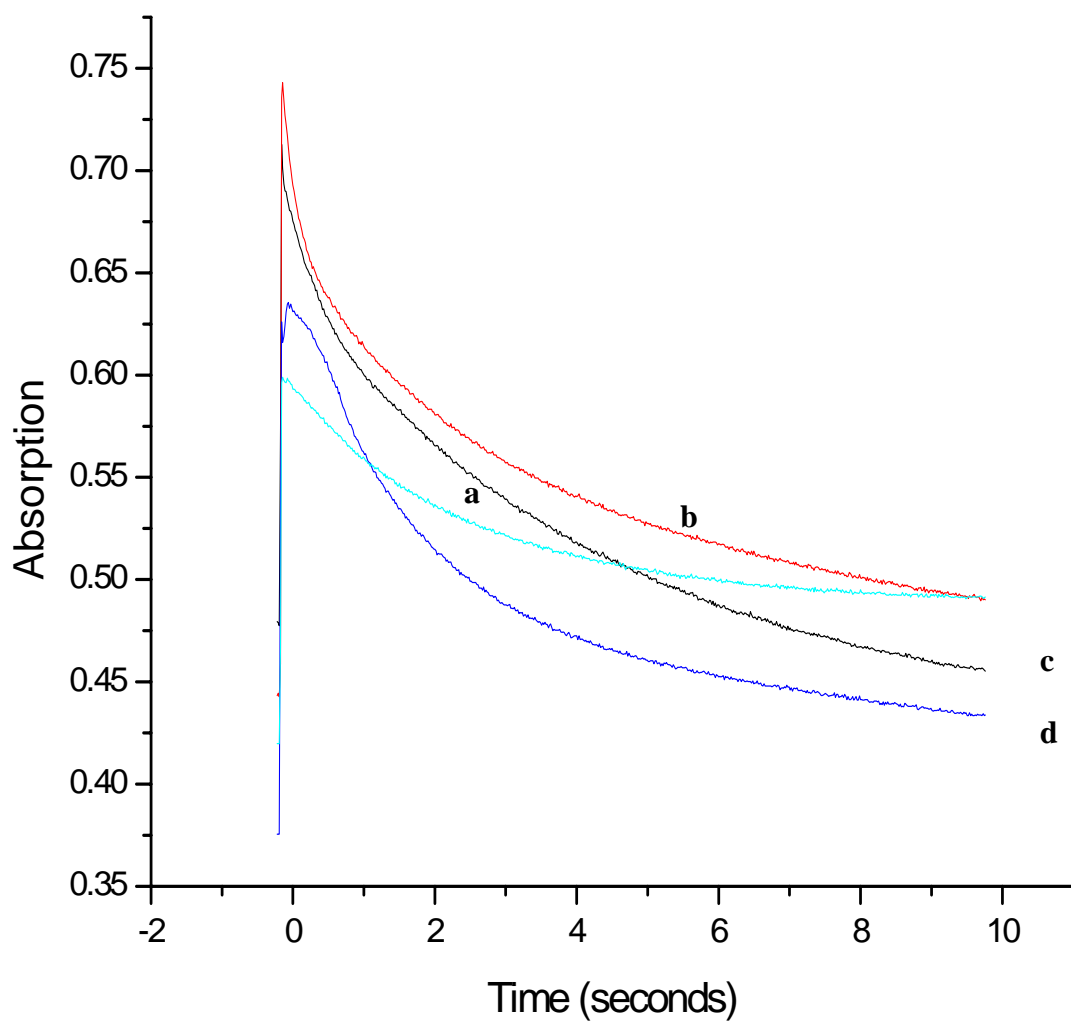


Figure 4.12 Stopped-flow kinetic trace for the reaction of *L. pectinata* HbII and HbI PheB10Tyr with hydrogen peroxide for 10 seconds at 400 nm. (a) HbII and (b) HbI PheB10Tyr in the reaction at pH 7.5. (c) HbI PheB10Tyr and (d) HbII in the reaction at pH 5.0.

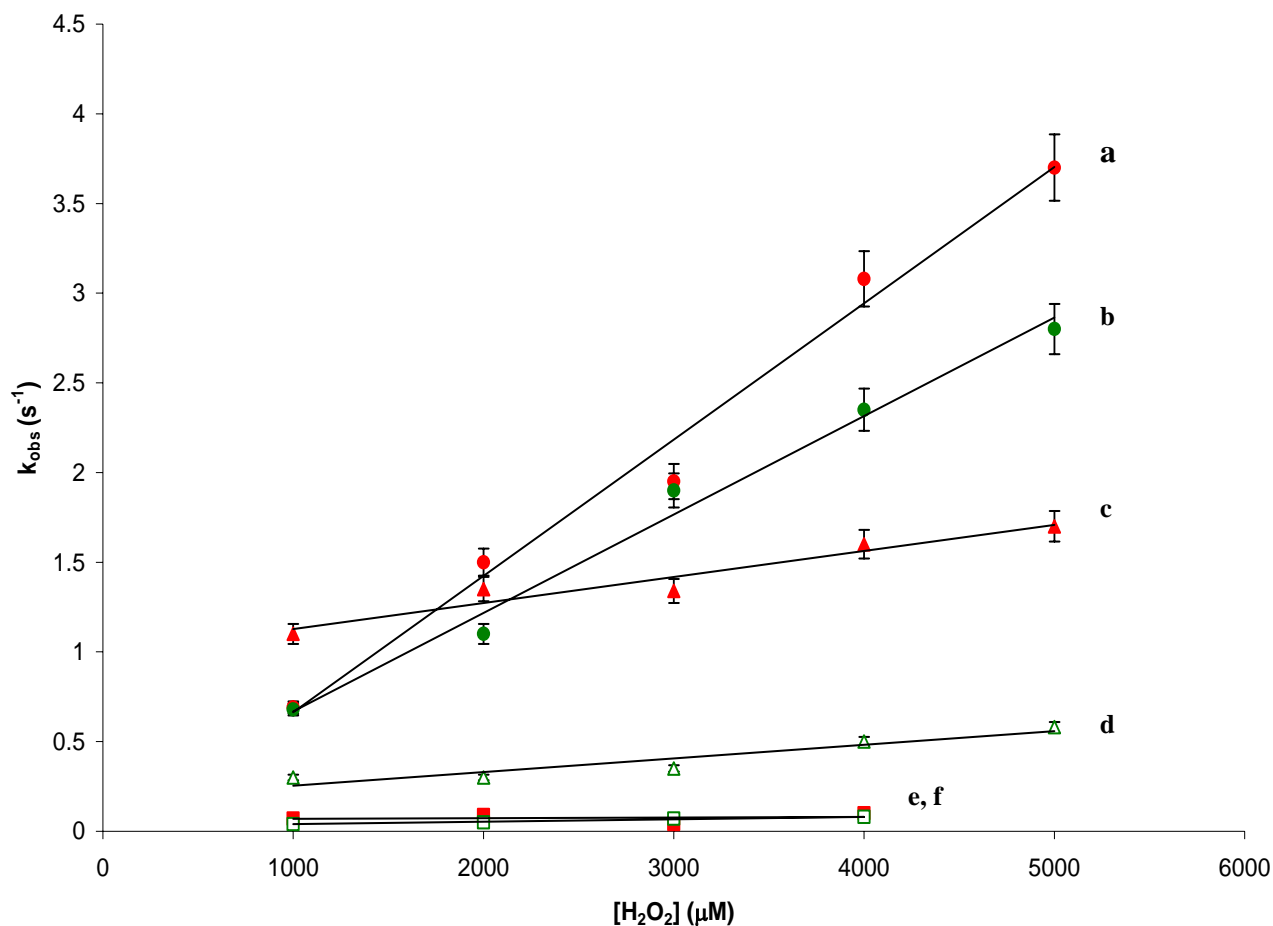


Figure 4.13 Plot of the apparent rate constants for the reaction of *L. pectinata* hemoglobins with H_2O_2 as function of H_2O_2 . (a) HbII at pH 5, (b) HbI PheB10Tyr mutant at pH 5, (c) HbII at pH 7.5, (d) HbI PheB10Tyr at pH 7.5, (e) HbII at pH 11.2, (f) HbI PheB10Tyr at pH 11.2. The hemoglobins were reacted with H_2O_2 in ratios from 1:100 to 1:5000. The formation of the ferryl compound I was monitored at 400 nm, at 5 ms intervals and over periods ranging from 1 to 10 seconds. The kinetic rate constants are the mean of four independent experiments.

Table 4.2 Kinetic rate constants for the hydrogen peroxide oxidation of *L. pectinata* complexes monitored at 400 nm.

pH	HbII (M ⁻¹ s ⁻¹)	His PheB10Tyr (M ⁻¹ s ⁻¹)
5.0	141.60 ± 2.5	103.45 ± 2.2
7.5	77.79 ± 4.6	69.00 ± 5.3
11.2	2.96 ± 0.5	1.56 ± 0.3

Fluorescent heme degradation products were detected using the stopped flow technique in the reaction of the hemoglobins with H₂O₂ excess.

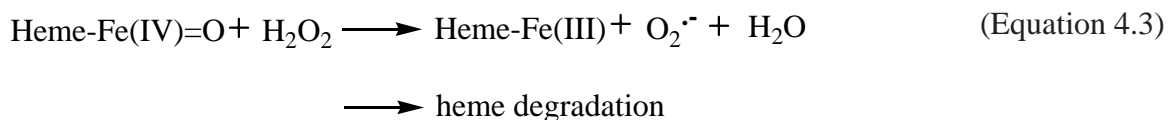


Figure 4.14 shows the kinetic traces for the *L. pectinata* hemoglobins with 4 mM H₂O₂. A double exponential equation was used to fit the HbII, HbI, HbI PheB10Tyr and α -DBBF-Hb kinetic traces. Figures 4.15 graph the observed kinetic rate constants versus the hydrogen peroxide concentration for each one of the hemoglobins. Table 4.3 shows the kinetic rate constants for the production of heme degradation products of α -DBBF-Hb, HbI, and HbII and the HbI PheB10Tyr mutant with values of 8.0 M⁻¹s⁻¹, 37 M⁻¹s⁻¹, 1.1 M⁻¹s⁻¹, and 1.2 M⁻¹s⁻¹, respectively. The susceptibility of HbI to oxidative modification and heme degradation is clearly indicated and ranked the same, if not higher, than those established for

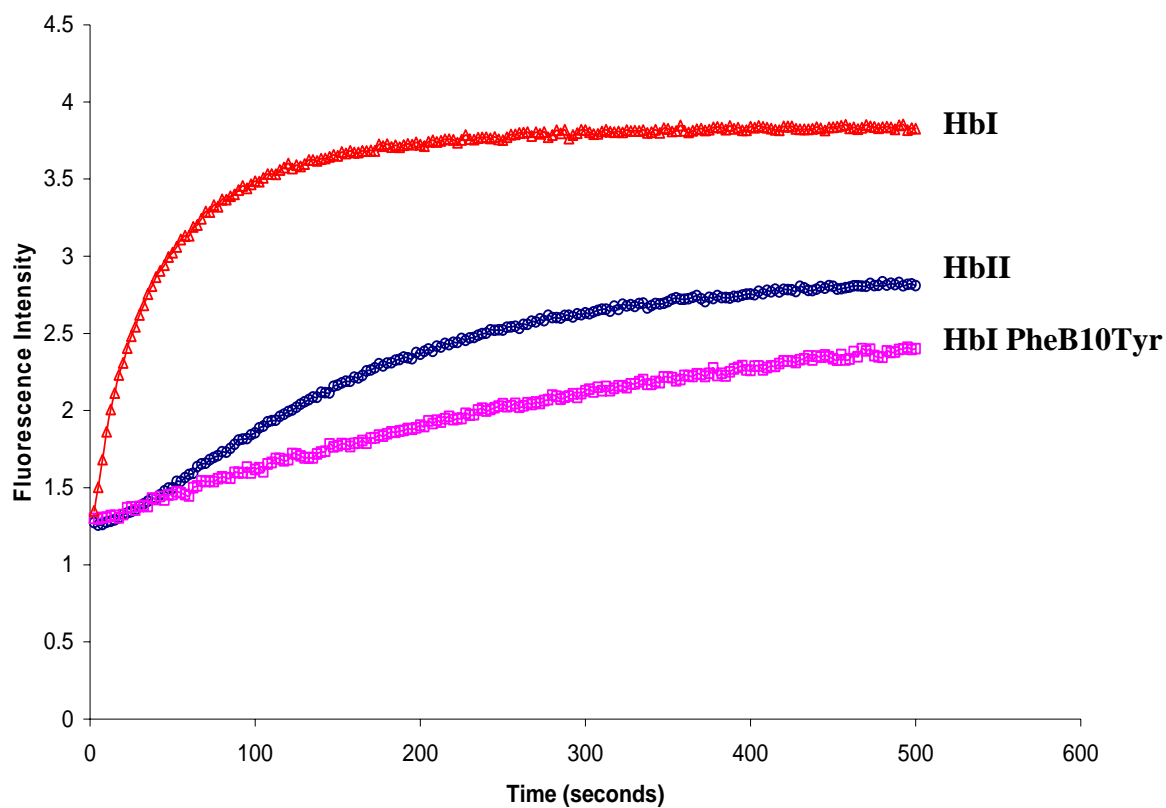


Figure 4.14 Stopped-flow fluorescence time courses of the reaction between 10 μM *L. pectinata* HbI, HbII, and HbI PheB10Tyr and 4 mM H_2O_2 (after mixing). The fluorescence was measured using a stopped-flow spectrophotometer in 50 mM sodium phosphate buffer, pH 7.4, with an excitation wavelength of 321 nm and emission at 360 nm.

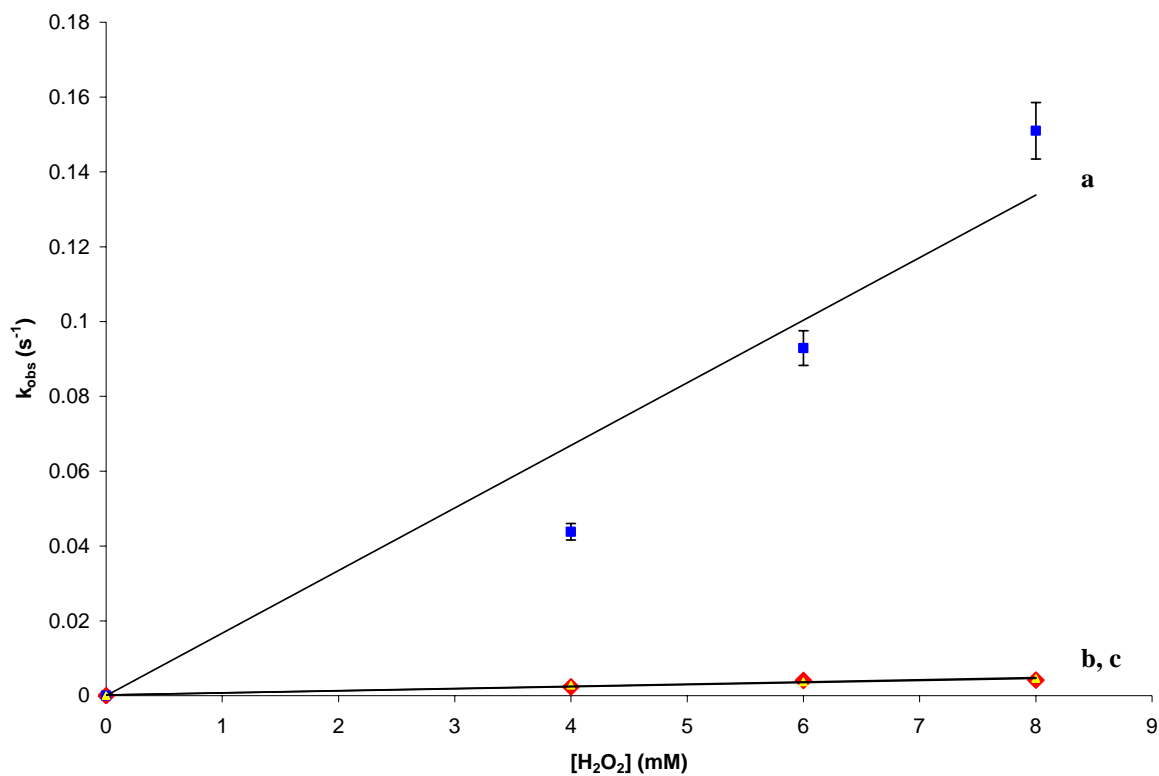


Figure 4.15 Plot of the apparent rate constants for the formation of heme degradation products. Reaction of 10 μ M oxy HbI (a), HbII (b), and HbI PheB10Tyr (c) as function of H₂O₂ monitored in a stopped-flow spectrophotometer. The kinetic rate constants are the mean of at least three independent experiments.

Table 4.3. Peroxide-mediated oxidation reactions rate constants of ferric Hb by H₂O₂ measured at 400 nm, and the formation of heme fluorescent products induced by H₂O₂.

Hemoglobin	k_{H₂O₂, ox} (M⁻¹s⁻¹)	k_{heme degradation} (M⁻¹s⁻¹)
α-DBBF Hb	120.5 ± 5.6	8.0 ± 1.6
HbI	403.2 ± 2.7	37.0 ± 6.3
HbII	64.0 ± 2.3	1.1 ± 0.6
HbI PheB10Tyr	52.0 ± 4.7	1.2 ± 0.04

α-DBBF Hb as measured by its reactivity with H₂O₂ and the presence of fluorescent heme degradation products. The rate constants for the reaction of the ferric forms of HbII and HbI PheB10Tyr mutant with bolus H₂O₂ (k_{H₂O₂, ox}, Table 4.3) and the rate constants for the presence of fluorescent heme degradation products in these solutions as a result of addition of excess peroxide are approximately 2.5 fold slower than that obtained for HbI. This clearly distinguishes that HbII and the HbI PheB10Tyr mutant are extremely stable and acts towards damaging by autoxidative and oxidative side reactions.

4.4 Discussion

Cell free hemoglobins are exposed to different tissues and molecules that can react with them causing reactions that may disturb the physiological equilibrium. The success of intracellular oxygen carriers in invertebrates is due, in large part, to the packaging of these molecules with reductants and allosteric modifiers of the hemoglobin affinity within red blood cells. The challenges of preparing cell free hemoglobins that achieve all the advantages of natural intracellular oxygen carriers have been overcome in some species by the evolutionary development of the high molecular weight heme proteins, erythrocruorins, which serve as oxygen carriers in marine and terrestrial worms. These naturally occurring respiratory proteins have high capacity for oxygen binding due to the presence of many oxygen binding sites, avoid adverse osmotic pressure effects via formation of multi-subunit ensembles, and allow for subunit interactions that are the basis of cooperativity in oxygen binding and heterotropic functional control of oxygen binding affinity (Bonaventura et al., 1975). The high molecular weight polymeric *Lubricous terrestris* Hb is another successful example in which oxygen carrying abilities are combined with unusually stable heme pockets with a well control oxidation reactions in extracellular environment (Hirsch et al., 1997). Therefore, the study of the redox chemistry of the hemoglobins is very important to understand the chemistry behind these reactions, and thereafter use this information to engineer a hemoglobin-based oxygen carrier.

Previous studies showed that the heme pocket double substitution HisE7Gln/LeuB10Phe enhances the autoxidation resistant of the hemoglobin in absence of antioxidant enzymes (Rogers et al., 1995). These experiments also suggested that

hemoglobins with lower oxygen affinity tend to autoxidize faster than the ones with high affinity. In this respect, HbI and HbII demonstrate that this statement is not always true due to the fact that both hemoglobins have high oxygen affinity, but they behave very different in their autoxidation reactions. *L. pectinata* HbI naturally has the substitution HisE7Glu/LeuB10Phe, which in vertebrates is unique in the elephant myoglobin, while HbII differs by a TyrB10 instead of the PheB10. HbI and HbII have a very high oxygen affinity with P_{50} of 0.18 and 0.13 mmHg, respectively (Kraus and Wittenberg, 1990), while α -DBBF Hb has a P_{50} of 26.0 mmHg (D'Agnillo & Alayash, 2000). However, HbI has a higher oxidation rate compared to HbII who has the lower autoxidation among all the hemoglobins studied here (Table 4.1). The autoxidation data shows that the kinetic rate for HbII is 9 times slower than that of the human cross-linked α -DBBF Hb. In the presence of the antioxidant enzymes SOD and catalase, α -DBBF Hb reduces its autoxidation by 40% while HbII reduces the reaction by 6%. The HbI PheB10Tyr mutant obtains an autoxidation rate similar to HbII, suggesting that the autoxidation is influenced by the TyrB10 residue. This autoxidation reduction in the reaction with SOD and catalase suggests that *L. pectinata* HbII produces less oxidative modifications that mediate the accumulation of oxygen free radicals. Moreover, the catalase assay shows a small enzymatic activity in HbII for H_2O_2 consumption, which is not present in HbI neither in α -DBBF Hb. This enzymatic behavior of *L. pectinata* HbII may be due as a self protective mechanism to maintain its ferrous oxidation state in the clam sulfide rich environment.

Regarding this, the PheB10 substitution of the Leu residue in mutant Mb was shown to decrease the rate of autoxidation by at least ten fold when compared to the rate of autoxidation of the native Mb. The large benzyl side chain inhibits autoxidation reactions by

both stabilizing bound O₂ and by filling the space adjacent to the bound oxygen. However, our data show that the presence of TyrB10 in HbII and HbI PheB10Tyr appear to afford a more stable O₂ adduct in the oxygenated form of these Hbs than does PheB10 in HbI. In this respect, Figure 4.16 shows the amino acids that form hydrogen bonds in the binding of oxygen to HbII (Gavira et al., 2008). The distances between amino acids or heme iron that creates the hydrogen network in the distal and proximal cavities are: Fe to O1, 2.94 Å; Fe to O2, 2.14 Å; O1 to NE1 of GlnE7, 3.00 Å; the oxygen in the OH of the TyrB10 to O1, 1.94 Å; the oxygen in the OH of the TyrB10 to the NE2 of GlnE7, 3.00 Å; OE1 of GlnE7 to NZ of LysF3, 2.64 Å; O1D of the heme propionate to NZ of LysF3, 2.71 Å; O2A of the heme propionate to NH1 of ArgF11, 2.95 Å; O1A of the heme propionate to NH2 of ArgF11, 2.64 Å; NE2 of HisF8 to the heme Fe, 2.11 Å. Thus the hydrogen network, specially between the oxygen ligand with TyrB10 and GlnE7, helps to protect HbII from the change in the heme oxidation state from heme-Fe(II) to heme-Fe(III). Therefore, it is suggested a contribution of the TyrB10 towards the stability of the heme pocket of HbII and HbI PheB10Tyr in the face of peroxide attack due to the presence of hydrogen bonding between the ferryl moiety and the heme pocket amino acids including TyrB10 which ultimately enhance the removal of peroxide by the peroxidative cycle (De Jesús-Bonilla et al., 2006).

The hydrogen peroxide can be formed as secondary product from the superoxide dismutation during the hemoglobins autoxidation. Amino acids play an important role in the steps through the formation of the ferryl species, compound I and compound II. Titrations for the reaction of the HbII, or the HbI mutant, with H₂O₂ show that starting with a deoxy hemoglobin, the iron protonates to form a ferric state and finally reacts with unreacted H₂O₂ showing a mixture between ferric and oxy hemoglobin with a Soret band at 412 nm. The

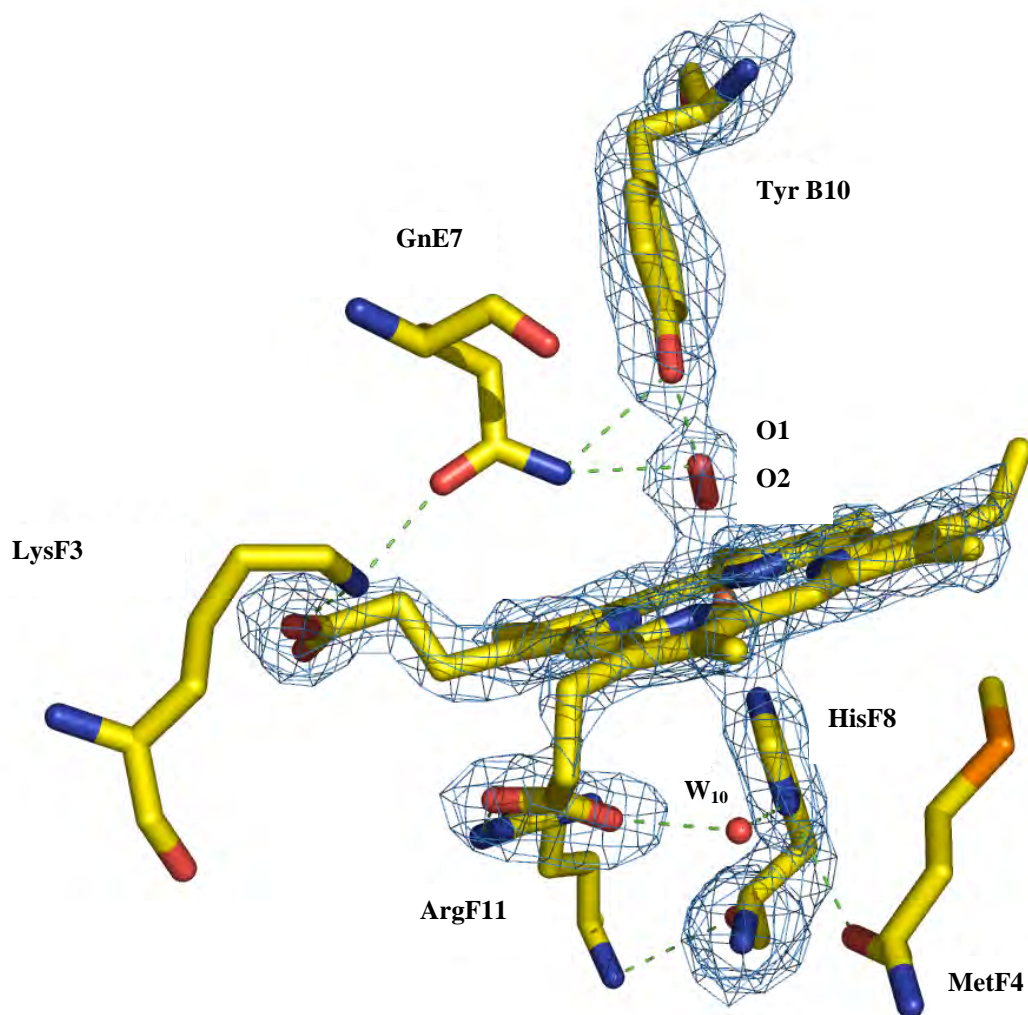


Figure 4.16 *L. pectinata* oxy HbII hydrogen bonding network. The TyrB10 and GlnE7 point towards the bound oxygen stabilizing it by means of hydrogen bonding. Fe - O1, 2.94 Å; Fe - O2, 2.14 Å; O1 - GlnE7 (NE1), 3.00 Å; TyrB10 (OH) - O1, 1.94 Å; TyrB10 (OH) - GlnE7 (NE2), 3.00 Å; GlnE7 (OE1) - LysF3 (NZ), 2.64 Å; heme (O1D) - LysF3 (NZ), 2.71 Å; heme (O2A) - ArgF11 (NH1), 2.95 Å; heme (O1A) - ArgF11 (NH2), 2.64 Å; HisF8 (NE2) - Fe, 2.11 Å (Gavira et al., 2008).

panorama is different for HbI wild type in where starting from a deoxy state the reaction with H_2O_2 proceeds with the binding of O_2 to form the oxy HbI and then reacting with additional H_2O_2 produces the final compound II with the Soret band at 419 nm. Figure 4.17 shows the proposed mechanism for the reaction of HbII or HbI PheB10Tyr mutant with H_2O_2 . These *L. pectinata* hemoglobins have a pattern similar to human hemoglobin and myoglobin (Yeh & Alayash, 2003, Reeder et al., 2002). One of the starting points in the mechanism is the hemoglobin in the ferric state [1] with a water molecule as the ligand. The addition of H_2O_2 forms either ferryl compound I [2], ferryl compound II [3] or both ferryl species. At some conditions, compound I is going to have a longer life time, as in the reaction of hydrogen peroxide with ferric HbI (De Jesús et al., 2001), and then the porphyrin radical goes to some place of the protein, forming the compound II ferryl species. In this special case, and different from the most of the proteins, k_{13} is higher than k_{12} and k_{23} . The reaction is going to behave different when a networking between a distal amino acid and the radicals formed in the reaction with H_2O_2 can take place. The reaction with the HbII and the HbI PheB10Tyr mutant showed, like to other globins, a non-stable compound I monitoring the characteristic band at 648 nm indicative of this species. Different to HbI, HbII and the HbI PheB10Tyr mutant have a tyrosine in the B10 position. The tyrosine amino acid in the heme pocket creates a hydrogen bond networking that neutralizes very quickly the compound I radical leading to a rapid formation of the compound II without the detection of the compound I through the 648 nm band. Therein the rate constant k_{23} has to be higher and faster than $(k_{12}+k_{13})$, rate constant for the formation of compound II. Previous works with myoglobin show similar networking between the ferryl porphyrin radical and the amino acids tryptophan and tyrosine (Østdal et al., 2001, DeGray et al., 1997, Catalano et al., 1989).

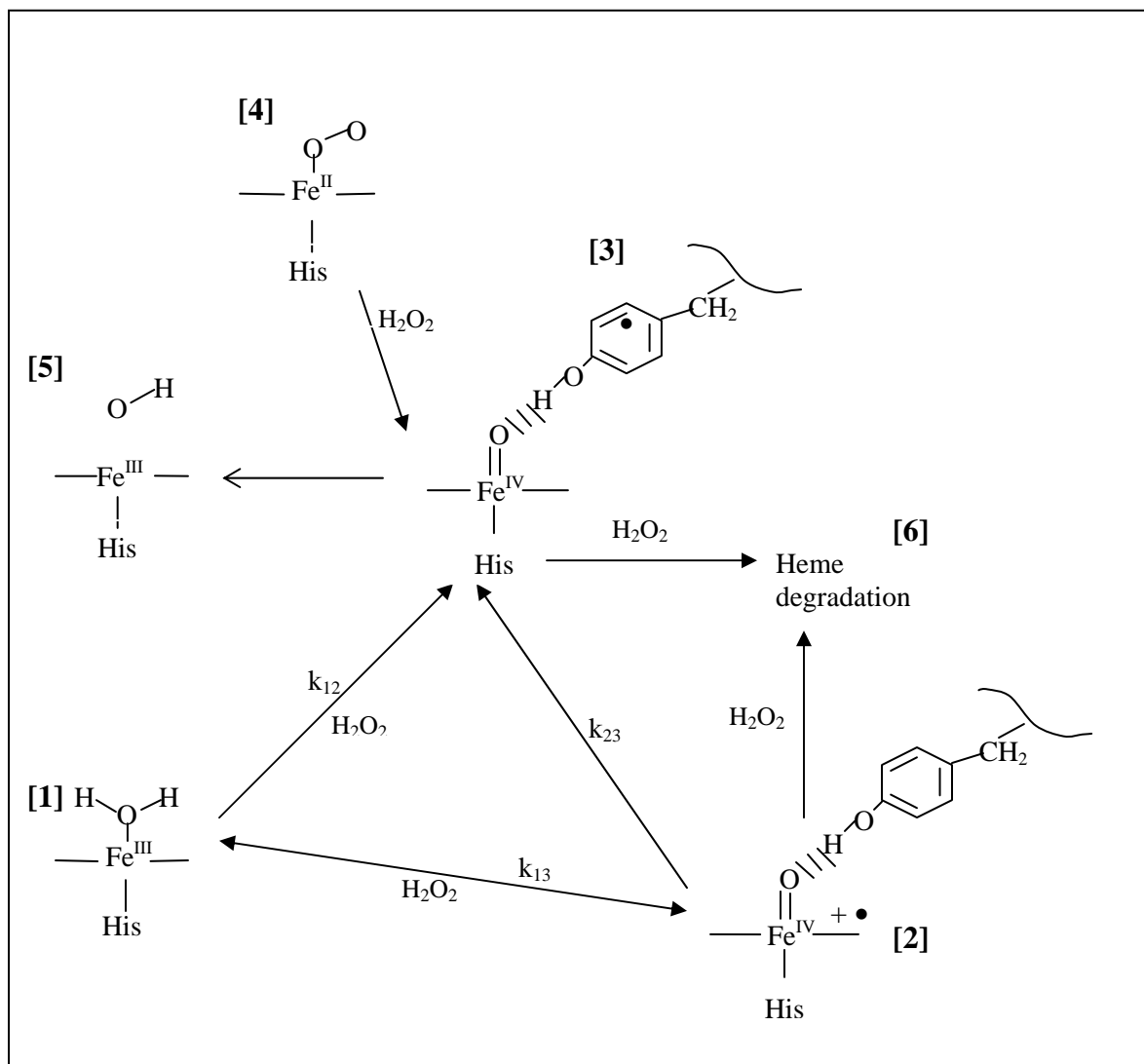
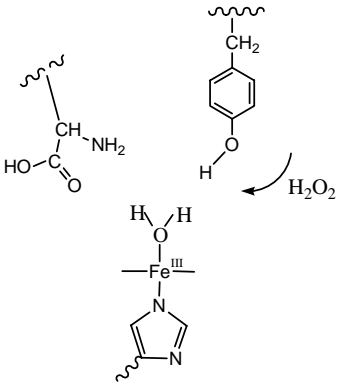
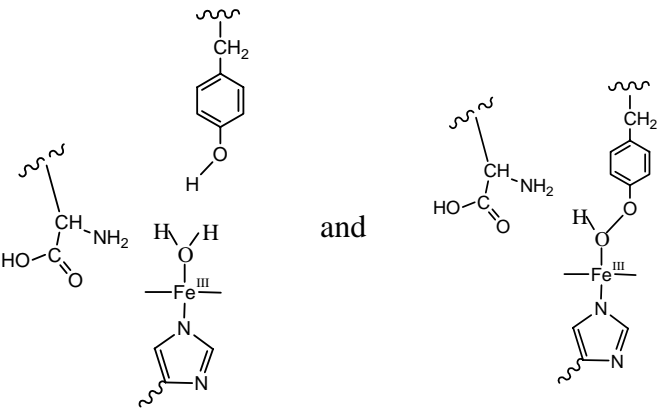
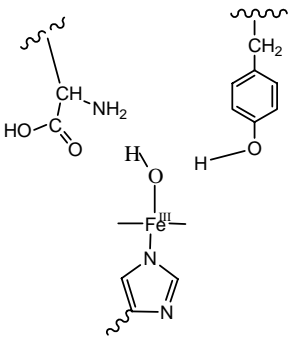


Figure 4.17 Proposed mechanism for the reaction of HbII and HbI PheB10Tyr with H_2O_2 . The oxy hemoglobin [2] autoxidizes to form the ferric heme [1], which reacts with H_2O_2 to form, compound I [3] or compound II [4]. The formation of the ferryl compound I proceeds by the decay to compound II or depending on the H_2O_2 concentration can go back to the ferrous heme. The reaction at high concentrations tends to the production of degradation species and to heme degradation.

When oxy hemoglobin [4] reacts with hydrogen peroxide produces the ferryl compound II [3] and then undergoes a one electron reduction to ferric hemoglobin [5]. The reaction of the hemoglobin with large hydrogen peroxide concentrations leads to heme degradation [6]. The formation of the tyrosine radical is a very important step toward the understanding of dimerization reactions and heme protein degradation.

Moreover, the kinetic rate constants shown in Table 4.2 demonstrate that the rate constant values for HbII and the HbI PheB10Tyr are very similar. Table 4.4 shows the suggested structures for HbII at pH 5.0, 7.4 and 11.0. The kinetic rate constants for the reaction of HbII and HbI PheB10Tyr with hydrogen peroxide at pH 5.0, were $141.60 \text{ M}^{-1}\text{s}^{-1}$ and $103.45 \text{ M}^{-1}\text{s}^{-1}$, respectively. The reaction suggests that the incoming H_2O_2 displaces the water molecule in the heme-Fe(III) active center, and then is stabilized by a hydrogen bond between the TyrB10 and the GlnE7. At pH 7.4, the ferric heme is in equilibrium with the iron tyrosine moiety. Since the H_2O_2 and the hemoglobin concentrations governed the rate constants, and the amount of hemoglobin available to interact is lower than that for a pH of 5.0, thus the rate constants decreased to $77.79 \text{ M}^{-1}\text{s}^{-1}$ and $69.00 \text{ M}^{-1}\text{s}^{-1}$ for HbII and HbI PheB10Tyr, respectively. At pH 11.0, the strong interaction between the iron and the OH ligand does not allow the rapid reaction of the peroxide. This behavior for the rate of the ferryl formation is similar to previous work in the reaction of myoglobin with hydrogen peroxide (Reeder et al., 2002). In spite that the kinetic constants for the formation of compound II are similar for HbII and the HbI PheB10Tyr, the values for the later are smaller. The heme freedom in the HbI PheB10Tyr mutation allows a change in the structure conformation that slows the entrance of H_2O_2 , therefore it is also slower the formation of the

Table 4.4 Proposed heme pocket interactions when HbII is exposed to different pHs.

pH 5.0	
pH 7.4	
pH 11.0	

compound II ferryl species.

In the blood fluids the reactions of cell free hemoglobins with hydrogen peroxide lead to heme degradation and toxicity. The kinetic rate constant for the formation of fluorescent heme degradation products (Table 4.3) is 13 times less in HbII than in α -DBBF Hb. In this experiment the mutation of the tyrosine in the B10 position affects positively the stability of the pocket with a kinetic rate constant similar to HbII. The difference is very dramatic for HbI, having the higher formation of degradation products. The general behavior of the hemoglobins indicates that HbII is less susceptible to oxidative damage. Previous studies showed that the double insertion of Phe at both the B10 and E11 positions (i.e., L29F/V68F) produces a myoglobin mutant that reacts slowly with H_2O_2 , forms less ferryl iron intermediate, but it retains an extremely high affinity towards O_2 which disqualify this combination as basis for further development as an oxygen carrier prototype. However, Mb mutants in which His64 was replaced with Gln singularly or in combination with PheB10 showed similar enhanced pseudoperoxidase activity, favorable NO and O_2 binding characteristics, (Olson et al., 2004) but an enhanced heme loss and breakdown. Uncontrolled oxidative reactions and subsequent heme degradation or loss were among the most undesirable side reactions that hampered the development of current generation chemically modified hemoglobins. (Alayash, 2004). Resonance Raman, X-ray crystal structure studies and functional studies showed that both GlnE7 and PheB10 contribute towards stabilizing bound ligands and that the flexibility of the HbI distal site, is directed mainly by GlnE7, which controls ligand reactivity. The stabilizing of the heme-bound O_2 by the TyrB10 residue in HbII as well as in other nonvertebrate hemoglobins, such as those from *Mycobacterium tuberculosis*, *Ascaris suum* and bacterial flavohemoglobin has been

demonstrated recently (Pietri et al., 2005, Mukai et al., 2001, Yeh et al., 2000). Therefore, the autoxidation, the hydrogen peroxide and heme degradation experiments in this study strongly suggests that the Gln64 is not responsible for the hemoglobins oxidative damage and heme breakdown. Indeed, the substitution of an apolar and big residue like phenylalanine in the B10 position, like in HbI, can increase heme damage. In addition, the substitution to a tyrosine polar residue and in combination with the glutamine in E7, as in HbII, creates a hydrogen bonding network that includes the GlnE7, TyrB10 and O₂ bound to the heme that results in a tight gage for the oxygen networking providing better resistant to oxidative damage.

5 REACTIONS WITH GLUCOSE OXIDASE IN BOVINE AORTIC ENDOTHELIAL CELLS

5.1 Introduction

One application for the hemoglobin-based oxygen carriers is its transfusion, as for example in cases of anemia, where the cells are in stress for the lack of oxygen. Despite the absence of oxygen, there is an overproduction of reactive oxygen species (ROS). The hydrogen peroxide, a ROS, can also be produced by the mammalian endothelial cells (D'Agnillo & Alayash, 2000). Therefore, one way to study the extracellular oxidative stress is to expose endothelial cells to ROS generating enzymes, such as glucose oxidase (Gow et al., 1999). The reactive oxygen species that are generated extracellularly attack surface proteins, blood elements, and the outer leaflet of the plasma membrane. Previous studies with human HbA₀ and modified human α -DDBF Hb show that the cell death induced by H₂O₂ was inhibited by these hemoglobins. This is consistent with the hemoglobin suggested pseudoperoxidative activity in which consumes H₂O₂ as it cycles between the ferric and the ferryl species (Goldman et al., 1998). Therefore, the redox cycling in which H₂O₂ is consumed (Figure 5.1) produces the ferryl species that is toxic to cells and alters the route of death (D'Agnillo & Alayash, 2000). The studies also suggested that the intermolecular and intramolecular cross-linking in the hemoglobins lock the protein conformation to have a more stable ferryl species (Goldman et al., 1998).

In this respect, D'Agnillo and Alayash (2001) studied the reaction of α -DDBF Hb and hydrogen peroxide generated by the glucose oxidase (GOX) system. The reaction oxidizes

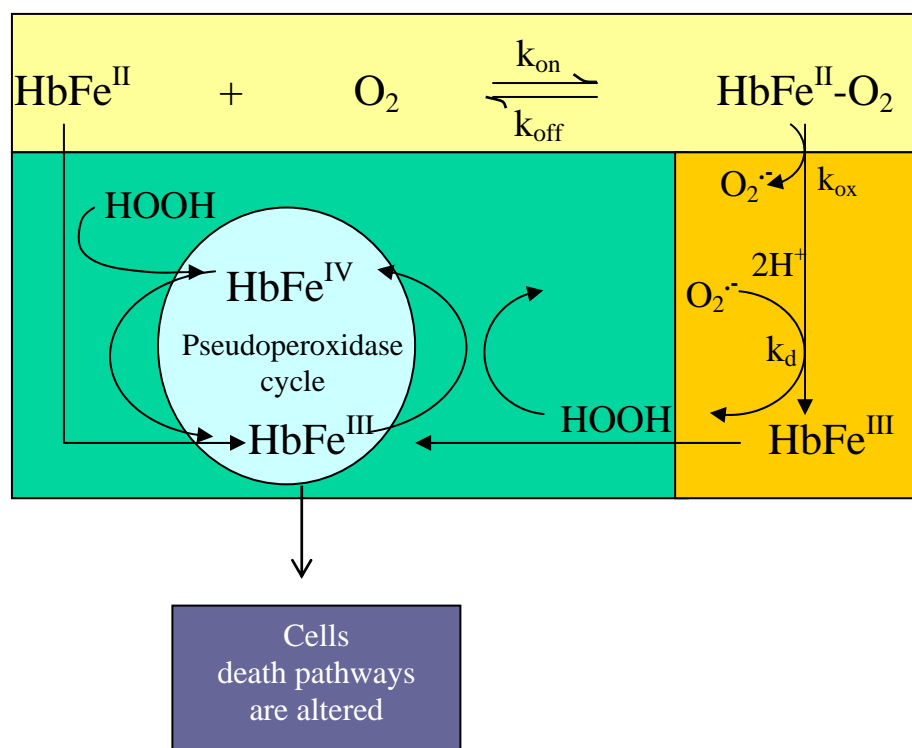


Figure 5.1 Hemoglobins redox cycle. The hemoglobins autoxidation forms the superoxide ion which dismutates to hydrogen peroxide. The hemoglobin reacts with hydrogen peroxide in a ferric-ferryl cycle that produces high concentrations of ROS. This balance disruption alters cell death pathways.

oxy α -DBBF Hb, but during the process the redox cycling of ferric and ferryl α -DBBF Hb was identified. Moreover, these reactions showed changes in cell morphology and apoptotic features including cell rounding, swelling, detachment, and phosphatidylserine externalization. This endothelial dysfunction takes in abnormalities in the factors that regulate vasodilation (Dworakowski et al., 2008).

Therefore, this part of the study investigates the oxidation reactions of the hemoglobins HbI, HbI PheB10Tyr, and HbII and the formation of the ferryl species in the reaction with a low steady flux of H_2O_2 generated by GOX. The cytotoxicity of the hemoglobins in culture bovine aortic endothelial cells was also monitored by apoptosis and cell viability analysis. The modified human cross-linked α -DBBF Hb was used as control in the experiments.

5.2 *L. pectinata* hemoglobins oxidation with glucose oxidase

Spectral analysis of *L. pectinata* HbI and HbII with H_2O_2 and GOX allowed to monitor the behavior of the hemoglobins previous to their incubation with bovine aortic endothelial cells. The reaction with moderate concentrations of H_2O_2 produces the ferryl species, while the addition of high H_2O_2 concentrations leads to heme degradation products (De Jesús-Bonilla et al., 2007). Regarding this, experiments were performed to compare the behavior of the hemoglobins when reacting with the H_2O_2 , but in this analysis the H_2O_2 was produced by the reaction of GOX with oxygen. Figure 5.2 shows the UV-Vis overlaid spectra for the reaction of 50 μ M oxy HbI with 250 μ M of H_2O_2 . The intensity of the visible

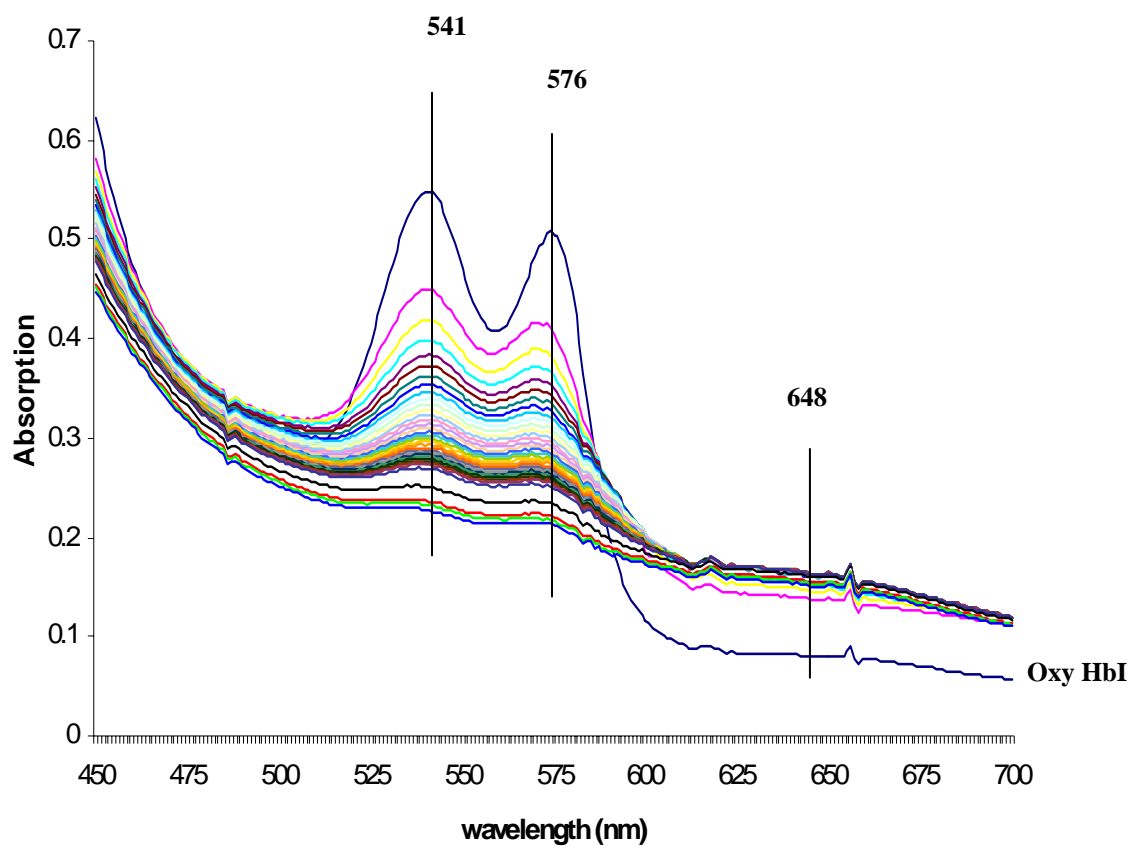


Figure 5.2 Overlaid spectra for the reaction of 50 μM oxy HbI with 250 μM H_2O_2 . Oxy HbI 541nm and 576 nm bands decrease while increases the ferryl band at 648 nm and the formation of hemichrome species.

bands at 541 nm and 576 nm assigned to the oxy HbI species decreases, and at the same time, a very weak and broad band near the 648 nm increases, characteristic of the ferryl compound I species (De Jesús et al., 2001). Similarly, the spectra suggest heme degradation in less than 1 hour. However, the overlaid spectra of 50 μ M oxy HbI with 10 mU/mL GOX, Figure 5.3, shows that the oxidation of HbI with GOX is slower than the reaction with hydrogen peroxide. During the one hour analysis, the spectra evidenced the formation of the ferryl species compound II. The bands at 633 nm and 502 nm indicate a mixture of the hemoglobins oxidation state suggesting the cyclic ferric-ferryl reaction. The spectra in the reaction with GOX also show formation of hemichrome species. The hemichrome is a six coordinated low-spin heme characterized by the occurrence of peaks at 530 nm and 565 nm (Vitagliano et al., 2004). The loss of isobestic points near 515 nm and 590 nm is also indicative of the presence of these species during the hemoglobin oxidation (Sugawara et al., 2003). In addition, changes in the baseline between spectra suggest that the oxidation by hydrogen peroxide leads to heme degradation. Figure 5.4 (A) shows the reaction of HbI with 10 mU/mL GOX at the end of 6 hours. The spectrum is nearly flat with a small band at 561 nm suggesting the presence of hemichrome species and is indicative of heme degradation. After 6 hours, sodium dithionite was added to the hemoglobin solution (Figure 5.4 B), but instead of the formation of the deoxy species by the reduction with the sodium dithionite, the spectrum shows only one band with a maximum at 648 nm. This band suggests the presence of intermediate species; however, the overall behavior of the protein is indicative of a non functional heme protein.

The one hour reaction of 50 μ M oxy HbII with 250 μ M H_2O_2 is illustrated in Figure 5.5. The overlaid spectra show that the oxidation of HbII by H_2O_2 is slower than the HbI

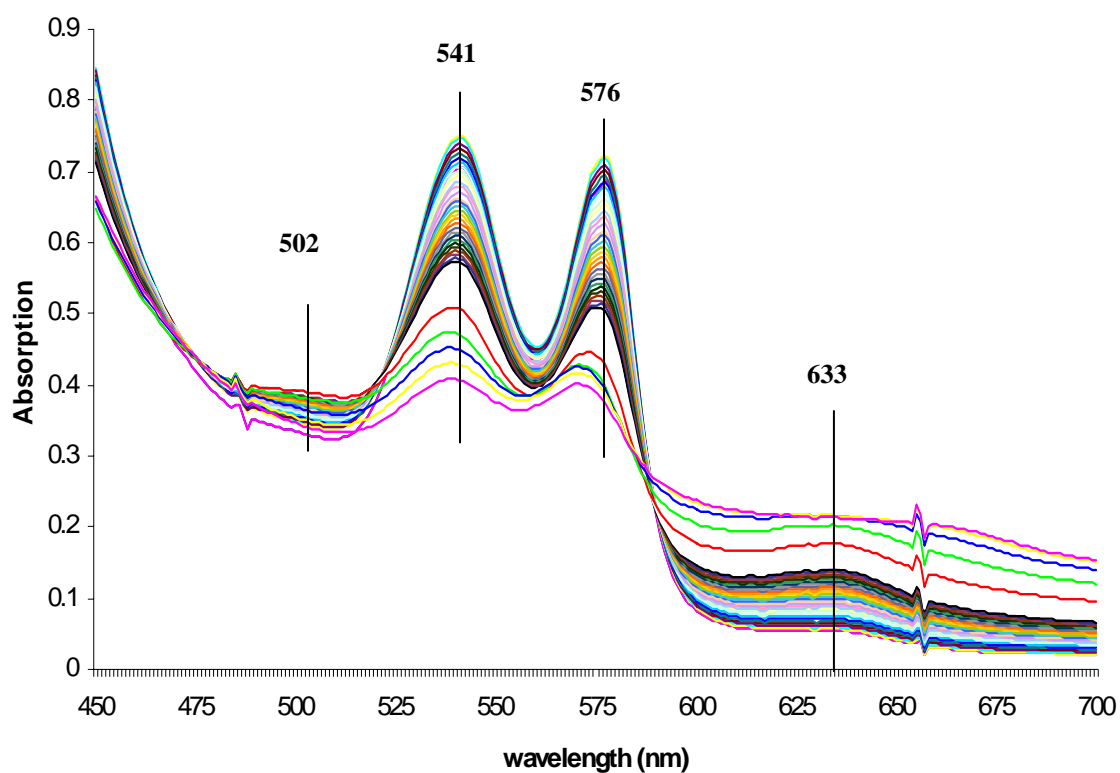


Figure 5.3 Overlaid spectra for the reaction of 50 μM HbI with 10 mU/mL GOX. Oxy HbI 541nm and 576 nm bands decrease while increases ferric bands at 502 nm and 633 nm. The change in baseline between spectra and the decrease in the bands intensity suggests heme degradation.

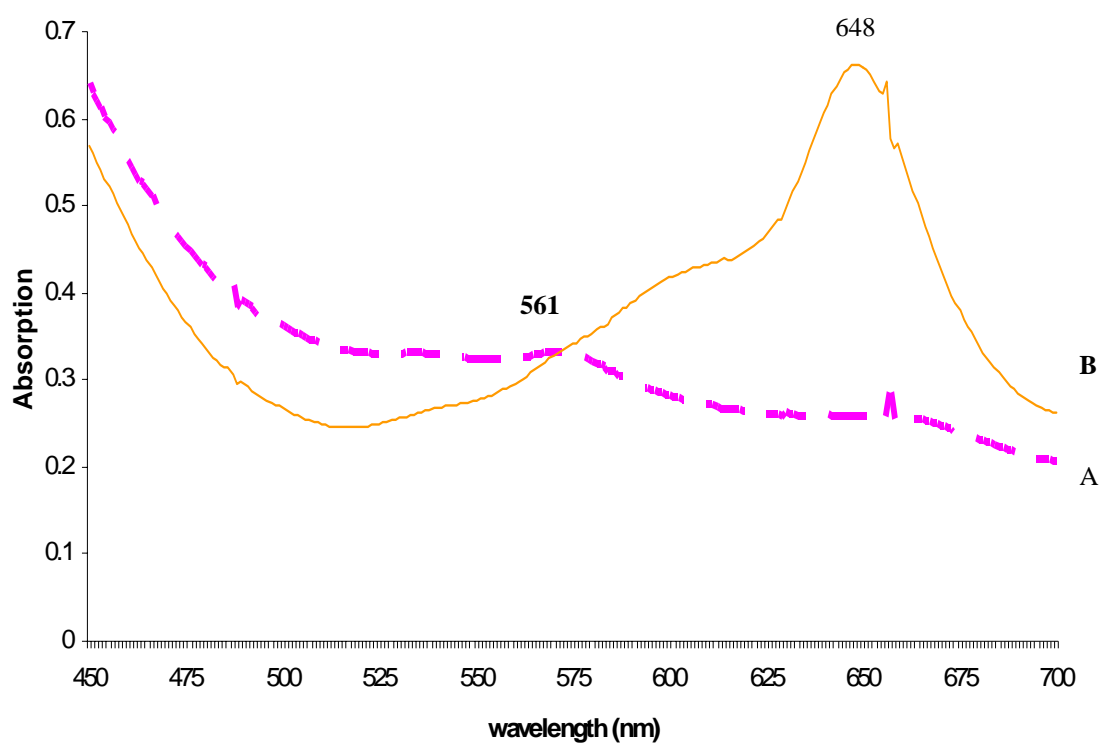


Figure 5.4 UV-vis spectra for the reaction of 50 μM HbI with 10 mU/mL GOX after 6 hrs (A), and after the addition of sodium dithionite (B). After 6 hours the spectrum only shows the hemichrome band at 561 nm. The addition of sodium dithionite did not form the deoxy hemoglobin, instead forms a band at 648 nm.

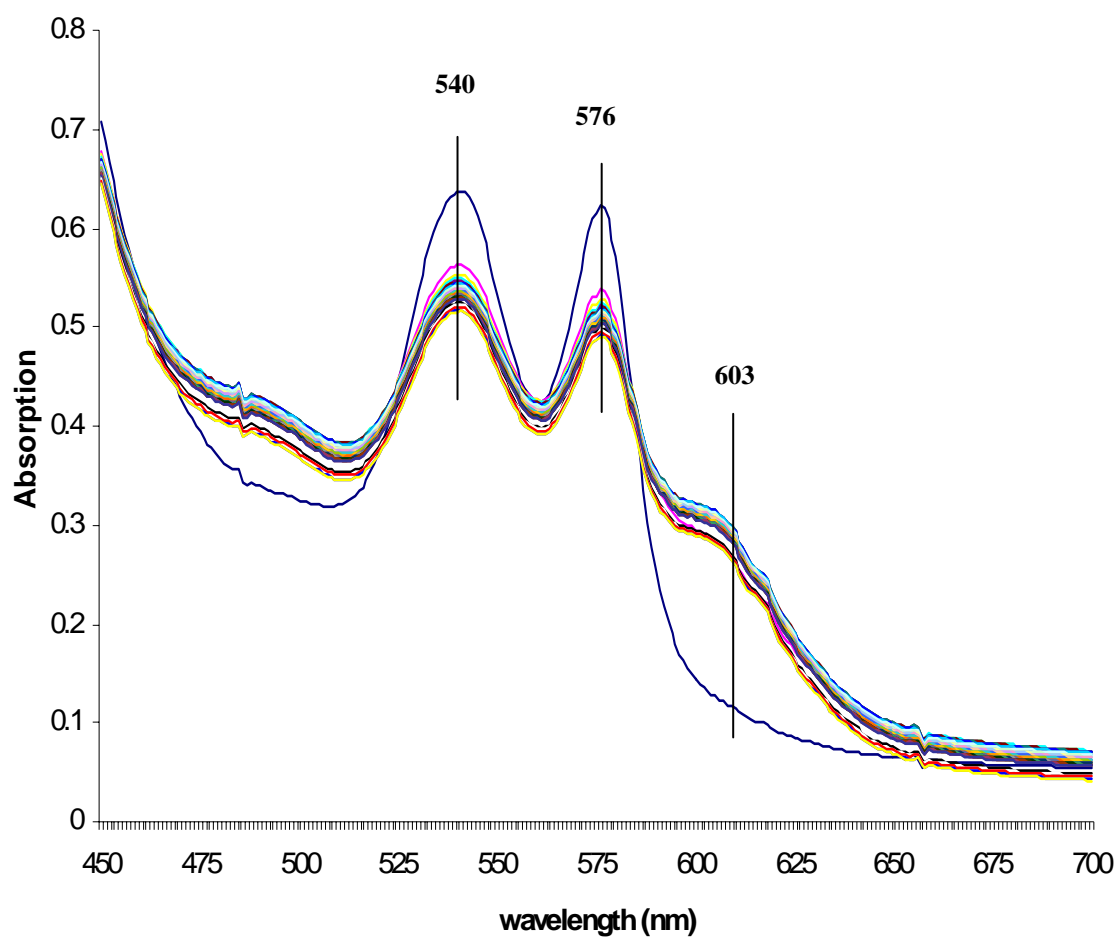


Figure 5.5 Overlaid spectra for the reaction of 50 μM HbII with 250 μM H_2O_2 . Oxy HbII 541nm and 576 nm bands have a small decrease while increases the heme-tyrosianate moiety band at 603 nm.

using the same experimental conditions. The oxy bands at 540nm and 576 nm have a little decrease in intensity, while a band appears at 603 nm. This band was assigned to HbII tyrosinate moiety with pH value between 6 and 8 (Pietri et al., 2005). In addition, the spectra did not show signals of hemichrome species, neither of heme degradation, since lack changes in the isobestic points or the presence of the 561 nm band. As a result, the change in the oxy bands intensity in part is due to the molar extinction coefficients of the species that is higher in the oxy than in the ferric species, thus giving middle intensities in the case of a oxy-ferric mixture (Table 2.1). Figure 5.6 shows the reaction of HbII with 10 mU/mL GOX for 6 hours. In the presence of hydrogen peroxide the small changes in the oxy bands of HbII suggest that it is strongly resistant to oxidation when it is exposed to continuous additions of low concentrations of the oxidant species. Figure 5.7 A shows the UV-Vis spectrum for the reaction after 6 hours. This spectrum (A) presents oxy HbII bands at 540 nm and 576 nm, and the band at 603 nm. When sodium dithionite was added to the 6 hour solution, the deoxy HbII species was formed with its characteristic band at 556 nm (Figure 5.7 B). Therefore, comparing HbI with HbII, the latter shows resistance to oxidation when reacts with high concentrations of H_2O_2 or with small fluxes of H_2O_2 produced by the glucose oxidase. Figure 5.8 A shows a proposed reaction mechanism in which the reaction of oxy HbII [1] with GOX produces the ferryl heme-Fe(IV) species [2]. The ferryl heme can be reduced forming ferric heme [3]. Thus, the ferric HbII reacts with available H_2O_2 forming again ferryl species [2]. The continuous flux of hydrogen peroxide allows the reaction of H_2O_2 with the hemoglobin suggesting a pseudoperoxidative cycle of H_2O_2 consumption. However, the spectral data indicates that HbI produces the ferryl species in a short time period, and that

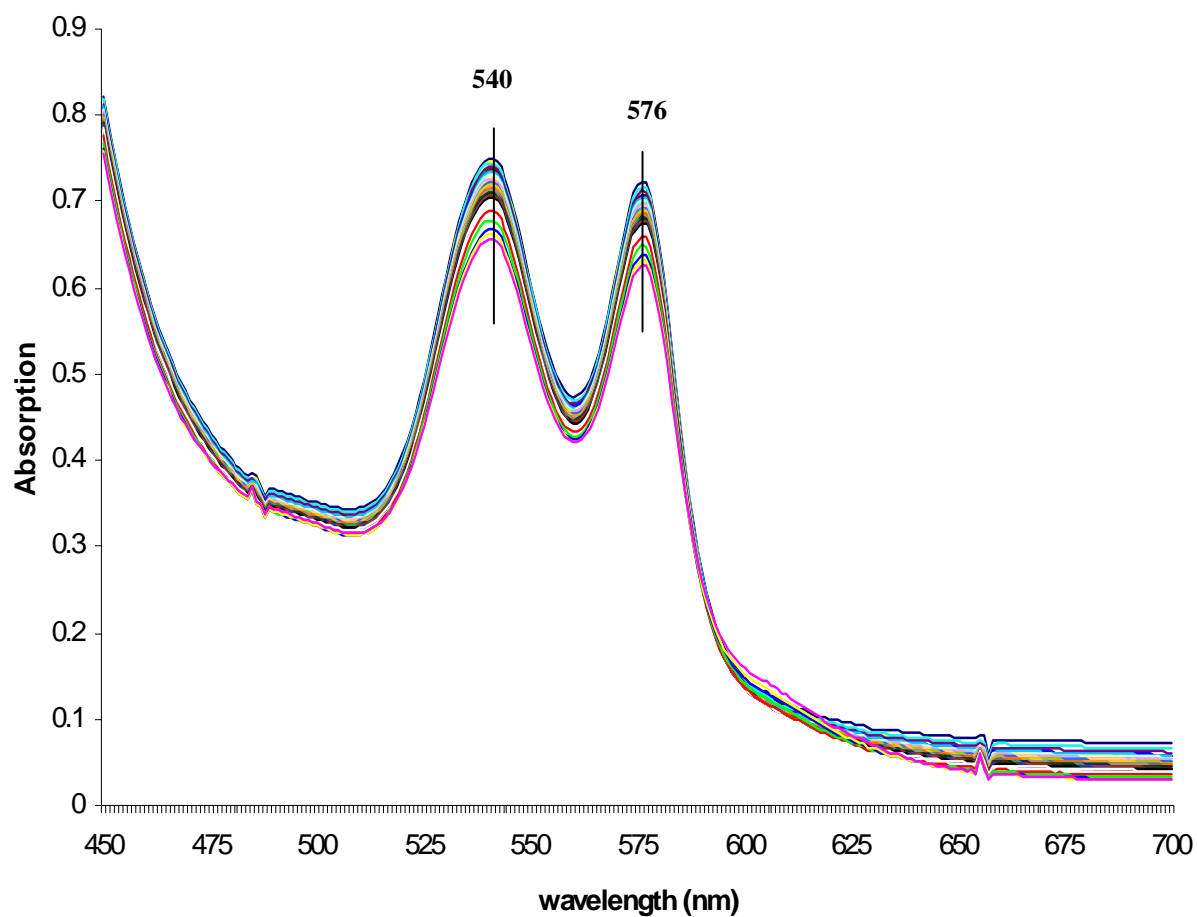


Figure 5.6 Overlaid spectra for the reaction of 50 μM HbII with 10 mU/mL GOX. Oxy HbII 541nm and 576 nm bands have a very small reduction, but without signals of ferric or ferryl species.

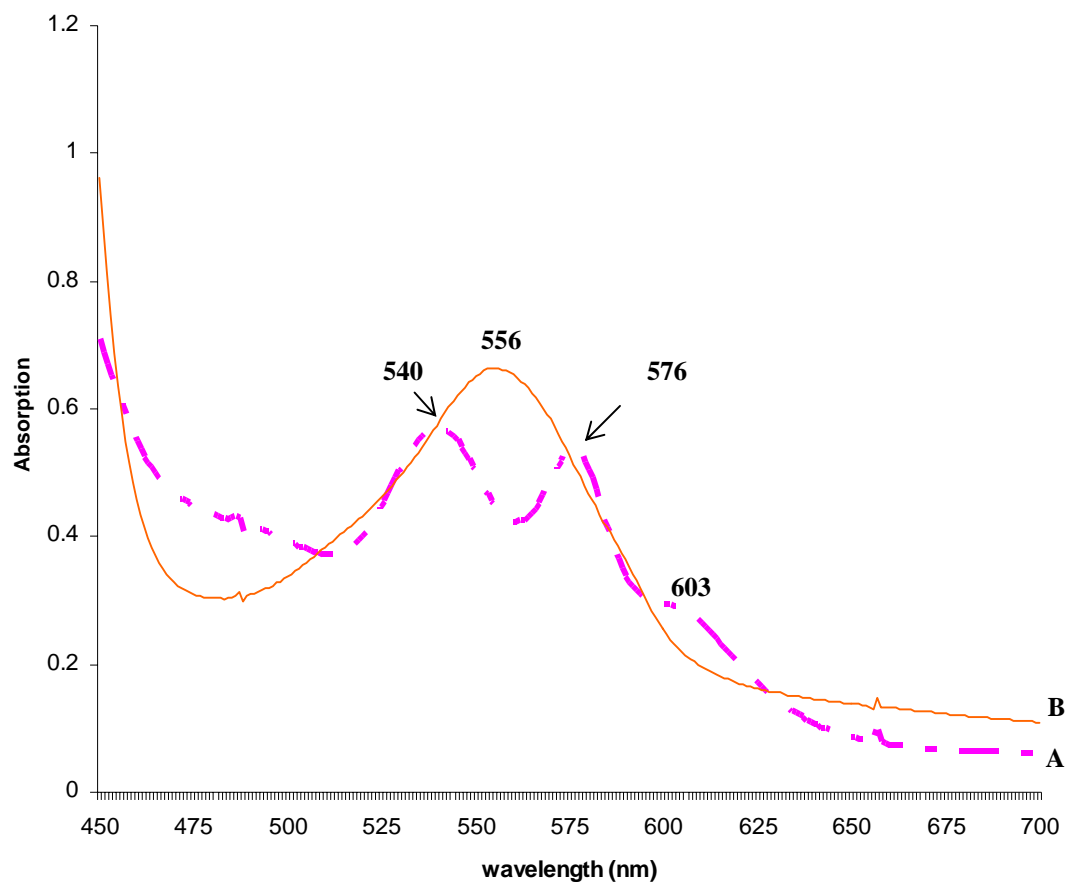
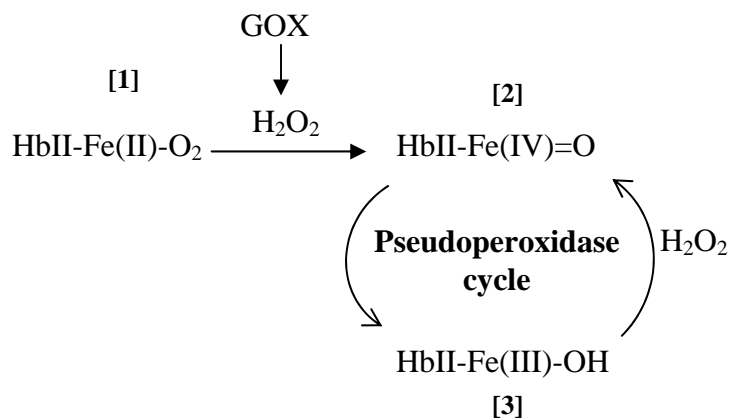


Figure 5.7 UV-Vis spectra for the reaction of 50 μM HbII with 10 mU/mL GOX after 6 hrs, and addition of sodium dithionite. In spectrum A, the reaction at 6 hours resemble the reaction with 250 μM H_2O_2 , with an increase in the 603 nm band. Deoxy HbII was formed after the addition of sodium dithionite (B).

A



B

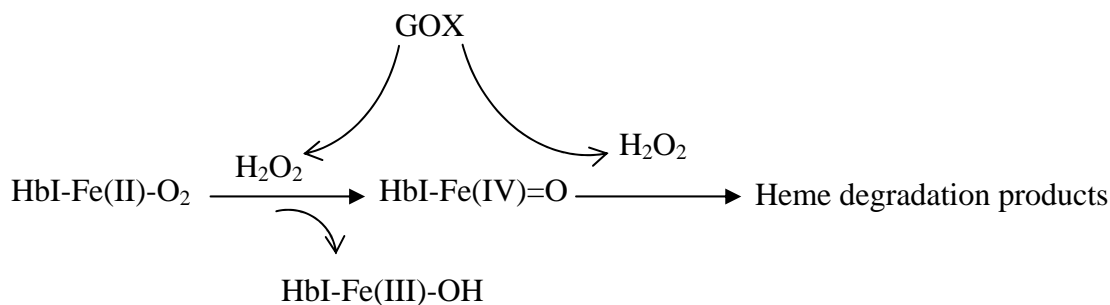


Figure 5.8 Schematic representation for the reaction of *Lucina pectinata* HbII and HbI with glucose oxidase. **A.** HbII reacts with the H₂O₂ produced by GOX forming the ferryl species. Continuous flux of H₂O₂ makes HbII to act as a pseudoperoxidase, thus consuming H₂O₂ in a ferric-ferryl cycle. **B.** HbI reacts with the produced H₂O₂ forming ferric and the ferryl species. Continuous H₂O₂ production leads to HbI heme degradation.

the continuous H₂O₂ flux generates many degradation products forming green hemoglobin, as depicted in the reaction in Figure 5.8 B.

5.3 Apoptosis and cell morphology in the reaction of the hemoglobins with glucose oxidase

The endothelial cells recover the blood vessels, consequently, have direct contact with blood or with infused cell free hemoglobin. Therefore, it is important to study the impact of the cell free hemoglobin to the cells. In this respect, the Cell titer-blue viability assay was performed for endothelial cells treated with α -DBBF Hb, HbII, HbI, and HbI PheB10Tyr mutant. Figure 5.9 indicates that at 2 hours more than 85% of the cells are viable after exposed to hemoglobins. The statistical analysis showed a probability in the range of 0.051 to 0.63 ($p < 0.05$ are significantly different) when the treated and untreated cells with hemoglobins were compared. Therefore, there is not a significant difference in the viability of the cells treated and untreated with hemoglobins at 2 hours. The graph at 6 hours illustrates that the viability for α -DBBF Hb decreases only 7%; while the cells incubated with HbII and HbI have a reduction of 21% and 24%, respectively, showing a significant difference in viability from cells without treatment. The cells treated with HbI PheB10Tyr only have a 13% decrease in the viability assay showing no significance difference with untreated cells ($p = 0.06$). The experiments for 24 hours show that α -DBBF Hb decreases only a 10% without a significant difference compared to untreated cells. However, the experiments for the *L. pectinata* hemoglobins for periods longer than 6 hours showed that during the incubation time, at 37°C in a humidified incubator with 5% CO₂ and 95% air, HbI, HbII, and HbI PheB10Tyr aggregate. In this respect, previous experiments (Pietri et al.,

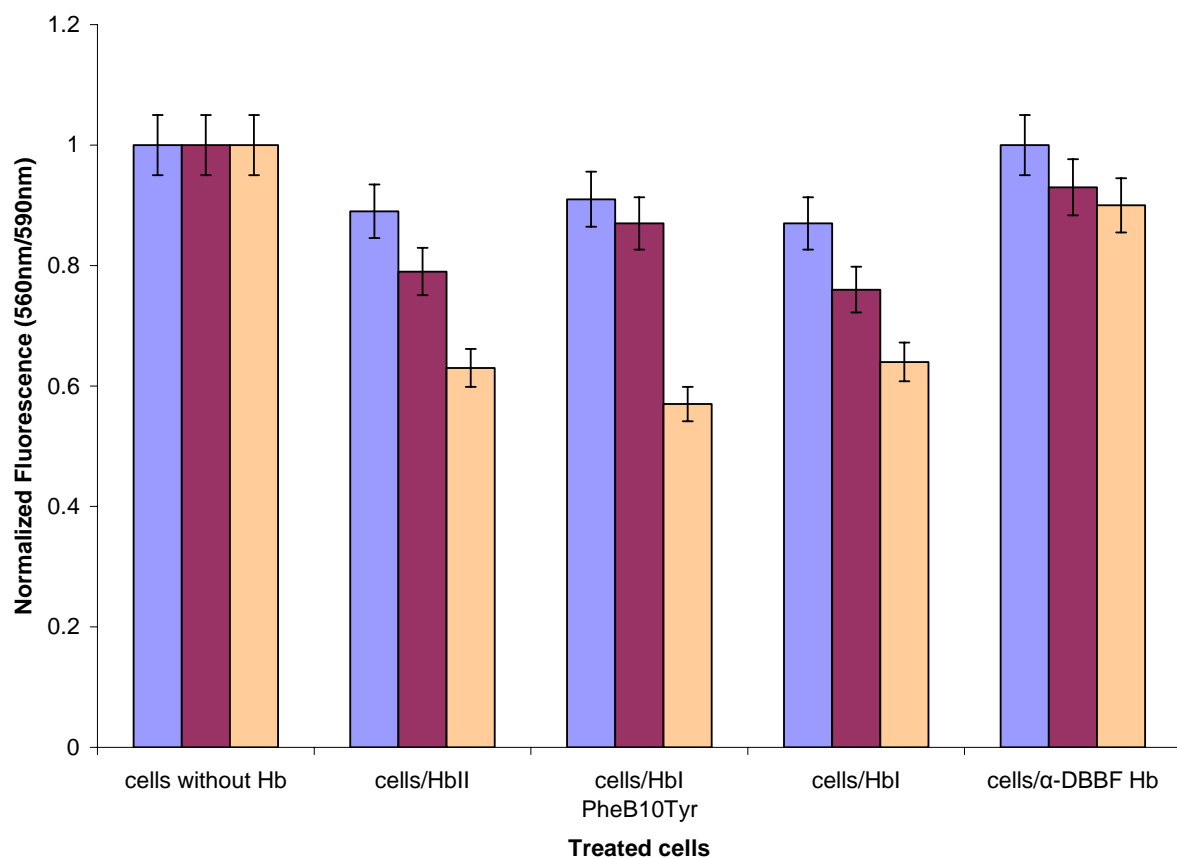


Figure 5.9 Bovine aortic endothelial cells viability assay after exposed to α -DBBF Hb, HbII, HbI, and HbI PheB10Tyr mutant. ■ 2 hr, ■ 6hr, ■ 24 hr. Values at each time represent the mean \pm SE of 15 - 30 assays for three different experiments.

2005) showed that the hemoglobins are stable in a pH range from 5.5 to 10.5, thus eliminating the pH as possible factor for the aggregation. To check the factor of temperature, the hemoglobins were incubated with and without the cells at 37°C for 72 hours. During this time, the hemoglobins remained stable without signals of aggregation or degradation. Preliminary assays were carried with HbII exposed to CO₂ and showed hemoglobin aggregation and oxidation. Therefore, these experiments suggested a conformational change in *L. pectinata* hemoglobin's structure when exposed to an atmosphere exchanging 5% CO₂. This aggregation makes the hemoglobin toxic to endothelial cells causing that only a 65% of the endothelial cells can be viable for periods longer than 6 hours.

Figure 5.10 graphs the viability assay for the bovine aortic endothelial cells incubated with the hemoglobins during the production of H₂O₂ induced by glucose oxidase. At 2 hours, the cells incubated with GOX did not present a significant difference compared to the cells without treatment. However, the cells undergo arrest in a time dependent manner at 6 and 24 hours with decreases in their viability of 16% and 44%, respectively. The addition of α -DBBF Hb shows the same behavior as the cells alone with GOX, indicative that this hemoglobin does not affect the cell viability significantly, with $p > 0.05$. Comparing the cells treated with GOX and α -DBBF Hb with the ones having GOX and *L. pectinata* hemoglobins, the cells treated with the latter show a cell viability reduction in all the experiments. The 2 hours assay, compared to the control cells with GOX, shows that HbII and HbI reduces the cells viability by 16% and 18%, respectively, while the HbI PheB10Tyr has only a 5% decrease. These values are nearly the same as the viability of the cells without the GOX, without a significant difference between the values. At 6 hours, HbI and the

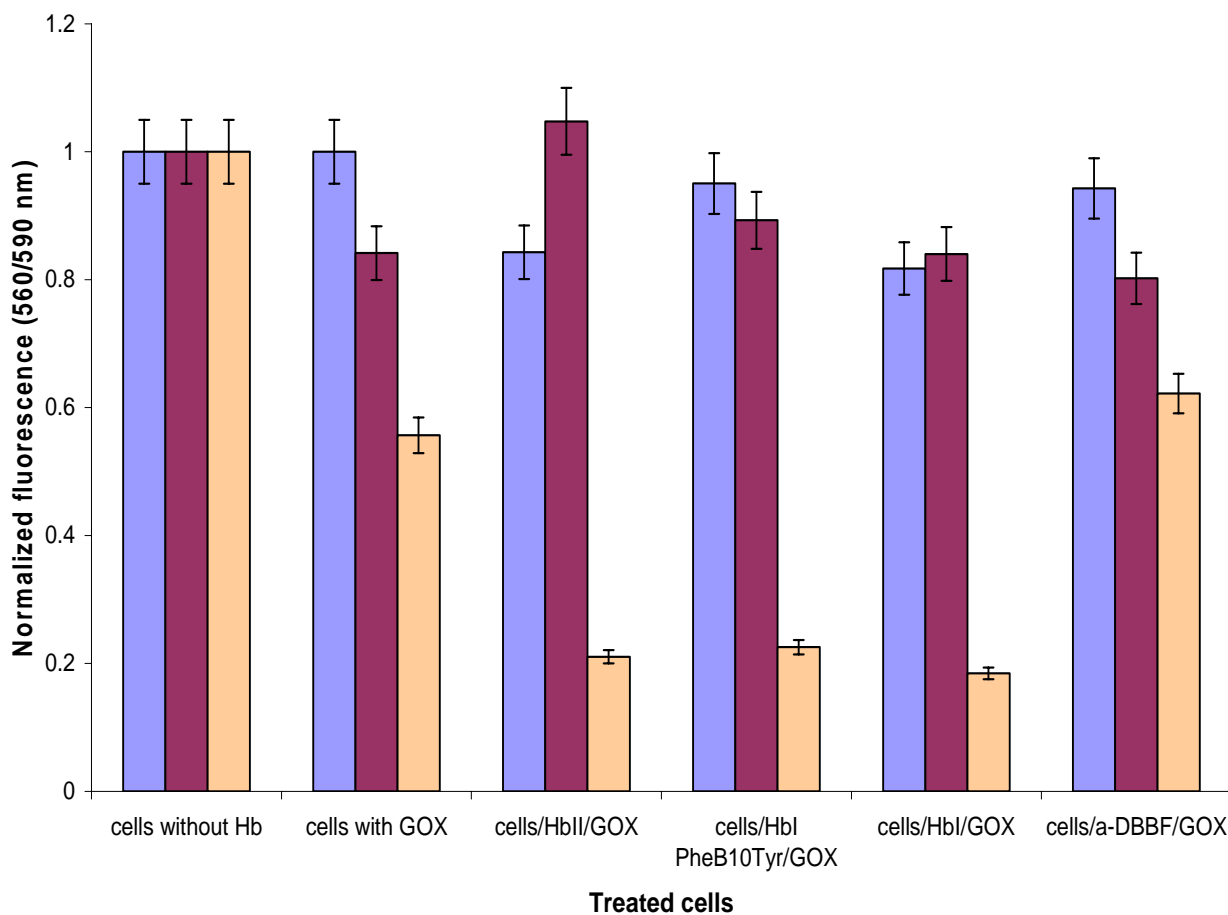


Figure 5.10 Bovine Aortic Endothelial Cells Viability Assay after exposed to α -DBBF Hb, HbII, HbI, and HbI PheB10Tyr mutant and GOX. ■ 2 hr, ■ 6hr, ■ 24 hr. Values at each time represent the mean \pm SE of 15 - 30 assays for three different experiments.

mutant did not affect the cell viability, showing a behavior similar to the cell control with GOX. In the case of HbII, the viability increased from 85% to 100%. This change is significant with a p of 0.001 ($p < 0.5$). The living cells at 24 hours are very few, only approximately 20%, when they are exposed to the three *L. pectinata* hemoglobins. These values mean that *L. pectinata* hemoglobins reduces the viability of the endothelial cells by 45% when exposed for long times.

The cells media containing the hemoglobins was removed from the 6-well plate and the redox transitions of the hemoglobins were monitored using a UV-Vis spectrophotometer. Figure 5.11 A shows the overlaid spectra for 50 μ M α -DBBF Hb, HbII, HbI PheB10Tyr, and HbI after incubated with the endothelial cells for 2 hours. All the hemoglobins show bands characteristics of the oxy species, with the exception of HbI, which starts to oxidize, having an initial small band at 633 nm. When the hemoglobins reacted with the small fluxes of H_2O_2 , produced by GOX, oxidized faster as illustrated in the Figure 5.11 B spectra. α -DBBF Hb oxy bands shifts from 416 nm to 410 nm, and from 540 nm and 576 nm to 542 and 578 nm, respectively, with a slight band at 633 nm indicating a mixture between the ferric and the ferryl species. HbII shows similar ferric-ferryl species bands at 410 nm, 542, 578 and 603 nm, with a decrease in intensity due to the initial steps of protein aggregation. The HbI PheB10Tyr mutant spectrum only shows bands that correspond to the ferryl species at 417nm, 542, and 578 nm. The scenery is very different for HbI, which has the hemichrome band at 561 nm with almost flattened Soret band indicative of heme degradation. These experiments agree with the autoxidation and the oxidation of the *L. pectinata* hemoglobins with H_2O_2 results discussed in Chapter 4. HbI has a very high oxidation rate and produces a

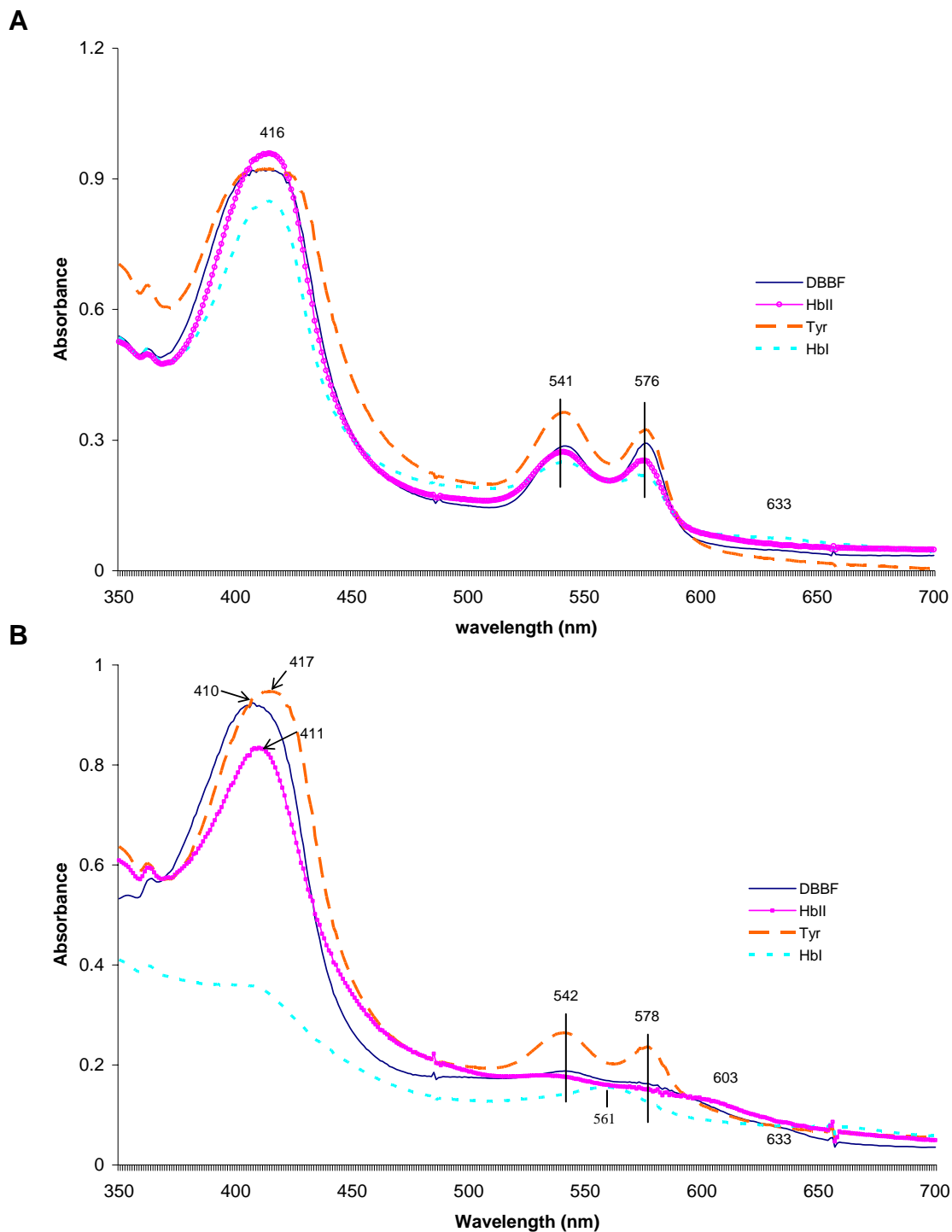


Figure 5.11 UV-Vis spectra of the hemoglobins after incubated with BAEC for 2 hours. (A) The incubation of 50 μ M hemoglobin in the cells media at 37°C only shows bands for oxy hemoglobin. (B) Hemoglobins after reaction with 10 mU/mL GOX in the cells media for 2 hours. α -DBBF Hb and HbII exhibit oxidation and ferryl formation, while the HbI PheB10Tyr mutant forms the ferryl species. The band at 561 nm suggests the HbI hemichrome species.

ferryl species with further formation of heme degradation products. Moreover, this result corroborates the resistant of HbII and the TyrB10 mutant to oxidize under the same experimental conditions. Figure 5.12 shows the oxidation process of the hemoglobins in the endothelial cells for a period of 6 hours without (A) or in the presence of GOX (B). The spectrum for the hemoglobins in Figure 5.12 A is very similar to that of the 2 hours. The only difference is the PheB10TyrB10 mutant spectrum that has the oxy bands and the band at 603 nm. The 6 hours period incubation with GOX in Figure 5.12 B shows that the HbI PheB10Tyr is more resistant to oxidation than α -DBBF Hb. The pseudoperoxidative cycle is maintained in the HbI PheB10Tyr mutant showing bands for the ferryl species at 417 nm, 545, and 577 nm, with few or nothing of heme degradation. Oxy HbII Soret band decreased in intensity and shifted from 416 nm to 412 nm indicative of the oxidation of the oxy heme. This hemoglobin, which starts to aggregate during the incubation time, shows the 561 nm band characteristic of the hemichrome species, and a decrease in the intensity of the Soret band suggesting heme degradation. When the media containing HbI was analyzed, the color of the hemoglobin was green. The spectrum for HbI was flat and without recognizable hemoglobin bands. Figure 5.13 A shows the redox transitions of the hemoglobins after incubated in the endothelial cells for 24 hours. The spectrum of α -DBBF hemoglobin has a mixture between the oxy and the ferric species, with bands at 407 nm, 540, 577 and 633 nm. HbII has a ferric-ferryl mixture with bands at 412 nm, 540 and 573 nm and shows the formation of the hemichrome species observed in the increase in the baseline. HbI, which also remained oxy during 2 and 6 hours, starts to oxidize with a shift in the Soret band from 416 nm to 411 nm. The broad band with maximum at 561 nm shows the presence of the hemichrome species and the decrease in intensity suggests heme degradation. The HbI

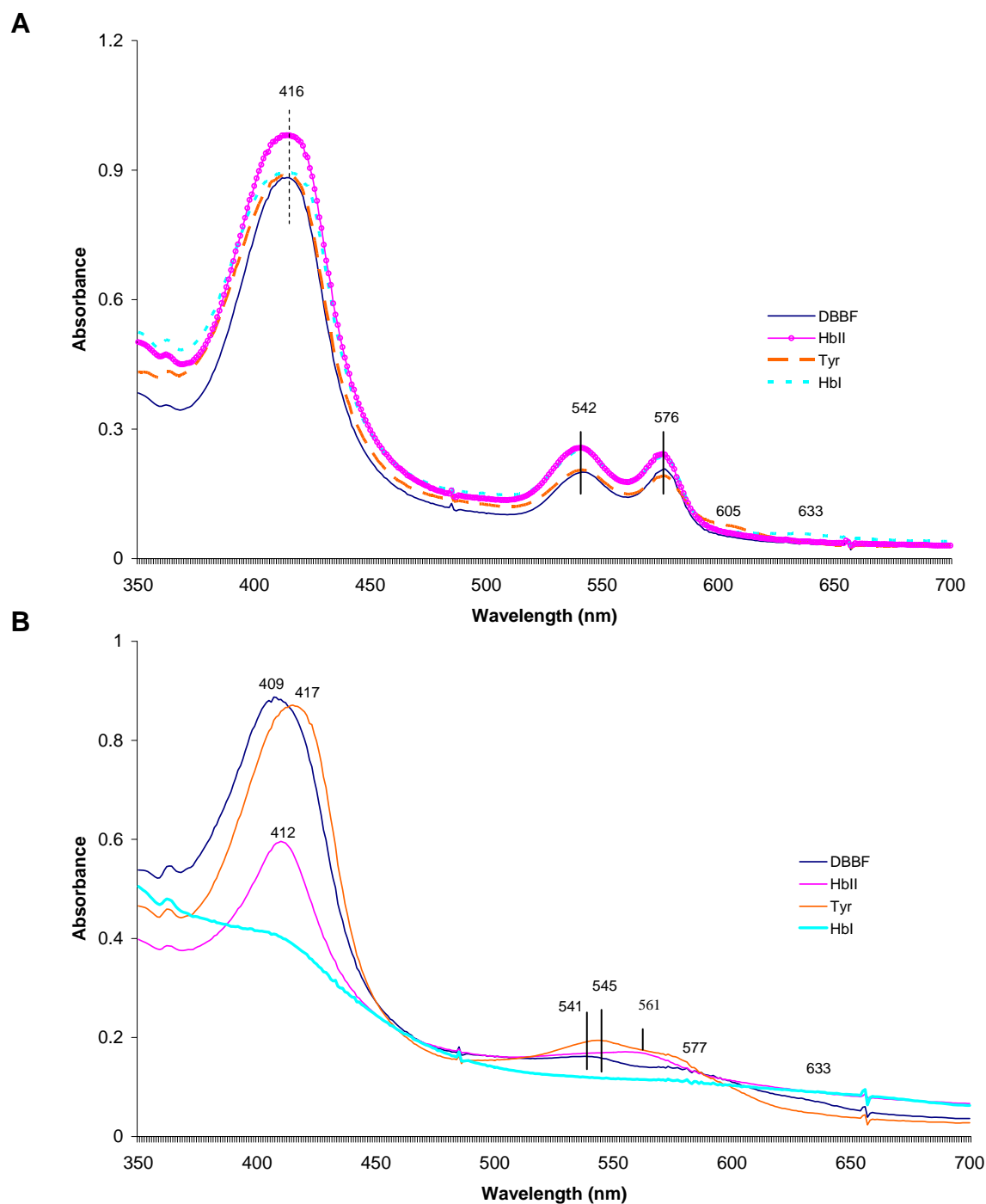


Figure 5.12 UV-Vis spectra of the hemoglobins after incubated with BAEC for 6 hours. (A) The incubation of 50 μ M hemoglobin in the cells media at 37°C remains in the oxy species. (B) Hemoglobins after reaction with 10 mU/mL GOX in the cells media for 6 hours. α -DBBF Hb shows ferric-ferryl bands, HbII oxidizes and forms hemichrome species, HbI PheB10Tyr mutant shows ferryl bands, and HbI is almost degrade.

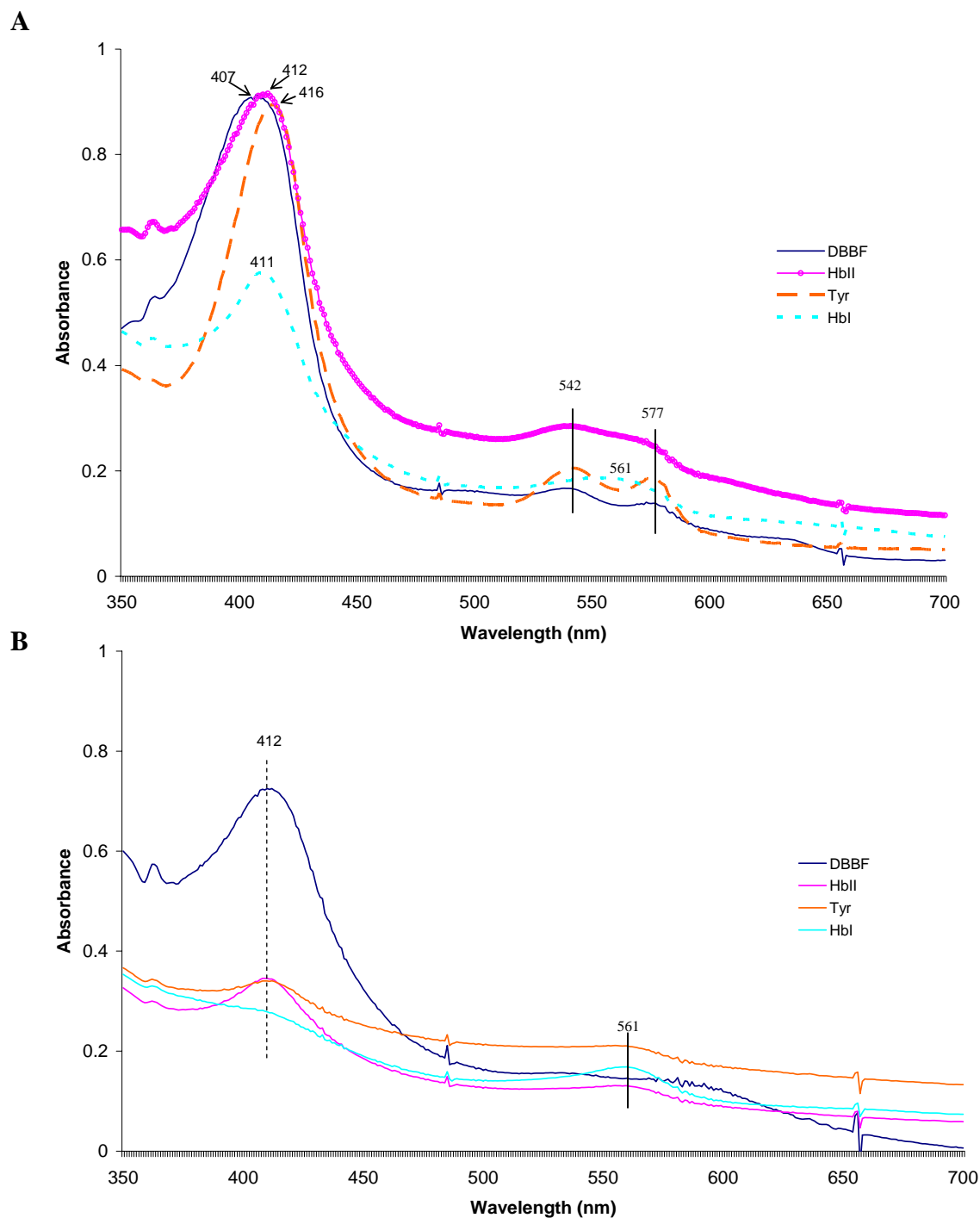


Figure 5.13 UV-Vis spectra of the hemoglobins after incubated with BAEC for 24 hours. (A) α -DBBF Hb shows oxy bands, while HbII and HbI PheB10Tyr oxidize and form hemichrome species. (B) Hemoglobins after reaction with 10 mU/mL GOX in the cells media for 24 hours. α -DBBF Hb shows ferric-ferryl bands and small degradation. *L. pectinata* hemoglobins forms hemichrome species and degrade.

PheB10Tyr mutant remains with bands characteristics of the oxy species without signals of oxidation. During the incubation of the hemoglobins in the cells containing 10 mU/mL GOX for 24 hours (Figure 5.13 B), the unique hemoglobin that has a spectrum characteristic of the hemoglobins was α -DBBF Hb, showing a band at 412 nm, and broadened ferryl bands in the Q region. The HbI PheB10Tyr mutant oxidizes fast during the last hours with a behavior similar to HbI. The spectrum of HbII for 6 hours with GOX is almost the same as for the 24 hours, with a little decrease in the intensity of the Soret band suggesting a slower oxidation rate and possible a longer turnover during the pseudoperoxidative cycle. Table 5.1 summarizes the hemoglobins spectral data when were exposed to endothelial cells with and without GOX. The hemoglobins without GOX maintained its oxy bands for up to 6 hours. After 6 hours, the human modified α -DBBF Hb showed autoxidation, while *L. pectinata* hemoglobins started to aggregate and degrade. From the three hemoglobins HbI PheB10Tyr shows more resistant towards degradation. In the reactions with GOX all the hemoglobins formed the ferryl species at two hours, as expected by the reaction with the hydrogen peroxide. At 6 hours, HbI was degraded and HbII started to degrade, while α -DBBF Hb and HbI PheB10Tyr showed a mixture of ferric and ferryl species. At 24 hours, all *L. pectinata* hemoglobins were degraded.

After the analysis of the redox transition of the hemoglobins and the capacity for the cells to proliferate at 2, 6 and 24 hours, the endothelial cells morphology and apoptosis were monitored. First, the morphology of the cells was observed using phase contrast microscopy. Figure 5.14 shows the morphology of confluent endothelial cells incubated with α -DBBF Hb, HbII, HbI PheB10Tyr, and HbI, with or without GOX, for 2 hours. The left column corresponds to the cells incubated only with the hemoglobins. The cell morphology is

Table 5.1 Spectral characteristic of the hemoglobins exposed to endothelial cells with and without glucose oxidase

	2 hour	6 hour	24 hour
HbI	<div> <div>→</div> <div>Oxy HbI</div> </div> <div> <div>GOX</div> <div>→</div> <div>Heme degradation</div> </div>	<div>Oxy HbI</div> <div>Degraded protein</div>	<div>Oxidation and High levels of degradation</div> <div>Degraded protein</div>
HbII	<div> <div>→</div> <div>Oxy HbI</div> </div> <div> <div>GOX</div> <div>→</div> <div>Oxidation-ferryl</div> </div>	<div>Oxy HbI</div> <div>Oxidation-hemichrome</div>	<div>Oxidation to ferric Hb and heme degradation</div> <div>Degraded protein</div>
HbI PheB10 Tyr	<div> <div>→</div> <div>Oxy HbI</div> </div> <div> <div>GOX</div> <div>→</div> <div>Ferryl Species</div> </div>	<div>Oxy HbI</div> <div>Ferryl Species</div>	<div>Oxy HbI</div> <div>Degraded protein</div>
α -DBBF Hb	<div> <div>→</div> <div>Oxy α-DBBF Hb</div> </div> <div> <div>GOX</div> <div>→</div> <div>Ferric-ferryl Species</div> </div>	<div>Oxy α-DBBF Hb</div> <div>Ferric-ferryl Species</div>	<div>Oxidation to ferric Hb</div> <div>Ferric-ferryl species and heme degradation</div>

indistinguishable for this time period, except that for HbI, in which cells begin to elongate. Figure 5.14, right column, shows the cells treated with hemoglobins and 10 mU/mL GOX. The incubation with α -DBBF Hb and HbI PheB10Tyr did not produce any remarkable changes in the cells monolayer density. In contrast, HbII shows cell elongation and HbI

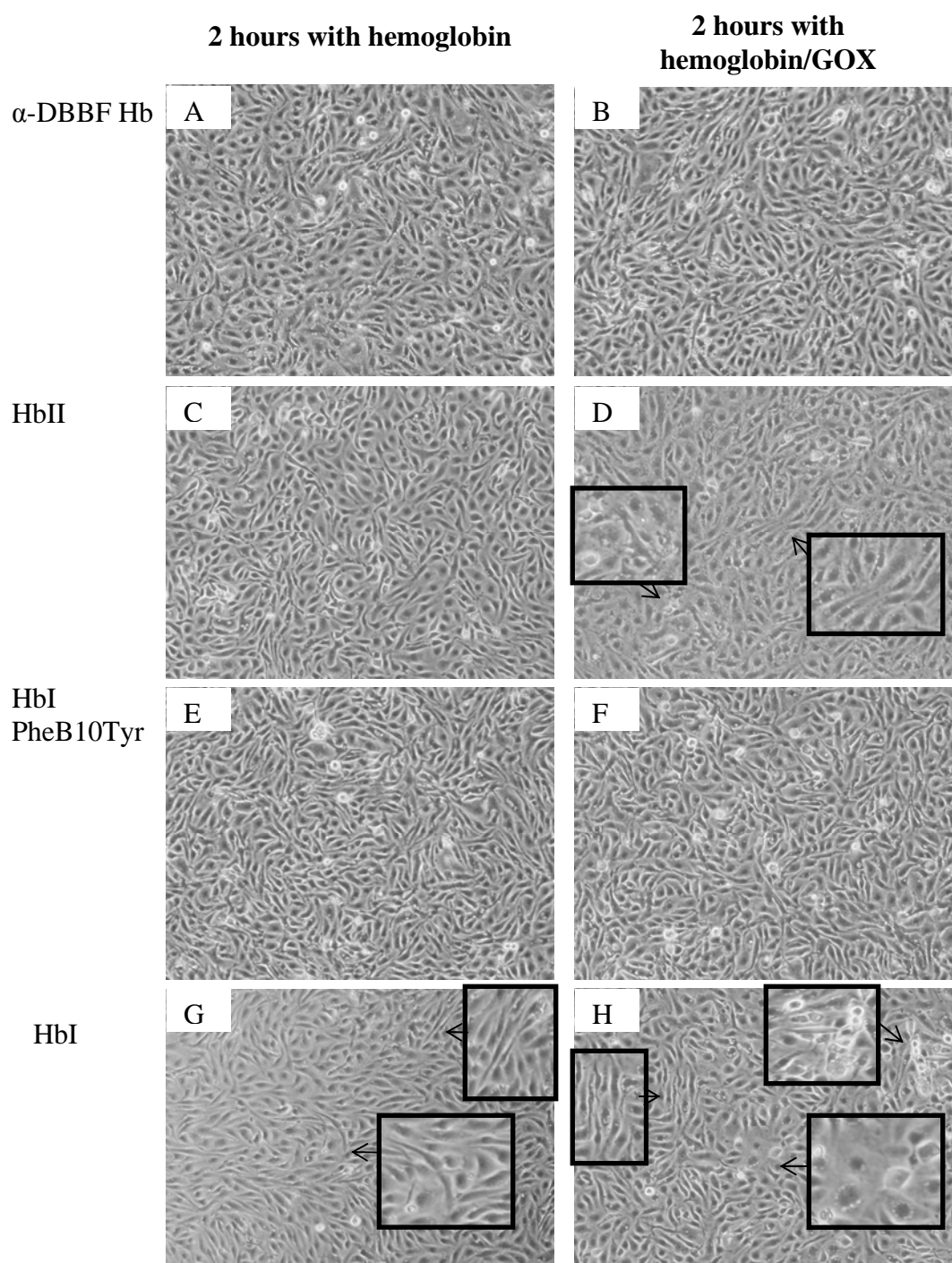


Figure 5.14 Morphologic changes in endothelial cells induced by the redox cycling of the hemoglobins for 2 hours. Arrows in micrograph D and G show cell elongation. Arrows in H show cell detachment and rounding.

starts to exhibit cell rounding and detachment. Figure 5.15 shows the morphologic changes of the endothelial cells for 6 hours in the presence of the hemoglobins and 10 mU/mL GOX. At 6 hours of exposure to the hemoglobins, there are no visible changes from the reaction at 2 hours between α -DBBF Hb and HbII. The cells incubated with HbI and HbI PheB10Tyr continues their elongation. The cells incubated for 6 hours with the hemoglobin and the GOX are illustrated in Figure 5.15, right column. The cells treated with α -DBBF Hb, HbII, and HbI PheB10Tyr do not show differences from the cells also treated with the hemoglobins, but without the GOX. Perhaps, the cells media containing the HbII starts to show hemoglobin aggregation. All endothelial cells exposed to HbI and GOX for 6 hours have elongated morphology. Figure 5.16 shows the phase contrast morphology of the endothelial cells with the hemoglobins without (left column) or with GOX (right column) at 24 hours. The α -DBBF Hb did not affect the cells morphology for periods of 24 hours, and the reaction of the hemoglobin with GOX shows cell rounding, shrinkage and detachment from the monolayer, at a smaller level than the *L. pectinata* hemoglobins. HbII, HbI, and HbI PheB10Tyr show hemoglobin aggregation, large levels of cell rounding and detachment from the cell monolayer. The cells treated with GOX and the hemoglobins were washed carefully to eliminate the hemoglobin aggregation. HbII and HbI micrographs show the largest levels of accumulation of debris from cells insoluble precipitates.

Morphological alterations of BAEC after treatment for 24 hours with hemoglobins and GOX were also analyzed by fluorescence microscopy. Figure 5.17 shows nuclear morphologic changes typical of apoptosis detected by the observation of the cells stained with Hoechst 33342, Annexin V-Alexa Fluor conjugate, and propidium iodide. Micrographs of the endothelial cells exposed to 10mU/mL GOX for 24 hours are shown in Figures 5.17 A

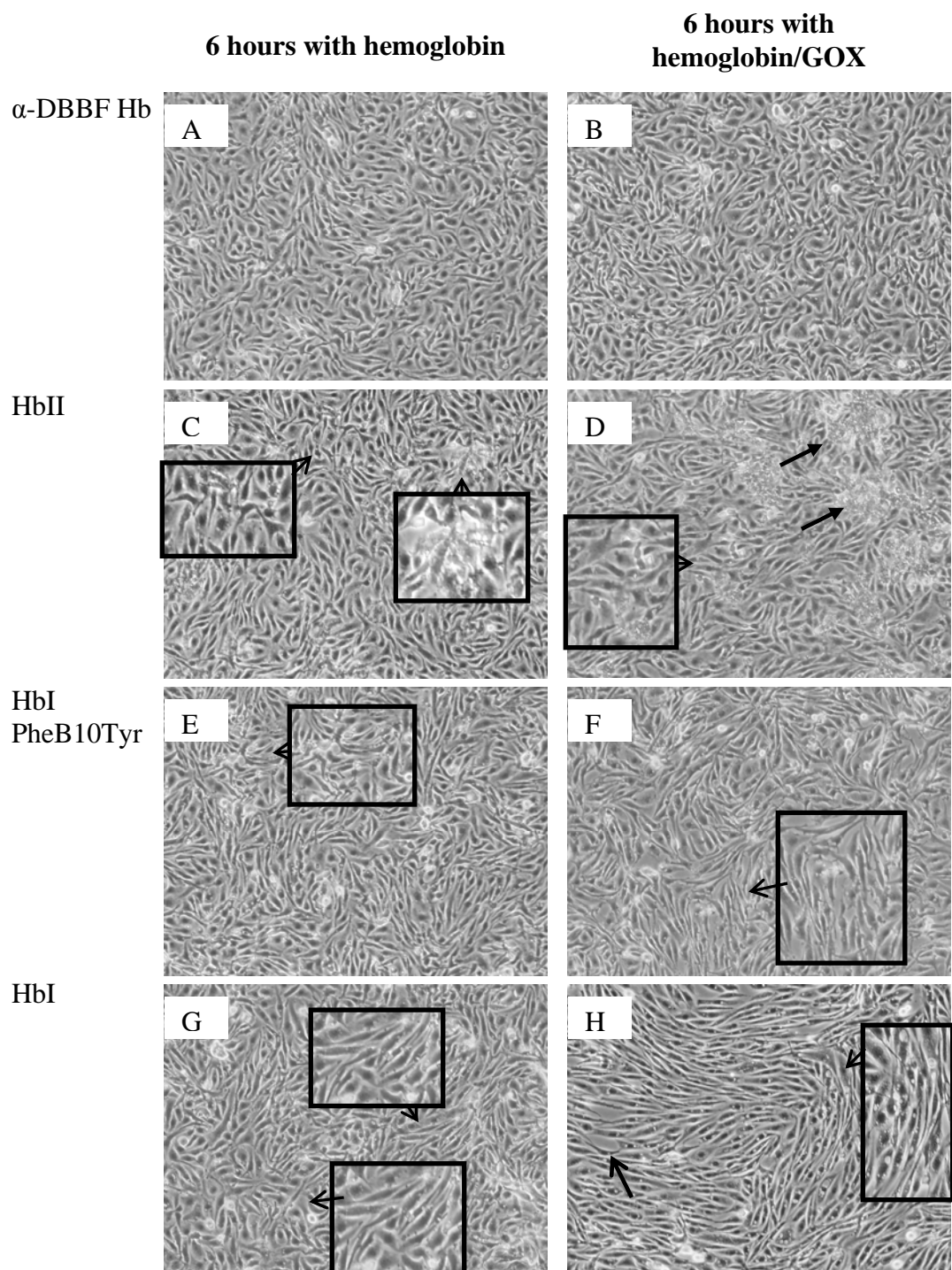


Figure 5.15 Morphologic changes in endothelial cells induced by the redox cycling of the hemoglobins during 6 hours. Arrows in micrograph D show initial steps of hemoglobin aggregation. Arrows in micrographs E and G show cells elongation. Micrograph H shows that all the cells have elongated morphology.

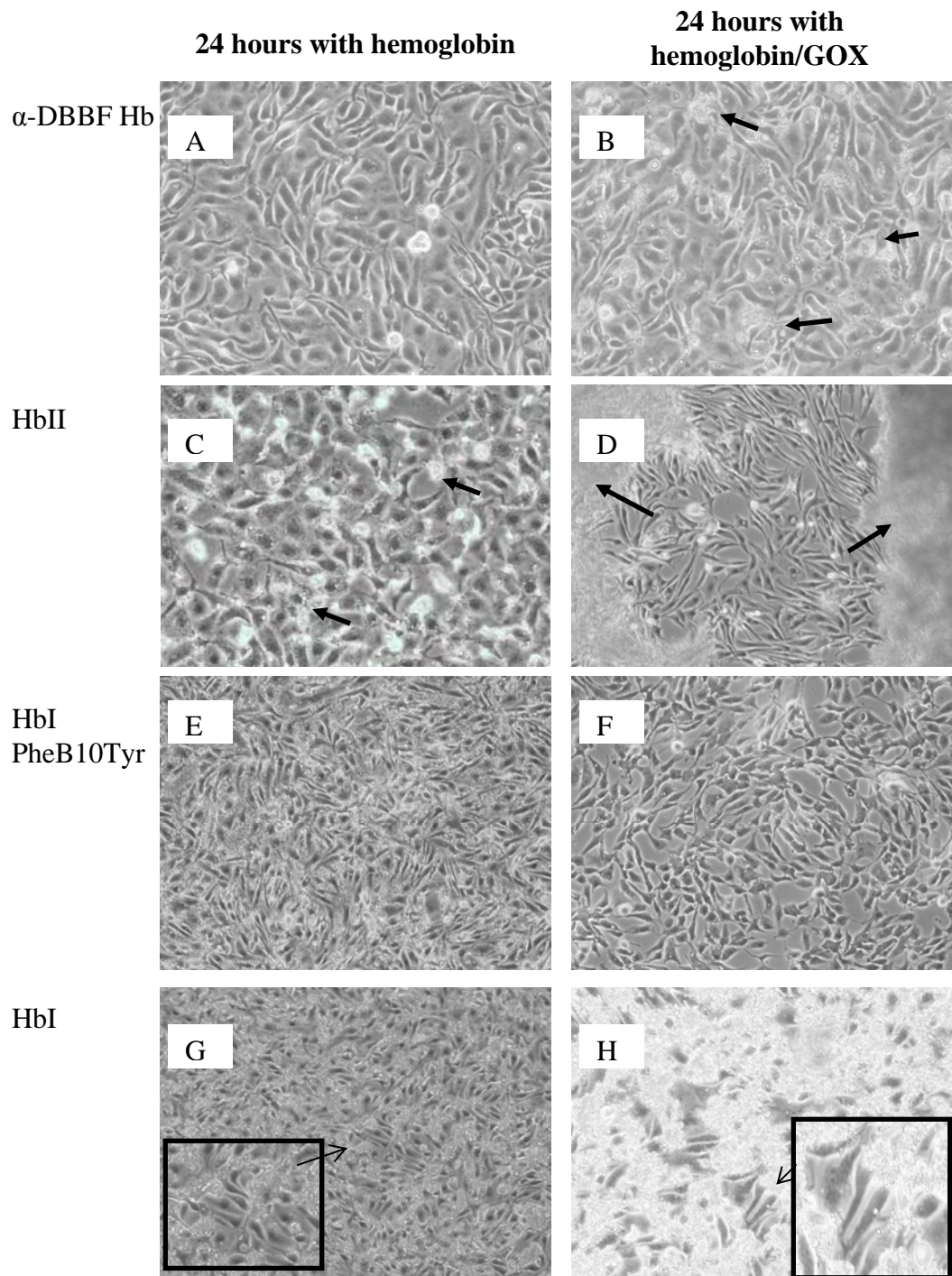


Figure 5.16 Morphologic changes in endothelial cells induced by the redox cycling of the hemoglobins during 24 hours. Micrograph B shows cells rounding and fragments. The cells exposed to *L. pectinata* hemoglobins show cell detachment from the layer. Micrographs D and H show the hemoglobin aggregation on the cell monolayer.

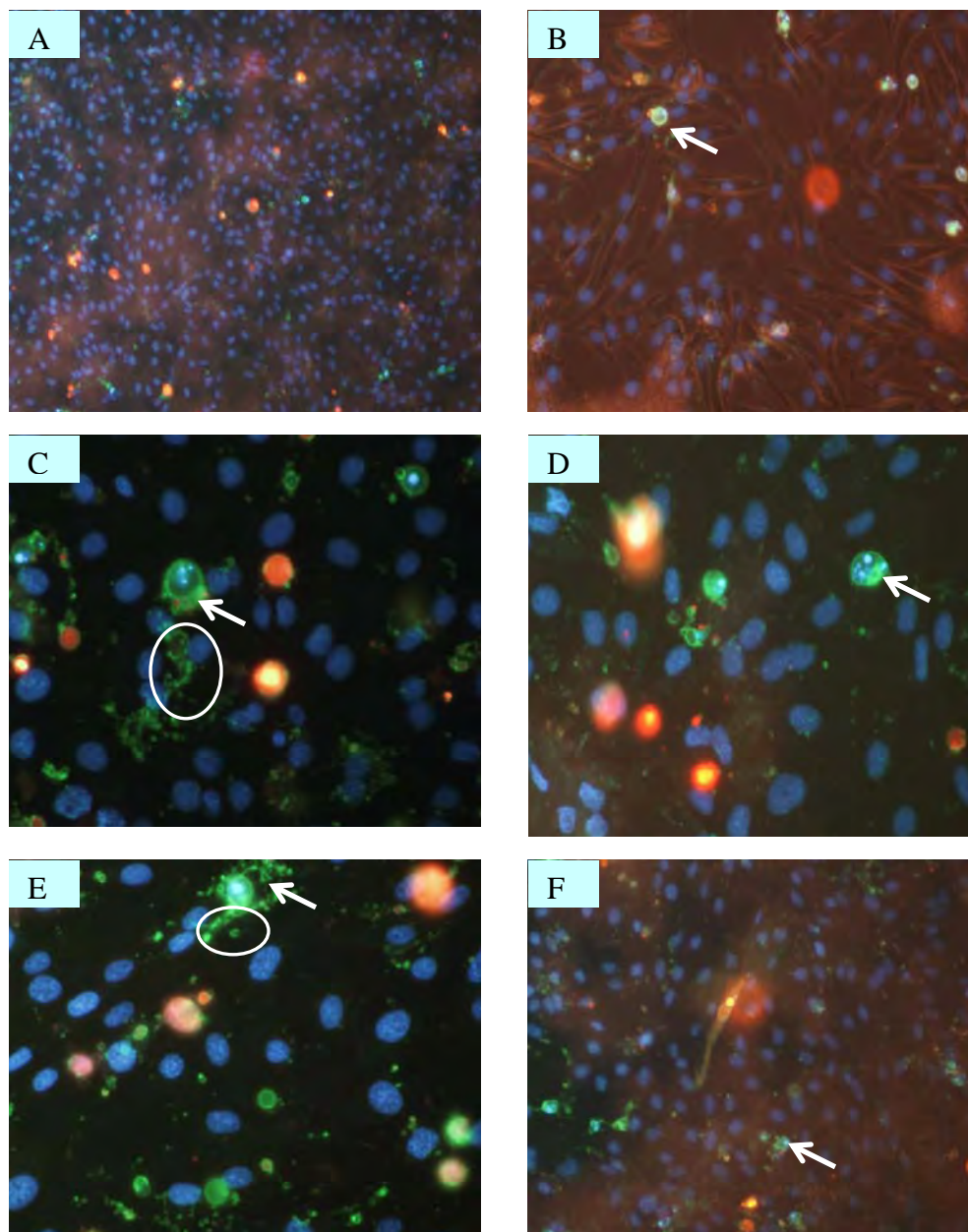


Figure 5.17 Endothelial cells treated with hemoglobins and 10 mU/mL GOX for 24 hours. Micrographs A and B show cells treated only with GOX, C – F show cells treated with GOX and α -DBBF Hb, HbII, HbI, or HbI PheB10Tyr, respectively. Examples of nucleus condensation are point up with white arrows.

and B. Changing the contrast of the light intensity made it easier to see that the cell membrane was elongated, as shown in Figure 5.17 B. The Hoechst 33342 stained blue the nuclei of living cells, and the red spots are the cells in necrosis stained with the propidium iodide. The propidium iodide enters the cells that have permeable plasma membranes, thus staining cells that are necrotic or in later apoptotic stages. To evidence that the phosphatidylserine exposure occurs in the endothelial cells treated for 24 hours, cultures were dual-labeled with annexin V and propidium iodide. The phospholipid protein annexin V binds to exposed phosphatidylserine on the surface of plasma membrane on apoptotic cells. Because the propidium iodide is excluded from cells with intact plasma membranes, it was used to determine if the annexin V labeling was due to phosphatidylserine externalization. Therefore, the bright green staining with bubble appearance are the cells under apoptosis which show the condensed nucleus. Figures 5.17 C-F show endothelial cells treated for 24 hours with 10 mU/mL GOX and 50 μ M α -DBBF Hb, HbII, HbI, or HbI PheB10Tyr, respectively. All the hemoglobins in the reaction with GOX for long time periods lead to apoptotic and necrotic cells as evidenced by the condensed nuclei and the red stain in the micrographs. Table 5.2 summarizes the cell morphological changes when treated with the hemoglobins. In two (2) hours the cells showed more than 85% viability without morphological changes, except the cells treated with HbI that started to exhibit membrane elongation. At 6 hours the viability of the cells treated with *L. pectinata* hemoglobins decreased also showing membrane elongation. The decrease in cell viability at 24 hours was accompanied with membrane elongation, cell debris and membrane detachment. Table 5.3 summarizes the cell morphological changes when treated with the hemoglobins and GOX. In the first 2 hours the cells showed a prompt membrane elongation. At 6 hours the cells

Table 5.2 Endothelial cell morphological changes and media features after treatment with hemoglobins

Hemoglobin	2 hours	6 hours	24 hours
His	<ul style="list-style-type: none"> • 85% viable cells • Initial steps of membrane elongation 	<ul style="list-style-type: none"> • 75% viable cells • Initial steps of membrane elongation 	<ul style="list-style-type: none"> • 45% viable cells • membrane elongation • protein aggregation
HbII	<ul style="list-style-type: none"> • 90% viable cells 	<ul style="list-style-type: none"> • 85% viable cells • Initial steps of membrane elongation 	<ul style="list-style-type: none"> • 51% viable cells • membrane elongation, cell debris and detachment • protein aggregation
HbI PheB10Tyr	<ul style="list-style-type: none"> • 85% viable cells 	<ul style="list-style-type: none"> • 83% viable cells • Initial steps of membrane elongation 	<ul style="list-style-type: none"> • 45% viable cells • membrane elongation, cell debris and detachment • protein aggregation
α -DBBF Hb	<ul style="list-style-type: none"> • 98% viable cells 	<ul style="list-style-type: none"> • 90% viable cells 	<ul style="list-style-type: none"> • 87% viable cells • Initial steps of membrane elongation

Table 5.3 Endothelial cell morphological changes and media features after treatment with hemoglobins and glucose oxidase

Hemoglobin	2 hours/GOX	6 hours/GOX	24 hours/GOX
His	<ul style="list-style-type: none"> • 82% viable cells • membrane elongation • cell rounding and detachment 	<ul style="list-style-type: none"> • 84% viable cells • All cells exhibit membrane elongation 	<ul style="list-style-type: none"> • 18% viable cells • membrane elongation • cell detachment • protein aggregation • nuclei condensation
HbII	<ul style="list-style-type: none"> • 84% viable cells • Cell membrane elongation 	<ul style="list-style-type: none"> • 90% viable cells • membrane elongation • cell rounding 	<ul style="list-style-type: none"> • 21% viable cells • membrane elongation, cell debris and detachment • protein aggregation • nuclei condensation
HbI PheB10Tyr	<ul style="list-style-type: none"> • 95% viable cells • Cell rounding and membrane elongation 	<ul style="list-style-type: none"> • 89% viable cells • membrane elongation 	<ul style="list-style-type: none"> • 23% viable cells • membrane elongation, cell debris and detachment • protein aggregation • nuclei condensation
α -DBBF Hb	<ul style="list-style-type: none"> • 94% viable cells • Initial steps of membrane elongation 	<ul style="list-style-type: none"> • 80% viable cells • Initial steps of membrane elongation 	<ul style="list-style-type: none"> • 62% viable cells • membrane elongation • Cell rounding • nuclei condensation

started to round and detach, and at 24 hours the hemoglobins aggregate and degrade helping to the cell deterioration, thus showing detachment, nuclei condensation, and cell debris.

Moreover, the cells DNA was extracted to detect DNA fragmentation which is an apoptotic feature. Figure 5.18 shows the agarose gels containing endothelial cells DNA that evidences DNA damage by apoptosis or necrosis. Agarose gels A-B correspond to cells

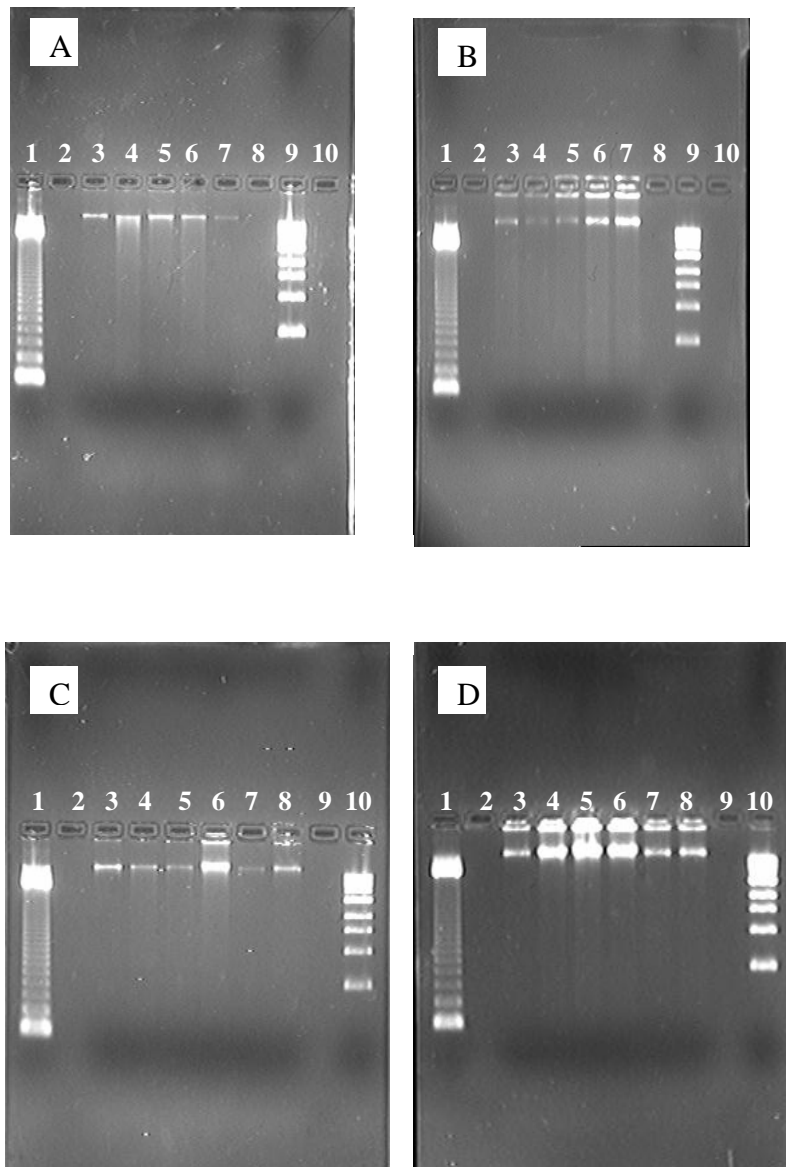


Figure 5.18 Endothelial cells DNA extraction. Agarose gels A and B show the extracted DNA of cells treated for 2 hours and 6 hours, respectively. Lanes were filled with: 1- 123 bp DNA ladder marker; 3- untreated cells DNA; 4 to 7- DNA of cells treated with HbII, HbI PheB10Tyr, HbI, and α -DBBF Hb, respectively; 9- 1 kb DNA ladder. Agarose gel C and D show the extracted DNA of cells treated with 10 mU/mL GOX for 2 hours and 6 hours, respectively. Lanes 1 and 10 were filled with the 123 bp and 1 kb DNA ladder marker; 3- untreated cells DNA; 4 to 8- DNA of cells treated with HbII, HbI PheB10Tyr, HbI, α -DBBF Hb, and cells only with GOX, respectively.

treated with the hemoglobins during 2 hours and 6 hours, respectively. Lanes 1 and 9 have DNA 123 bp ladder and 1kb ladder markers, while lanes 3-7 have DNA of cells: without treatment, HbII, HbI PheB10Tyr, HbI, and α -DBBF Hb, respectively. The gel of the cells treated for 2 hours shows an undamaged DNA for the cells without treatment and for cells treated with α -DBBF Hb. The *L. pectinata* hemoglobins show a smear pattern characteristic of DNA damage. At 6 hours, all cells treated and untreated exhibit DNA damage. Figure 5.18 C-D show the agarose gels containing DNA extracted from endothelial cells treated with GOX and the hemoglobins. Lanes 1 and 10 have DNA 123bp ladder and 1kb ladder markers, lane 3 contains DNA of cells without treatment, lanes 4-7 have DNA from cells treated with GOX and HbII, HbI PheB10Tyr, HbI, or α -DBBF Hb, respectively, and lane 8 have DNA from cells treated only with GOX. The behavior of the cells after treated for 2 hours in the reactions with GOX (Figure 5.18 C) was similar to that without GOX (Figure 5.18 A). The lanes containing the cells without treatment or exposed to α -DBBF Hb do not show DNA damage, while the lanes containing DNA from the *L. pectinata* hemoglobins have a smear pattern. The agarose gels show that all cells treated with GOX for 6 hours, with or without the hemoglobins, show a smear pattern. These results agree with previous experiments that suggest the indirect DNA damage induced by the redox cycling of α -DBBF Hb for periods longer than 4 hours (D'Agnillo & Alayash, 2001).

Once the cells apoptosis was evidenced by the morphological features and by the DNA ladders in the agarose gels, the apoptotic levels were measured using the activities of the caspases-3 and 7. Figure 5.19 shows the results for the Apo-One Homogeneous Caspase-3/7 assay for the endothelial cells treated during 2 hours, 6, and 24 hours with the hemoglobins. Each point represents the mean \pm SE for 5 to 7 independent experiments,

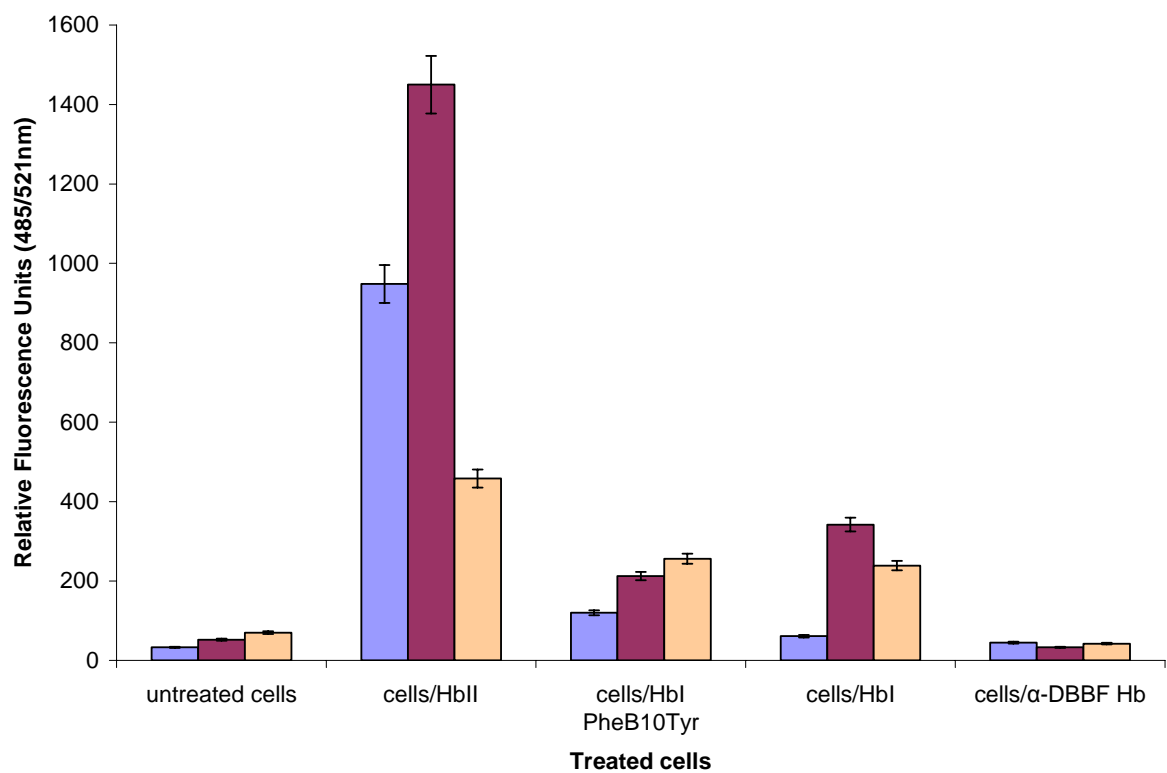


Figure 5.19 Bovine aortic endothelial cells apoptosis assay after exposed to HbII, HbI PheB10Tyr, HbI, or α-DBBF Hb for 2 hours, 6 hours, and 24 hours. Values at each time represent the mean \pm SE of 5-7 samples.

where $p < 0.05$ was obtained versus the untreated cells (control). The statistical analysis is shown in Appendix A. The untreated cells exhibit a little increase in apoptosis in a time dependent manner, which is not significant. The same behavior is found in the cells treated with the modified human α -DBBF Hb, with relative fluorescence units (RFU) of 45, 38, and 42 at 2 hours, 6 and 24 hours, respectively, with no significant difference between them when compared to untreated cells. The results for 2 hours show that the hemoglobin that induces significantly high apoptotic levels in endothelial cells ($p = 0.022$) is HbII, while the cells treated with HbI and its mutant were indistinguishable from the control level. At 6 hours the apoptotic levels increased in a significant manner for all *L. pectinata* hemoglobins, HbII reaching the higher apoptotic levels. The cells treated for 24 hours also show significant high apoptotic levels, but with lower values than at 6 hours. One possible explanation for this result is that at 6 hours, there are many cells undergoing apoptosis which are nearly to die, thus showing high RFU values, while at 24 hours there are many necrotic or died cells showing a decrease in the RFU values. The cells morphology in Figure 5.16 supports this statement showing at 6 hours cell membrane elongation, and at 24 hours high levels of cell fragments and detached cells. The results for the cells treated with GOX in Figure 5.20 show the same pattern as without the production of small H_2O_2 fluxes. Similar to the cells morphology results, the apoptosis of cells treated for 2 and 6 hours with GOX is very small and insignificant when compared with the untreated cells. The cells treated with α -DBBF Hb and GOX show to be viable for long time periods indicative of the high stability of this hemoglobin.

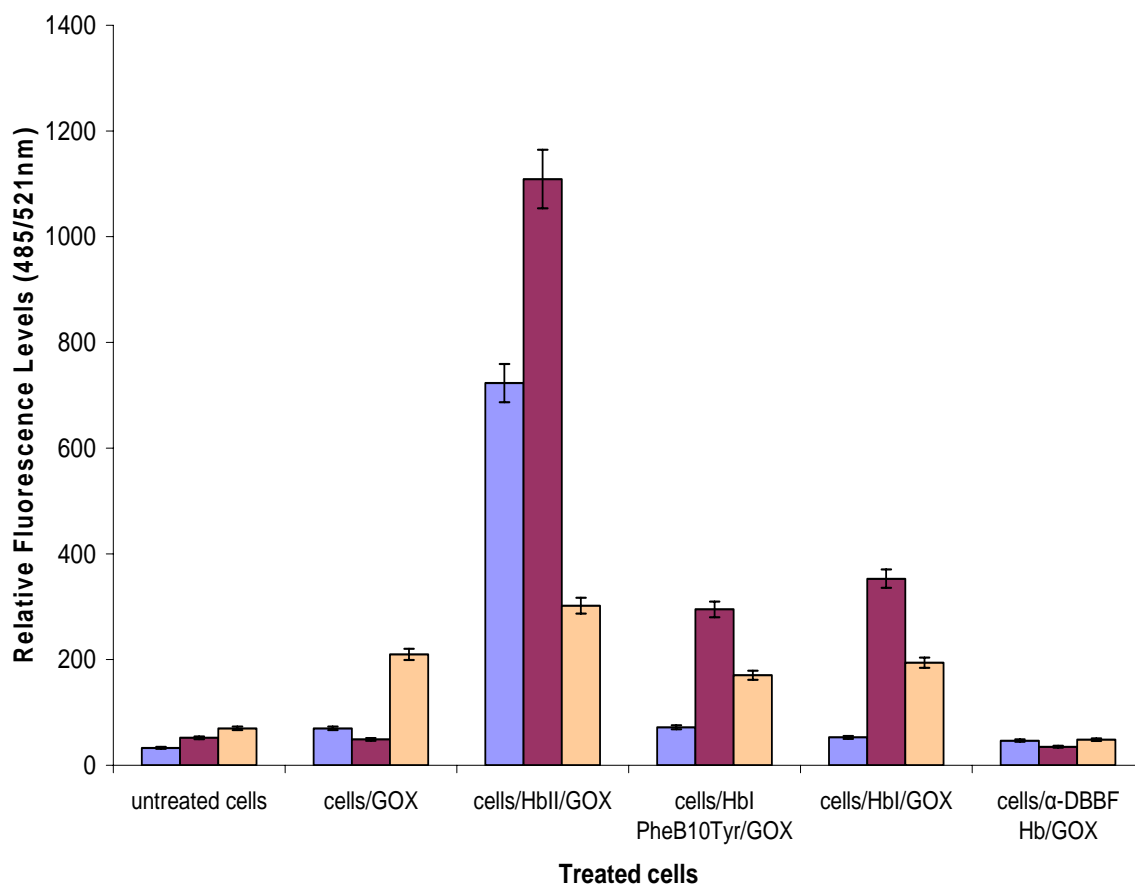


Figure 5.20 Bovine aortic endothelial cells apoptosis assay after exposed to 10 mU/mL GOX and HbII, HbI PheB10Tyr, HbI, or α-DBBF Hb for 2 hours, 6 hours, and 24 hours. Values at each time represent the mean \pm SE of 5-7 samples.

5.4 Discussion

The reaction of hemoglobin with hydrogen peroxide produces the ferryl species in a redox cycle that leads to non functional hemoglobin. If the concentration of hydrogen peroxide is high the hemoglobin starts to degrade. The spectral data of the hemoglobins with glucose oxidase showed that a continuous production of small concentrations of hydrogen peroxide oxidizes HbII and HbI PheB10Tyr mutant in small amounts. In solution, HbII demonstrates to have a special amino acid arrangement that makes it more resistant to peroxidative damage compared to modified human hemoglobin. Thus, this data agrees with the kinetic reactions with hydrogen peroxide discussed previously and the detection of fluorescent heme degradation products in Chapter 4. However, the same reaction of the hemoglobins with hydrogen peroxide produced by GOX in a endothelial cell media aggregates the *L. pectinata* hemoglobins.

These oxidative reactions in cell free hemoglobin infused to plasma are linked to endothelial cell injury and damage (D'Agnillo & Alayash, 2001), where the cells with apoptotic features are accumulated in the G2/M phase. This is due to the oxidative stress caused to the cells by the intracellular generation of the hydrogen peroxide and by the oxidative species generated in the reaction with the hemoglobins (Gow et al., 1999; D'Agnillo & Alayash, 2001). The resistance of HbII to oxidation and heme degradation by reactions with hydrogen peroxide allows the study of this hemoglobin in a cell environment and compared its behavior with HbI and the HbI PheB10Tyr mutant. Thus, bovine aortic endothelial cells were treated with *L. pectinata* hemoglobins to characterize morphological changes in the cells resulting from oxidative stress. It was found that the cells viability was maintained during the 2 hour and 6 hour treatment with all the hemoglobins, despite the

media contained or not glucose oxidase. However, the UV-Vis spectra of the *L. pectinata* hemoglobins started to show hemichrome species and heme degradation when were exposed to the endothelial cells with the media containing GOX for more than 6 hours. From the three studied hemoglobins, HbI PheB10Tyr mutant shows to be the more resistant to heme degradation. This behavior was not observed in the modified human hemoglobin α -DBBF Hb which the UV-Vis spectrum for each experiment evidences formation of the ferryl species without heme degradation. Therefore, the viable cells exposed to *L. pectinata* hemoglobins decreased to 20% in the 24 hours assay, while the ones exposed to α -DBBF Hb remained with more than a 70%.

These results show a relationship with the qualitative and quantitative apoptosis analysis. The exposition of endothelial cells to HbII, HbI, and HbI PheB10Tyr deteriorates in a larger proportion the cells. The cells show changes in plasma membrane asymmetry which are one of the earliest features of cells undergoing apoptosis, displaying an elongated morphology, cell rounding, and detachment from the monolayer. The fluorescence microscopy with Hoechst 33342, Annexin-V Alexa flour conjugated, and propidium iodide confirms chromatin condensation, phosphatidylserine externalization, and necrosis in the cells treated with the hemoglobins and GOX for 24 hours. Moreover, the time dependent activation of caspases -3 and 7 allowed for the apoptosis quantification. The levels of apoptosis increased significantly at 6 and 24 hours, with and without GOX, compared to the untreated cells and cells exposed to α -DBBF Hb. Apoptosis is a controlled cell death program in response to several stimuli. During incubation with the endothelial cells, at 37°C (similar conditions studied in Chapter 4), the hemoglobins autoxidizes producing the ferric species and superoxide ions which are ROS. This is one of the routes for cell damage that

stimulates apoptosis. Moreover, the reaction of the hemoglobins with the hydrogen peroxide, produced by GOX, forms the ferryl species and subsequent heme degradation products which also are ROS. Therefore, in 6 hours and 24 hours, the induction of apoptosis correlates with the formation of the ferryl hemoglobins, as was evidenced in Figures 5.12 and 5.13.

This behavior was not expected for HbII and HbI PheB10Tyr since the kinetic data for the reactions with hydrogen peroxide in Chapter 4 suggested that these hemoglobins are very stable, even more than α -DBBF Hb. Furthermore, the reaction of HbII with 10 mU/mL GOX, in solution, shows that HbII is more resistant to peroxidative damage due to the slow production of H_2O_2 . Therefore, one hypothesis is that the CO_2 present in the cell culture media, as also present in the plasma, may cause a conformational change in the hemoglobins which make them susceptible to peroxidation and heme damage. Previous studies of human Hb (Perrella et al., 1975) showed that CO_2 binds to the α -amino group of the β chain. However, in the α chain CO_2 binds in the interior of the protein near the heme group. HbII and HbI that are a dimer and monomer, respectively, have the chains more exposed to the solvent allowing the entrance of the CO_2 molecule and consequently, a change in the tertiary structure. Figure 5.21 A shows a schematic view for the reaction of HbII and HbI in a solution containing GOX. In the first 6 hours both hemoglobins reacts with the produced hydrogen peroxide forming the ferryl species. Up to 24 hours HbII shows resistance to heme damage, while HbI degrades and forms a green adduct. Figure 5.21 B illustrates the reaction in presence of CO_2 . From 2 to 6 hours the *L. pectinata* hemoglobins form the ferryl species, but for periods longer than 6 hours the hemoglobins aggregate and degrade, increasing the concentration of reactive oxygen species. Moreover, one of the initial problems of the infused cell-free hemoglobin was its short vascular retention time (Greenburg et al.,

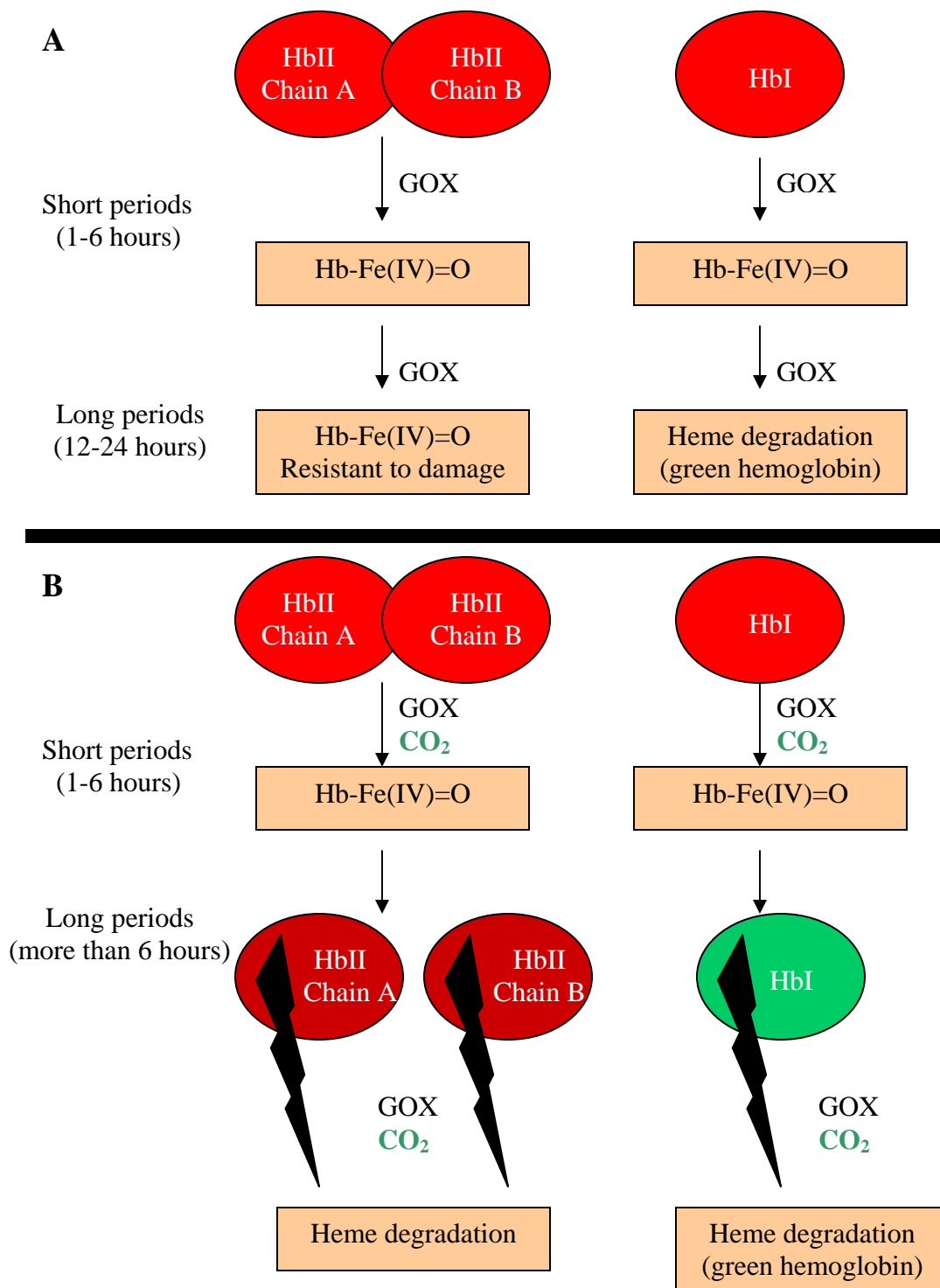


Figure 5.21 Schematic representations of HbII and HbI hemoglobins when treated with endothelial cells and GOX incubated at 37°C without (A) or with (B) a CO₂ atmosphere.

1977) and structure dissociation into dimers. To overcome this problem, chemical and genetic modifications were designed to provide the infused hemoglobin with high stability (Greenburg et al., 1977; Alayash, 1999). In this respect, this set of experiments evidences that the tertiary structure of hemoglobins of *L. pectinata* needs to be stabilized, for example by crosslinking, previous to exposition to endothelial cells.

The endothelial cells, in addition to form a semi-permeable barrier between blood and the vessel walls, have important physiological functions including the synthesis and release of nitric oxide (Dworakowski et al., 2008). It was suggested that the generation of superoxide and hydrogen peroxide reactive oxygen species up regulates the expression of endothelial nitric oxide synthase (Zhen et al., 2008). This behavior was also seen when endothelial cells were treated with human hemoglobin (Yeh & Alayash, 2004). It was suggested that the expression was regulated in part by the NO scavenging activity of the hemoglobin limiting the NO availability. Thus, *L. pectinata* hemoglobins autoxidizes fast under a CO₂ atmosphere allowing a change in conformation that finally breaks the heme, produce heme degradation products, and increase the reactive oxygen species concentration. Figure 5.22 illustrates the *L. pectinata* hemoglobins mechanism exposed to bovine aortic endothelial cells. The endothelial cells, which form the layer that lines the lumen of the blood vessels, produced NO. Then, the infused oxy hemoglobin reacts with the nitric oxide oxidizing the hemoglobin to its ferric species and forming very fast the peroxynitrite ion. Moreover, one of the products from the hemoglobins autoxidation is the superoxide ion. Finally, if GOX is added to the system, small fluxes of H₂O₂ are produced leading to the formation of the ferryl species and subsequent heme degradation. This increase in oxidative stress disrupts the physiological balance between the production of physiological amounts of

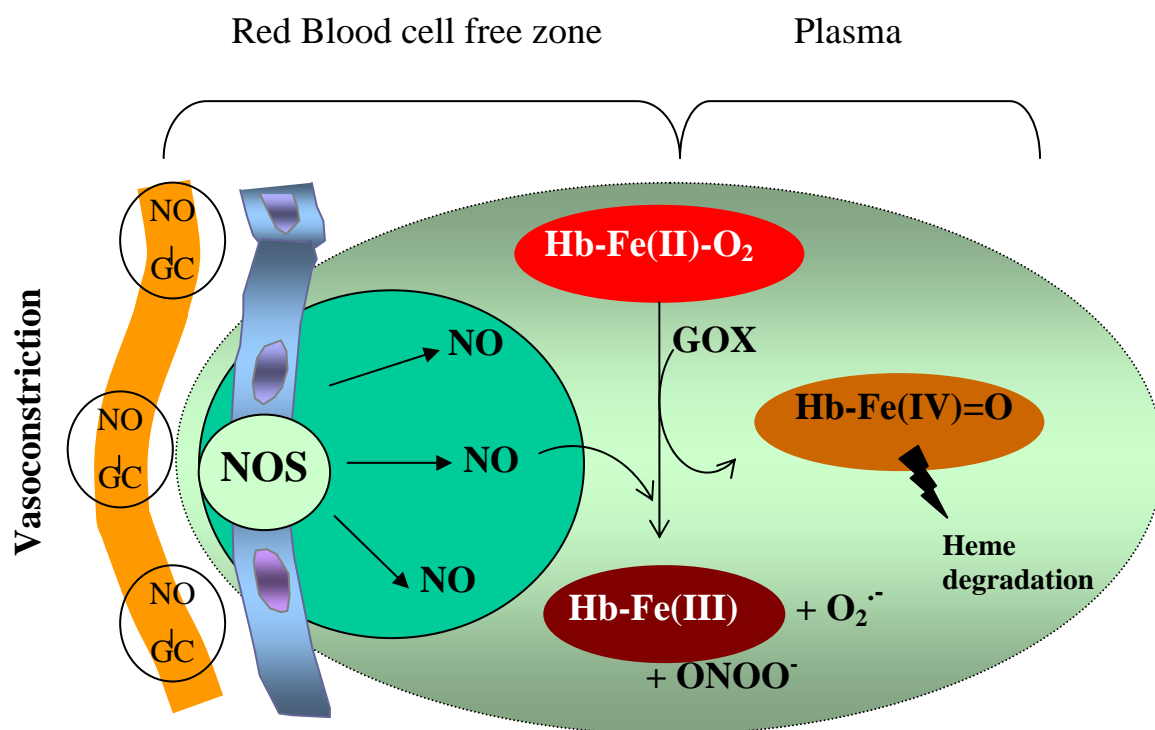


Figure 5.22 Proposed mechanism for the reaction of *L. pectinata* HbI and HbII when exposed to the endothelial cells media. The hemoglobins autooxidize producing the superoxide ion. In addition, the hemoglobins react with NO forming ferric hemoglobin and the peroxynitrite ion. The accumulation of H₂O₂, formed by GOX, produces the ferryl species and subsequent heme degradation. The formation of high concentrations of ROS creates a balance disruption that can cause physiological diseases, for example vasoconstriction.

ROS and antioxidants. As a direct consequence, the cells deteriorate inducing apoptosis, necrosis, and physiological disease as vasoconstriction. The reactions of *L. pectinata* HbII with nitric oxide in Chapter 3 showed that this hemoglobin reacts slowly with the NO. Consequently, the part in the reaction that contributes largely to the formation of reactive oxygen species is the degradation of the heme as a result of its reaction with the carbon dioxide. Therefore, it is suggested to stabilize the HbII structure to decrease its interaction with CO₂, thus avoiding the hemoglobin aggregation.

6 REDOX CHEMISTRY OF THE HEMOGLOBINS EXPOSED TO BOVINE AORTIC ENDOTHELIAL CELLS DURING HYPOXIA

6.1 Introduction

The induction of reactive oxygen species by hypoxia is other mechanism in which the oxidative stress can be studied (Gow et al., 1999). Hypoxia is a lack of tissue oxygenation, which is associated with respiratory diseases. The partial pressure, pO_2 , of human hemoglobin HbA₀ and the human modified α -DBBF Hb is 26 mmHg and 29 mmHg, respectively. During hypoxia, these oxygen levels can decrease to 2 - 5 mmHg. The hemoglobin autoxidation process was already discussed, in where the hemoglobin oxidizes and produces the superoxide ion, which dismutates forming hydrogen peroxide. Recent experiments reported that this increase in reactive oxygen species concentration in the red blood cells induced hypoxic inflammation (Kiefmann et al., 2008).

Moreover, previous studies have shown that the hydrogen peroxide molecule has a cell signaling role activating the hypoxia-inducible factor, HIF-1 α . The HIF-1 α transcriptional factor is an oxygen regulator, that in cases of oxygen deprivation helps in the oxygen delivery or to the adaptation in that environment. HIF-1 α binds only to DNA of cells or proteins that are under hypoxia. Therefore, the HIF-1 α expression, which is directly linked to the O₂ transport, increases gradually during hypoxic conditions as function of time (Scharte et al., 2003). Valuable data of the interaction of α -DBBF Hb with endothelial cells in hypoxic media has been shown (Yeh & Alayash, 2004; McLeod & Alayash, 1999). The cells treated with hypoxic gas in presence of oxy α -DBBF Hb show that the HIF-1 α

expression increases 2 to 3 fold. The HIF-1 α expression is 2 fold higher when the experiments were carried out with ferric α -DBBF Hb compared with the values obtained for oxy α -DBBF Hb. Besides this, the addition of α -DBBF Hb in concentrations below 100 μ M caused a reduction in the hydrogen peroxide concentration with an increase in lipid peroxidation. In this regard during the hypoxic period the α -DBBF Hb autoxidation is 3 times faster, increasing the ferric α -DBBF Hb levels from 0% to 82%. Linearly with the ferric species increases was found a decrease in the oxy α -DBBF Hb levels from 95 % to 2 - 4 %. The formation of approximately 16% of the ferryl species, induced by the reaction of the hemoglobin with the ROS produced in the redox cycle was also evident (Yeh & Alayash, 2004).

This chapter discusses the redox reactions of the hemoglobins HbI, and HbII from the clam *Lucina pectinata* when exposed to bovine aortic endothelial cells (BAEC) in a hypoxic environment. The results show formation of intracellular superoxide ion and ferryl hemoglobin. Moreover, it was confirmed that the addition of the hemoglobins to the cells media under hypoxia affect the reactive oxygen species cell signaling mechanism and increases the HIF-1 α protein levels.

6.2 Intracellular superoxide ion formation and oxygen tension results

The levels of intracellular superoxide ion were detected by luminescence measuring the light emission of the compound lucigenin, which emits light when reacts with the superoxide ion. Figure 6.1 illustrates the time courses for the intracellular O₂⁻ formation in

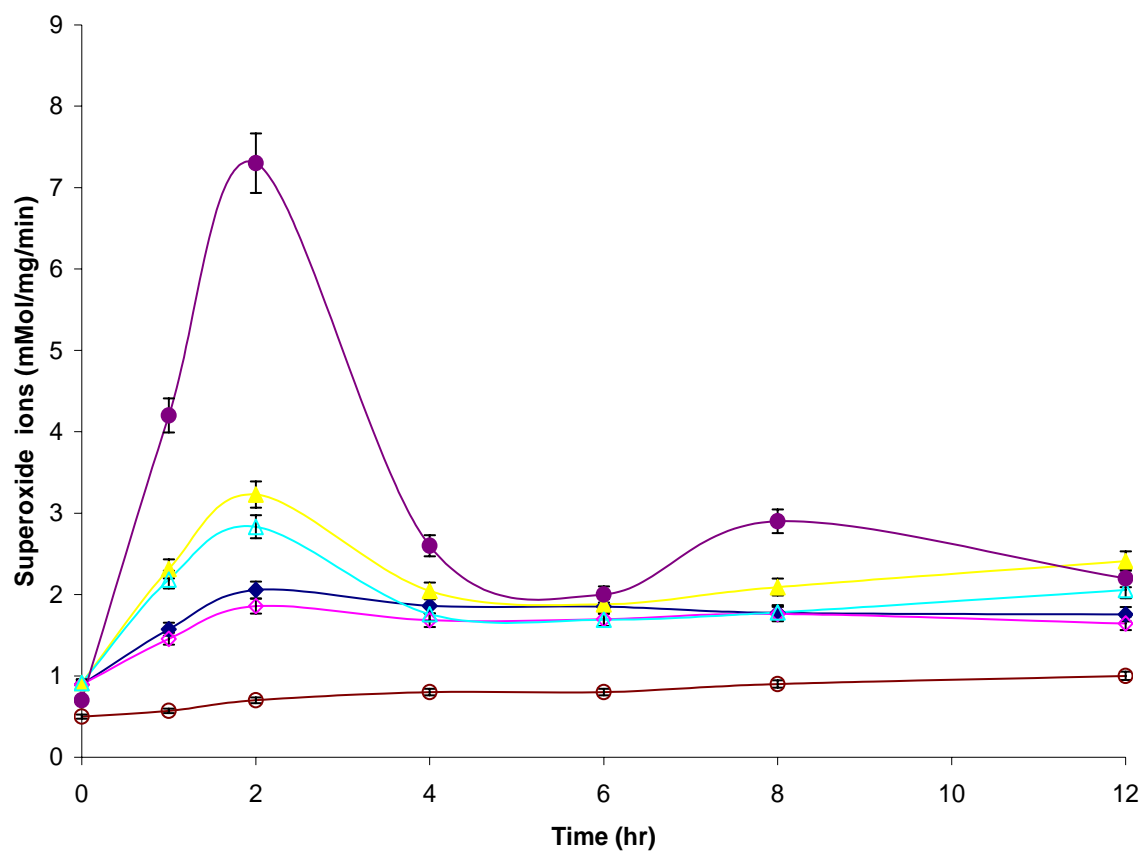


Figure 6.1 Time course for the intracellular $O_2^{\cdot -}$ formation during hypoxia in the presence or without SOD. Cells were incubated under hypoxic conditions (95% N_2 , 5% CO_2) with 50 μM Hb and with or without 100 U SOD for 12 hrs. The $O_2^{\cdot -}$ was measured in a TopCount Luminescence counter. ● α -DBBF Hb/hypoxia; ○ α -DBBF Hb/hypoxia/SOD; ◆ HbII/hypoxia; ◇ HbII/hypoxia/SOD; ▲ HbI/hypoxia; △ HbI/hypoxia/SOD.

BAEC exposed to hypoxia and to HbI and HbII hemoglobins. The graph shows that during the hypoxic conditions α -DBBF Hb produces 1 to 7 mMol/mg/min $O_2^{\cdot -}$, reaching the higher concentration at 2 hours. The addition of the antioxidant enzyme SOD to the cells media reduces the $O_2^{\cdot -}$ levels to approximately 0.5 - 0.8 mMol/mg/min. This data is in agreement with previous experiments for this hemoglobin (Yeh & Alayash, 2004). The concentration of intracellular $O_2^{\cdot -}$ when the cells were incubated with HbII was between 1 - 2 mMol/mg/min, while the concentration in the cells incubated with HbI was between 1-3 mMol/mg/min. Both *L. pectinata* hemoglobins also show that the levels of $O_2^{\cdot -}$ have the higher concentration at 2 hours. After 2 hours, the superoxide ion concentration decreases and oscillates between 1.5 and 2.5 mMol/mg/min for the following 12 hours. The formation of the superoxide ion in the hypoxic environment concurs with the increase of the hemichrome species and the decrease in the oxy species. The graph also illustrates the superoxide ion concentration when SOD was added to the cells media containing hemoglobins. The low detection of $O_2^{\cdot -}$ levels, less than 1 mMol/mg/min, in the reaction of α -DBBF Hb with SOD demonstrates that α -DBBF Hb produces high amounts of $O_2^{\cdot -}$ which are consumed in the presence of SOD. However, the reaction for HbI and HbII with SOD do not show a significant difference from that without the SOD. In agreement with the autoxidation data, this experiment also suggests that HbII induces less formation of ROS.

Oxygen tension experiments were performed to monitor the oxygen-carrying capabilities of the oxy hemoglobins exposed to cells during normal and hypoxic conditions. Figure 6.2 shows that under normal conditions the cells media has an oxygen tension (pO_2) of approximately 208 mmHg, which was used as control. When the cells media was exposed

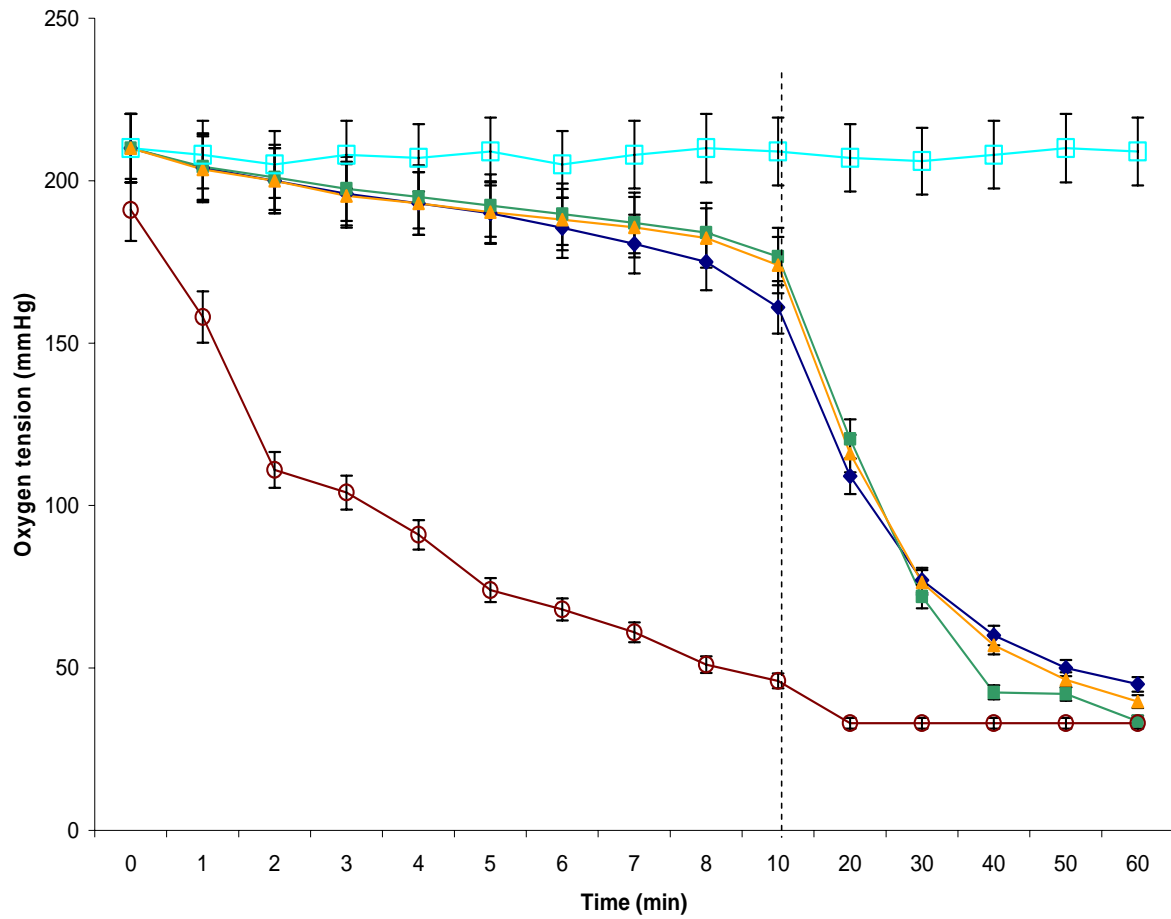


Figure 6.2 Oxygen tension of endothelial cells medium during hypoxia. Confluent endothelial cells were placed inside a chamber containing 3mL of basal medium and with or without 50 μ M Hb (\blacklozenge : α -DBBF Hb; \blacktriangle : HbII; \blacksquare : HbI). Normoxia experiments (\square : control) were carried out when 5% CO_2 and 95% air were fed into the chamber. Hypoxia experiments (\circ : cells during hypoxia) were conducted when mixed gas (5% CO_2 and 95% N_2) was flushed into the chamber. Values at each time represent the mean \pm SE of 3 independent experiments.

to the hypoxia period, the pO_2 decreases gradually to approximately 33 mmHg in 20 minutes, which was the lower value obtained. At the same time, the decrease in pO_2 in the presence of α -DBBF Hb is slower with pO_2 of ~175 mmHg at 10 minutes, and ~110 mmHg at 20 minutes, accordingly with previous experiments (Yeh & Alaysh, 2004). Under the same hypoxic conditions, the oxygen tension for HbI and HbII was nearly 180 mmHg at 10 minutes, and 112 mmHg at 20 minutes, having pO_2 values similar to α -DBBF Hb. The measurement of pO_2 at 30 minutes was approximately 80 mmHg for the three hemoglobins, but thereafter, the pO_2 in the cells media exposed to HbI decreases faster than HbII and α -DBBF Hb. At 60 minutes, HbI reaches a pO_2 of 33 mmHg that was the same minimum value that reached the cells without the hemoglobins under hypoxia, while HbII and α -DBBF Hb remains with pO_2 of ~40 mmHg and ~ 45 mmHg, respectively. These measurements suggested that under hypoxic stress the oxy form of HbII has similar oxygen carrying capabilities than the human cross-linked α -DBBF hemoglobin.

6.3 *Lucina pectinata* redox chemistry during hypoxia

Previous experiments (Yeh & Alayash, 2004) show that, in a time frame of 12 hours, the oxy levels of α -DBBF Hb when exposed to cell cultured media were reduced from 95% to 70%, increasing the ferric-ferryl forms nearly 30%. Under hypoxic conditions, at the end of the 12 hours the spectra showed that the oxidation was faster decaying the oxy α -DBBF Hb levels to 4%, and increasing the ferric and hemichrome levels 82% and 17%, respectively. In this respect, Figure 6.3 shows the overlay spectra of HbII exposed to the

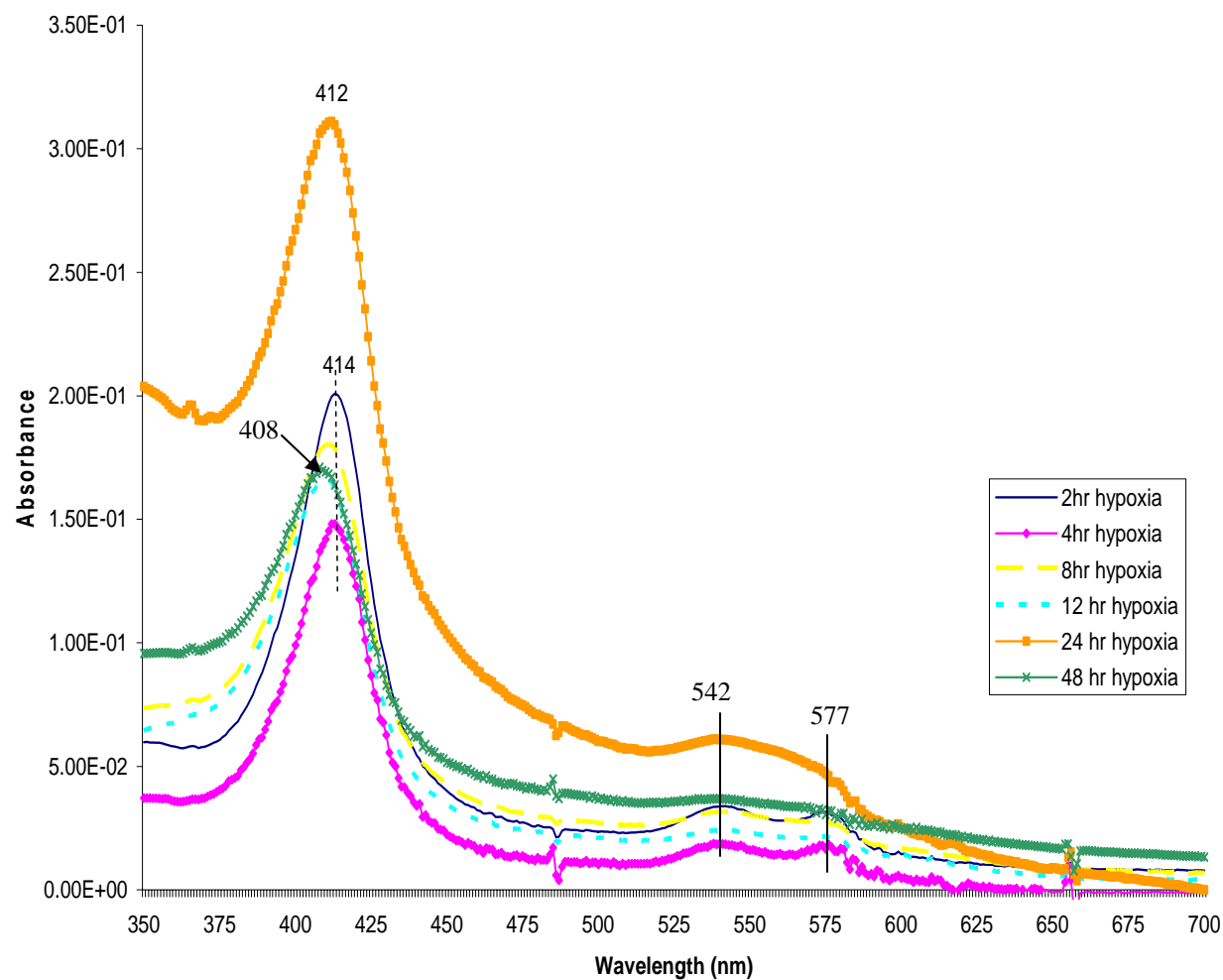


Figure 6.3 UV-Vis overlaid spectra of *Lucina pectinata* HbII after exposed to bovine aortic endothelial cells subjected to hypoxia. The formation of reactive oxygen species lead to the production of the ferryl HbII.

BAECs under hypoxia. During 2 and 4 hours, the HbII remains in the oxy form showing a band at 414 nm, and initial formation of the ferryl species with bands at 542 nm and 577 nm, with a small decrease in the of the Soret band between times. The HbII oxidation starts around 8 hours where the Soret band shifts to 413 nm and the Q bands broadens. Bands characteristic of the hemichrome-ferryl species appear near 24 hours. The decrease in the intensity of the Soret band with an increase in the base line suggests heme degradation. Figure 6.4 shows the percent of oxy, ferric and hemichrome HbII species plotted as function of time during the exposition to BAEC cells cultured under normoxic and hypoxic conditions. Each point in the plot represents the average of three independent experiments and was calculated from the spectra following the Winterbourn equations described in section 2.1.2 (Winterbourn, 1985). The first graph plots the percent of the oxy species during normoxic conditions showing a gradual decrease from 82% at the beginning of the experiment, to 8% at the end of the 24 hours. This change was in part due to the autoxidation of oxy HbII. The percent of ferric species during normoxia shows that corresponding to the decrease in the oxy HbII, is 35 - 40% of ferric hemoglobin formed at the end of the 24 hours, while the hemichrome species increases around 56% of the total heme. Under hypoxic conditions the oxy HbII autoxidizes more quickly. At 2 hours, the percent in ferric HbII did not show a difference between the normoxic and hypoxic values, therefore it is suggested that the main contribution to the oxy percent change was due to the formation of the hemichrome species. The change in oxy species between the normoxic and hypoxic experiment was about 10% between 4 hours, 6, 8 and 12 hours. During these times the percent in hemichrome species were constant, increasing only the percent in ferric species.

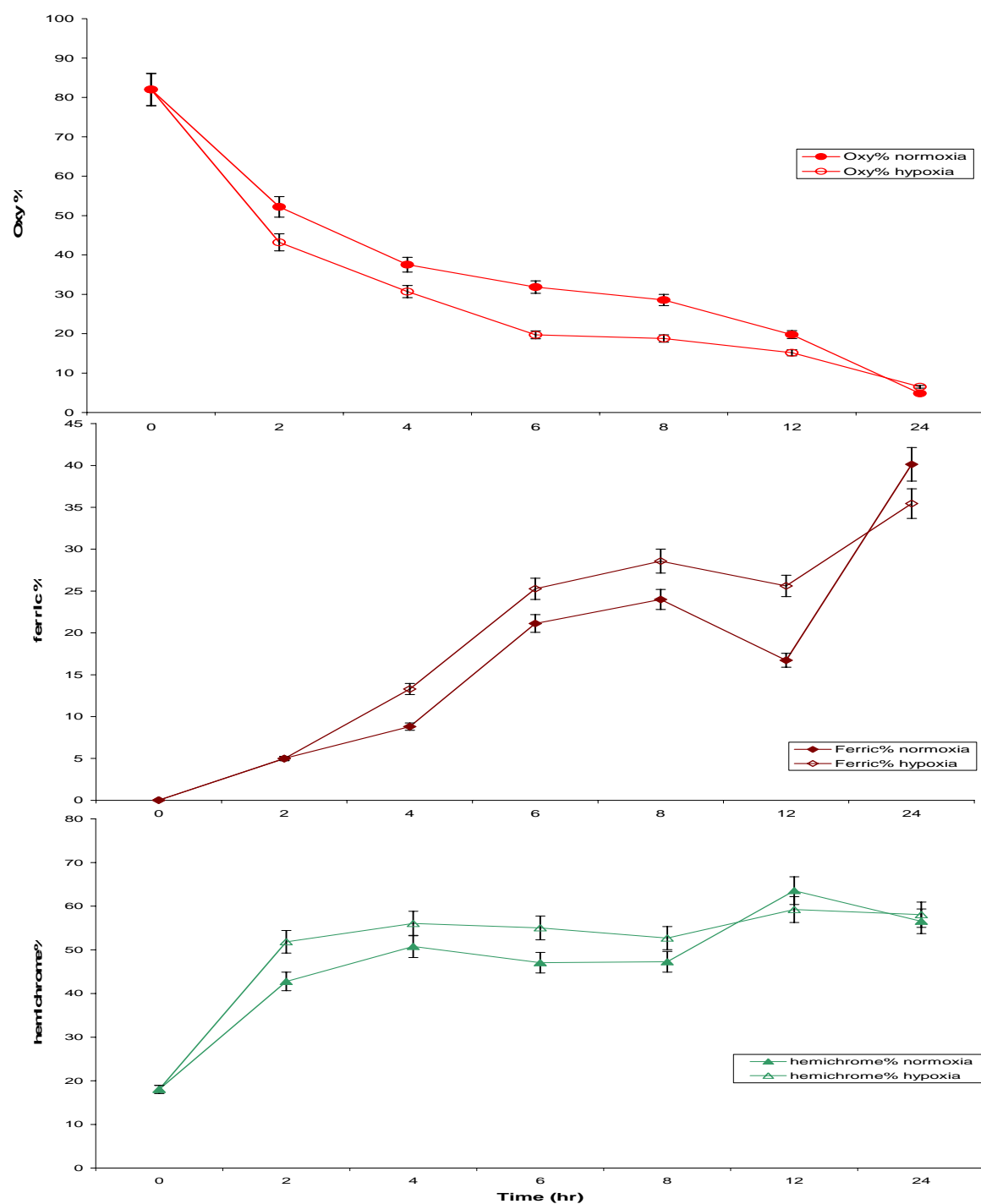


Figure 6.4 Time course spectra analysis for the oxidation of HbII in cells culture media under normoxic and hypoxic conditions. HbII (25 μ M) was incubated with BAEC's at 2, 4, 6, 8, 12 and 24 hrs. At each time interval the spectrum was recorded and the percentage of oxy, ferric and hemichrome was calculated following the Winterbourn equations (Material and methods, Section 2.1.2).

Figure 6.5 shows the UV-Vis spectra for HbI when was exposed to endothelial cells during hypoxia. The spectrum at 2 hours shows mixture of the oxy and ferric HbI with a Soret band at 412 nm and Q bands at 543 nm and 577 nm suggesting the formation of ferryl species, and broad bands at 502 nm and 633 nm indicating oxidation to the ferric species. During 4 and 6 hours the Q ferryl bands decreased, increasing the 502 nm and 633 nm bands, and the Soret band shifted to 409 nm. From 8 to 12 hours bands characteristic of ferric HbI governs the reaction. Figure 6.6 shows the percent of oxy, ferric and hemichrome HbI species exposed to the endothelial cell culture under normoxic and hypoxic conditions calculated from the UV-Vis spectra. The percent of oxy HbI during the first 4 hours of incubation in normoxic conditions show a gradual decrease from 77% to 31%. This decrease corresponds mainly to an increase in the percent of ferric hemoglobin. Between 4 hours and 6 hours the percent of oxy HbI remained constant, while increased with the same proportion as the ferric and hemichrome species. The graphs show that in 8 hours the oxy HbI percent decreased to nearly 0%, and corresponding to this decrease only a 20% of ferric hemoglobin was formed, while the hemichrome species (degradation products or ferryl species) increased 60% of the total heme. Under hypoxia, the decay in the percent of oxy HbI was faster showing ~10% at 4 hours, and 0% at 6 hours. Different from normoxia, in hypoxic conditions the ferric form reaches a 65%, and the hemichrome species were near the 35%. These experiments clearly indicate, as previously showed by the heme degradation products formation, that HbII is more resistant to autoxidize than HbI, and that the latter degrades faster forming hemichrome species. This is also shown in the HbII behavior during normoxia versus hypoxia, with small spectral changes between both periods (Figure 6.4) while HbI shows faster changes in the oxidation states (Figure 6.6).

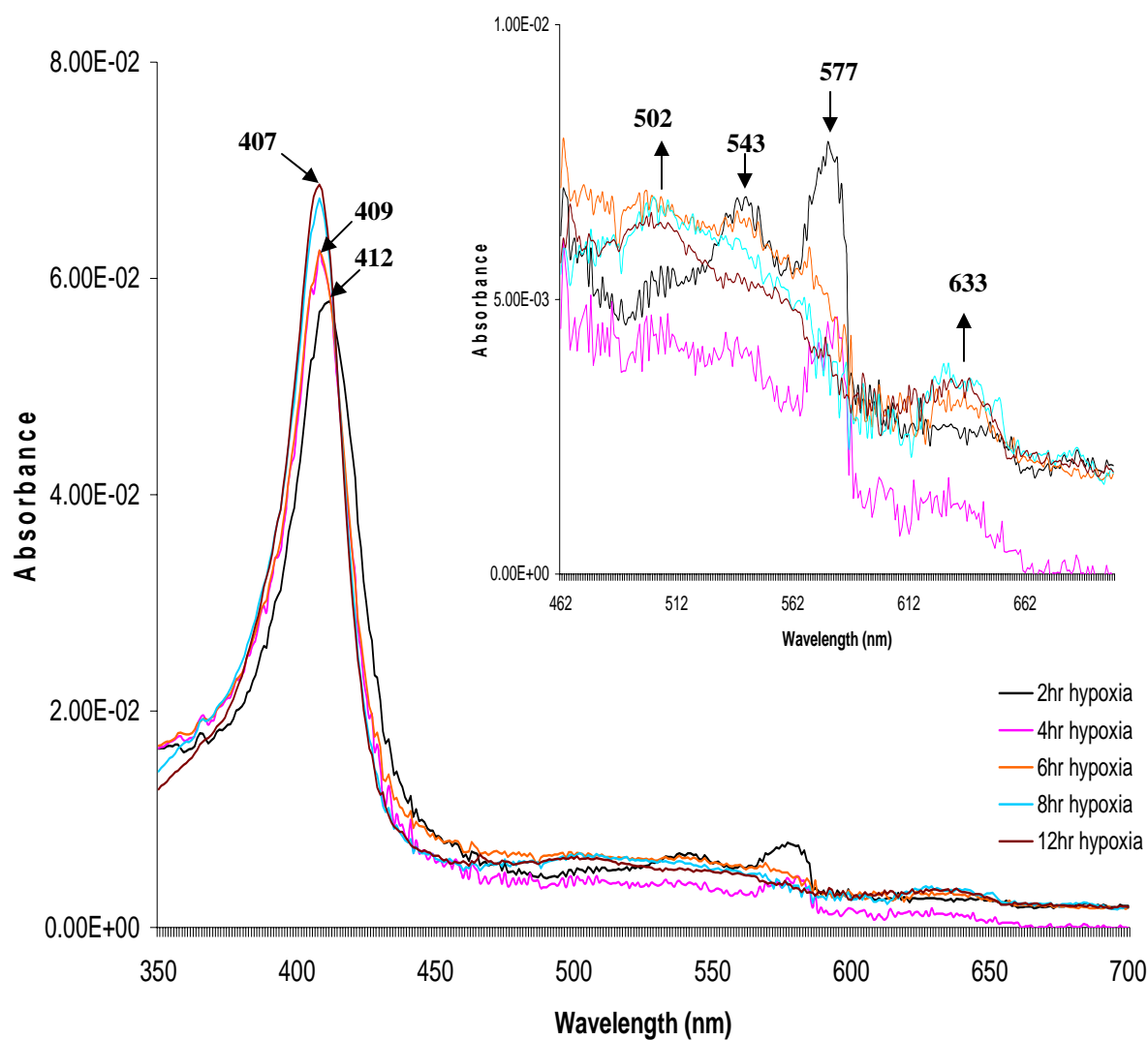


Figure 6.5 UV-Vis overlaid spectra of *Lucina pectinata* HbI after exposed to bovine aortic endothelial cells subjected to hypoxia. The initial spectrum at 2 hours already shows a mixture between the ferric and the ferryl species with a Soret band at 412 nm and Q bands at 543 nm and 577 nm.

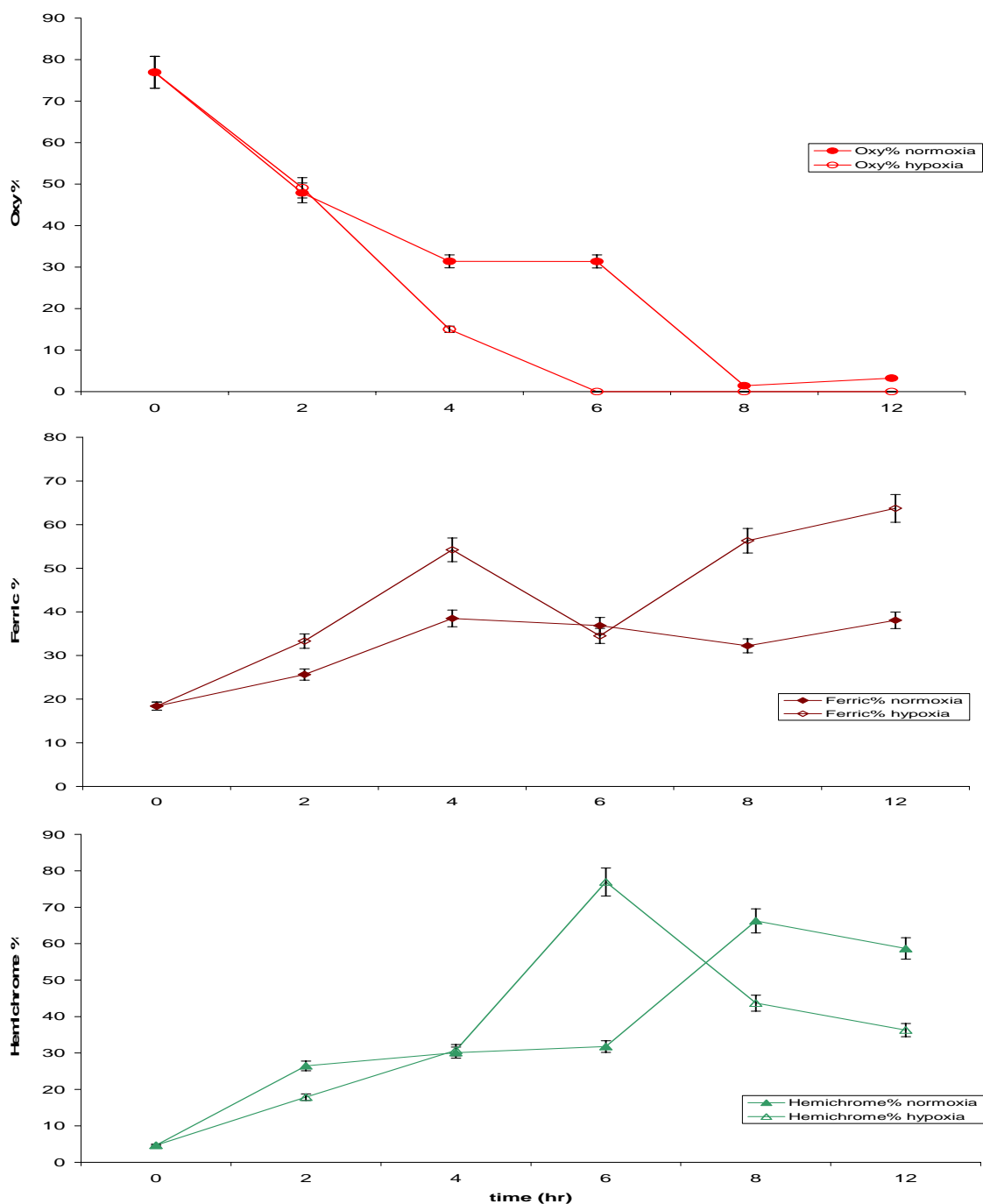


Figure 6.6 Time course spectra analysis for the oxidation of HbI in cells culture media under normoxic and hypoxic conditions. HbI (25 μ M) was incubated with BAEC's at 2, 4, 6, 8, and 12 hrs. At each time interval the spectrum was recorded and the percentage of oxy, ferric and hemichrome was calculated following the Winterbourn equations.

6.4 HIF-1 α protein expression during hypoxic conditions

Studies of bovine aortic endothelial cells under hypoxic conditions and with α -DBBF Hb showed an increase in the HIF-1 α expression as a function of time. Thus, α -DBBF Hb can modulate cell signaling pathways. In this respect, Figure 6.7 screens the detection of HIF-1 α expression by Western immunoblot for the endothelial cells under hypoxia with and without oxy HbII and HbI. According to earlier observations, the expression of HIF-1 α in the cells under hypoxia used as control, presents a slight gradual increase in the intensity and width of the bands in a time dependent manner (Yeh & Alayash, 2004). The expression of HIF-1 α in the experiments where the cells were exposed to HbII (Figure 6.7 A) also shows that the density of the bands increases in a time dependent behavior. But compared to the control, these bands are more intense. Thus, indicating a higher HIF-1 α expression when HbII was added to the cells media. Figure 6.7 B shows the immunoblot of HIF-1 α expression during cells incubation with HbI in the hypoxic media. Like the results for HbII, the HIF-1 α expression increases in the presence of His, showing an increase dependent of time in the band density. This increase in intensity is due to the high formation of ROS that activates redox signal pathways, thus enhancing the expression of HIF-1 α .

Figure 6.8 shows the densitometry of the bands plotted as a function of time taking as control the normoxic conditions. This representation quantifies the bands in the western blot indicating that the relative HIF-1 α expression levels increased in the cells under hypoxia. The Student's t-Test statistical analyses to consider if the HIF-1 α expression relative levels

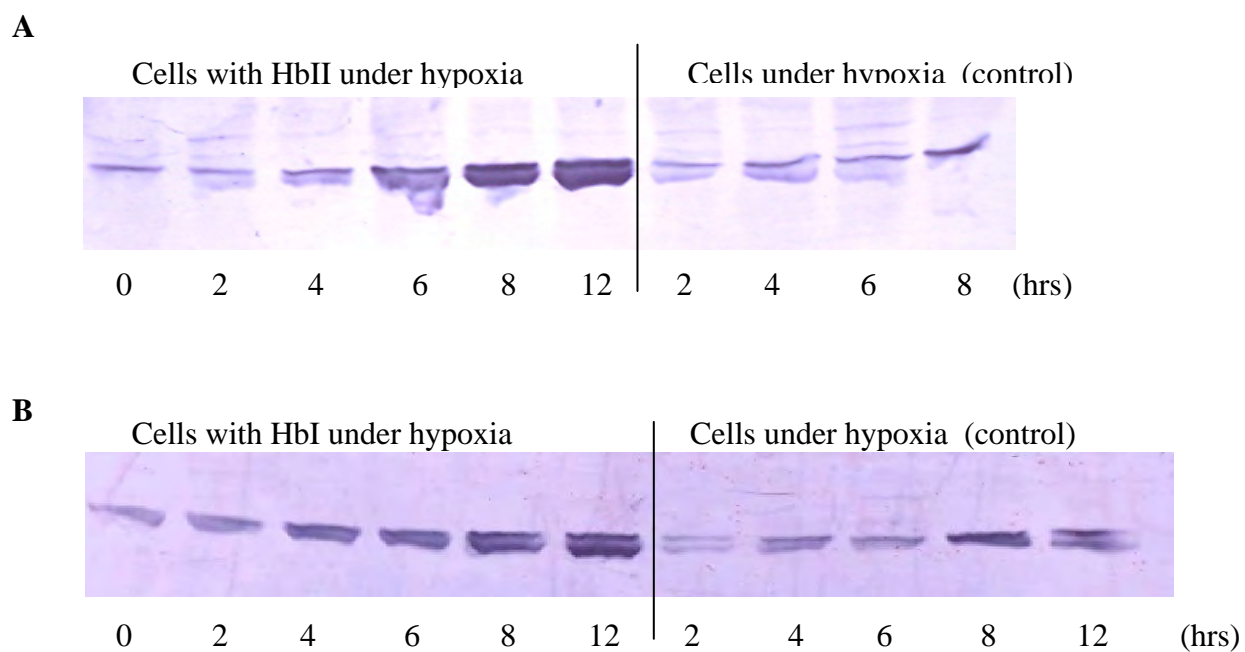


Figure 6.7 HIF-1 α expression in bovine aortic endothelial cells under hypoxia with or without 25 μ M oxy HbII (A) or HbI (B). Hypoxic gas (95% N₂, 5% CO₂) was flushed in a sealed chamber containing the cell cultured media with or without 50 μ M HbII or HbI. After each experiment, cell lysates were analyzed by western blot for HIF-1 α protein.

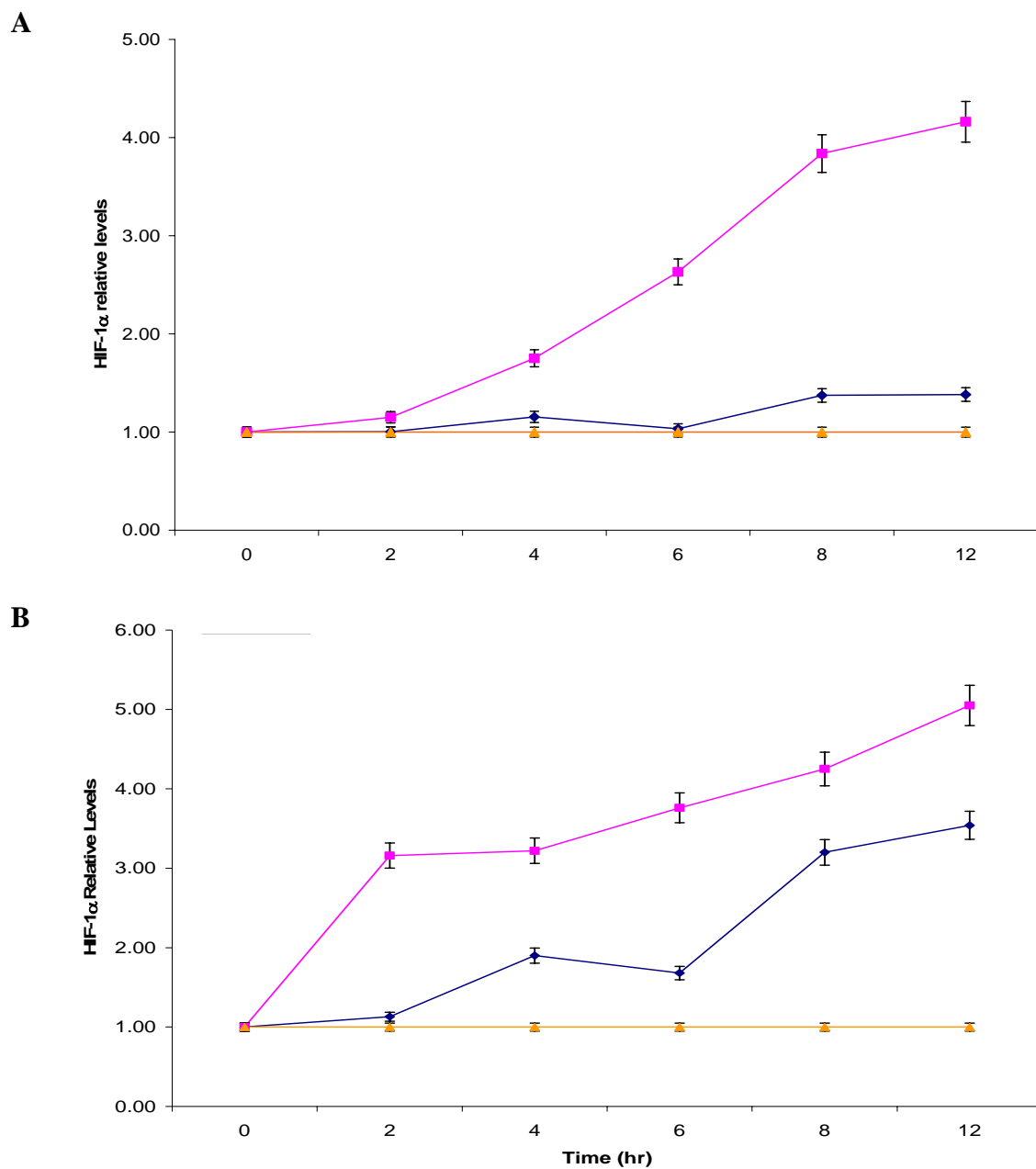


Figure 6.8. Relative HIF-1 α protein expression levels in BAEC's during incubation with (A) HbII or (B) HbI under hypoxia. Densitometry for the immunoblot detection of HIF-1 α was performed and plotted as function of time. ▲ -cells under normoxia, ■ -cells under hypoxia treated with HbII (A) or HbI (B), ◆ -untreated cells under hypoxia. The probability (p) is less than 0.05; therefore the increase between cells in hypoxia and with Hb is significant.

are significant are shown in Appendix B. Figure 6.8 A indicates a small change in the intensity of the HIF-1 α expression band for the cells incubated with HbII at 2 hours that is not significant since $p = 0.065$. Thereafter, the graph indicates that HIF-1 α expression have 2 fold to 3 fold time dependent increases when HbII was added to the system for a period of 12 hours. Figure 6.8 B plots the HIF-1 α expression when hypoxic cells were exposed to HbI. At 2 hours the HIF-1 α expression shows a 2 fold increase. At each time, the expression increased gradually reaching a 4 fold increase after 12 hours of incubation. The analysis of probability for the cells under normoxia compared with the cells with HbI under hypoxic conditions is $p < 0.05$ for all the plots. This means that the difference between the HIF-1 α levels in the cells under hypoxia exposed to HbI is significant. These results suggest that the *L. pectinata* HbI and HbII can also alter cell signaling pathways that cause increases in the HIF-1 α expression.

6.5 Discussion

During accidents with blood loss, or in cases of infections the blood flow is limited. Therefore, ischemia might occur in some tissues. The oxygen delivery to tissues and organs is reduced causing hypoxia, as in the case of hemorrhagic shock. Generally, blood is infused during these situations causing reperfusion or tissue re-oxygenation. It was evidenced that many reactive oxygen species can be generated when the tissue is re-oxygenated (Therade-Matharan et al., 2004). In this respect, *L. pectinata* HbII and HbI have a high oxygen affinity of 0.46 μ M and 0.37 μ M, respectively, compared to α -DBBF Hb that has an affinity of 3.33 μ M (Kraus & Wittenbeerg, 1990; D'Agnillo & Alayash, 2000). Therefore, at low partial pressures HbII and HbI do not have cooperative kinetics. Thus, the carrying capabilities of

these hemoglobins when exposed to endothelial cells subjected to hypoxia are interesting. During hypoxia, the oxygen tension of the media can be decreased between 2 to 35 mmHg. In this study, the oxygen tension of the cells under normoxia was 208 mmHg and during hypoxia drops off to approximately 33 mmHg. However, the addition of 50 μ M HbII or HbI to the media contributes to the oxygen tissue content maintaining it above 175 mmHg in the first 10 minutes, and thereafter decreasing the oxygen tension slowly for an hour. Thus, the oxygen from oxy hemoglobin is down loaded from the heme and diffuses through the hypoxic media. Then, the cells take the oxygen and convert it to superoxide ion via the membrane complex NADPH oxidase (Nox) which in the mechanism oxidizes NADPH to NADP^+ , as depicted in Figure 6.9. It was suggested that the NADPH oxidases are the main source of ROS generation and are involved in redox signaling pathways (Cave et al., 2006). Therefore, the increase in reactive oxygen species in the endothelial cells treated with the *L. pectinata* hemoglobins generate a disruption between reductases and the oxidants that activates the HIF-1 α expression during hypoxia.

These results can be correlated with the intracellular superoxide formation. During hypoxia, the superoxide ion is formed intracellularly. Moreover, the addition of HbI or HbII to the hypoxic cells media increases its formation showing a maximum concentration of 7.2 mMol/mg/min at 2 hours. The results of the experiments when the enzyme SOD was added to the system were similar to the autoxidation results discussed in Chapter 4. In the presence of HbII or HbI, the difference in intracellular superoxide concentration between the experiment performed with the SOD and that performed without the SOD was very small. The small changes in the reaction adding the SOD, compared to the reaction without it, clearly indicates that HbII produces low concentrations of reactive oxygen species.

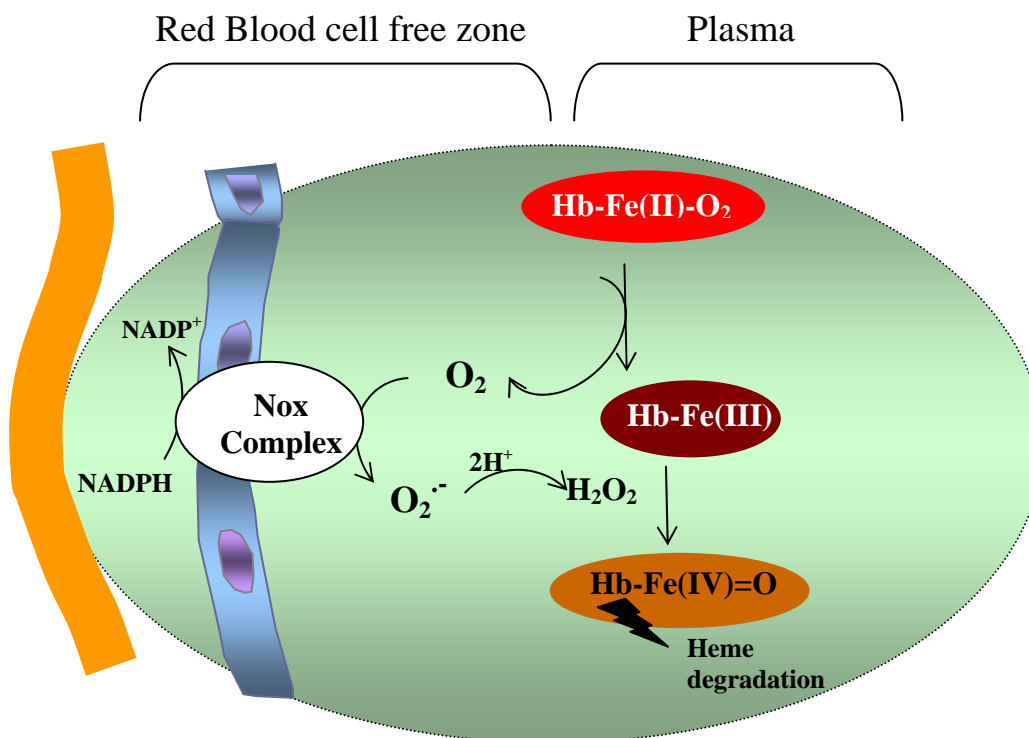
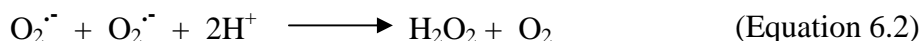


Figure 6.9 Schematic representation for the reaction of the *Lucina pectinata* hemoglobins HbI and HbII. During the hypoxic period, oxy hemoglobin down loads the oxygen which is converted to superoxide ion by Nox1. The reaction of the hemoglobin with the hydrogen peroxide, formed by the superoxide dismutation, produces the Hb-ferryl species. Model adapted from Dworakowski et al., 2008 & Alayash, 2004.

The superoxide ion can react with hemoglobin or can undergo dismutation to produce hydrogen peroxide (Nagababu et al., 2002).



The formation of the superoxide ion and hydrogen peroxide prolongs the oxidation process of the hemoglobins. It was previously reported that the concentration of hydrogen peroxide produced by the endothelial cells is less than 10 μM (McLeod & Alayash, 1999). When the hemoglobins were subjected to cells under hypoxia, the percent of oxy HbII and HbI was reduced to 22% in HbII and 0% in HbI in a period of 6 hours. An increase in the ferric and hemichrome species correlates with the decrease in the oxy species. As a result, the formation of ferryl HbI species and ferric bands at 2 hours evidences the cyclic reaction of pseudoperoxidase of this hemoglobin. For the first 4 hours, HbII shows to be more resistant to oxidation forming oxy-ferryl bands, and then oxidizing to the ferric species with ferric-ferryl bands. Therefore, these reactions agree with formation of the intracellular superoxide ion in the cells exposed to hypoxia and 50 μM HbI or HbII. Thus, under the hypoxic stress the ferryl hemoglobin is formed, as evidenced in the HbII and HbI spectra in Figures 6.3 and 6.5, respectively. The scheme in Figure 6.9 also shows that the superoxide ion can dismutate producing hydrogen peroxide, which reacts with the hemoglobin forming the ferryl species and subsequent heme degradation. As it was discussed in Chapter 5, the oxidation and formation of the ferryl hemoglobin represents an oxidative stress to cells and may cause cell damage.

Moreover, the reactive oxygen species have direct effects that lead to the modulation of redox-sensitive signaling pathways in the endothelial cells (Dworakowski et al., 2008). These changes can affect the expression of different proteins, as for example HIF-1 α protein (Deudero et al., 2008). In this respect, the formation of the superoxide ion functions as a redox signaling molecule activating the expression of the HIF-1 α protein. Endothelial cells under hypoxia increase the HIF-1 α expression in a time dependent manner, showing to be more intense when 50 μ M hemoglobin was added to the system. The increase in the expression of the HIF-1 α protein exhibits a direct correlation with the oxy and ferric species of HbI and HbII. Figures 6.10 and 6.11 present the percent of oxy or ferric hemoglobin species versus the HIF-1 α relative levels when treated in endothelial cells during hypoxia. Figure 6.10 A shows that while the percent of oxy HbII decreases the HIF-1 α expression increases. Figure 6.10 B shows a positive correlation between the increase of the ferric HbII and the increase of the HIF-1 α expression. A similar behavior was seen for HbI in Figure 6.11 A and B.

Therefore, in this study the endothelial cells sense stress in two different ways. The first one was by using an anaerobic system, thus generating hypoxia in the tissue and media. The second one was by the addition of the hemoglobins to the media. From both paths, the system produces high concentrations of reactive oxygen species that creates a physiological balance disruption. Moreover, the overproduction of the reactive oxygen species activates cell signaling mechanisms to overcome the balance disruption, as is the case of the HIF-1 α protein. The increase in the cell media partial pressure during hypoxic periods when endothelial cells were exposed to *L. pectinata* HbI or HbII suggests that these hemoglobins can transport oxygen to the media, thus oxygenating tissues that are in hypoxic stress.

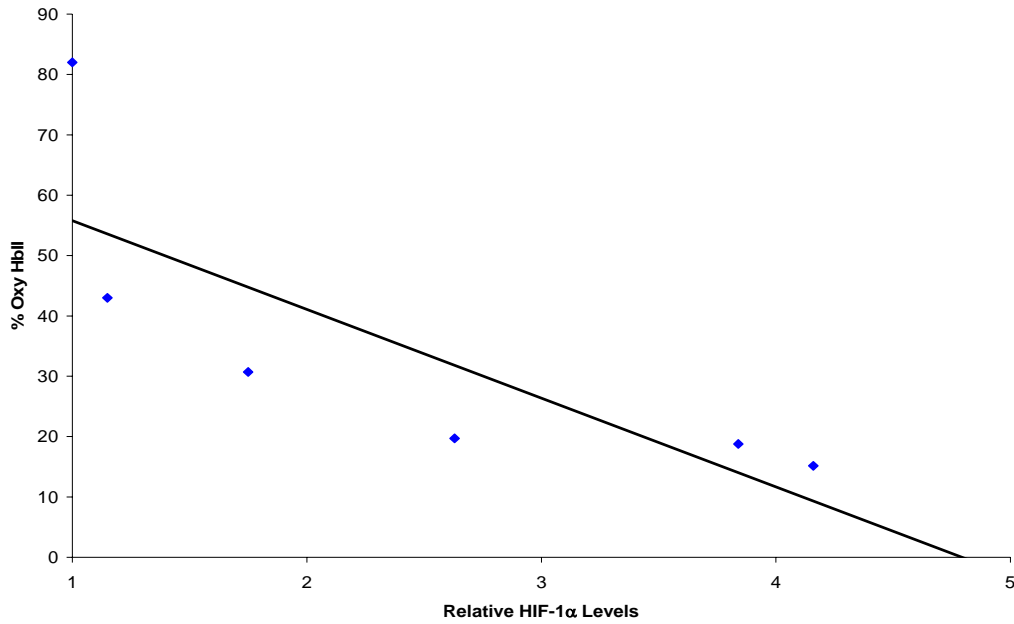
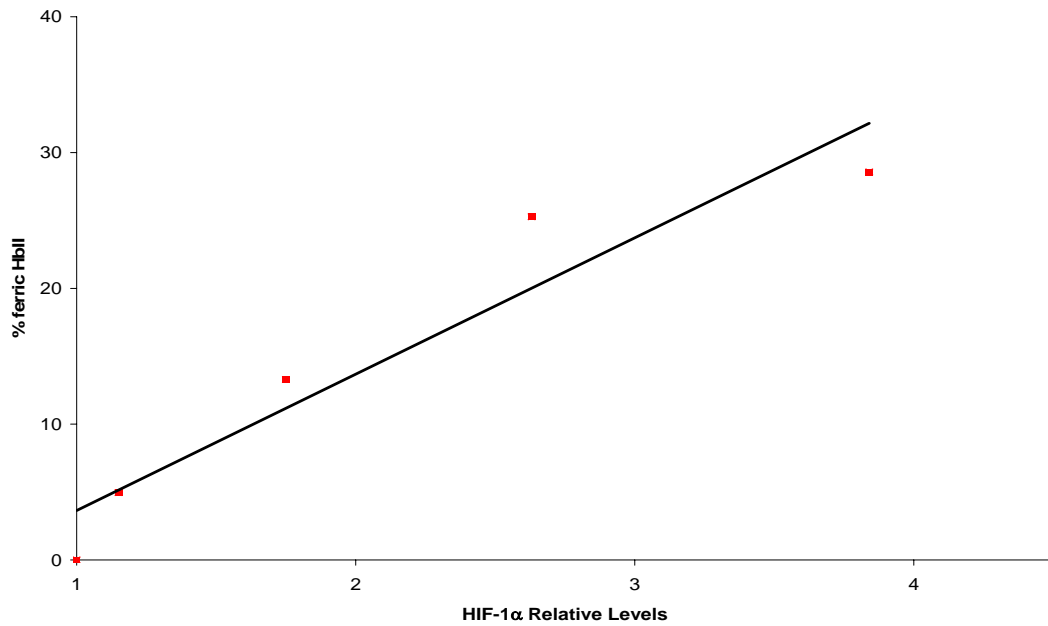
A**B**

Figure 6.10 Correlation between the percent of oxy (A) or ferric (B) HbII and HIF-1 α relative levels. Graph A shows a negative correlation between the decrease in the percent of oxy HbII and the expression of HIF-1 α . Graph B shows a positive correlation between the increase in the percent of ferric HbII and the expression of HIF-1 α .

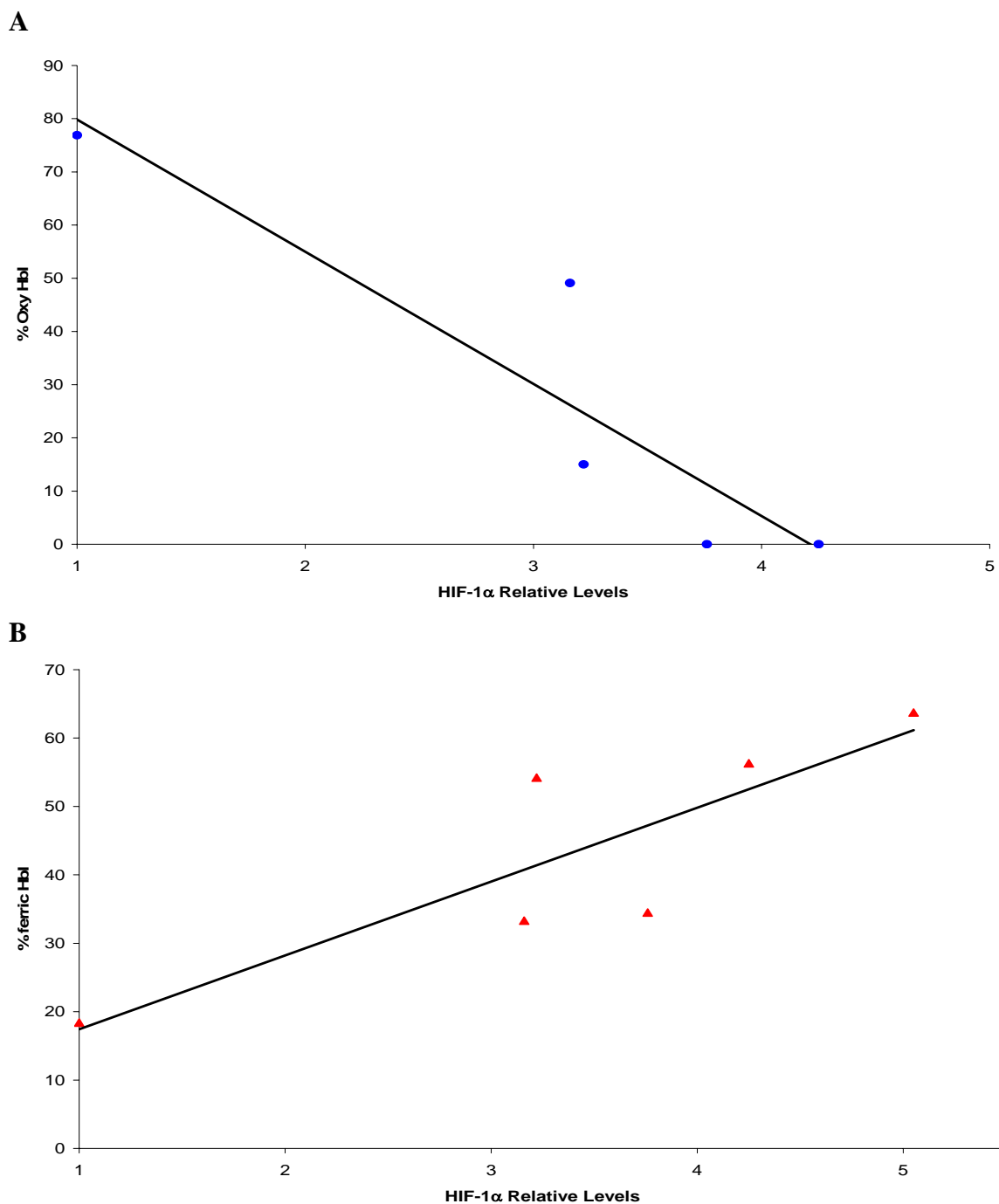


Figure 6.11 Correlation between the percent of oxy (A) or ferric (B) HbI and HIF-1 α relative levels. Graph A shows a negative correlation between the decrease in the percent of oxy HbI and the expression of HIF-1 α . Graph B shows a positive correlation between the increase in the percent of ferric HbI and the expression of HIF-1 α .

However, this over production of reactive oxygen species leads to the formation of hydrogen peroxide and as a result, the production of the ferryl species and degradation products can damage the cells. In this respect, Figure 6.3 shows that the HbII spectra exhibit oxy bands for up to 4 hours, and ferric-ferryl bands for the reaction at 48 hours, while HbI shows in Figure 6.5 a fast formation of the ferryl species at 2 hours and ferric bands with heme degradation at the end of the 12 hours. Therefore, these results agree with the results of hemoglobins oxidation by hydrogen peroxide, where HbII is more resistant to oxidation than HbI.

7 CONCLUSIONS

The design of an oxygen carrier has been a goal for researchers for many years (Chang, 1997, Estep et al., 2008), but several factors prevent the utilization of the produced hemoglobin based oxygen carriers. The first barriers were to control the dissociation of the hemoglobin alpha and beta chains and to improve its retention time in the vascular system, given that the reactions involved in the process caused cellular damage and renal dysfunction in patients (Alayash, 1999; Kim & Greenurg, 2004). To overcome this problem, it was necessary to perform crosslinking of the chains and polymerization of the hemoglobin. Thereafter, the infusion of the hemoglobins was causing physiological diseases by their interaction with the cellular tissue. Therefore, two major problems need to be controlled in the actual oxygen carrier prototypes. First, the hemoglobins oxidation and formation of reactive oxygen species, which are affecting the cell redox and death signaling pathways (Baldwin, 2004), and second, to control the nitric oxide scavenging by the hemoglobin which causes vascular stress and vasoconstriction (Kim & Greenburg, 2004; Doherty et al., 1998).

In this respect, the heme pocket of hemoglobin and myoglobin has been modified to find a mutation that discriminates from the reaction with hydrogen peroxide and nitric oxide. *L. pectinata* HbI and HbII have a special arrangement of amino acids in the heme cavity that differs from human hemoglobin and myoglobin (Rizzi et al., 1994; Gavira et al., 2008). Glutamine, GlnE7, is found in the distal position, while phenylalanine is found in positions CD1 and E11. The main difference between HbI and HbII is the B10 position where HbI has a phenylalanine and HbII has a tyrosine. Therefore, this research analyzed the reaction of

HbI and HbII with hydrogen peroxide and nitric oxide. HbI PheB10Tyr mutant was also used to help understand the role of TyrB10 in these reactions.

One of the findings in this work is that the reaction of the three studied hemoglobins from *L. pectinata* with nitric oxide showed that both oxy and ferric forms of HbII reacted extremely slowly with NO. The kinetic and structural data suggest that the TyrB10 or polar amino acid substitutions in this position are not the only factor affecting the decrease in the reaction with NO. The main feature in this response is the proximity of TyrB10 and GlnE7 to the heme iron in HbII that minimizes the exposure of heme to solvent, thus maintaining an oxidative stability and reducing its reactivity towards NO.

Other important finding is that HbII oxidizes in air slowly and exhibits unusual stability towards hydrogen peroxide and heme-ferryl formation. Therefore, the autoxidation, the hydrogen peroxide and heme degradation experiments in this study strongly suggest that the GlnE7 is not responsible for the hemoglobins oxidative damage and heme breakdown. Indeed, the substitution of an apolar and big residue like phenylalanine in the B10 position, like in HbI, can increase heme damage. In addition, the substitution to a tyrosine polar residue and in combination with the glutamine in E7, as in HbII and confirmed with the reaction of the HbI PheB10Tyr mutant, creates a hydrogen bonding network that includes the GlnE7, TyrB10 and O₂ bound to the heme that results in a tight gage for the oxygen networking providing better resistant to oxidative damage.

Moreover, the redox chemistry of the hemoglobins exposed to bovine aortic endothelial cells and glucose oxidase was studied. The spectral analysis evidences that the reaction of HbI, HbII and the HbI PheB10Tyr mutant exposed to a cell cultured media with H₂O₂ formed the heme-ferryl species. The hydrogen peroxide was produced by the reaction

of GOX with oxygen or from the dismutation of the superoxide ion in the reaction of oxygen with NADPH oxidase in a hypoxic period. HbII and HbI PheB10Tyr mutant showed to be more resistant against peroxidative damage than HbI. However, for periods longer than 6 hours the hemoglobins start to aggregate, thus suggesting a possible conformational change by their reaction with CO₂. The change in the hemoglobins structure also modifies their behavior towards oxidation converting them in hemoglobins susceptible to peroxidation, forming reactive oxygen species and degradation products. This formation of high concentrations of reactive oxygen species creates a balance disruption that caused cell morphology changes, cell apoptosis and necrosis. Besides this, the addition of the hemoglobins to the cells media under hypoxia increased the HIF-1 α protein levels. This part of the research confirms that the balance disruption caused by the generation of reactive oxygen species affect the cell signaling and the cell death mechanisms.

In the overall reactions, HbII produces low concentrations of reactive oxygen species and has low reactivity with nitric oxide. One limitation of the hemoglobins from the clam *L. pectinata* is their high oxygen affinity and lack of cooperativity (Kraus & Wittenberg, 1990), a factor that needs to be overcome in future studies. Therefore, regardless of the precise role of HbII in the NO physiology of the clam *Lucina pectinata*, the unusually well controlled NO entry in heme pocket, based on the kinetic and structural data presented, may represent a model for the design of future oxidatively stable oxygen therapeutics with little or no vasoactivity.

REFERENCES

- Abassi, Z., Kotob, S., Pieruzzi, F., Abouassali, M., Keiser, H.R., Fratantoni, J.C. & Alayash, A.I. (1997). Effects of polymerization on the hypertensive action of diaspirin cross-linked hemoglobin in rats. *J. Lab. Clin. Med.*, 129, 603-610.
- Abu-Soud, H.M. & Hazen, S.L. (2000). Nitric oxide is a physiological substrate for mammalian peroxidases. *J. Biol. Chem.*, 275, 37524-37532.
- Alayash, A.I. (1999). Hemoglobin-based blood substitutes: oxygen carriers, pressor agents, or oxidants? *Nature Biotechnol.*, 17, 545-549.
- Alayash, A.I. (2004). Oxygen therapeutics: can we tame hemoglobin? *Nature*, 3, 152-159.
- Alayash, A.I., Brockner Ryan, B.A., Eich, R.F., Olson, J.S. & Cashion, R.E. (1999). Reactions of sperm whale myoglobin with hydrogen peroxide. Effects of distal pocket mutations on the formation and stability of the ferryl intermediate. *J. Biol. Chem.*, 274 (4), 2029-2037.
- Alayash, A.I., Brockner Ryan, B.A. & Cashion, R.E. (1998). Peroxynitrite-mediated heme oxidation and protein modification of native and chemically modified hemoglobins. *Arch. Biochem. Biophys.*, 349, 65-73.
- Alayash, A.I., Fratantoni, J.C., Bonaventura, J. & Cashion, R.E. (1993). Nitric oxide binding to human ferrihemoglobins cross-linked between either alpha or beta subunits. *Arch. Biochem. Biophys.*, 303, 332-338.
- Alayash, A.I., Summers, A.G., Wood, F. & Jia, Y. (2001). Effects of glutaraldehyde polymerization on oxygen transport and red properties of bovine hemoglobin. *Arch. Biochem. Biophys.*, 391, 225-234.
- Antommattei-Pérez, F.M., Rosado Ruiz, T., Cadilla, C.L. & López Garriga, J. (1999). The DNA-derived amino acid sequence of hemoglobin I from *Lucina pectinata*. *J. Protein. Chem.*, 18, 831-836.
- Baldwin, A.L. (2004). Blood substitutes and redox responses in the microcirculation. *Antioxid. Redox Signal.*, 6, 1019-1026.
- Becker, C. (2001). Budgets may get bloodied. American Red Cross plans to raise average price of blood by nearly one-third. *Modern Healthcare*, 2001, 31-38.
- Bolognesi, M., Boffi, A., Coletta, M., Mozareli, A., Pesce, A., Tarricone, C., et al. (1999). Anticooperative ligand binding properties of recombinant ferric Vitreoscilla homodimeric hemoglobin: a thermodynamic, kinetic and X-ray crystallographic study. *J. Mol. Biol.*, 291, 637-650.

- Buhler, P. & Alayash, A.I. (2004). Oxygen sensing in the circulation: “cross talk” between red blood cells and the vasculature. *Antioxid. Redox Signal.*, 6, 1000-1010.
- Burmester, T., Weich, B. & Reinhardt, T.H. (2000). “A vertebrate globin expressed in the brain”. *Nature*, 407, 520-523.
- Cashon, R.E. & Alayash, A.I. (1995). Reaction of human hemoglobin HbAo and two cross-linked derivatives with hydrogen peroxide: differential behavior of the ferryl intermediate. *Arch. Biochem. Biophys.*, 316, 461-469.
- Catalano, C.E., Choe, Y.S. & Ortiz de Montellano, P.R. (1989). Reactions of the protein radical in peroxide-treated myoglobin. Formation of a heme-protein cross-link. *J. Biol. Chem.*, 264, 10534-10541.
- Cave, A.C., Brewer, A.C., Narayanapanicker, A., Ray, R., Grieve, D.J., Walker, S., & Shah, A.M. (2006). NADPH oxidases in cardiovascular health and disease. *Antioxid. Redox. Signal.*, 8, 691-728.
- Chang, T.M.S. (2003). Future generations of red blood cell substitutes. *J. Inter. Med.*, 253, 527-535.
- Chang, T.M.S. (2004). Hemoglobin-based red blood cell substitutes. *Artificial Organs*, 28, 789-794.
- Chang, T.M.S. & Montreal, P.Q. (1997). Blood substitutes: Principles, Methods, Products and Clinical Trials. Volume 1. *Karger Landes Systems*, Basel, Switzerland.
- Chen, K., Piknova, B., Pittman, R.N., Schechter, A.N. & Popel, A.S. (2008). Nitric Oxide from nitrite by hemoglobin in the plasma and erythrocytes. *Nitric Oxide*, 18, 47-60.
- Chiancone, E., Norne, J.E., Forsen, S., Bonaventura, J., Brunori, M., Antonini, E. & Wyman, J. (1975) Identification of chloride-binding sites in hemoglobin by nuclear-magnetic-resonance quadrupole-relaxation studies of hemoglobin digests. *Eur. J. Biochem.* 55, 385-390.
- Cohen, R.A. (1999). Endothelium, nitric oxide, and atherosclerosis. From Basic mechanisms to clinical implications. *Futura Publishing Company, Inc.* Armonk, New York, USA. pp 49-56.
- Collazo, E., Pietri, R., De Jesús-Bonilla, W., Ramos, C., Del Toro, A., León, R.G., et al. (2004). Functional characterization of the purified holo form of hemoglobin I from *Lucina pectinata* overexpressed in *Escherichia coli*. *Protein J.*, 23, 239-245.

- D'Agnillo, F. & Alayash, A.I. (2000). Interactions of hemoglobin with hydrogen peroxide alters thiol levels and course of endothelial cell death. *Am. J. Physiol.*, 279, H1880-H1889.
- D'Agnillo, F. & Alayash A.I. (2001). Redox cycling of diaspirin cross-linked hemoglobin induces G2/M arrest and apoptosis in cultured endothelial cells. *Blood*, 98, 3315-3323.
- D'Agnillo, F. & Alayash A.I. (2002). A role for the myoglobin redox cycle in the induction of endothelial cell apoptosis. *Free Radic. Biol. Med.*, 33, 1153-1164.
- DeGray, .A., Gunther, M.R., Tschirret-Guth, R., Ortiz de Montellano, P.R. & Mason, R.P. (1997). Peroxidation of a specific tryptophan of metmyoglobin by hydrogen peroxide. *J. Biol. Chem.*, 264, 10534-10541.
- De Jesús-Bonilla, W., Cortés-Figueroa, J.E., Souto-Bachiller, F.A., Rodríguez, L. & López-Garriga, J. (2001). Formation of Compound I and Compound II Ferryl Species in the reaction of Hemoglobin I from *Lucina pectinata* with hydrogen peroxide. *Arch. Biochem. Biophys.*, 390, 304-308.
- De Jesús-Bonilla, W., Cruz, A., Lewis, A., Cerda, J., Bacelo, D.E., Cadilla, C.L. & López-Garriga, J. (2006). Hydrogen-bonding conformations of tyrosine B10 tailor the hemeprotein reactivity of ferrylspecies. *J. Biol. Inorg. Chem.*, 11, 334-342.
- De Jesús-Bonilla, W., Jia, Y., Alayash, A.I. & López-Garriga, J. (2007). The heme pocket geometry of *Lucina pectinata* hemoglobin II restricts nitric oxide and peroxide entry: model of ligand control for the design of a stable oxygen carrier. *Biochemistry*, 46, 10451-10460.
- De Jesús-Bonilla, W., Ramirez-Meléndez, E. Cerda, J. & López-Garriga, J. (2002). Evidence for nonhydrogen bonded compound II in cyclic reaction of hemoglobin I from *Lucina pectinata* with hydrogen peroxide. *Biopolymers (Biospectroscopy)*, 67, 178-185.
- Deudero, J.J., Caramelo, C. Castellanos, M.C., Neria, F., Fernández-Sánchez, R., Calabia, O., et al. (2008). Induction of hypoxia-inducible factor 1 alpha gene expresion by vascular endotelial growth factor. Role of a superoxide-mediated mechanism. *J. Biol. Chem.*, 283, 11435-11444.
- Dimino, M. L. & Palmer, A. F. (2007). Hemoglobin-based O2 carrier O2 affinity and capillary inlet pO2 are importaant factors that influence O2 transport in a capillary. *Biotechnol. Prog.*, 23, 921-931.
- Doherty, D.H., Doyle, M.P., Curry, S.R., Vali, R.J., Fattor, T.J., Olson, J.S. & Lemon, D.D. (1998). Rate of reaction with nitric oxide determines the hypertensive effect of cell-free hemoglobin. *Nat. Biotechnol.*, 16, 672-676.

- Dou, Y., Maillet, D.H., Eich, R.F. & Olson, J.S. (2002). Myoglobin as a model system for designing heme protein based blood substitutes. *Biophys. Chem.*, 98, 127-148.
- Draghi, F., Mieli, A.E., Travaglini-Allocatelli, C., Vallone, B., Brunori, M., Gibson, Q.H. & Olson, J.S. (2001). Controlling Ligand binding in myoglobin by mutagenesis. *J. Biol. Chem.*, 277, 7509-7519.
- Dworakowski, R., Alom-Ruiz, S.P. & Shah, A. M. (2008). NADPH oxidase-derived reactive oxygen species in the regulation of endothelial phenotype. *Pharmacological Reports*, 60, 21-28.
- Egawa, T., Shimada, H. & Ishimura, Y. (2000). Formation of compound I in the reaction of native myoglobins with hydrogen peroxide. *J. Biol. Chem.*, 275, 34858-34866.
- Eich, R.F., Li, T., Lemon, D.D., Doherty, D.H., Curry, S.R., Aitken, J.F., et al. (1996). Mechanism of NO-induced oxidation of myoglobin and hemoglobin. *Biochemistry*, 35, 6976-6983.
- Estep, T., Bucci, E., Farmer, M., Greenburg, G., Harrinton, J., Kim, H.W., et al. (2008). Basic science focus on blood substitutes: a summary of the NHLBI Division of Blood Diseases and Resources Working Group Workshop, March 1 2006. *Transfusión*, 48, 776-782.
- Euro Blood Substitutes. <http://www.eurobloodsubstitutes.com>
- Farrés, J., Rechsteiner, M.P., Herold, S., Frey, A.D. & Kallio, P.T. (2005). Ligand binding properties of bacterial hemoglobin and flavohemoglobins. *Biochemistry*, 44, 4125-4234.
- Fernández-Alberti, S., Bacelo, D.E., Binning, R.C., Echave, J., Chergui, M. & López-Garriga, J. (2006). Sulfide-binding hemoglobins: effects of mutations on the dynamic. *Biophysical J.*, 91, 1698-1709.
- Fridovich, I. (1995). Superoxide radical and superoxide dismutases. *Annu. Rev. Biochem.*, 64, 97-112.
- Gainey, L.F. Jr. & Greenberg, M.J. (2005). Hydrogen sulfide is synthesized in the gills of the clam *Mercenaria mercenaria* and acts seasonally to modulate branchial muscle contraction. *Biol. Bull.*, 209, 11-20.
- Galaris, D., Eddy, L., Arduini, A., Cadenas, E. & Hochstein, P. (1989) *Biochem. Biophys. Res. Commun.*, 160, 1162-1168.
- Gardner, P.R. (2008) Assay and characterization of the NO dioxygenase activity of Flavohemoglobins. *Methods Enzymol.*, 436C, 217-237.

- Gardner, P.R., Gardner, A.M., Brashear, W.T., Suzuki, T., Hvitved, A.N., Setchell, K.D.R. & Olson, J.S. (2006) Hemoglobins deoxygenate nitric oxide with high fidelity. *J. Inorg. Biochem.*, 100, 542-550.
- Gavira, J.A., Cámara-Artigas, A., De Jesús-Bonilla, W., López-Garriga, J. Lewis, A., Pietri, R., Yeh, S.R., et al. (2008, January 10). Structure and ligand selection of hemoglobin II from *Lucina pectinata*. *J. Biol. Chem.*, 283, 9414-9423.
- Gavira, J.A., De Jesús-Bonilla, W., Cámara-Artigas, A., López- Garriga, J. & García-Ruiz, J.M. (2006). Capillary crystallization and molecular replacement solution of hemoglobin II from the clam *Lucina pectinata*. *Acta Crystallograph. Sect. F Struct. Biol. Cryst. Commun.*, 62, (Pt 3), 196-9.
- Goldman, D.W., Breyer III, R.J., Yeh, D., Brockner-Ryan, B.A. & Alayash, A.I. (1998). Acellular hemoglobin-mediated oxidative stress toward endothelium: a role for ferryl iron. *Am. J. Physiol.*, 275, (Heart Circ Physiol 44). H1046-H1053.
- Gow, A.J., Branco, F., Christfidou-Solomidou, M., Black-Schultz, L-, Albelda, S.M. & Muzykantov, V.R. (1999). Immunotargeting of glucose oxidase: intracellular production of H₂O₂ and endothelial oxidative stress. *Am. J. Physiol.*, 277, L271-L281.
- Gow, A.J., Payson, A.P. & Bonaventura, J. (2005). Invertebrate hemoglobins and nitric oxide: how heme pocket structure controls reactivity. *J. Inorg. Biochem.*, 99, 903-911.
- Hemarina. <http://www.hemarina.com>
- Herold, S. & Rock, G. (2003). Reactions of deoxy-, oxy-, and methemoglobin with nitrogen monoxide. Mechanistic studies of the S-nitrosothiol formation under different mixing conditions. *J. Biol. Chem.*, 278, 6623-6634.
- Hirsch, R.E., Jelicks, L.A., Wittenberg, B.A., Kaul, D.K., Shear H.L. & Harrington, J.P. (1997). A first evaluation of the natural high molecular weight polymeric *Lumbricus terrestris* hemoglobin as an oxygen carrier. *Artif Cells, Blood Substitutes, Immobilization, Biotechnol.*, 25, 429-444.
- Ho, R.C. (1995). Medical management of stage IV malignant melanoma. *Medical Issues. Cancer*, 75, 735-741.
- Ignarro, L.J., Fukuto, J.M., Griscavage, J.M., Rogers, N.E. & Byrns, R.E. (1993). Oxidation of nitric oxide in aqueous solution to nitrite but not nitrate: comparison with enzymatically formed nitric oxide from L-arginine. *Proc. Natl. Acad. Sci., USA*, 90, 8103-8107.

- Jia, Y. & Alayash, A.I. (2002). Stopped-flow fluorescence method for the detection of heme degradation products in solutions of chemically modified hemoglobins and peroxide. *Anal. Biochem.*, 308, 186-188.
- Jia, Y., Wood, F., Menu, P., Faivre, B., Caron, A. & Alayash, A.I. (2004). Oxygen binding and oxidation reactions of human hemoglobin conjugated to carboxylate dextran. *Biochim. Biophys. Acta.*, 1672, 164-173.
- Joyner, J.L., Peyer, S.M. & Lee, R.W. (2003, December). Possible roles of sulfur-containing amino acids in a chemoautotrophic bacterium-mollusc symbiosis. *Biol. Bull.*, 205, 331-338.
- Kiefmann, R., Rifkind, J.M., Nagababu, E. & Bhattacharya, J. (2008). RBC induce hypoxic lung inflammation. *Blood*, Retrieved from PubMed, March 1, 2008, PMID: 18270324.
- Kim, H.W. & Greenburg, A.G., (2004). Artificial oxygen carriers as red blood cell substitutes: a selected review and current status. *Artif. Organs*, 28, 813-828.
- King, N.K. & Winfield, M.E. (1963). The mechanism of metmyoglobin oxidation. *J. Biol. Chem.*, 238, 1520-1528.
- Kraus, D.W. & Wittenberg, J.B. (1990). Hemoglobins of the *Lucina pectinata*/bacteria symbiosis. *J. Biol. Chem.*, 65, 16043-16053.
- Kraus, D.W., Wittenberg, J.B., Ping-Fen, L. & Peisach, J. (1990). Hemoglobins of the *Lucina pectinata*/bacteria symbiosis. *J. Biol. Chem.*, 265, 16054-16059.
- Kvietikova, I., Wenger, R. H., Marti, H.H. & Gassmann, M. (1995). The transcription factors ATF-1 and CREB-1 bind constitutively to the hypoxia-inducible factor-1 (HIF-1) DNA recognition site. *Nucleic Acids Res.*, 23, 4542-4550.
- León, R.G., Munier-Lehmann, H., Barzu, O., Baudin Creuza, V. Pietri, R. & López-Garriga, J. (2004). High-level production of recombinant silfide-reactive hemoglobin I from *Lucina pectinata* in *Escherichia coli*. High yields of fully functional holoprotein synthesis in the Bli5 *E. coli* strain. *Protein Expr. Purif.*, 38, 184-95.
- Mackenzie, C. (2005). Synthetic blood: myth or reality? *ITACCS, Winter*, 13-17.
- Mackenzie, C. & Bucci, C. (2004). Artificial oxygen carriers for trauma: myth or reality? *Hosp. Med.*, 65, 582-588.
- Manning, J.M. (1995). Blood substitutes. Physiological Basis of Efficacy. Birkhauser, Boston, USA. pp 76-85.

- Martin, W., Smith, J.A. & White, D.G. (1986). The mechanisms by which haemoglobin inhibits the relaxation of rabbit aorta induced by nitrovasodilators, nitric oxide, or bovine retractor penis inhibitor factor. *Br J. Pharmacol.*, 89, 563-571.
- McLeod, L.L. & Alayash, A.I. (1999). Detection of a ferrylhemoglobin intermediate in an endothelial cell model after hypoxia reoxygenation. *Am. J. Physiol.*, 277, H92-H99.
- Mukai, M., Mills, C.E., Poole, R.K. & Yeh, S.R. (2001). Flavohemoglobin, a globin with a peroxidase-like catalytic site. *J. Biol. Chem.*, 276, 7272-7277.
- Nagababu, E., Fabry, M.E., Nagel, R.L. & Rifkind, J.M. (2008). Heme degradation and oxidative stress in murine models for hemoglobinopathies: Thalassemia, sickle cell disease and hemoglobin C disease. *Blood Cells Mol. Dis.*, Retrieved from PubMed, March 20, 2008, PMID: 17880185.
- Nagababu, E., Ramasamy, S. & Rifkind, J.M., Jia, Y. & Alayash, A.I. (2002). Site-specific cross-linking of human hemoglobins differentially alters oxygen binding and redox side reactions producing rhombic heme degradation. *Biochemistry*, 41, 7407-7415.
- Nagababu, E., & Rifkind, J.M. (2004). Heme degradation by reactive oxygen species. *Antioxid. Redox Signal.*, 6, 967-978.
- Navarro, A., Maldonado, M., González-Lago, J. López-Mejías, R., Colón, J.L. & López-Garriga, J. (1996). Control of carbon monoxide binding sites and dynamics in hemoglobin I of *Lucina pectinata* by nearby aromatic residues. *Inorg. Chim. Acta*, 243, 161-166.
- Olson, J.S., Foley, E.W., Rogge, C., Tsai, A.L., Doyle & M.P. Lemon, D.D. (2004). NO scavenging and the hypertensive effect of hemoglobin-based blood substitutes. *Free Rad. Biol. Med.*, 36, 685-697.
- Østdal, H., Sjøgaard, S.G., Bendixen E. & Andersen H.J. (2001). Protein radicals in the reaction between H₂O₂-activated metmyoglobin and bovine serum albumin. *Free Rad. Res.*, 35, 757-766.
- Ouellet, H., Ranguelova, K., Labarre, M., Wittenberg, J.B., Wittenberg, B.A., Magliozzo, R.S. & Guertin, M. (2007). Reaction of *Mycobacterium tuberculosis* truncated hemoglobin O with hydrogen peroxide: evidence for peroxidatic activity and formation of protein-based radicals. *J. Biol. Chem.*, 282, 7491-7503.
- Perella, M., Kilmartin, J.V. & Fogg, J. (1975). Identification of the high and low affinity CO₂-binding sites of human haemoglobin. *Nature*, 256, 759-761.

- Pietri, R., Granell, L., Cruz, A., De Jesús-Bonilla, W., Lewis, A., León, R. et al. (2005). Tyrosine B10 and heme-ligand interactions of *Lucina pectinata* hemoglobin II: control of heme reactivity. *Biochim. Biophys. Acta*, 1747, 195-203.
- Privalle, C., Talarico, T., Keng, T. & DeAngello, J. (2000). Pyridoxalate hemoglobin polyoxyethylene: a nitric oxide scavenger with antioxidant activity for the treatment of nitric oxide-induced shock. *Free Rad. Biol. Med.*, 28, 1507-1517.
- Read, K.R.H. (1965). The characterization of the hemoglobins of the bivalve mollusk *Phacoides pectinatus*. *Comp. Biochem. Physiol.*, 15, 137-158.
- Reeder, B.J., Svistunenko, D.A., Sharpe, M.A. & Wilson M.T. (2002). Characteristics and mechanism of formation of peroxide-induced heme to protein cross-linking in myoglobin. *Biochemistry*, 41, 367-375.
- Rizzi, M., Wittenberg, J.B., Coda, A., Fasano, M., Ascenzi, P. & Bolognesi, M. (1994). Structure of the sulfide-reactive hemoglobin from the clam *Lucina pectinata*. *J. Mol. Biol.*, 244, 86-89.
- Rizzi, M., Wittenberg, J.B., Coda, A., Ascenzi, P. & Bolognesi, M. (1996). Structural bases for sulfide recognition in *Lucina pectinata* hemoglobin I. *J. Mol. Biol.*, 258, 1-5.
- Ródenas, J., Mitjavila, M.T. & Carbonell T. (1998). Nitric oxide inhibits superoxide production by inflammatory polymorphonuclear leukocytes. *Cell Physiol.*, 43, C827-C830.
- Rogers, M.S., Ryan, B.B., Cashon, R.E. & Alayash, A.I. (1995). Effects of polymerization on the oxygen carrying and redox properties of diaspirin cross-linked hemoglobin. *Biochim. Biophys. Acta*, 1248, 135-142.
- Rohlf, R.J., Bruner, E., Chiu, A., González, A., Gonzáles, M.L., Magde, D. et al. (1998). Arterial blood pressure responses to cell-free hemoglobin solutions and the reaction with nitric oxide. *J. Biol. Chem.*, 273, 12128-12134.
- Rousselot, M., Delpy, E., Drieu La Roche, C., Lagente, V., Pirow, R., Rees, J.F., et al. (2006). *Arenicola marina* extracellular hemoglobin: a new promising blood substitute. *Biotechnol. J.*, 1, 333-45.
- Rydberg, P., Sigfridsson, E. & Ryde, U. (2004). On the role of the axial ligand in heme proteins: a theoretical study. *J. Biol. Inorg. Chem.*, 9, 203-223.
- Sakai, H., Sato, A., Masuda, K., Takeoka, S. & Tsuchida, E. (2008). Encapsulation of concentrated hemoglobin solution in phospholipids vesicles retards the reaction with NO, but not CO, by intracellular diffusion barrier. *J. Biol. Chem.*, 283, 1508-1517.

- Sakai, H., Sou, K., Horinouchi, H., Kobayashi, K. & Tsuchida, E. (2008). Haemoglobin-vesicles as artificial oxygen carriers: present situation and future visions. *J. Intern. Med.*, 263, 4-15.
- Scharte, M., Xiaonan, H., Bertges, D.J., Fink, M.P. & Delude, R.L. (2003). Cytokines induce HIF-1 DNA binding and the expression of HIF-1-dependent genes in cultures rat enterocytes. *Am. J. Physiol. Gastrointest. Liver Physiol.*, 284, G373-384.
- Sharma V.S., & Ranney, H.M., (1978) the dissociation of NO from nitrosylhemoglobin. *J. Biol. Chem.*, 253, 6467-6472.
- Sharma, V.S., Isaacson, R.A., John, M.E., Waterman, M.R. & Chevion M. (1983). Reaction of nitric oxide with heme proteins: studies on methemoglobin, opossum methemoglobin, and microperoxidase. *Biochemistry*, 22, 3897-3902.
- Sharp, F.R., Ran, R., Lu, A., Tang, Y., Strauss, K.I., Todd, G. et al. (2004). Hypoxic preconditioning protects against ischemic brain injury. *NeuroRx_The Journal of the American Society for Experimental Neuro Therapeutics*, 1, 26-35.
- Stowell, C. P., Levin, J., Spiess, B.D. & Winslow, R.M. (2001). Progress in the development of RBC substitutes. *Transfusion*, 41, 287-299.
- Sugawara, Y., Kadono, E., Suzuki, A., Yukuta, Y., Shibasaki, Y., Nishimura, N. et al. (2003). Hemichrome formation observed in human haemoglobin A under various buffer conditions. *Acta Physiol. Scand.*, 179, 49-59.
- Therade-Matharan, S., Laemmel, E., Duranteau, J. & Vicaut, E. (2004). Reoxygenation after hypoxia and glucose depletion causes reactive oxygen species production by mitochondria in HUVEC. *Am. J. Physiol. Regul. Integr. Comp. Physiol.*, 287, R1037-R1043.
- Tinmouth, A.T., McIntyre, L.A. & Fowler, R.A. (2008). Blood conservation strategies to reduce the need for red blood transfusion in critically ill patients. *CMAJ*, 178, 49-57.
- Torres-Mercado, E., Renta, J.Y., Rodríguez, Y., López-Garriga, J. & Cadilla, C. L. (2003). The cDNA-derived amino acid sequence of hemoglobin II from *Lucina pectinata*. *J. Prot. Chem.*, 22, 683-690.
- Trent, J.T.^{3rd}, & Hargrove, M.S. (2002). A ubiquitously expressed human hexacoordinate hemoglobin. *J. Biol. Chem.*, 277, 19538-19545.
- Vandergriff, K.D. (2000). Haemoglobin-based oxygen carriers. *Exper. Opin. Invest. Drugs*, 9, 1967-1984.

- Vitagliano, L., Bonomi, G., Riccio, A., Di Prisco, G., Smulevich, G. & Mazarella, L. (2004). The oxidation process of Antarctic fish hemoglobins. *Eur. J. Biochem.*, 271, 1651-1659.
- Watkins, J.A., Kawanishi, S. & Caughey, W.S. (1985). Autoxidation reactions of hemoglobin A free from other red cell components: a minimal mechanism. *Biochem. Biophys. Res. Commun.*, 132, 742-748.
- Weber, E. & Vinogradov, S.N. (2001). Nonvertebrate hemoglobins: functions and molecular adaptations. *Physiol. Rev.*, 81, 569-628.
- Winslow, R.M. (2006). Current status of oxygen carriers ("blood substitutes"). *Vox Sang*, 91, 102-110.
- Winterbourn, C.C. (1985). In CRC handbook of methods for oxygen radical research (Greenwald, R.A., ed), *CRC Press*, Boca Raton, FL, USA. pp 137-141.
- Wittenberg, J.B. & Krauss D.W. (1991). In structure and functions of invertebrate oxygen carriers (Vvinogradov, S.N. & Kapp O.H., eds). *Springer Verlag*, New York, USA. pp 323-330.
- Wittenberg, J.B. & Wittenberg, B.A. (1990). Mechanisms of cytoplasmic hemoglobin and myoglobin function. *Annu. Rev. Biochem. Biophys. Commun.*, 19, 217-241.
- Yang, T. & Olsen, K.W. (1994). Enzymatic protection from autoxidation for crosslinked hemoglobins. *Artif Cells, Blood Substitutes, Immobilization Biotechnol.*, 22, 709-717.
- Yeh, L.H. & Alayash, A.I. (2003). Redox side reactions of haemoglobin and cell signaling mechanisms. *J. Intern. Med.*, 253, 518-526.
- Yeh, L.H. & Alayash, A.I. (2004). Effects of cell-free hemoglobin on hypoxia-inducible factor (HIF-1 α) and heme oxygenase (HO-1) expression in endothelial cells subjected to hypoxia. *Antioxid. Redox Signal.*, 6, 944-953.
- Yeh, L.H., Couture M., Ouellet, Y., Guertin, M. & Rousseau, D.L. (2000). A cooperative oxygen binding hemoglobin from *Mycobacterium tuberculosis*. Stabilization of heme ligands by a distal tyrosine residue. *J. Biol. Chem.*, 275, 1679-1684.
- Zhang, X., Liu, C., Yuan, Y. Shan, X., Sheng, Y. & Xu, F. (2008). Key parameters affecting the initial leaky effect of hemoglobin-loaded nanoparticles as blood substitutes. *J. Mater. Sci. Mater. Med.*, 19, 2463-2470.

Zhen, J., Lu, H., Wang, X.Q., Vaziri, N.D. & Zhou, X.J. (2008). Upregulation of endothelial and inducible nitric oxide synthase expression by reactive oxygen species. *Am. J. Hypertenses*, 21, 28-34.

APPENDIX A

Student's t-Test statistical analysis for the bovine aortic endothelial cells apoptotic levels cells incubated for 2 hours, 6 and 24 hours.

A. Analysis for untreated endothelial cells at 2 hours versus 6 hours

t-Test: Paired Two Sample for Means		
	untreated cells 2 hrs	untreated cells 6 hrs
	<i>Variable 1</i>	<i>Variable 2</i>
Mean	34.0166	52.3338
Variance	77.14089	14.34305
Observations	5	5
Pearson Correlation	0.790881	
Hypothesized Mean Difference	0	
df	4	
t Stat	-6.5696	
P(T<=t) one-tail	0.001389	
t Critical one-tail	2.131847	
P(T<=t) two-tail	0.002778	
t Critical two-tail	2.776445	

B. Analysis for untreated endothelial cells at 2 hours versus 24 hours

t-Test: Paired Two Sample for Means		
	untreated cells 2 hrs	untreated cells 24 hrs
	<i>Variable 1</i>	<i>Variable 2</i>
Mean	34.0166	70.9742
Variance	77.14089	64.61648
Observations	5	5
Pearson Correlation	0.646733	
Hypothesized Mean Difference	0	
df	4	
t Stat	-11.6363	
P(T<=t) one-tail	0.000156	
t Critical one-tail	2.131847	
P(T<=t) two-tail	0.000312	
t Critical two-tail	2.776445	

Student's t-Test statistical analysis for the bovine aortic endothelial cells apoptotic levels after treated for 2 hours

A. Analysis for the endothelial cells treated with HbII versus untreated cells

t-Test: Paired Two Sample for Means		
	untreated cells	HbII
	<i>Variable 1</i>	<i>Variable 2</i>
Mean	33.34483	948.664
Variance	64.42033	466515.1
Observations	6	6
Pearson Correlation	0.325931	
Hypothesized Mean Difference	0	
df	5	
t Stat	-3.295	
P(T<=t) one-tail	0.010797	
t Critical one-tail	2.015048	
P(T<=t) two-tail	0.021594	
t Critical two-tail	2.570582	

B. Analysis for the endothelial cells treated with HbI versus untreated cells

t-Test: Paired Two Sample for Means		
	untreated cells	HbI
	<i>Variable 1</i>	<i>Variable 2</i>
Mean	33.34483	60.7685
Variance	64.42033	785.3451
Observations	6	6
Pearson Correlation	-0.36148	
Hypothesized Mean Difference	0	
df	5	
t Stat	-2.1112	
P(T<=t) one-tail	0.044244	
t Critical one-tail	2.015048	
P(T<=t) two-tail	0.088487	
t Critical two-tail	2.570582	

C. Analysis for the endothelial cells treated with α -DBBF Hb versus untreated cells

t-Test: Paired Two Sample for Means		
	untreated cells	A-DBBF Hb
	<i>Variable 1</i>	<i>Variable 2</i>
Mean	33.34483	45.21183
Variance	64.42033	229.8955
Observations	6	6
Pearson Correlation	-0.33862	
Hypothesized Mean Difference	0	
df	5	
t Stat	-1.49761	
P(T<=t) one-tail	0.09725	
t Critical one-tail	2.015048	
P(T<=t) two-tail	0.194499	
t Critical two-tail	2.570582	

D. Analysis for the endothelial cells treated with HbI PheB10Tyr versus untreated cells

t-Test: Paired Two Sample for Means		
	untreated cells	HbI PheB10Tyr
	<i>Variable 1</i>	<i>Variable 2</i>
Mean	33.34483	119.7192
Variance	64.42033	9199.46
Observations	6	6
Pearson Correlation	-0.46138	
Hypothesized Mean Difference	0	
df	5	
t Stat	-2.11846	
P(T<=t) one-tail	0.043838	
t Critical one-tail	2.015048	
P(T<=t) two-tail	0.087676	
t Critical two-tail	2.570582	

E. Analysis for the endothelial cells treated with GOX versus untreated cells

t-Test: Paired Two Sample for Means		
	untreated cells	cells/GOX
	<i>Variable 1</i>	<i>Variable 2</i>
Mean	33.34483	70.24817
Variance	64.42033	2603.091
Observations	6	6
Pearson Correlation	-0.17497	
Hypothesized Mean Difference	0	
df	5	
t Stat	-1.705	
P(T<=t) one-tail	0.074457	
t Critical one-tail	2.015048	
P(T<=t) two-tail	0.148913	
t Critical two-tail	2.570582	

F. Analysis for the endothelial cells treated with GOX and HbII versus untreated cells

t-Test: Paired Two Sample for Means		
	untreated cells	HbII/GOX
	<i>Variable 1</i>	<i>Variable 2</i>
Mean	33.34483	723.4515
Variance	64.42033	372978.2
Observations	6	6
Pearson Correlation	0.919807	
Hypothesized Mean Difference	0	
df	5	
t Stat	-2.80173	
P(T<=t) one-tail	0.018958	
t Critical one-tail	2.015048	
P(T<=t) two-tail	0.037916	
t Critical two-tail	2.570582	

- G. Analysis for the endothelial cells treated with GOX and HbI PheB10Tyr versus untreated cells

t-Test: Paired Two Sample for Means		
	untreated cells	HbI PheB10Tyr/GOX
	<i>Variable 1</i>	<i>Variable 2</i>
Mean	33.34483	72.14233
Variance	64.42033	2690.551
Observations	6	6
Pearson Correlation	-0.30251	
Hypothesized Mean Difference	0	
df	5	
t Stat	-1.7331	
P(T<=t) one-tail	0.071808	
t Critical one-tail	2.015048	
P(T<=t) two-tail	0.143617	
t Critical two-tail	2.570582	

- H. Analysis for the endothelial cells treated with GOX and HbI versus untreated cells

t-Test: Paired Two Sample for Means		
	untreated cells	HbI/GOX
	<i>Variable 1</i>	<i>Variable 2</i>
Mean	33.34483	52.90233
Variance	64.42033	534.7695
Observations	6	6
Pearson Correlation	-0.35041	
Hypothesized Mean Difference	0	
df	5	
t Stat	-1.77397	
P(T<=t) one-tail	0.068125	
t Critical one-tail	2.015048	
P(T<=t) two-tail	0.136249	
t Critical two-tail	2.570582	

- I. Analysis for the endothelial cells treated with GOX and α -DBBF Hb versus untreated cells

t-Test: Paired Two Sample for Means		
	untreated cells	A-DBBF Hb/GOX
	<i>Variable 1</i>	<i>Variable 2</i>
Mean	33.34483	46.73317
Variance	64.42033	301.8743
Observations	6	6
Pearson Correlation	-0.42881	
Hypothesized Mean Difference	0	
df	5	
t Stat	-1.48776	
P(T<=t) one-tail	0.098488	
t Critical one-tail	2.015048	
P(T<=t) two-tail	0.196975	
t Critical two-tail	2.570582	

Student's t-Test statistical analysis for the bovine aortic endothelial cells apoptotic levels after treated for 6 hours

A. Analysis for the endothelial cells treated with HbII versus untreated cells

t-Test: Paired Two Sample for Means		
	untreated cells	HbII
	<i>Variable 1</i>	<i>Variable 2</i>
Mean	52.3338	1449.756
Variance	14.34305	53428.89
Observations	5	5
Pearson Correlation	-0.52453	
Hypothesized Mean Difference	0	
df	4	
t Stat	-13.4019	
P(T<=t) one-tail	8.96E-05	
t Critical one-tail	2.131847	
P(T<=t) two-tail	0.000179	
t Critical two-tail	2.776445	

B. Analysis for the endothelial cells treated with HbI versus untreated cells

t-Test: Paired Two Sample for Means		
	untreated cells	HbI PheB10Tyr
	<i>Variable 1</i>	<i>Variable 2</i>
Mean	52.3338	212.4822
Variance	14.34305	7403.57
Observations	5	5
Pearson Correlation	0.390517	
Hypothesized Mean Difference	0	
df	4	
t Stat	-4.23105	
P(T<=t) one-tail	0.006679	
t Critical one-tail	2.131847	
P(T<=t) two-tail	0.013359	
t Critical two-tail	2.776445	

D. Analysis for the endothelial cells treated with HbI PheB10Tyr versus untreated cells

t-Test: Paired Two Sample for Means		
	untreated cells	HbI
	<i>Variable 1</i>	<i>Variable 2</i>
Mean	52.3338	342.0824
Variance	14.34305	17365.1
Observations	5	5
Pearson Correlation	0.581069	
Hypothesized Mean Difference	0	
df	4	
t Stat	-4.99872	
P(T<=t) one-tail	0.003749	
t Critical one-tail	2.131847	
P(T<=t) two-tail	0.007497	
t Critical two-tail	2.776445	

C. Analysis for the endothelial cells treated with α -DBBF Hb versus untreated cells

t-Test: Paired Two Sample for Means		
	untreated cells	A-DBBF Hb
	<i>Variable 1</i>	<i>Variable 2</i>
Mean	52.3338	38.1238
Variance	14.34305	3.205304
Observations	5	5
Pearson Correlation	0.114504	
Hypothesized Mean Difference	0	
df	4	
t Stat	7.944727	
P(T<=t) one-tail	0.00068	
t Critical one-tail	2.131847	
P(T<=t) two-tail	0.001359	
t Critical two-tail	2.776445	

E. Analysis for the endothelial cells treated with GOX versus untreated cells

t-Test: Paired Two Sample for Means ²¹⁰		
	untreated cells	cells/GOX
	<i>Variable 1</i>	<i>Variable 2</i>
Mean	52.3338	49.1532
Variance	14.34305	222.9104
Observations	5	5
Pearson Correlation	0.253424	
Hypothesized Mean Difference	0	
df	4	
t Stat	0.492428	
P(T<=t) one-tail	0.324111	
t Critical one-tail	2.131847	
P(T<=t) two-tail	0.648221	
t Critical two-tail	2.776445	

F. Analysis for the endothelial cells treated with GOX and HbII versus untreated cells

t-Test: Paired Two Sample for Means		
	untreated cells	HbII/GOX
	<i>Variable 1</i>	<i>Variable 2</i>
Mean	52.3338	1109.843
Variance	14.34305	18905.24
Observations	5	5
Pearson Correlation	0.452712	
Hypothesized Mean Difference	0	
df	4	
t Stat	-17.4098	
P(T<=t) one-tail	3.19E-05	
t Critical one-tail	2.131847	
P(T<=t) two-tail	6.39E-05	
t Critical two-tail	2.776445	

- G Analysis for the endothelial cells treated with GOX and HbI PheB10Tyr versus untreated cells

t-Test: Paired Two Sample for Means		
	untreated cells	HbI PheB10Tyr/GOX
	<i>Variable 1</i>	<i>Variable 2</i>
Mean	52.3338	295.0738
Variance	14.34305	11561.42
Observations	5	5
Pearson Correlation	0.443801	
Hypothesized Mean Difference	0	
df	4	
t Stat	-5.12554	
P(T<=t) one-tail	0.00343	
t Critical one-tail	2.131847	
P(T<=t) two-tail	0.00686	
t Critical two-tail	2.776445	

- H. Analysis for the endothelial cells treated with GOX and HbI versus untreated cells

t-Test: Paired Two Sample for Means		
	untreated cells	HbI/GOX
	<i>Variable 1</i>	<i>Variable 2</i>
Mean	52.3338	353.4032
Variance	14.34305	7702.254
Observations	5	5
Pearson Correlation	0.522157	
Hypothesized Mean Difference	0	
df	4	
t Stat	-7.84211	
P(T<=t) one-tail	0.000714	
t Critical one-tail	2.131847	
P(T<=t) two-tail	0.001428	
t Critical two-tail	2.776445	

- I. Analysis for the endothelial cells treated with GOX and α -DBBF Hb versus untreated cells

t-Test: Paired Two Sample for Means		
	untreated cells	α -DBBF Hb/Gox
	<i>Variable 1</i>	<i>Variable 2</i>
Mean	52.3338	34.9318
Variance	14.34305	4.612835
Observations	5	5
Pearson Correlation	-0.07967	
Hypothesized Mean Difference	0	
df	4	
t Stat	8.646702	
P(T<=t) one-tail	0.000492	
t Critical one-tail	2.131847	
P(T<=t) two-tail	0.000984	
t Critical two-tail	2.776445	

Student's t-Test statistical analysis for the bovine aortic endothelial cells apoptotic levels after treated for 24 hours

A. Analysis for the endothelial cells treated with HbII versus untreated cells

t-Test: Paired Two Sample for Means		
	untreated cells	HbII
	<i>Variable 1</i>	<i>Variable 2</i>
Mean	70.01214	458.2257
Variance	50.31343	31482.38
Observations	7	7
Pearson Correlation	0.544475	
Hypothesized Mean Difference	0	
df	6	
t Stat	-5.9141	
P(T<=t) one-tail	0.00052	
t Critical one-tail	1.94318	
P(T<=t) two-tail	0.00104	
t Critical two-tail	2.446912	

B. Analysis for the endothelial cells treated with HbI versus untreated cells

t-Test: Paired Two Sample for Means		
	untreated cells	HbI PheB10Tyr
	<i>Variable 1</i>	<i>Variable 2</i>
Mean	70.01214	256.2386
Variance	50.31343	9831.488
Observations	7	7
Pearson Correlation	0.314818	
Hypothesized Mean Difference	0	
df	6	
t Stat	-5.0714	
P(T<=t) one-tail	0.001142	
t Critical one-tail	1.94318	
P(T<=t) two-tail	0.002285	
t Critical two-tail	2.446912	

C. Analysis for the endothelial cells treated with HbI PheB10Tyr versus untreated cells

t-Test: Paired Two Sample for Means		
	untreated cells	HbI
	<i>Variable 1</i>	<i>Variable 2</i>
Mean	70.01214	238.8446
Variance	50.31343	12043.97
Observations	7	7
Pearson Correlation	0.457839	
Hypothesized Mean Difference	0	
df	6	
t Stat	-4.18702	
P(T<=t) one-tail	0.002884	
t Critical one-tail	1.94318	
P(T<=t) two-tail	0.005768	
t Critical two-tail	2.446912	

D. Analysis for the endothelial cells treated with α -DBBF Hb versus untreated cells

t-Test: Paired Two Sample for Means		
	untreated cells	A-DBBF Hb
	<i>Variable 1</i>	<i>Variable 2</i>
Mean	70.01214	42.35043
Variance	50.31343	279.1819
Observations	7	7
Pearson Correlation	0.64068	
Hypothesized Mean Difference	0	
df	6	
t Stat	5.491222	
P(T<=t) one-tail	0.000764	
t Critical one-tail	1.94318	
P(T<=t) two-tail	0.001527	
t Critical two-tail	2.446912	

E. Analysis for the endothelial cells treated with GOX versus untreated cells

t-Test: Paired Two Sample for Means		
	untreated cells	cells/GOX
	<i>Variable 1</i>	<i>Variable 2</i>
Mean	70.01214	209.7239
Variance	50.31343	3881.991
Observations	7	7
Pearson Correlation	0.242856	
Hypothesized Mean Difference	0	
df	6	
t Stat	-6.06245	
P(T<=t) one-tail	0.000457	
t Critical one-tail	1.94318	
P(T<=t) two-tail	0.000913	
t Critical two-tail	2.446912	

F. Analysis for the endothelial cells treated with GOX and HbII versus untreated cells

t-Test: Paired Two Sample for Means		
	untreated cells	HbII/GOX
	<i>Variable 1</i>	<i>Variable 2</i>
Mean	70.01214	301.9877
Variance	50.31343	6866.179
Observations	7	7
Pearson Correlation	0.12476	
Hypothesized Mean Difference	0	
df	6	
t Stat	-7.45937	
P(T<=t) one-tail	0.00015	
t Critical one-tail	1.94318	
P(T<=t) two-tail	0.000299	
t Critical two-tail	2.446912	

- G. Analysis for the endothelial cells treated with GOX and HbI PheB10Tyr versus untreated cells

t-Test: Paired Two Sample for Means		
	untreated cells	HbI PheB10Tyr/GOX
	<i>Variable 1</i>	<i>Variable 2</i>
Mean	70.01214	170.4443
Variance	50.31343	2936.336
Observations	7	7
Pearson Correlation	0.355003	
Hypothesized Mean Difference	0	
df	6	
t Stat	-5.10079	
P(T<=t) one-tail	0.00111	
t Critical one-tail	1.94318	
P(T<=t) two-tail	0.00222	
t Critical two-tail	2.446912	

- H. Analysis for the endothelial cells treated with GOX and HbI versus untreated cells

t-Test: Paired Two Sample for Means		
	untreated cells	HbI/GOX
	<i>Variable 1</i>	<i>Variable 2</i>
Mean	70.01214	194.1181
Variance	50.31343	1034.181
Observations	7	7
Pearson Correlation	0.068567	
Hypothesized Mean Difference	0	
df	6	
t Stat	-10.1177	
P(T<=t) one-tail	2.71E-05	
t Critical one-tail	1.94318	
P(T<=t) two-tail	5.42E-05	
t Critical two-tail	2.446912	

I. Analysis for the endothelial cells treated with GOX and α -DBBF Hb versus untreated cells

t-Test: Paired Two Sample for Means		
	untreated cells	A-DBBF Hb/GOX
	<i>Variable 1</i>	<i>Variable 2</i>
Mean	70.01214	48.59643
Variance	50.31343	180.1127
Observations	7	7
Pearson Correlation	0.698999	
Hypothesized Mean Difference	0	
df	6	
t Stat	5.742853	
P(T<=t) one-tail	0.000606	
t Critical one-tail	1.94318	
P(T<=t) two-tail	0.001212	
t Critical two-tail	2.446912	

APPENDIX B

Student's t-Test statistical analysis for the HIF-1 α expression in bovine aortic endothelial cells incubated with HbII for 2 hours, 4, 6, 8, and 24 hours.

- A. Analysis for the HIF-1 α expression of cells under normoxia versus cells treated with HbII during hypoxia for 2 hours

t-Test: Paired Two Sample for Means		
	2hr/HbII/Hypoxia	cells/Normoxia
	Variable 1	Variable 2
Mean	1.167433	1
Variance	0.000595	0
Observations	2	2
Pearson Correlation	1	
Hypothesized Mean Difference	0	
df	1	
t Stat	9.704654	
P(T<=t) one-tail	0.032684	
t Critical one-tail	6.313749	
P(T<=t) two-tail	0.065369	
t Critical two-tail	12.70615	

- B. Analysis for the HIF-1 α expression of cells under normoxia versus cells treated with HbII during hypoxia for 4 hours

t-Test: Paired Two Sample for Means		
	4hr/HbII/Hypoxia	cells/Normoxia
	Variable 1	Variable 2
Mean	1.777584	1
Variance	0.00138	0
Observations	2	2
Pearson Correlation	1	
Hypothesized Mean Difference	0	
df	1	
t Stat	29.59985	
P(T<=t) one-tail	0.01075	
t Critical one-tail	6.313749	
P(T<=t) two-tail	0.021499	
t Critical two-tail	12.70615	

C. Analysis for the HIF-1 α expression of cells under normoxia versus cells treated with HbII during hypoxia for 6 hours

t-Test: Paired Two Sample for Means		
	6hr/HbII/Hypoxia	cells/Normoxia
	Variable 1	Variable 2
Mean	2.671358	1
Variance	0.003117	0
Observations	2	2
Pearson Correlation	1	
Hypothesized Mean Difference	0	
df	1	
t Stat	42.33611	
P(T<=t) one-tail	0.007517	
t Critical one-tail	6.313749	
P(T<=t) two-tail	0.015034	
t Critical two-tail	12.70615	

D. Analysis for the HIF-1 α expression of cells under normoxia versus cells treated with HbII during hypoxia for 8 hours

t-Test: Paired Two Sample for Means		
	8hr/HbII/Hypoxia	cells/Normoxia
	Variable 1	Variable 2
Mean	3.89414	1
Variance	0.006624	0
Observations	2	2
Pearson Correlation	1	
Hypothesized Mean Difference	0	
df	1	
t Stat	50.29002	
P(T<=t) one-tail	0.006329	
t Critical one-tail	6.313749	
P(T<=t) two-tail	0.012657	
t Critical two-tail	12.70615	

- E. Analysis for the HIF-1 α expression of cells under normoxia versus cells treated with HbII during hypoxia for 12 hours

t-Test: Paired Two Sample for Means			
	12hr/HbII/Hypoxia	cells/Normoxia	
	Variable 1	Variable 2	
Mean	4.223287		1
Variance	0.007791		0
Observations	2		2
Pearson Correlation	1		
Hypothesized Mean Difference	0		
df	1		
t Stat	51.64438		
P(T<=t) one-tail	0.006163		
t Critical one-tail	6.313749		
P(T<=t) two-tail	0.012325		
t Critical two-tail	12.70615		

Student's t-Test statistical analysis for the HIF-1 α expression in bovine aortic endothelial cells incubated with HbI for 2 hours, 4, 6, 8, and 24 hours.

- A. Analysis for the HIF-1 α expression of cells under normoxia versus cells treated with HbI during hypoxia for 2 hours

t-Test: Paired Two Sample for Means		
	2hr/HbI/hypoxia	cells/Normoxia
	Variable 1	Variable 2
Mean	3.2074	1
Variance	0.004494	0
Observations	2	2
Pearson Correlation	-1	
Hypothesized Mean Difference	0	
df	1	
t Stat	46.56962	
P(T<=t) one-tail	0.006834	
t Critical one-tail	6.313749	
P(T<=t) two-tail	0.013668	
t Critical two-tail	12.70615	

- B. Analysis for the HIF-1 α expression of cells under normoxia versus cells treated with HbI during hypoxia for 4 hours

t-Test: Paired Two Sample for Means		
	4hr/HbI/hypoxia	cells/Normoxia
	Variable 1	Variable 2
Mean	3.2683	1
Variance	0.004666	0
Observations	2	2
Pearson Correlation	-1	
Hypothesized Mean Difference	0	
df	1	
t Stat	46.96273	
P(T<=t) one-tail	0.006777	
t Critical one-tail	6.313749	
P(T<=t) two-tail	0.013554	
t Critical two-tail	12.70615	

- C. Analysis for the HIF-1 α expression of cells under normoxia versus cells treated with HbI during hypoxia for 6 hours

t-Test: Paired Two Sample for Means		
	6hr/HbIHyp	cells/Normoxia
	Variable 1	Variable 2
Mean	3.8164	1
Variance	0.006362	0
Observations	2	2
Pearson Correlation	-1	
Hypothesized Mean Difference	0	
df	1	
t Stat	49.93617	
P(T<=t) one-tail	0.006373	
t Critical one-tail	6.313749	
P(T<=t) two-tail	0.012747	
t Critical two-tail	12.70615	

- D. Analysis for the HIF-1 α expression of cells under normoxia versus cells treated with HbI during hypoxia for 8 hours

t-Test: Paired Two Sample for Means		
	8hr/HbI/Hypoxia	cells/Normoxia
	Variable 1	Variable 2
Mean	4.31375	1
Variance	0.008128	0
Observations	2	2
Pearson Correlation	-1	
Hypothesized Mean Difference	0	
df	1	
t Stat	51.98039	
P(T<=t) one-tail	0.006123	
t Critical one-tail	6.313749	
P(T<=t) two-tail	0.012246	
t Critical two-tail	12.70615	

- E. Analysis for the HIF-1 α expression of cells under normoxia versus cells treated with HbI during hypoxia for 12 hours

t-Test: Paired Two Sample for Means		
	12hr/HbI/Hypoxia	cells/Normoxia
	Variable 1	Variable 2
Mean	5.12575	1
Variance	0.011476	0
Observations	2	2
Pearson Correlation	-1	
Hypothesized Mean Difference	0	
df	1	
t Stat	54.46535	
P(T<=t) one-tail	0.005844	
t Critical one-tail	6.313749	
P(T<=t) two-tail	0.011687	
t Critical two-tail	12.70615	